



**This electronic thesis or dissertation has been
downloaded from Explore Bristol Research,
<http://research-information.bristol.ac.uk>**

Author:

Eagling, Louise

Title:

Developing a 'Reverse-Biomimetic' Synthesis of Arogenate and its Analogues using a Dearomatising Intramolecular Acylation Strategy.

General rights

Access to the thesis is subject to the Creative Commons Attribution - NonCommercial-No Derivatives 4.0 International Public License. A copy of this may be found at <https://creativecommons.org/licenses/by-nc-nd/4.0/legalcode>. This license sets out your rights and the restrictions that apply to your access to the thesis so it is important you read this before proceeding.

Take down policy

Some pages of this thesis may have been removed for copyright restrictions prior to having it been deposited in Explore Bristol Research. However, if you have discovered material within the thesis that you consider to be unlawful e.g. breaches of copyright (either yours or that of a third party) or any other law, including but not limited to those relating to patent, trademark, confidentiality, data protection, obscenity, defamation, libel, then please contact collections-metadata@bristol.ac.uk and include the following information in your message:

- Your contact details
- Bibliographic details for the item, including a URL
- An outline nature of the complaint

Your claim will be investigated and, where appropriate, the item in question will be removed from public view as soon as possible.

Developing a ‘Reverse-Biomimetic’ Synthesis of Arogenate and its Analogues using a Dearomatising Intramolecular Acylation Strategy.

School of Chemistry

Louise Eagling

2020



University of
BRISTOL

A thesis submitted to the University of Bristol for the degree of Doctor of
Philosophy in the Faculty of Science

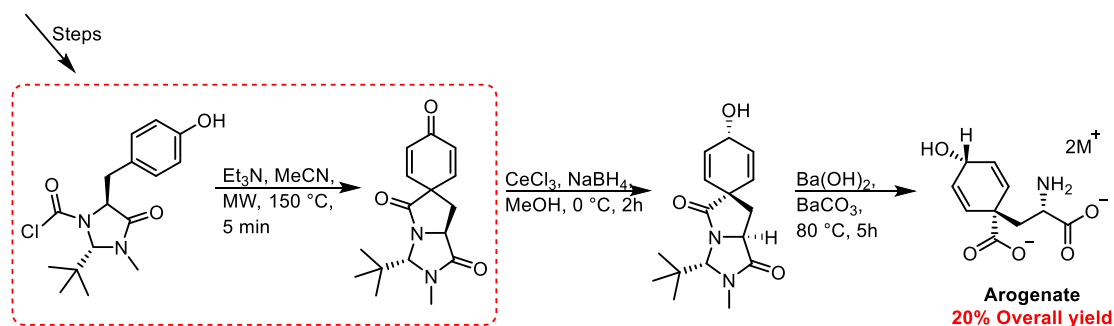
Project Supervisor – Professor Jonathan Clayden

Organic & Biological Chemistry

Abstract

Arogenate is a key intermediate in the shikimate biosynthetic pathway to aromatic amino acids tyrosine and phenylalanine. Though two previous syntheses have been reported in the literature, no functionalised derivatives have yet been reported. This work focuses on a ‘reverse-biomimetic’ synthesis of arogenate starting from the inexpensive, enantiopure amino acid L-tyrosine. Interestingly, the synthetic route proceeds via a novel and mechanistically unusual dearomatising spirocyclisation reaction. This intramolecular acylation, which utilises a carbamoyl chloride tether to produce a spirocyclic lactam, can be performed using low-cost reagents and without the need for heavy metals or toxic species. A synthesis of arogenate has been realised with a 19.6% overall yield in seven steps.

L-Tyrosine



The biosynthetic pathways to aromatic amino acids are present in plants, bacteria and fungi but completely absent in animals. It has long been thought that arogenate analogues may be potent competitive inhibitors of arogenate dehydrogenase and dehydratase and enable the development of new, safe and selective herbicides and/or antibiotics. Using the many points for derivatisation of the spirocyclic intermediate on the route to arogenate provides an opportunity for various functionalisations. The application of this new route to arogenate shows its efficacy to produce a collection of arogenate derivatives which may possess biological activity.

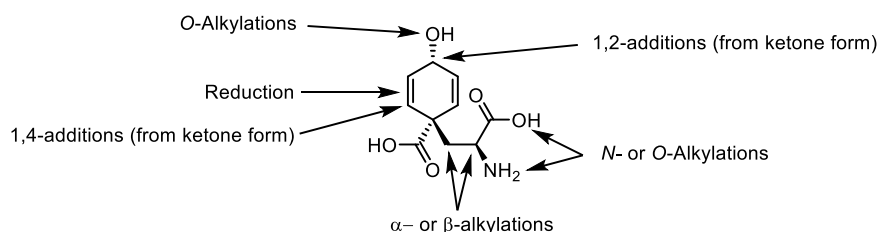


Table of Contents

Developing a ‘Reverse-Biomimetic’ Synthesis of Arogenate and its Analogues using a Dearomatising Intramolecular Acylation Strategy.		1
Abstract		3
Declaration		5
Acknowledgements		6
Abbreviations		7
1.	Introduction	11
1.1	Arogenate	11
1.2	Herbicides and metabolic diversity	15
1.2.1	Current herbicides.....	15
1.3	Previous syntheses.....	18
1.4	Dearomatising cyclisation	23
1.4.1	Dearomatising spirocyclisations in the Clayden group	23
1.4.2	Dearomatising spirocyclisations of phenols	28
1.4.3	Nucleophilic (oxidative) dearomatising spirocyclisations.....	29
1.4.4	Tyrosine-based spirocyclisations.....	32
1.4.5	Radical dearomatising spirocyclisations.....	36
1.4.6	Electrophilic dearomatising spirocyclisations	40
1.5	Previous work.....	46
2.	Results and discussion	49
2.1	Aims of the project	49
2.2	Unsuccessful routes	50
2.2.1	Hydantoin route	50
2.2.1.1	Silyl route	51
2.2.1.2	Benzyl route.....	53
2.2.2	Oxazolidinone route	55
2.3	Total synthesis of arogenate & its analogues	58
2.3.1	Arogenate synthesis via an imidazolidinone route	58
2.3.2	Synthesis of analogues.....	63
2.3.2.1	<i>ortho</i> -Arogenate.....	63
2.3.2.2	3-Methyl Arogenate.....	66
2.3.2.3	Grignard additions	70
2.3.2.4	Double bond reductions.....	72

2.3.2.5	Diels-Alder.....	75
2.3.2.6	Alkylation to produce aroenate-based quaternary amino acids	77
2.3.3	Hydrolysis of aroenate and its analogues.....	81
2.3.3.1	Purification.....	85
2.3.3.2	Hydrolysis of 3-Methyl Derivative	99
2.3.3.3	Hydrolysis of Grignard Derivatives	99
2.3.3.4	Hydrolysis of a Fully Saturated Derivative.....	101
2.3.3.5	Hydrolysis of Alkylation Derivatives	102
3.	Conclusions	103
4.	Future Directions	104
5.	Experimental	110
5.1	Hydantoin route	111
5.1.1	Silyl route.....	111
5.1.2	Benzyl route	115
5.2	Oxazolidinone route.....	118
5.3	Synthesis of aroenate	119
5.4	Aroenate derivatives	128
5.4.1	<i>Ortho</i> -tyrosine.....	128
5.4.2	3-Methyl Aroenate	134
5.4.3	Grignard addition derivatives.....	146
5.4.4	Hydrogenation.....	150
5.5	Alpha alkylations	154
6.	References.....	164

Declaration

I declare that the work in this dissertation was carried out in accordance with the requirements of the University's *Regulations and Code of Practice for Research Degree Programmes* and that it has not been submitted for any other academic award. Except where indicated by specific reference in the text, the work is the candidate's own work. Work done in collaboration with, or with the assistance of, others, is indicated as such. Any views expressed in the dissertation are those of the author.

SIGNED: DATE: / /

Acknowledgements

Firstly, a big thank you to Jonathan for allowing me to carry out such an interesting and challenging project in the Clayden group. Thank you for all your guidance and being so understanding throughout my time in the group.

Also, thank you to Professor Kevin Booker-Milburn, Emma Rose, Mar and Laura for giving me the opportunity to partake in CDT programme and all their help during PACT. Thank you to the University of Bristol, EPSRC and Syngenta for funding. Thank you to Steve Wailes (Syngenta) for his help and input throughout the project.

Thank you to all the members of the Clayden group for the all exceptional help and company throughout my time in the group. Dan, thanks for your guidance on the project, being such a fountain of knowledge and excellent company in the lab. Dabs, you have been there from the very beginning, thanks for all the lab chats, drunken nights and the numerous games you have introduced me to! Mo, you are such an incredibly kind-hearted person who can always cheer me up. I will never forget you abandoning me on the bus in Vienna ;). Makenzie, so many great chats in the lab, half of which I couldn't hear over the speaker, thanks for the SUPing session and keeping me calm(ish) in Athens. Roman, this last year in the group has been a blast working next to you – apologies for never shutting up! Mary, it's a shame we got kicked out of the library – it's been so nice working through these final few months of our PhD's with such a wonderful person. Matthew, thank you for listening to my numerous rants about the HPLC machine. Rachel, it was fantastic to have you in the lab – thank you for all your help on the project. Frank, Branca, Ellie, Rakesh, Steve, Quentin, Hossay, Jess, Josep, Romain, Johnno and John - thank you all.

A huge thank you to Makenzie, Dan, Matthew and Steve for the proof reading.

Lydia, thank you for your constant support and friendship. "She's my person. This is not about getting her approval. It's about telling her... if I murdered someone, she's the person I'd call to help me drag the corpse across the living room floor. She's my person." - Cristina Yang

The rest of the CDT family – Dabs, James and Jon, thanks for the nights I will never fully remember.

My friends and family for all their encouragement and support – thank you!

To my Mam and Dad, thank you for everything. From the long drives down to Bristol to putting Izzy on video call to cheer me up, you were always there to help me through the difficult times. You have always ensured that I could do anything and everything I ever wanted - your continuous support means the world to me. I am forever grateful for all you do.

Abbreviations

AAA	– aromatic amino acids
ADH	– arogenate dehydrogenase
ADT	– arogenate dehydratase
Aq	– aqueous
Asp	– aspartic acid
Boc	– <i>tert</i> -butoxycarbonyl
CM	– chorismate mutase
Conc.	– concentration
COSY	– correlation spectroscopy
CPBA	– chloroperoxybenzoic acid
DCE	– 1,2-dichloroethane
DCM	– dichloromethane
DIBAL	– diisobutylaluminium hydride
DIPEA	– N,N-Diisopropylethylamine
DMAP	– dimethylaminopyridine
DMF	– N,N-Dimethylformamide
DMP	– dimethylpyrazole
<i>dr</i>	– diastereomeric ratio
DMSO	– dimethylsulfoxide
E ⁺	– electrophile
<i>ee</i>	– enantiomeric excess
EPSP	– enolpyruvylshikimate-3-phosphate
eq.	– equivalents
ESI	– electrospray Ionisation
<i>et al.</i>	– and others
EWG	– electron-withdrawing group
Glu	– glutamic acid
HILIC	– hydrophobic interaction liquid chromatography
his	– histidine
HPLC	– high performance liquid chromatography
HPP-AT	– 4-hydroxyphenylpyruvate aminotransferase
KG	– ketoglutarate
KHMDS	– potassium hexamethyldisilazide
L	– ligand
LDA	– lithium diisopropylamide

Leu	– leucine
<i>m</i>	– <i>meta</i>
Met	– methionine
MW	– microwave
NAD/NADH	– nicotinamide adenine dinucleotide
NADP ⁺ /NADPH	– nicotinamide Adenine Dinucleotide Phosphate
NMR	– nuclear magnetic resonance
NOE	– nuclear overhauser effect
Nu [−]	– nucleophile
<i>o</i>	– <i>ortho</i>
OAc	– acetate
o/n	– overnight
<i>p</i>	– <i>para</i>
PDH	– prephenate dehydrogenase
PDT	– prephenate dehydratase
PGC	– porous graphitic carbon
Phe	– phenylalanine
pH	– power of hydrogen
PIDA	– (Diacetoxyiodo)benzene
PIFA	– [Bis(trifluoroacetoxy)iodo]benzene
Piv	– pivalate
PMB	– <i>para</i> -methoxybenzyl
PPA-AT	– prephenate aminotransferase
ppm	– parts per million
qNMR	– quantitative NMR
R ^x	– substituent
R _f	– retention factor
RT	– room temperature
SM	– starting material
TBS	– <i>tert</i> -butyldimethylsilane
TBDMS	– <i>tert</i> -butyldimethylsilyl
TEA	– triethylamine
Tf	– trifluoromethylsulfonyl
TFA	– trifluoroacetic acid
TFAA	– trifluoroacetic anhydride
TFE	– trifluoroethanol
THF	– tetrahydrofuran

Thr	– threonine
TLC	– thin layer chromatography
TMS	– trimethylsilyl
Ts	– tosyl
Trp	– tryptophan
Tyr	– tyrosine
VT	– variable temperature

1. Introduction

1.1 Arogenate

Arogenate **1** (Figure 1), also known as pretyrosine, is a key intermediate in the shikimate pathway towards aromatic amino acids (AAAs).¹

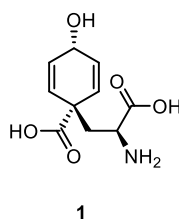
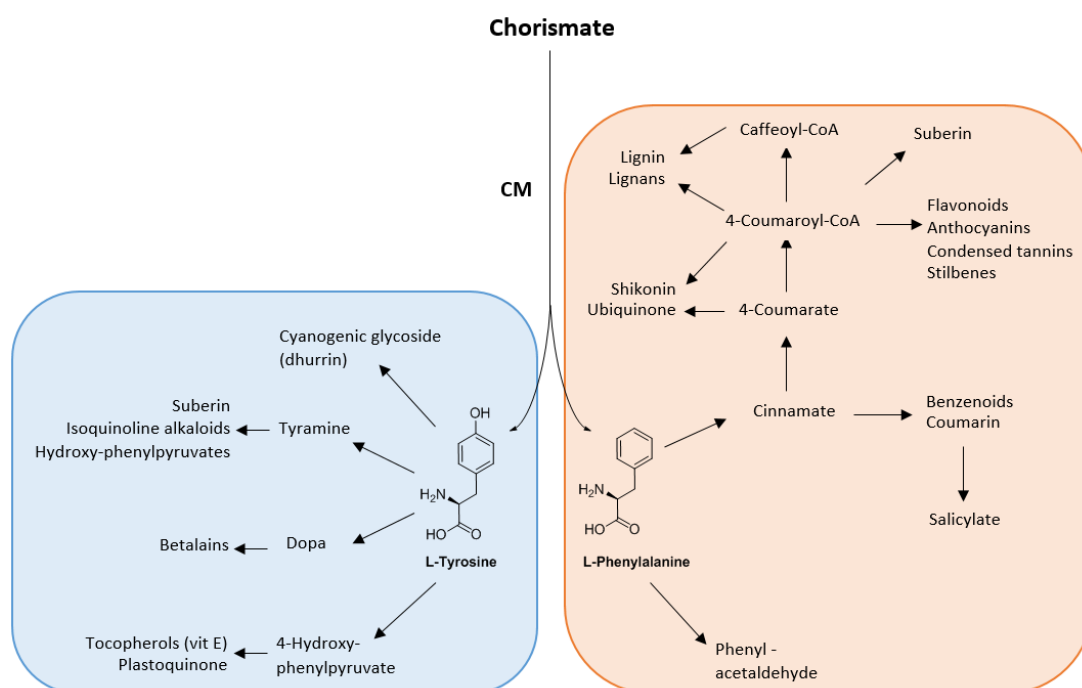


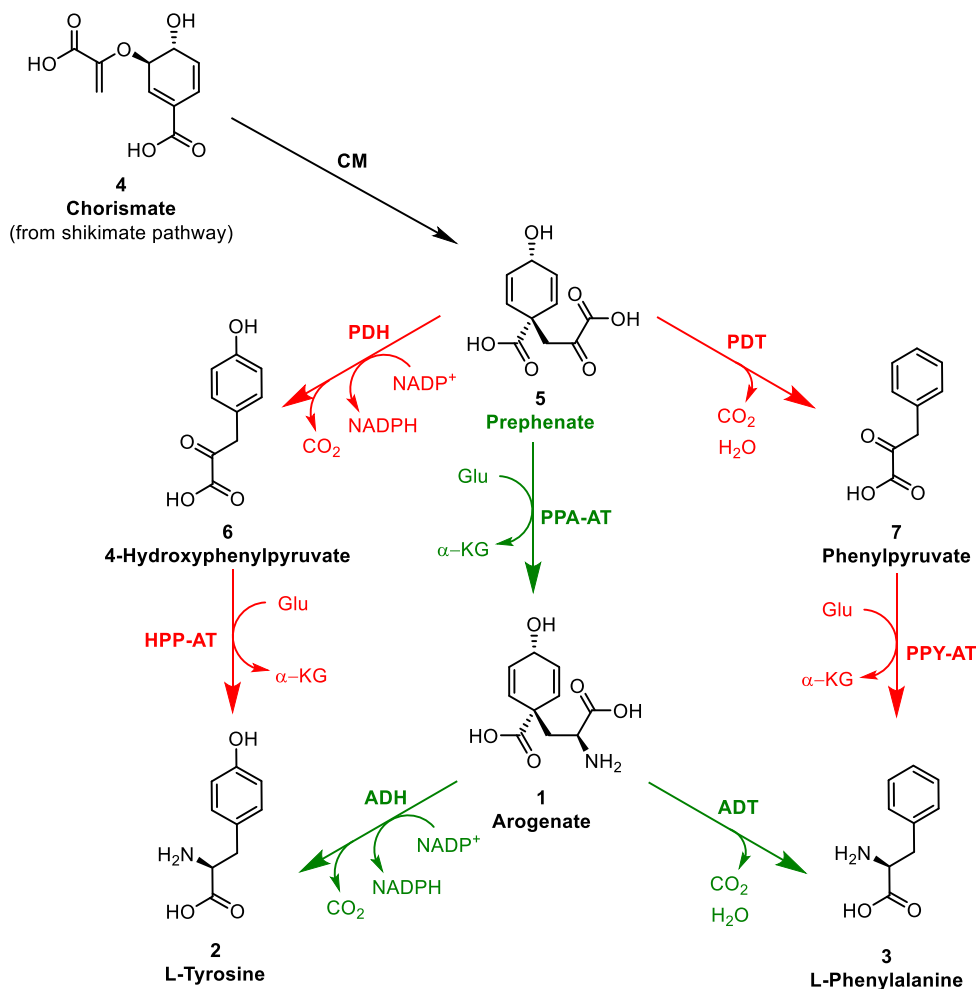
Figure 1 - The chemical structure of arogenate, β -(1-carboxy-4-hydroxy-2,5-cyclohexadien-1yl)alanine.

AAAs are essential for the synthesis of the vast majority of proteins.¹ In plants, AAAs function as precursors to numerous natural products which possess pharmacological or biological activities (Scheme 1), for example alkaloids, hormones, and salicylates; structural organic polymers, such as lignin, also often comprise large numbers of AAAs.^{1,2} Indeed, the AAAs Trp, Tyr and Phe, derived from the shikimate pathway, can account for up to 35% of a plant's dry weight.^{1,3}



Scheme 1 - Assortment of natural products from AAAs L-Tyrosine and L-phenylalanine, derived from the shikimate pathway.

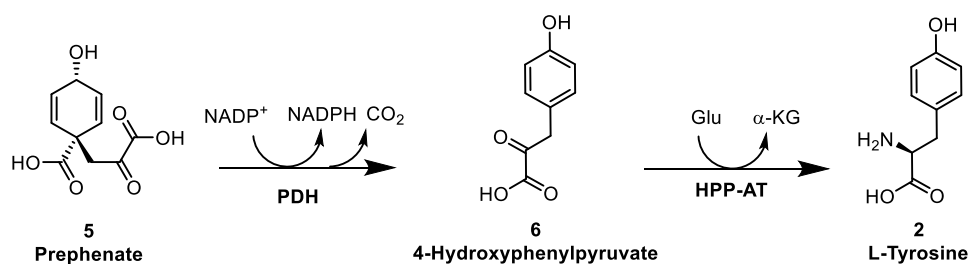
Further down the metabolic pathway, the shikimate pathway branches into two distinct routes towards the synthesis of L-tyrosine **2** and L-phenylalanine **3**. These are the phenylpyruvate/4-hydroxyphenylpyruvate and arogenate pathways (Scheme 2).⁴



Scheme 2 - Phenylpyruvate/4-hydroxyphenylpyruvate (red) and arogenate (green) pathways.

(NADP⁺/NADPH, Nicotinamide Adenine Dinucleotide Phosphate; α-KG, α-ketoglutarate; Glu, glutamate; CM, chorismate mutase; PDH, prephenate dehydrogenase; PDT, prephenate dehydratase; PPA-AT, prephenate aminotransferase; PPY-AT, phenylpyruvate aminotransferase; HPP-AT, 4-hydroxyphenylpyruvate aminotransferase; ADH, arogenate dehydrogenase; ADT, arogenate dehydratase.)

The discovery of arogenate and its pathway came in 1974 by Stenmark *et al.*, it was previously thought there was only one biosynthetic pathway to L-tyrosine **2**, known as the 4-hydroxyphenylpyruvate pathway (Scheme 3).⁵ The exact structure of arogenate was investigated in 1980 by Zamir *et al.*, and was established through a variety of spectroscopic techniques including UV, ¹H NMR, ¹³C NMR spectroscopies and mass spectrometry.⁶

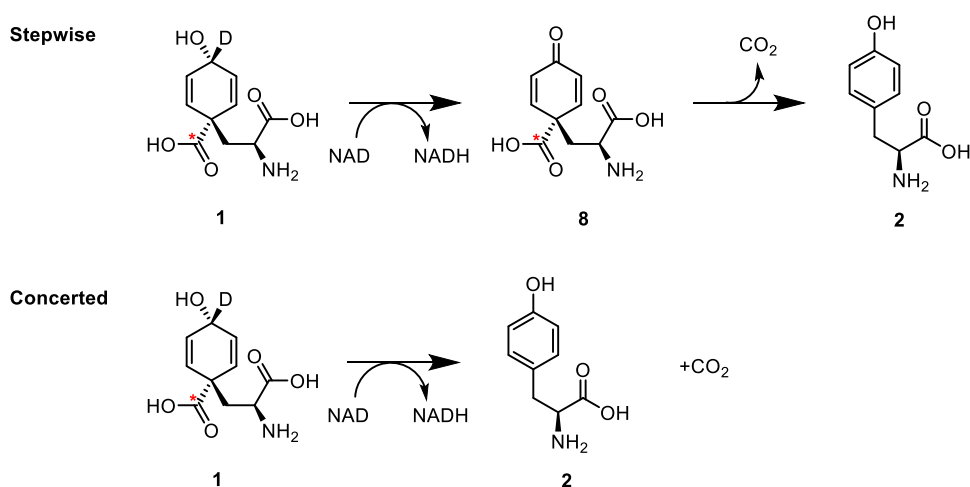


Scheme 3 - 4-hydroxyphenylpyruvate pathway to L-tyrosine.

(NADP⁺/NADPH, Nicotinamide Adenine Dinucleotide Phosphate; α -KG, α -ketoglutarate; Glu, glutamate; PDH, prephenate dehydrogenase; HPP-AT, 4-hydroxyphenylpyruvate aminotransferase.)

Stenmark's work revealed that several species of blue-green algae exploited this alternative arogenate pathway (Scheme 2) for the biosynthesis of AAAs.⁵ In this pathway arogenate is the last non-aromatic intermediate on the route to phenylalanine or tyrosine.⁷ The pathways to AAAs are present in plants, bacteria, fungi, and some protists. However, they are completely absent in animals, which must obtain these essential AAAs from their diet. Consequently, the pathway is an attractive target for herbicides, antimicrobial agents, and live vaccines.⁸⁻¹⁰

In 2006, Ferrer *et al.* isolated and characterised a crystal structure for arogenate dehydrogenase derived from a species of fresh water bacteria, *Synechocystis*.¹¹ The participation of a histidine residue in the prephenate dehydrogenase mechanism has been proven through site directed mutation.¹² The similarities between prephenate dehydrogenase and arogenate dehydrogenase, particularly with respect to their pH profiles, suggest a histidine residue was also present in the arogenate dehydrogenase mechanism. Cleland *et al.* suggested the mechanism of hydride transfer and decarboxylation in prephenate dehydrogenases, and so indirectly arogenate dehydrogenases, could either be stepwise or concerted (Scheme 4).^{11,13}



Scheme 4 - Possible stepwise or concerted mechanism for conversion of arogenate to tyrosine by arogenate dehydrogenase.

Cleland *et al.* studied the ^{13}C kinetic isotope effect of decarboxylation for both deuterated and non-deuterated substrates looking for a multiple isotope effect. Upon changing from non-deuterated to deuterated substrate, they observed an impact on the ^{13}C kinetic isotope effect for decarboxylation. Due to the deuterated substrate slowing down the ^{13}C kinetic isotope effect, it can be concluded the mechanism is concerted – heavier isotopes cause an increased stability and therefore a lower velocity.¹³

The crystal structure of arogenate dehydrogenase shows a water molecule is present in the active site, within 2.51 Å of His112. By replacing this water molecule with arogenate and performing a structure optimisation, a proposed model of active site showing key interactions between residues and arogenate was generated (Figure 2).¹¹

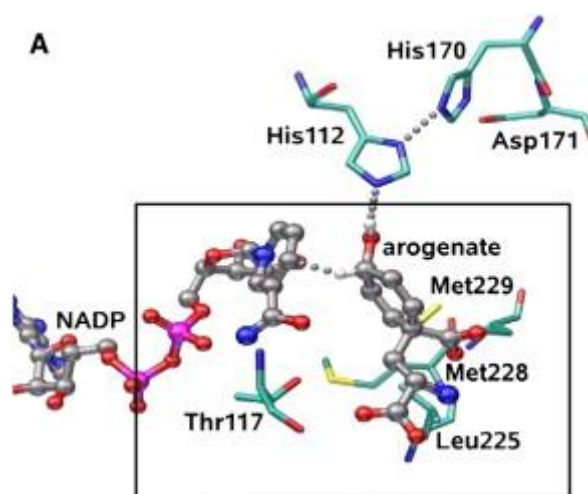
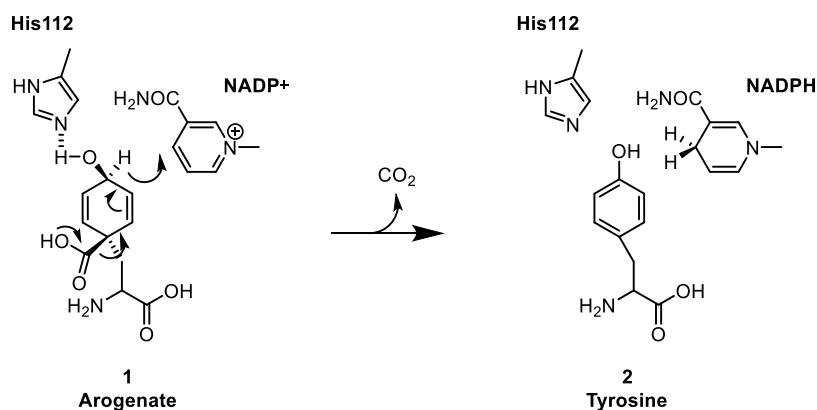


Figure 2 - Proposed model of the active site of Arogenate Dehydrogenase with Arogenate.¹¹

These projected interactions included the carboxyl group of arogenate pointing towards a hydrophobic pocket of Leu225, Met228 and Met229 which promotes the concerted decarboxylation reaction. The amino acid residue His112 is in close proximity to the 4-hydroxyl group of arogenate, whilst this facilitates hydride transfer it cannot abstract the hydroxyl proton preventing dienone formation as seen in the stepwise mechanism (Scheme 4). Whereas, the interaction between the C₄ of NADP and the hydride at the C₄ position of arogenate is optimised for hydride transfer. These modelled interactions also supported previous biochemical studies.^{11–13} They therefore proposed the mechanism within the active site is a concerted mechanism involving His112 and NADP⁺ (Scheme 5).¹¹



Scheme 5 - Reaction mechanism of arogenate dehydrogenase.

1.2 Herbicides and metabolic diversity

1.2.1 Current herbicides

There are various classes of herbicides depending on their mode of action. Of particular interest to this project are herbicides which inhibit the shikimate pathway toward AAAs. Both phosphonomethylglycinamide **9** (huangcaoling) and phosphonomethylglycine **10** (glyphosate) are enolpyruvylshikimate-3-phosphate (EPSP) synthase inhibitors, an enzyme involved early in the shikimate pathway (Figure 3).¹⁴

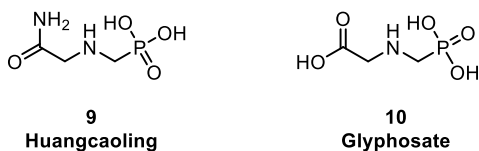
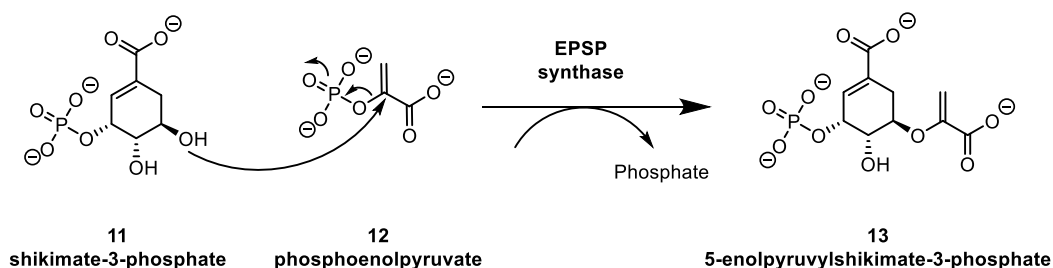


Figure 3 - EPSP synthase inhibitors.

These work by mimicking phosphoenolpyruvate **12** and binding competitively to EPSP synthase, the enzyme which catalyses the reaction of **11** to **13** (Scheme 6), and shuts down the pathway to AAAs.¹⁴⁻¹⁶



Scheme 6 - EPSP synthase catalysed reaction.

In 1970, Monsanto chemist John E. Franz first synthesised and tested glyphosate **10** for agrochemical uses, eventually leading to it becoming the most widely used herbicide in

history.^{17,18} In 2014, the total worldwide glyphosate use was over 825,000,000 kg. Since it came to market in 1974, the global production of glyphosate has topped 8,563,000,000 kg.¹⁹ Following the introduction of glyphosate resistant genetically modified crops in 1996, the sales of glyphosate have increased almost 15-fold.^{19,20} Despite this, there are conflicting reports as to the safety of its use. In 2015, a World Health Organisation assessment identified glyphosate as ‘probably carcinogenic to humans’.^{21,22} However, there have since been articles published to dispel this statement which state that the replacement of glyphosate with other herbicides ‘is likely to have a negative impact on chronic health risks faced by pesticide applicators’.²³ A meta-analysis published in 2019 by Zhang *et al.* reported that the risk of non-Hodgkins lymphoma was increased with the use of glyphosate-based herbicides particularly in high exposure groups.²⁴

1.2.2 Arogenate dehydrogenase and dehydratase inhibitors

It has long been thought the use of arogenate analogues would make for potent competitive inhibitors of arogenate dehydrogenase and dehydratase.^{8,9} Similarly to glyphosate, arogenate analogues could feasibly inhibit enzymes in the shikimate pathway; however, unlike glyphosate this would occur at a much later stage in the pathway. A quick and efficient synthesis of arogenate, which would be easily modified to produce analogues, would prove an attractive target. There are several possible sites for derivatisation of arogenate (Figure 4). However, to date there have been no reports of arogenate variants despite the two total syntheses published in the literature (Section 1.3).

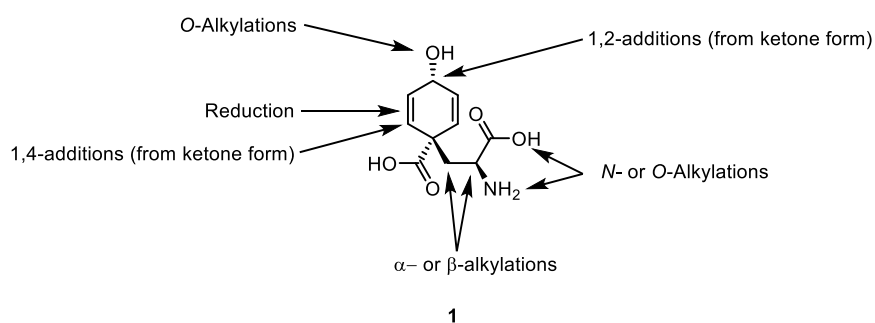
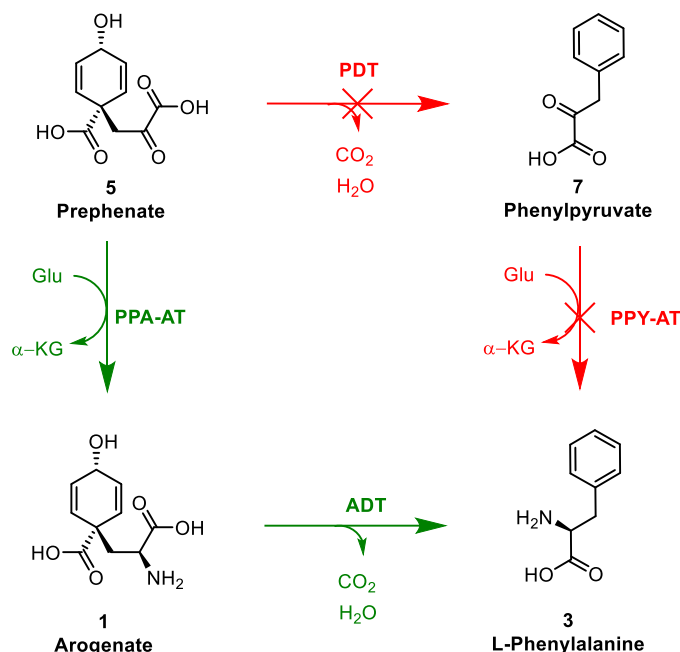


Figure 4 - Points of derivatisation of arogenate.

1.2.3 Metabolic diversity

Since arogenate’s discovery in 1974, it has been found that several plants and bacteria, including blue-green algae which was first discovered to utilise this pathway, produce AAAs via the arogenate pathway only.⁵ Others, such as the bacteria *Pseudomonas aeruginosa* utilise both the arogenate and phenylpyruvate pathways.²⁵ It has also been previously reported that prephenate dehydrogenase has not been detected in several species including mung bean,²⁶ corn,²⁷ Bervibacteria,²⁸ coryneform bacteria,^{29,30} sorghum³¹ and the yeast *Hansenula henricii*.³²

In 1986, Zamir *et al.* investigated the pathways in operation towards phenylalanine **3** in higher plants (Scheme 7), namely *Nicotiana sylvestris* (tobacco) and spinach.³³ They reported the presence of aroenate dehydratase in these vascular plants, whilst no prephenate dehydratase was found. The presence of only aroenate dehydratase suggests this pathway is used almost exclusively to produce AAAs.



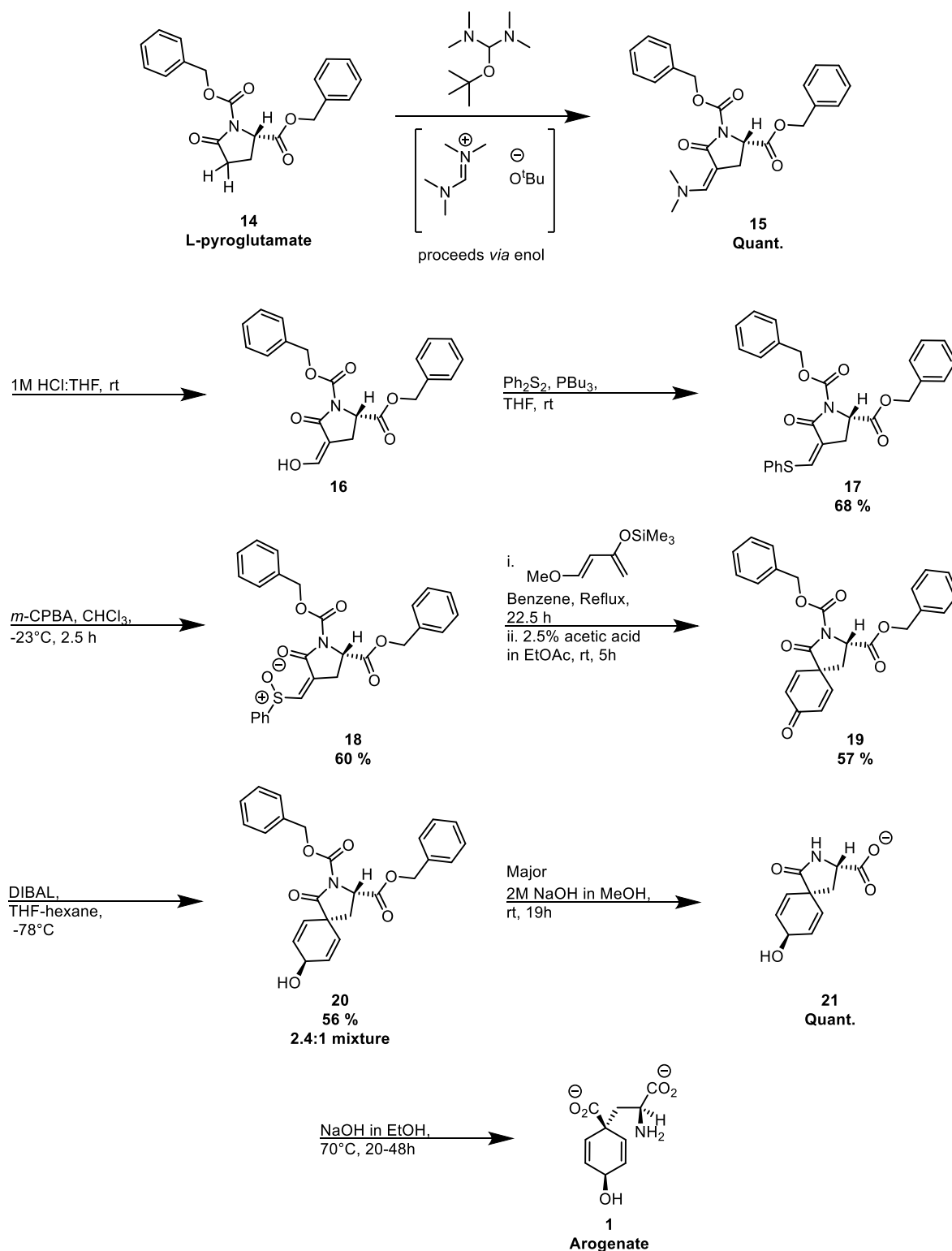
Scheme 7 - Pathways to L-phenylalanine; Aroenate pathway (green) and phenylpyruvate pathway (red).

In 2007, Lewis *et al.* further explored the dehydratases involved in production of L-phenylalanine (Scheme 7) in *Arabidopsis thaliana*.³⁴ The group cloned and expressed six genes from *Arabidopsis*; At1g11790, At3g07630, At2g27820, At3g44720, At5g22630, and At1g08250, and explored their activities. Previously these genes were considered PDT-like until 2005 when they were relabelled, by Douglas *et al.*, as ADTs (ADT1 to ADT6) despite a lack of functional characterisations.³⁵ From the work reported by Lewis *et al.* these have now all been provisionally characterised as aroenate dehydratases as a result of the functional characterisation carried out in this work. In particular, the genes ADT3, ADT4 and ADT5 utilised aroenate only, whereas, genes ADT1, ADT2 and ADT6 showed activity for mainly aroenate and low levels for prephenate.

These reports suggest there is considerable metabolic diversity in the biosynthesis of AAAs in plants, particularly in higher plants. It is hoped that this metabolic diversity may provide a source for exploitation to produce discriminative herbicides which operate by inhibiting only one pathway.

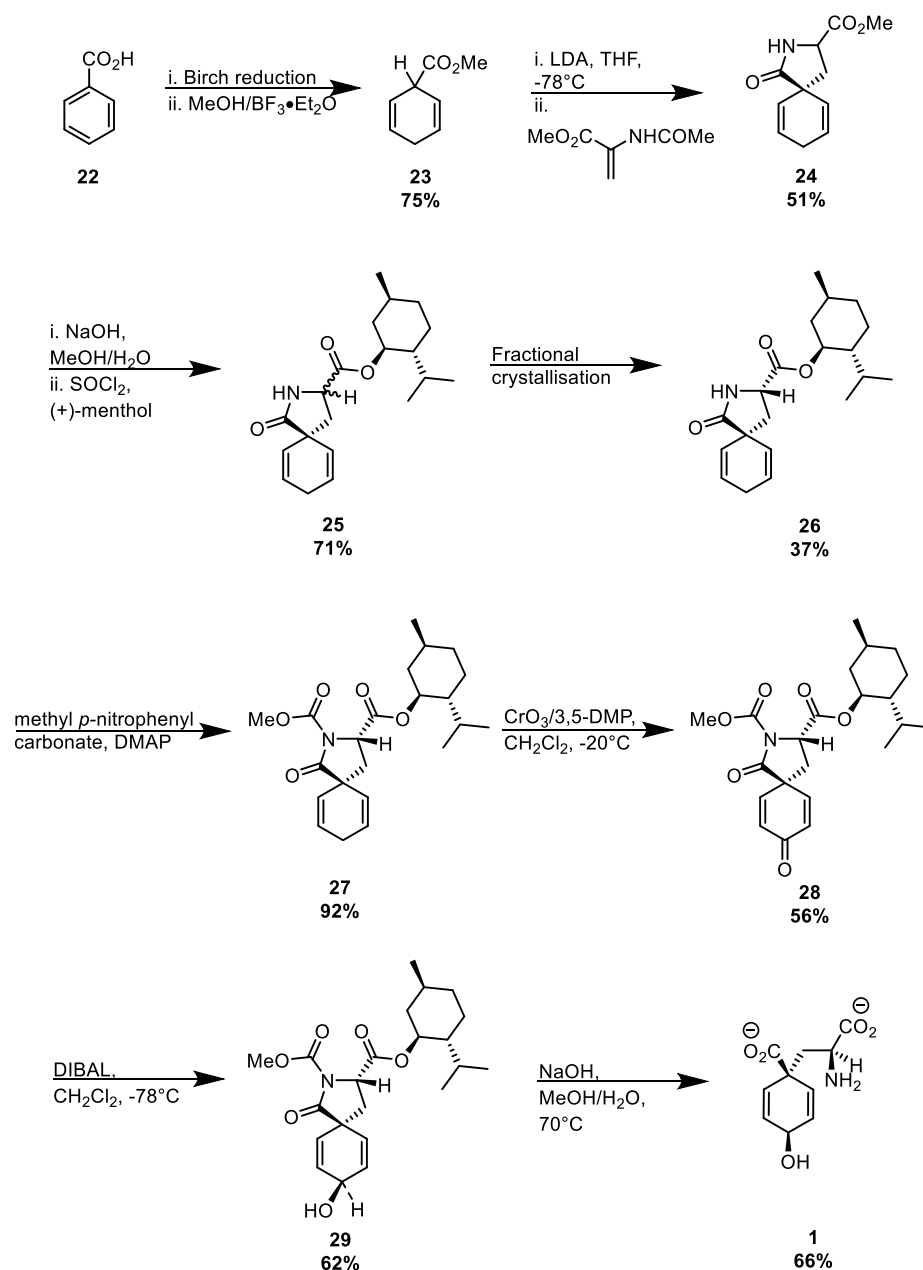
1.3 Previous syntheses

The first reported synthesis of arogenate was by Danishefsky *et al.* in 1981.³⁶ They achieved the synthesis of arogenate, and its epimer, in eight steps with a key Diels-Alder reaction used to construct the dienone core (Scheme 8).



Scheme 8 - Danishefsky *et al.* synthesis of arogenate.

Starting from L-pyroglutamate **14**, L-glutamic acid in its cyclic lactam form, the enol reacts with the imine to produce an enamine which is followed by hydrolysis. The hydrolysed species **16** is then reacted with diphenyl disulfide and tri-*n*-butylphosphine to produce the vinyl sulphide **17**. Oxidation using *m*-CPBA produced the sulfoxide **18** which then underwent the key Diels-Alder reaction to give **19**. This was followed by reduction of the ketone, hydrolysis of the carbamate and ester linkages and finally hydrolysis of the lactam ring to generate the desired aroenate product **1**. The authors stated that small amounts of phenylalanine and tyrosine were observed after the final step which could be separated using ion-exchange chromatography. It was also found that leaving the hydrolysis reaction for extended periods resulted in larger conversion to these undesired AAAs. However, a major drawback to this report is that no yield is quoted for the final step to aroenate itself and they do not discuss issues with instability of isolated aroenate.⁶

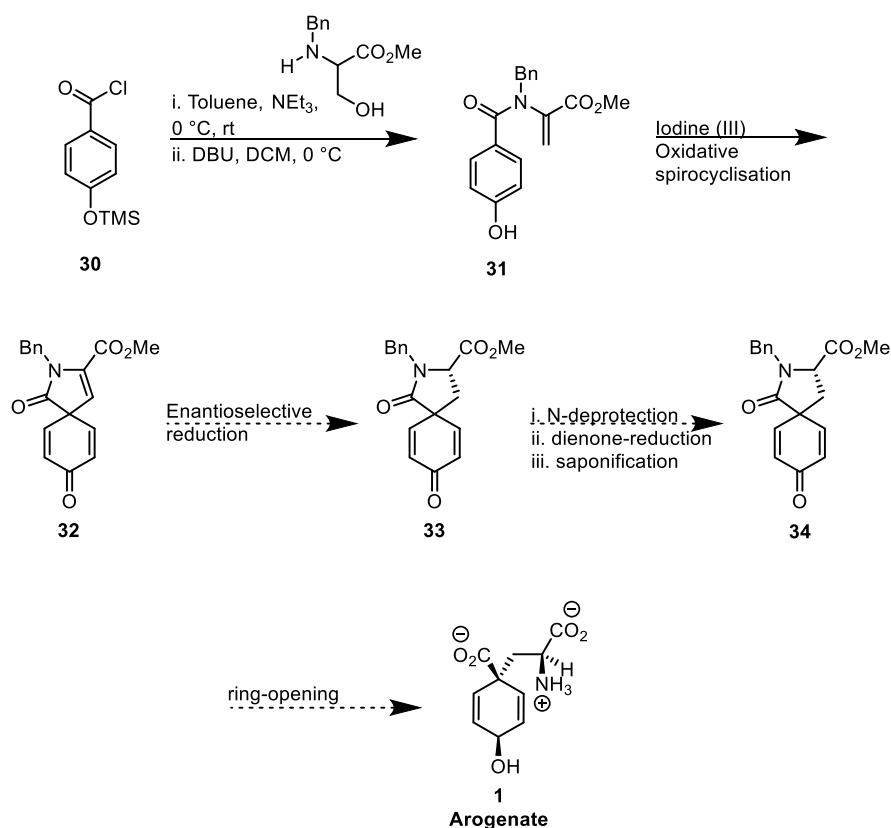


Scheme 9 - Crossley *et al.* synthesis of aroenate.

In 1994, Crossley *et al.* published an alternative synthesis of aroenate in nine steps, utilising a Michael addition as the key step with an overall yield of 2.1% (Scheme 9).³⁷ Using methyl benzoate **22** as the starting material, 1,4-dihydrobenzoate was produced using a Birch reduction followed by esterification using MeOH/BF₃•Et₂O to **23**, as reported by Folsom *et al.*³⁸ Deprotonation and quenching with methyl 2-acetamidoacrylate was then carried out to produce the spirocyclic lactam **24**. Hydrolysis of the ester, conversion to the acid chloride and finally esterification with (+)-menthol produced **25**. They then performed a fractional crystallisation in order to separate the diastereomers, followed by acylation of the nitrogen to give the carbamate **27**. Oxidation of the C₄ position with CrO₃/3,5-DMP followed by reduction with DIBAL produced the spirocyclic lactam-protected aroenate **29**. This species could then be hydrolysed under

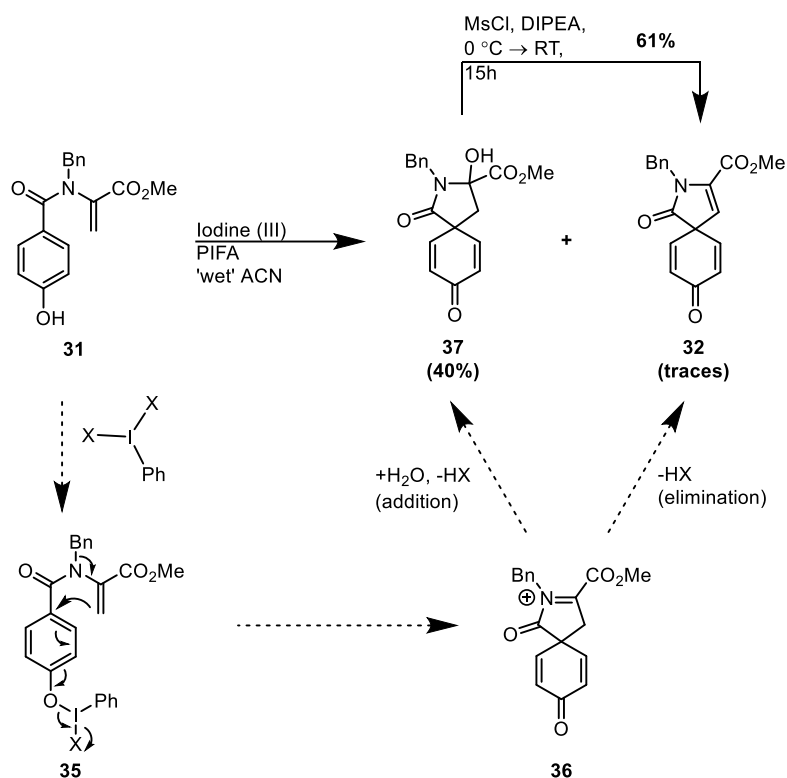
basic conditions to give aroenate **1** as the disodium salt. The authors noted issues with decomposition to phenylalanine and tyrosine being present in all samples of aroenate but provided no further information or a solution to overcome this. As part of this project, we reached out to Professor Maxwell Crossley in August 2019 who kindly supplied us with a copy of the thesis of Robert C. Reid in October 2019 to provide some more detail around this synthesis and provide insight into our own work.

Nachtsheim *et al.* reported a partial synthesis of the aroenate core in 2012 using an oxidative iodine(III)-mediated spirocyclisation.³⁹ Their work so far has produced a spirodienone lactam **32** which they envisage could then undergo enantioselective reduction, N-deprotection, dienone reduction, ester hydrolysis and finally ring opening to give aroenate **1** (Scheme 10).



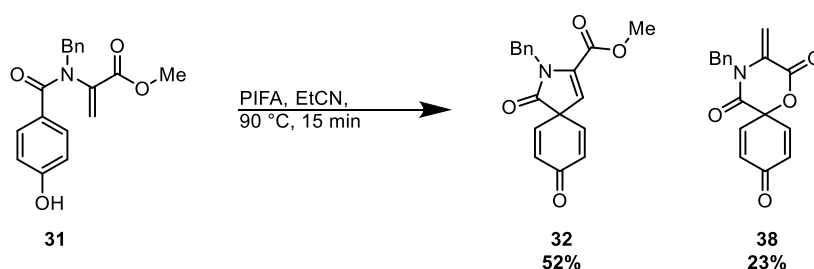
Scheme 10 - Nachtsheim *et al.* proposed aroenate synthesis.

First attempts at the spirocyclisation gave traces of the desired product **32** and a 40% yield of an undesired monohydroxylated product **37**. Conveniently, this species could be converted to the desired spirocyclic lactam via an elimination reaction (Scheme 11).



Scheme 11 - First attempts and mechanism of spirocyclisation.

Optimisations of the iodine(III)-mediated spirocyclisation were then carried out investigating temperatures, equivalents, solvents, generation of PIFA in situ and the effect of the ester substituent. The optimisation studies resulted in an increase in yield to 52% of the desired spirocyclic lactam **32**, conditions below (Scheme 12). However, a readily separable side product was observed and found to be the 6-membered spirolactone **38**. They state further studies into enantioselective reductions are underway, although to date no further papers have been published detailing this work.



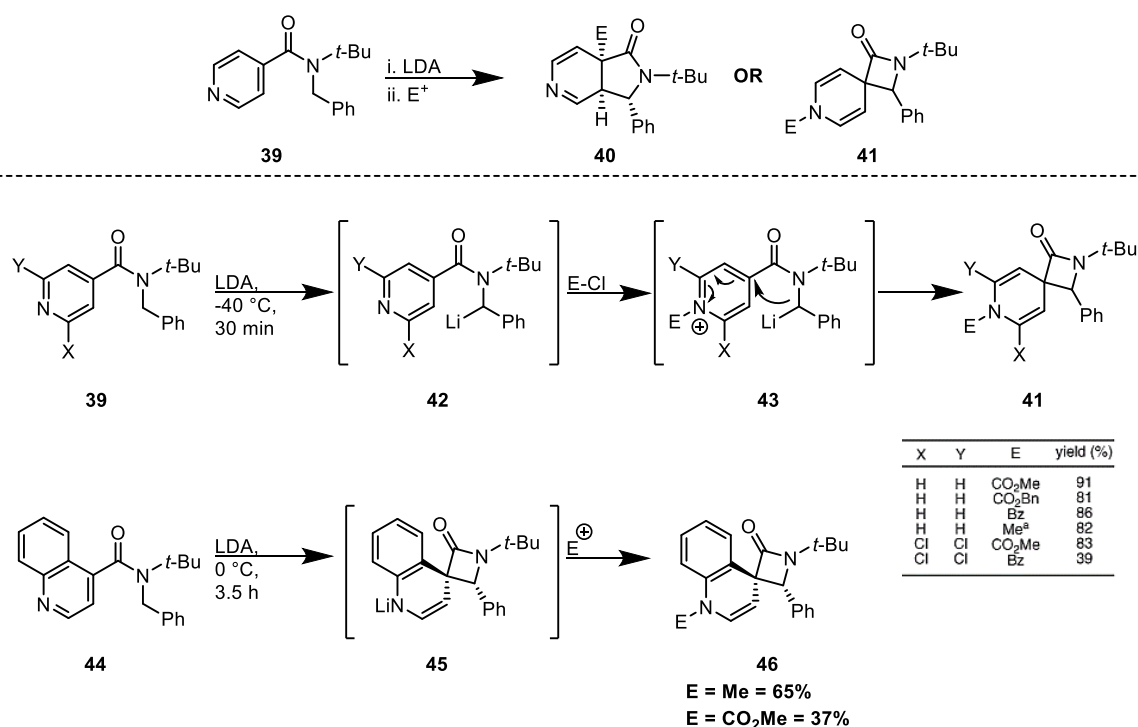
Scheme 12 – Optimised spirocyclisation to 32.

1.4 Dearomatising cyclisation

There are several classes of dearomatising cyclisations. These types of reactions have been performed on various aromatic starting materials such as pyridines,^{40,41} furans,^{42,43} indoles^{44,45} and phenols.^{46,47}

1.4.1 Dearomatising spirocyclisations in the Clayden group

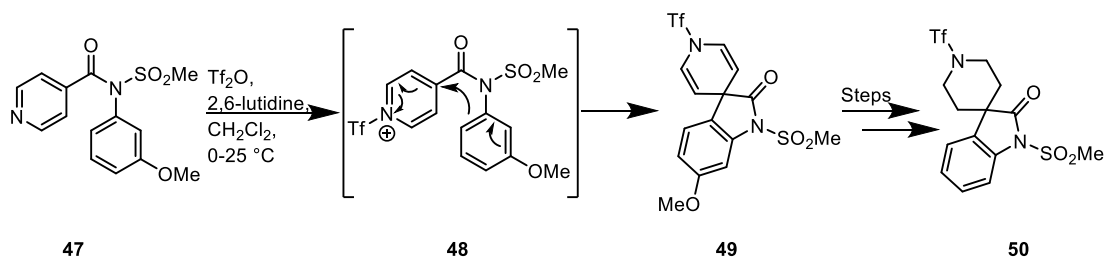
Work in the Clayden group has focused upon dearomatising spirocyclisations of pyridine using various nucleophilic tethers. Initial work explored using lithiation chemistry of benzyl amides to produce spirocyclic β -lactams. Lithiation could be carried out α to the nitrogen; the resulting carbanion could then undergo nucleophilic attack onto the pyridine and quinoline carboxamides. The use of LDA at 0 °C and addition of an electrophile produced *cis*-fused 5-*endo* cyclisation products **40**. However, it was found that with deprotonation with LDA at -40 °C, directly followed by addition of an acylating agent altered reactivity to favour the 4-*exo* spirocyclic product **41**. The reaction was successful with a range of acylating agents including methyl chloroformate, benzyl chloroformate, benzoyl chloride and methyl triflate (Scheme 13).⁴⁸



Scheme 13 - Pyridine and quinoline carboxamide spirocyclisations using LDA.

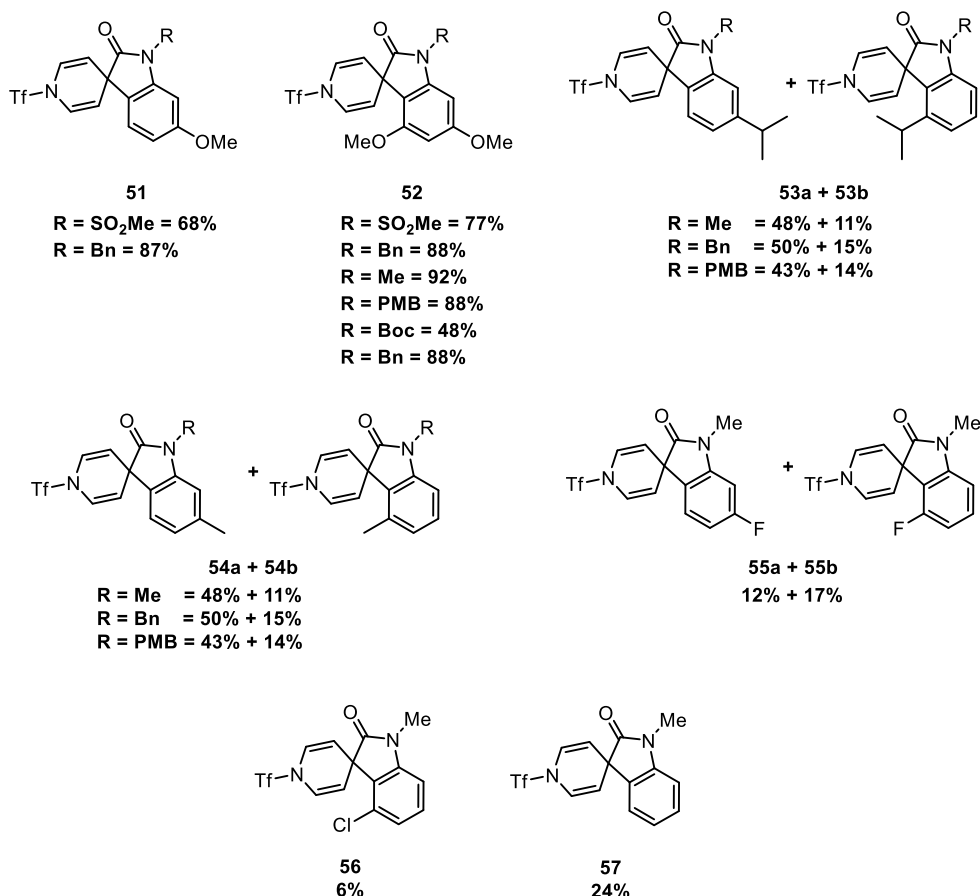
Later, dearomatising spirocyclisations of *N*-anisylisonicotinamides, **47**, with a tethered electron rich aryl group were found to occur upon exposure to trifluoromethanesulfonic anhydride (Scheme 14). This occurred via an intramolecular nucleophilic attack of the aryl ring to the

pyridinium ring **48**. This spirocyclic reaction was exploited to produce spirocyclic piperidines which are a moiety of interest in biologically active compounds such as MK-677 (Scheme 14).⁴⁹



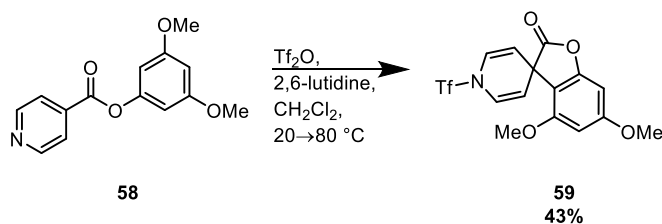
Scheme 14 – Spirocyclisation of *N*-anisylisonicotinamides leading to spirocyclic piperidines.

The spirocyclisation reaction was applied to a large range of derivatives to explore the substrate scope (Scheme 15). In most cases, the use of *meta*-substituted starting materials resulted in the regioisomeric products **53-55**. As might be expected, electron deficient phenylamides impeded the spirocyclisation whereas electron donating groups activated the aryl ring towards nucleophilic attack.⁴⁹



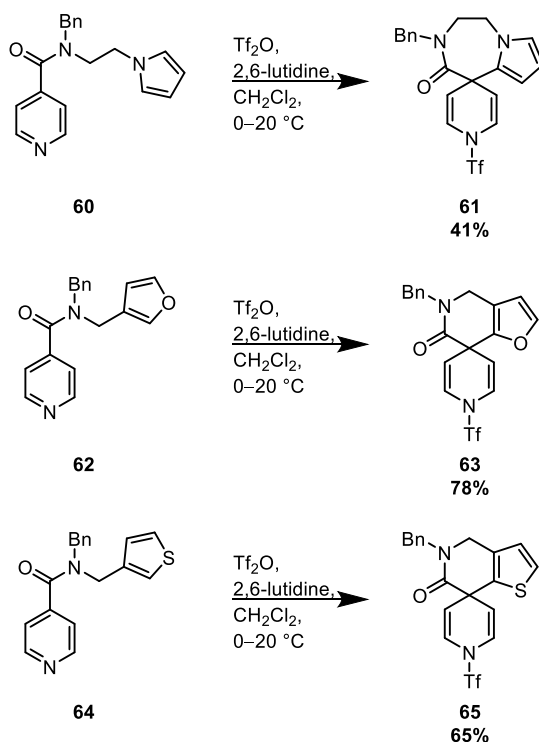
Scheme 15 -Various derivatives produced using the spirocyclisation method.

The reaction was then applied to produce an isonicotinamide analogue. Switching from the amide to the ester **58** resulted in a lower reactivity with a yield of 43%; this is likely due to the ester moiety being less activating and its favoured *s-cis* conformation (Scheme 16).⁴⁹



Scheme 16 - Isonicotinic ester spirocyclisation.

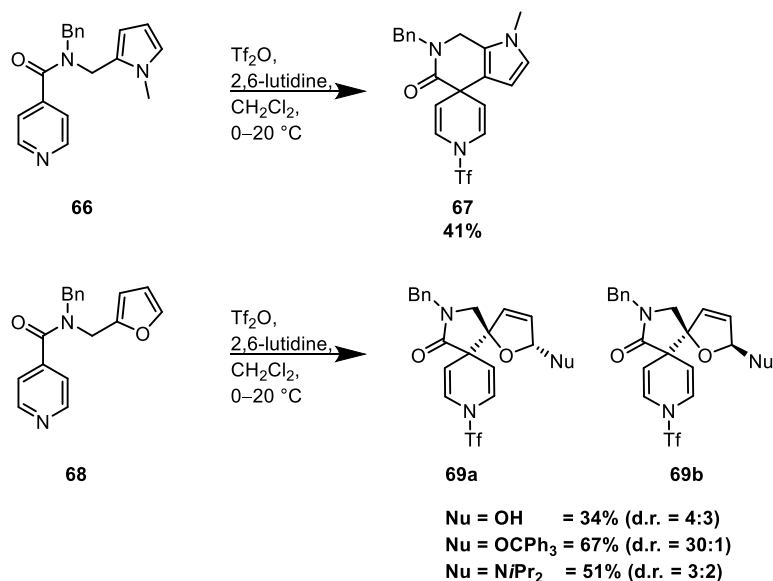
Further work in the group expanded these spirocyclisations of isonicotinamides to the use of nucleophilic heterocyclic tethers. Pyrroles, furans and thiofurans were used to explore the spirocyclisations reactions. A 1-substituted pyrrole and 3-substituted furan and thiophene all underwent spirocyclisation by nucleophilic attack from their 2-positions to give **61**, **63** and **65** respectively (Scheme 17).⁵⁰



Scheme 17 - 1-Substituted pyrrole and 3-substituted furan and thiophene spirocyclisations.

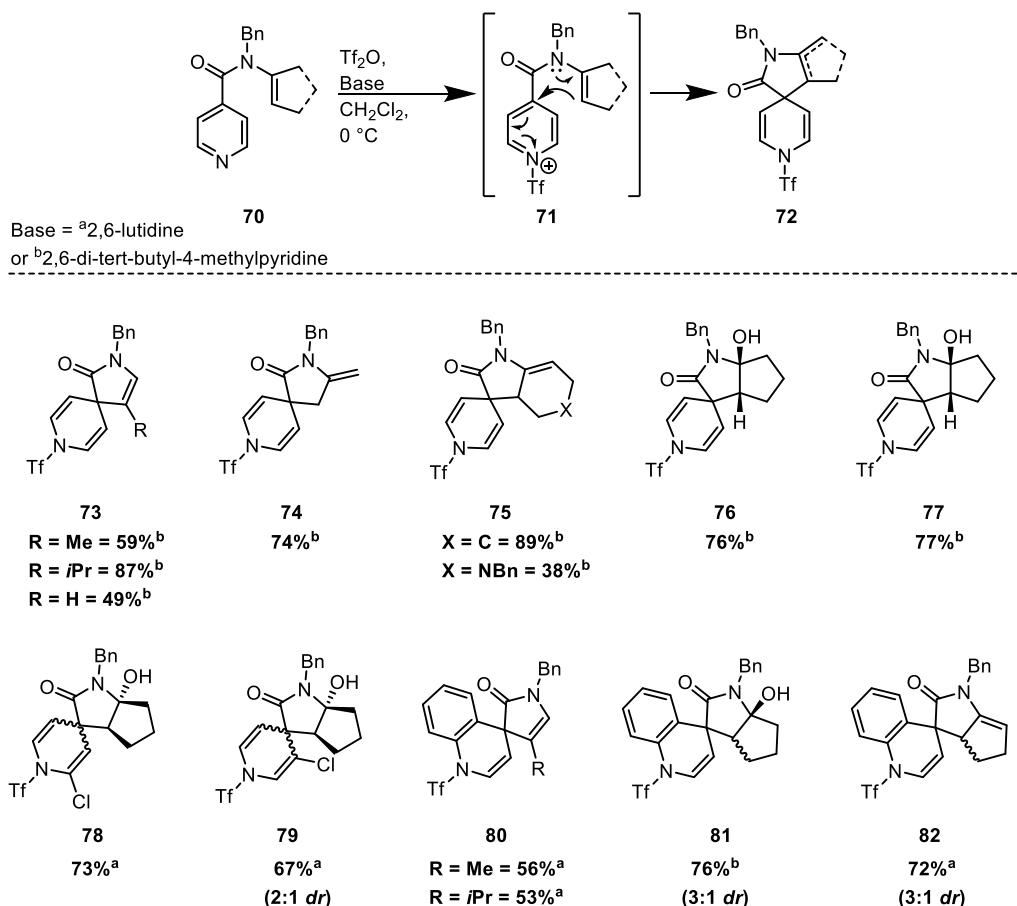
With 2-substituted pyrroles, cyclisation occurred from the 3-position to give **67**. Interestingly, the use of 2-substituted furans resulted in a doubly-dearomatised spirocyclisation producing two adjacent spirocyclic centres **69a/b** (Scheme 18). This product resulted from initial reaction at the 2-position of the furan; the resulting allylic oxonium ion was then trapped regioselectively by water in a nucleophilic attack. This was repeated using triphenylmethanol and diisopropylamine

as nucleophiles giving reasonable yields. The addition of the trityloxy group occurs on the less hindered face of the furan, **69a**, giving excellent diastereoselectivity.⁵⁰



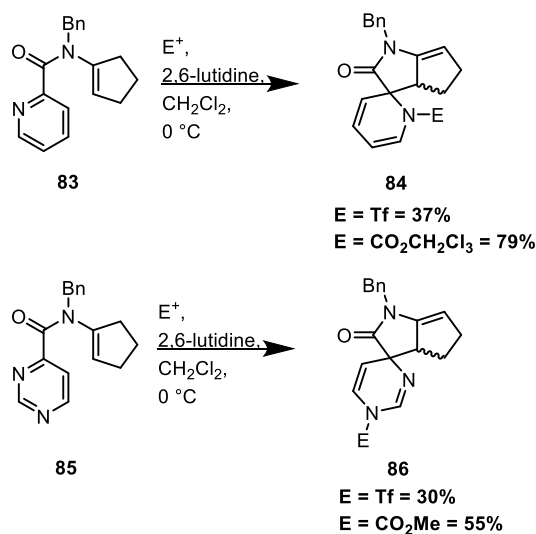
Scheme 18 – Spirocyclisation of a 2-substituted pyrrole and furan.

Finally, these spirocyclisations were applied to an alkenyl tether to give unsaturated 2,8-diazaspiro[4.5]decanes which are of potential biological interest. The methodology was applied to a large range of both acyclic and cyclic alkene tethers linked by an amide to a pyridine or quinoline ring (Scheme 19). Reactions where a new stereocentre is formed, due to the unsymmetrical nature of the starting material, gave little to no diastereoselectivity.⁵¹



Scheme 19 – Dearomatising spirocyclisations of pyridine and quinoline with alkenyl tethers.

Several related products were also produced using chloroformates in place of the triflate electrophile in moderate to excellent yields. The reaction was expanded to the use of a 2-pyridine ring to allow for an *ortho*-spirocyclisation to take place giving **84**. Pyrimidine rings were also found to undergo the dearomatising cyclisation to produce **86** (Scheme 20). All reactions proceed in between 5:1 and 9:1 *dr* but characterisation was not obtained due to their instability.⁵¹



Scheme 20 – Spirocyclisations of picolinamides and pyrimidinecarboxamide.

1.4.2 Dearomatising spirocyclisations of phenols

The dearomatisation of phenol is an important transformation, allowing complexity to be built from a simple planar core. It has been a prominent reaction in the synthesis of complex natural products.^{52,53} Examples of natural products which have been successfully synthesised by exploitation of a dearomatising spirocyclisation include (+)-maritidine,⁵⁴ dalesconol B,⁵⁵ platensimycin,^{56,57} and spirobacillene A⁵⁸ (Figure 5), all of which will be discussed in greater detail later.

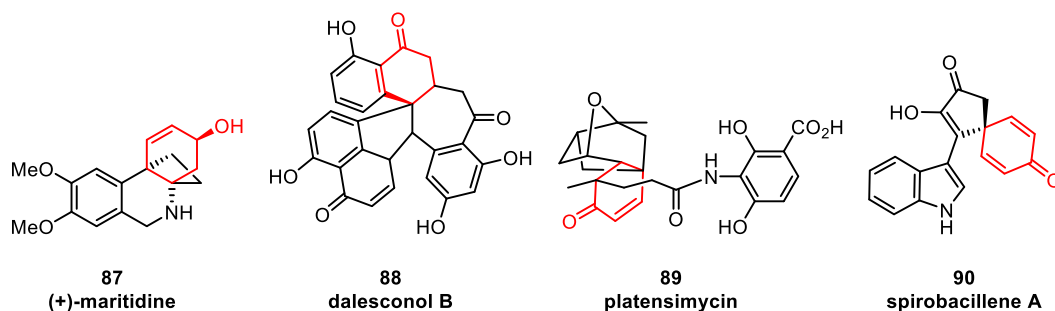


Figure 5 - Examples of natural products synthesised using a key dearomatising spirocyclisation.

Spirocyclic dienones are also an important motif in natural products such as argutosine D,⁵⁹ hopeanol,⁶⁰ glaziovine,⁶¹ stepharine,⁶² annosqualine⁶² and spirocalcaridine B⁶³ (Figure 6).

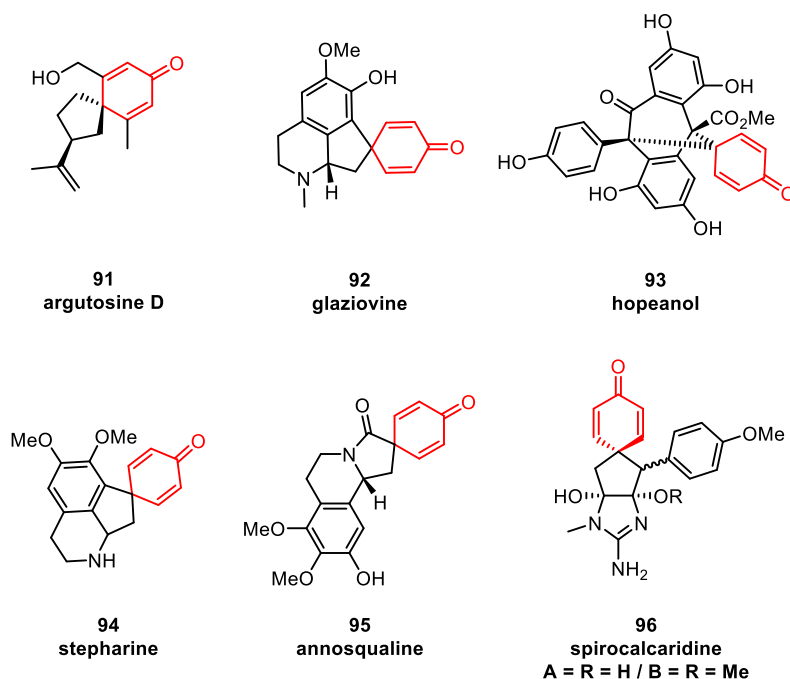
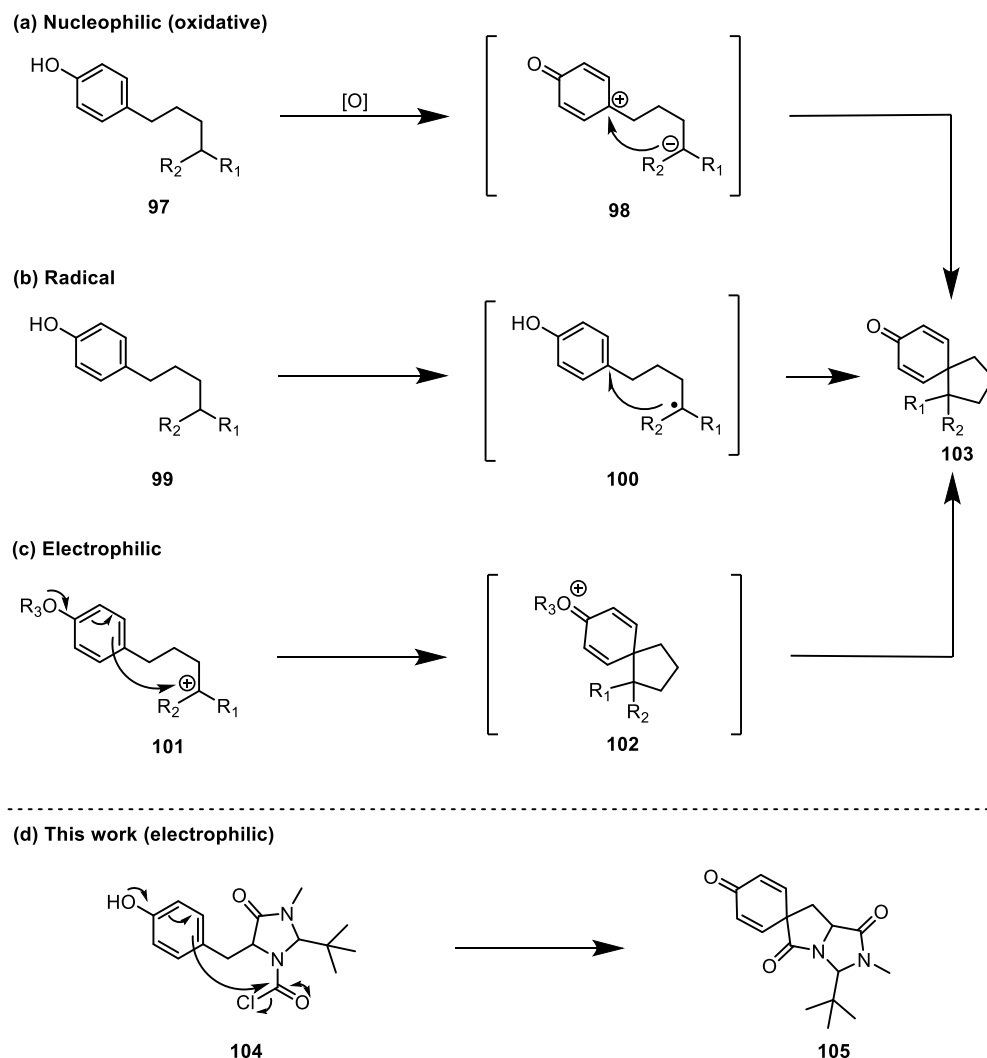


Figure 6 - Natural products containing the spirocyclic dienone motif.

The dearomatising spirocyclisation of phenols to yield spirocyclic dienones can be split into classifications depending on the mechanism involved. The most common method to produce spirocyclic dienones is using the nucleophilic method (Scheme 21a). In this method, two-electron

oxidation of the phenol occurs followed by intramolecular *ipso*-cyclisation with a carbon nucleophile. Other methods include radical (Scheme 21b) spirocyclisations, as well as electrophilic approaches (Scheme 21c) – which mirror the work carried out in this project (Scheme 21d).



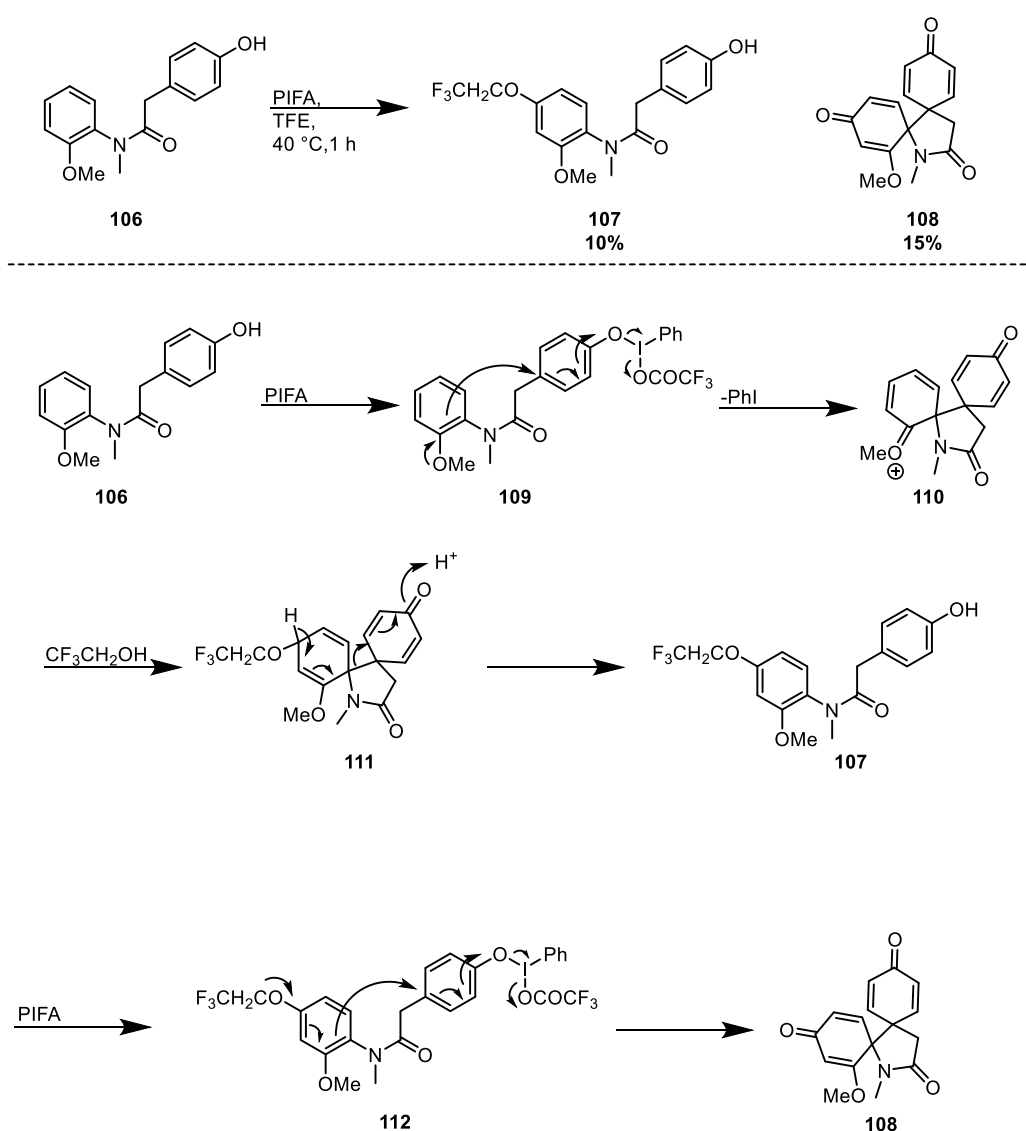
Scheme 21 - Various methods to prepare spirocyclic dienones.

Herein, we will discuss examples of these three methods to produce spirocyclic dienones, with a particular focus on the electrophilic approaches and tyrosine-based spirocyclisations which mirror our own work.

1.4.3 Nucleophilic (oxidative) dearomatising spirocyclisations

Oxidative nucleophilic approaches towards spirocyclic dienones are the most prevalent method seen in the literature. Numerous tethered nucleophiles have been utilised to achieve a variety of spirocyclic structures; herein are but a few of the many examples.

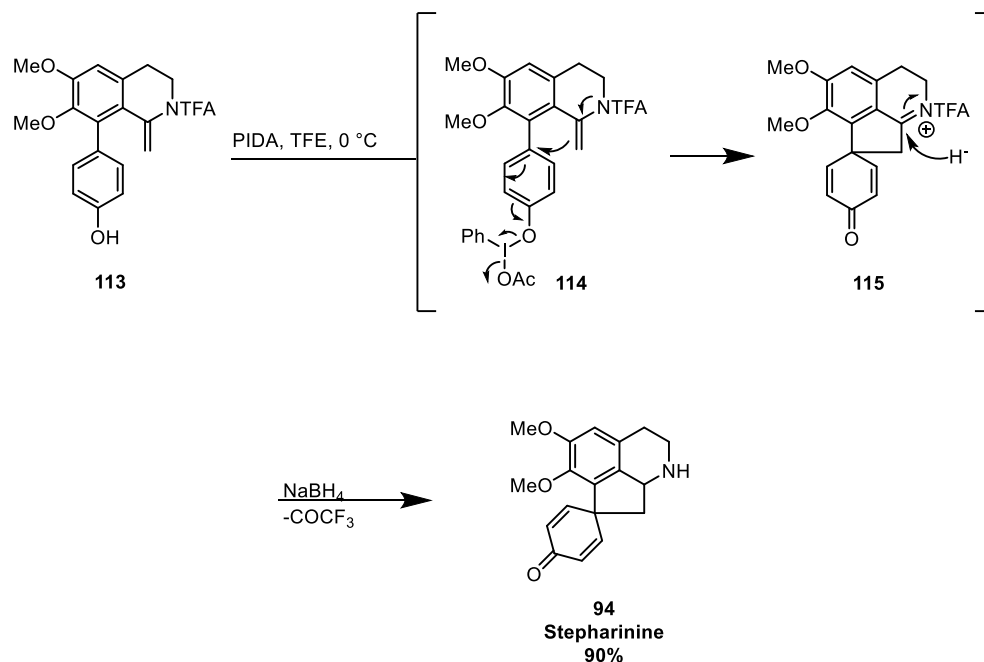
Guillou *et al.* employed a tethered aromatic ring in an oxidative spirocyclisation. The group discovered 1,2-dispirodienone **108** was produced in 15% yield from *p*-hydroxy acetanilide **106** using a hypervalent iodine-mediated oxidative spirocyclisation method. They proposed this product was produced via oxidation of the phenol **106** to give **107**, followed by loss of trifluoroethyl group. **107** was also isolated in 10% yield from the same reaction; to test this theory they subjected **107** to PIFA and obtained the spirocycle **108** exclusively in 75% yield. The group were able to produce a library of substituted 1,2-dispirodienones utilising this method and plan to further explore the method and the biological activities of these products (Scheme 22).⁶⁴



Scheme 22 - Proposed spirocyclisation mechanism of *p*-hydroxy acetanilides by Guillou *et al.*

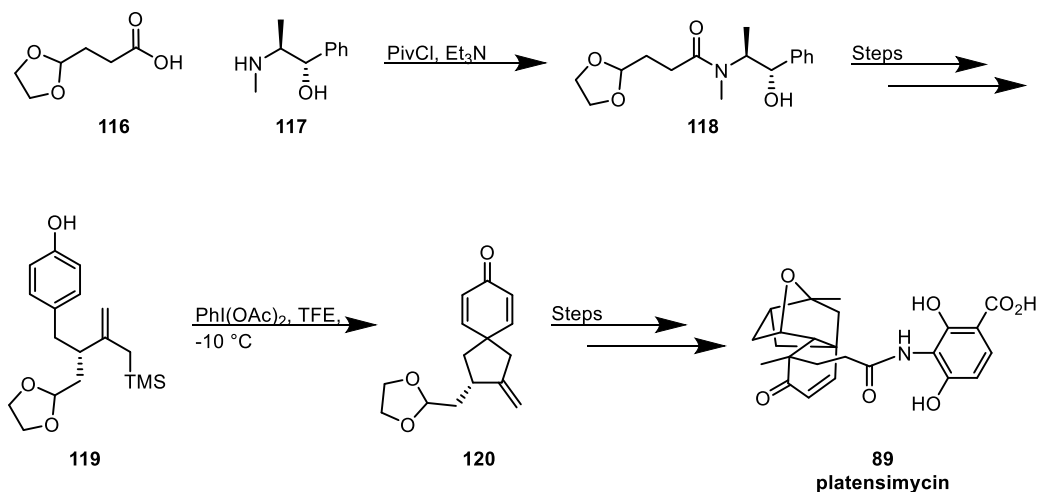
Shigehisa *et al.* exploited an enamide tether **113**, which could be prepared from the corresponding 3,4-dihydroisoquinoline by acylation, in their work towards a spirodienone moiety.⁶⁵ Using iodobenzene diacetate in trifluoroethanol at 0 °C, followed by reduction with NaBH₄, the oxidative spirocyclisation proceeded in high yield. This key spirocyclisation gave a short and

efficient route towards the proaporphine alkaloids Stepharinine (Scheme 23 - **94**) and Pronuciferine (NH→NMe).



Scheme 23 - Proposed mechanism of a tethered enamide spirocyclisation by Shigehisa *et al.*

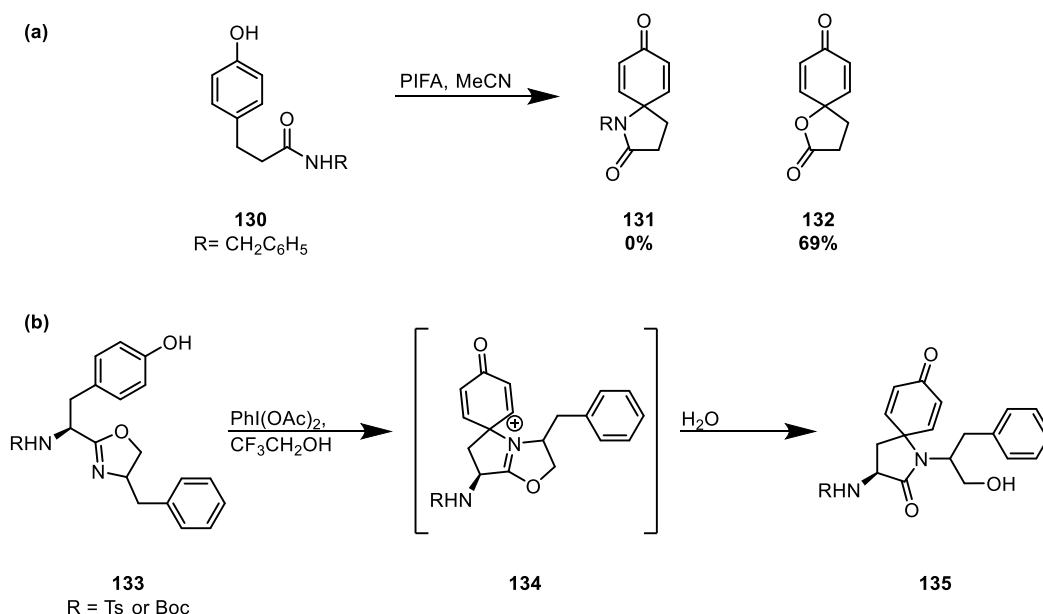
An oxidative spirocyclisation was exploited by Nicolaou *et al.* in their synthesis of platensimycin **89**. The reaction used PIDA as an oxidising agent in trifluoroethanol at -10 °C and afforded **120** with a 68% yield (Scheme 24).^{66,67}



Scheme 24 - Spirocyclisation used in Nicolaou *et al.* synthesis of platensimycin.

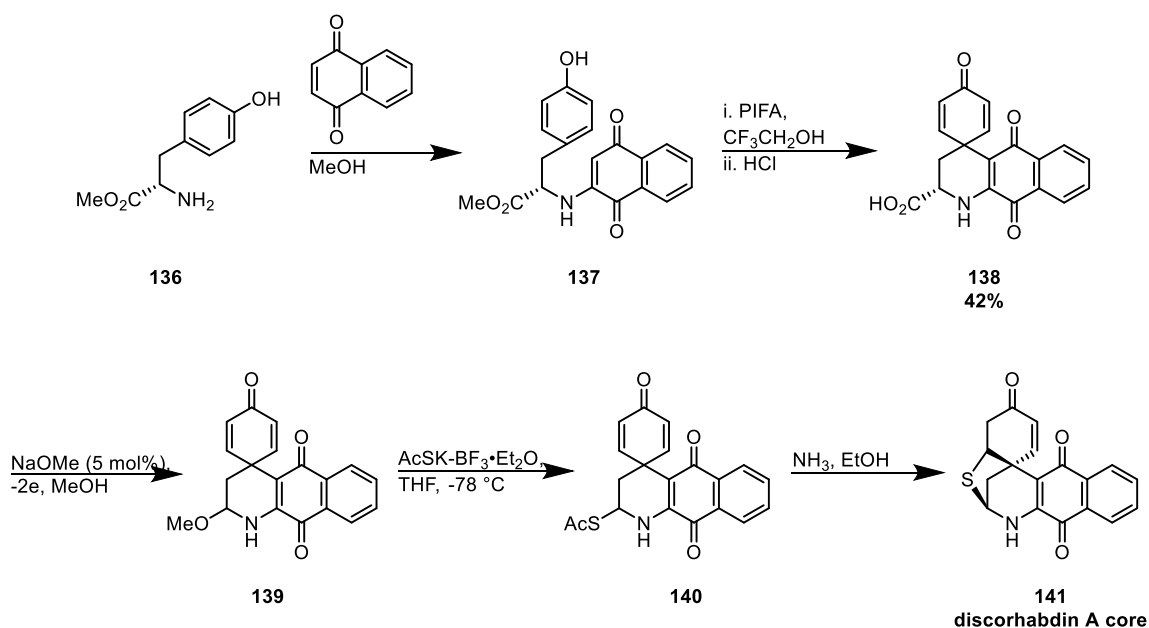
This method was later applied to alternative longer **121**, branched **123** and linear chains **125**; highlighting further possible applications of this spirocyclisation method (Scheme 25).⁶⁷

Spirolactams have been produced from tyrosine amides via oxidation using PIFA.⁶⁹ Previous work had found the tendency for the oxygen atom of an amide to react with the electrophilic phenol ring, via an iminoether, which gives rise to spirolactones rather than the desired spirolactams (Scheme 27a).⁷⁰ To overcome this, Peters *et al.* developed the 2-oxazolines **133** which favour attack from the nitrogen and give rise to spirolactones **135** (Scheme 27b).⁶⁹



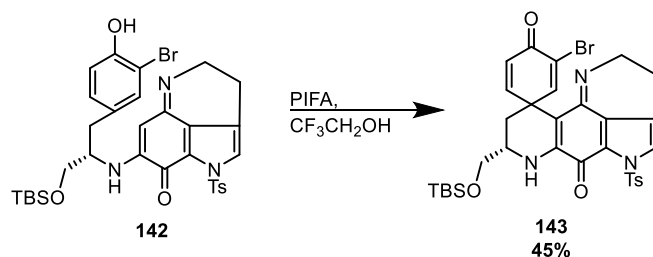
Scheme 27 – (a) Spirolactones from tyrosine amides and (b) Spirolactams from tyrosine oxazolines.

These types of spirocyclisations have also been utilised in the synthesis of natural product discorhabdin A starting from the tyrosine methyl ester. Initial attempts at the total synthesis looked at carrying out a synthetic study to produce the core of discorhabdin A (Scheme 28).^{71,72}



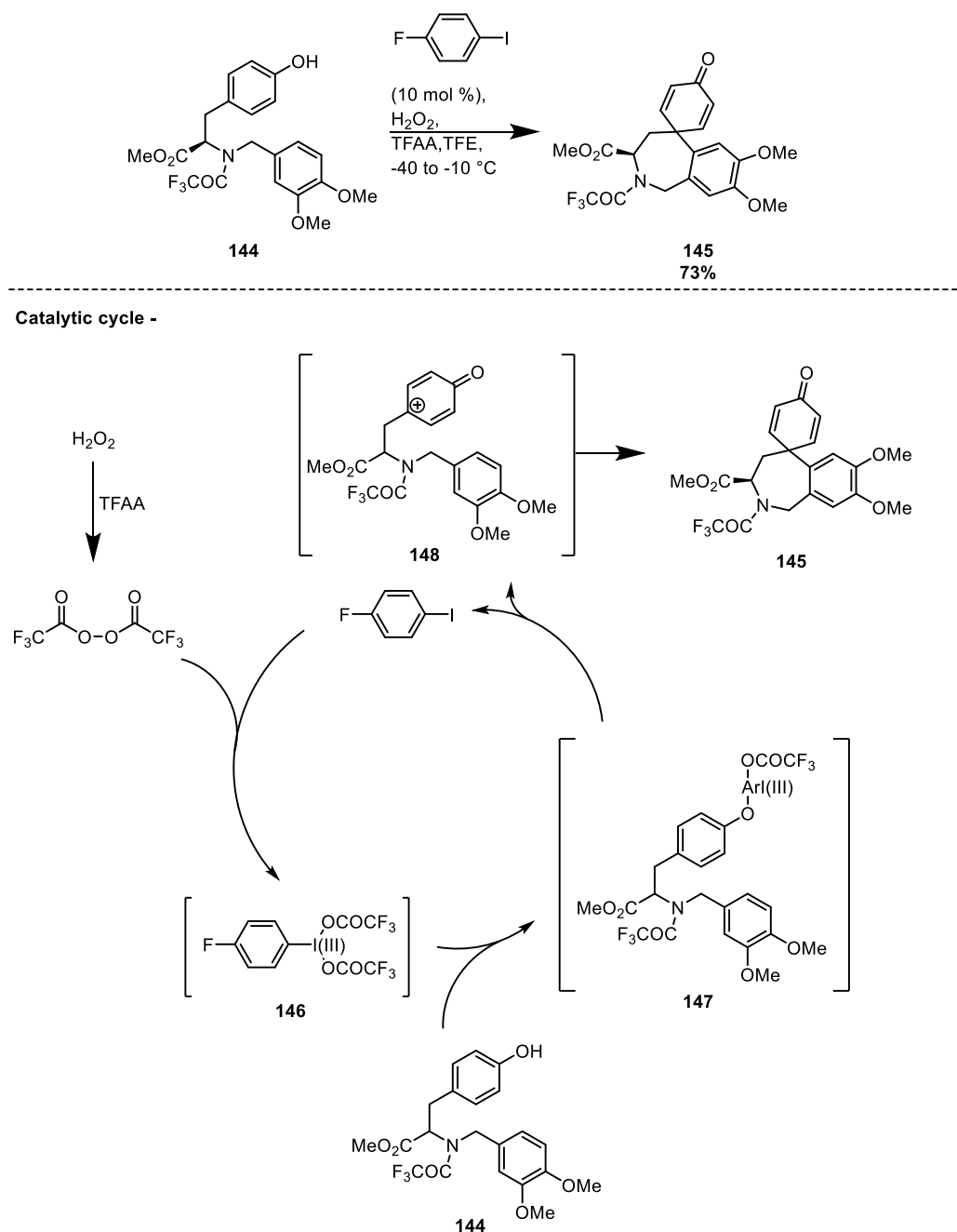
Scheme 28 – Tyrosine based spirocyclisation in synthetic studies towards a Discorhabdin A core.

This model study was then applied to the total synthesis in which spirocyclisation of the more complex **142** was carried out giving **143** as a mixture of two diastereomers in a 1.5:1 ratio (Scheme 29).



Scheme 29- Tyrosine based spirocyclisation seen in the synthesis towards Discorhabdin A.

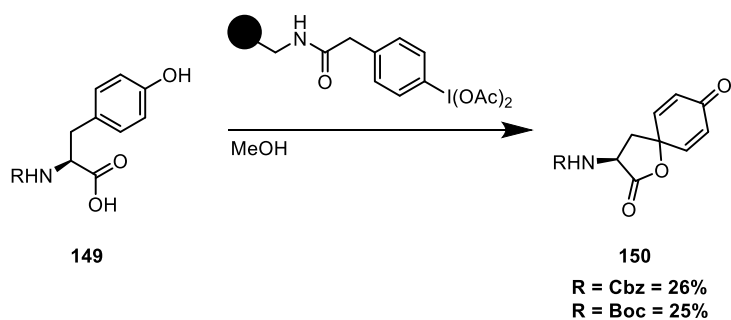
A catalytic, hypervalent iodine-mediated spirocyclisation has also been achieved with H_2O_2 as the terminal oxidant, in which a variety of phenols undergo dearomatisation to form a new C-C bond including a tyrosine-based derivative (Scheme 30).⁷³



Scheme 30 – Catalytic oxidative spirocyclisation of a tyrosine-based compound **144.**

In the reaction mechanism, bis(trifluoroacetyl) peroxide – generated in situ from TFAA and peroxide – oxidises the iodoarene giving the active catalyst species **146**. This reactant can then carry out oxidation of the phenolic oxygen of **144**, which in turn allows spirocyclisation to take place with concomitant regeneration of the iodoarene. The method has been applied to a variety of other phenolic substrates with yields between 51-80% (Scheme 30).⁷³

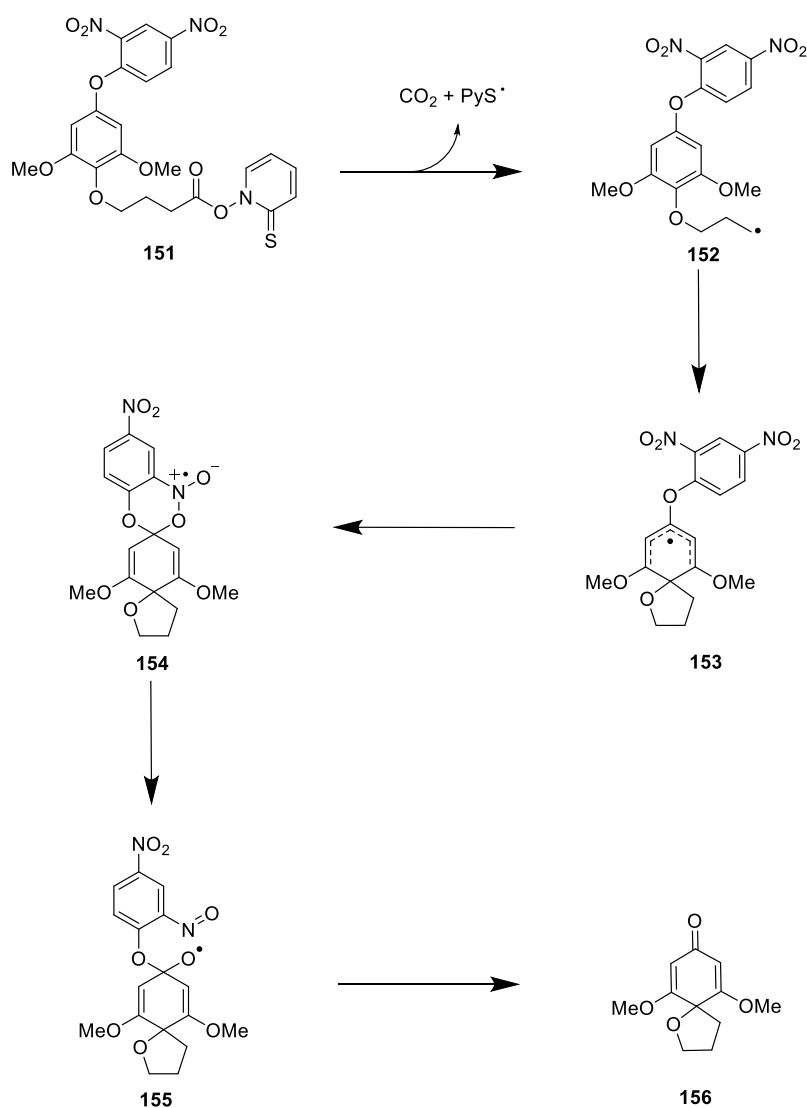
A spirocyclisation of N-protected tyrosine has been achieved using a polymer-supported hypervalent iodine oxidant (Scheme 31).⁷⁴ These types of spirocyclisations have also previously been achieved with non-resin hypervalent iodine in the synthesis of antitumor antibiotic Aranorosin in yields of 35-60%.^{75,76}



Scheme 31 – Spirocyclisation of N-protected tyrosines.

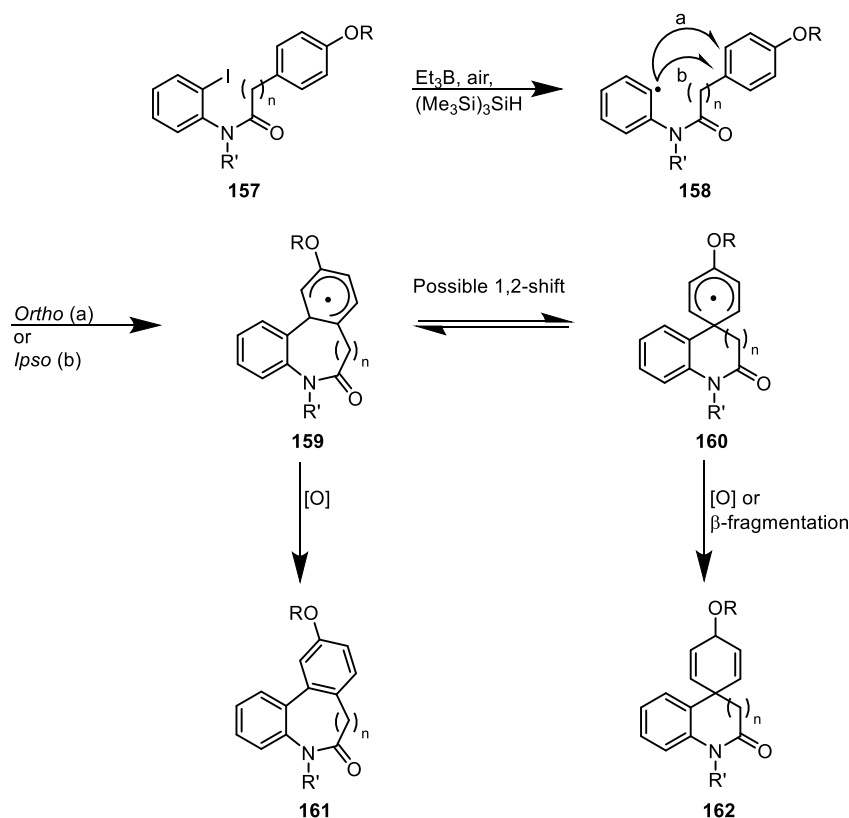
1.4.5 Radical dearomatising spirocyclisations

Radical dearomatisations are a subsection of nucleophilic spirocyclisations and are less prominent in the literature. However, a number of notable examples have been reported by several groups.



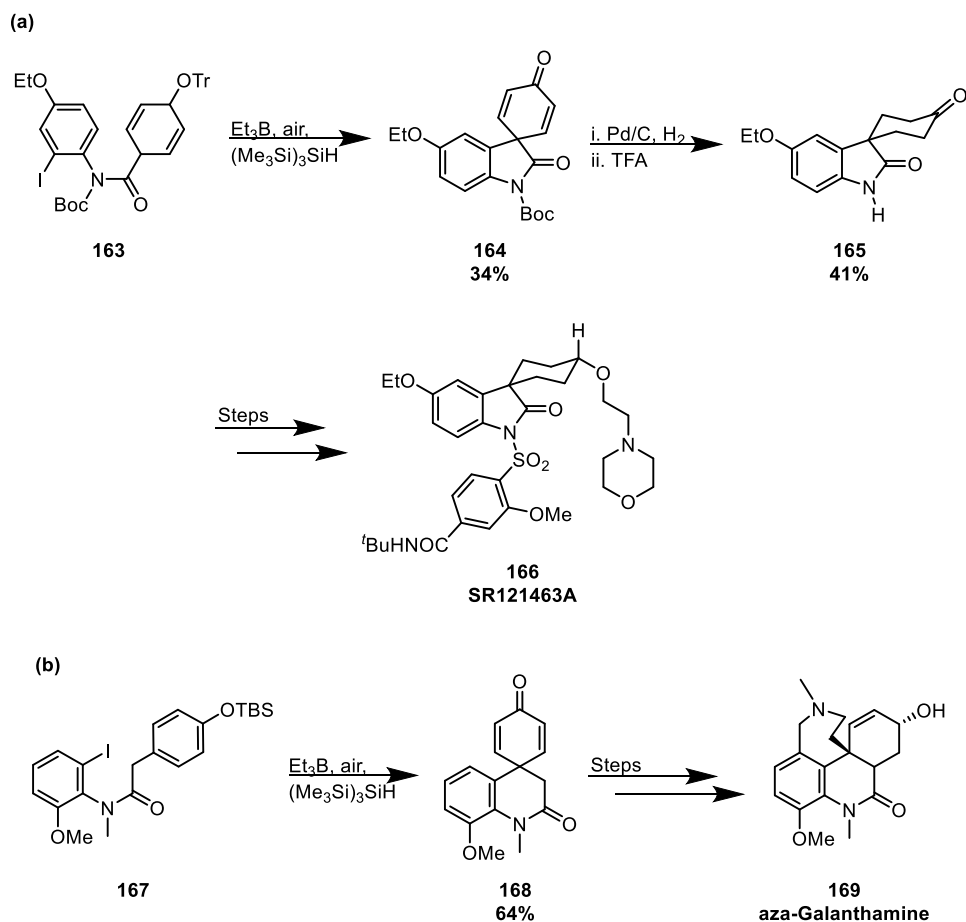
Scheme 32 - Proposed mechanism of thiohydroxamate ester spirocyclisation by Whiting *et al.*

Whiting *et al.* described a spirocyclisation of thiohydroxamate ester, **151**, when heated under reflux and irradiated with a tungsten lamp. They demonstrated a radical *ipso*-addition of a carbon radical to an aromatic unit to produce a *para*-spirodienone (Scheme 32).^{77,78} The group utilised ¹⁸O isotopic labelling of the biaryl ether to explore the mechanism. They proposed a mechanism in which an N-O homolysis occurs followed by decarboxylation to give **152** which can then undergo a cyclisation to **153**. A 6-*endo-trig* trapping of the carbon radical by oxygen of the *ortho*-nitro group occurs, followed by N-O α -scission and finally fragmentation of the intermediate oxygen radical to produce the spirodienone **156** in a 49% yield, with loss of the isotopic label.



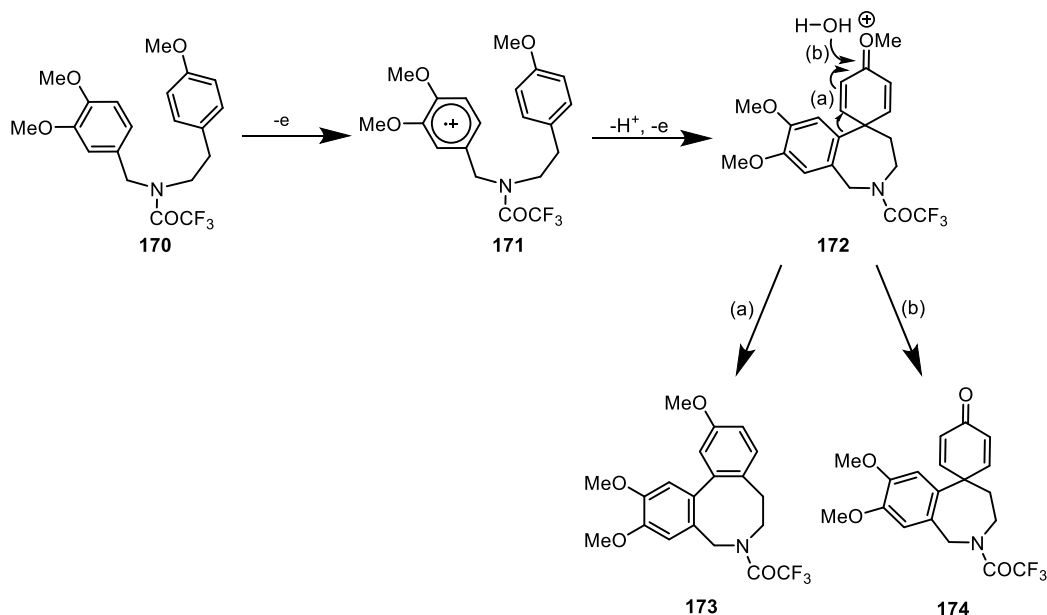
Scheme 33 - Proposed mechanism to spirocyclohexadienones Curran *et al.*

Curran *et al.* described a radical spirocyclisation procedure for spirooxindoles and spirodihydroquinolones.⁷⁹ They proposed the aryl radical **158** could cyclise in an *ortho* (a) or *ipso* (b) fashion to give **159** or **160** which can interconvert by a 1,2 shift. Oxidation or β -fragmentation of these products produced **161** or the spirodienone **162** (Scheme 33). They then utilised this technique in the formal synthesis of SR121463A, **166**, a selective vasopressin inhibitor, and *aza*-Galanthamine **169** (Scheme 34). These examples demonstrate the effectiveness of their method in producing complex molecules with biological activity.⁷⁹



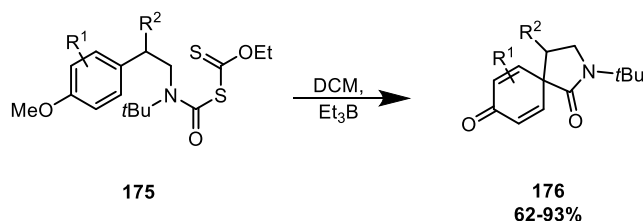
Scheme 34 - Curran *et al.* formal synthesis of (a) SR121463A via a spirooxindole and (b) aza-galanthamine.

A radical oxidative spirocyclisation reaction was reported by Kita *et al.* whilst studying aryl-aryl coupling using phenyliodine bis(trifluoroacetate) and a heteropoly acid, $\text{H}_3[\text{PW}_{12}\text{O}_{40}]$, as an alternative to heavy metal oxidising reagents. The use of phenol ether derivatives **170**, particularly *para*-methoxy, allowed for preferential formation of spirodienones **174** over biaryls **173** in the presence of a water source (Scheme 35).⁸⁰ They propose that the simplicity of the method, along with its lack of heavy metal reagent requirement and ease of handling of phenol ethers over phenols, could lead to a wide variety of applications in biaryl and spirodienone syntheses.⁸⁰



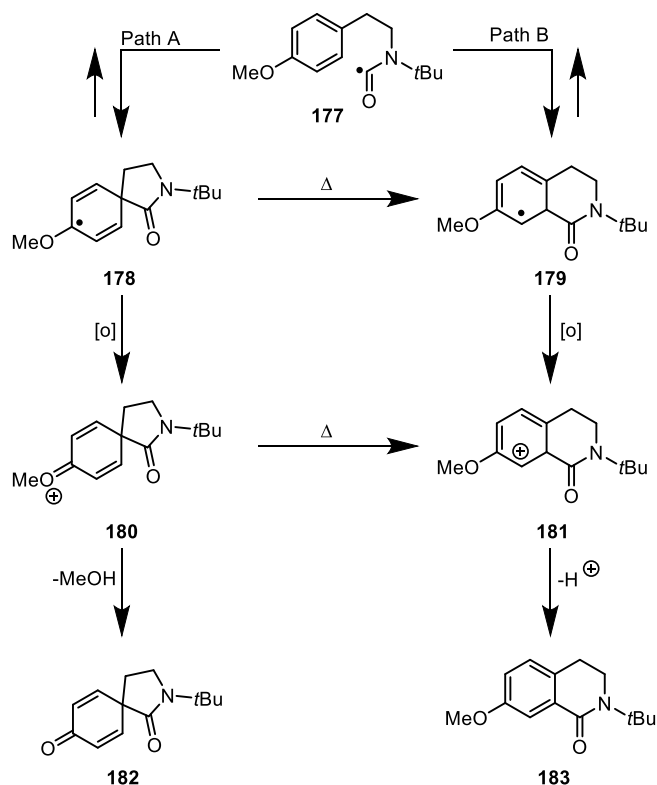
Scheme 35 - Proposed mechanism to biaryls and spirodienones by Kita *et al.*

A carbamoyl radical tether has been applied to a range of substituted phenol derivatives in a dearomatising spirocyclisation by Miranda *et al.* to produce spirodienonamides **176** (Scheme 36). By utilising carbamoylxanthates **175**, carbamoyl radicals capable of undergoing radical spirocyclisation were generated.⁸¹



Scheme 36 - Spirocyclisation with carbamoyl chlorides reported by Miranda *et al.*

In their initial study, which employed dilauroyl peroxide in dichloroethane under microwave irradiation, they observed an undesirable thermal decomposition to give *N*-*t*-butyl-dihydroisoquinolones **183** (Scheme 37 - path B). However, when the reaction was conducted at room temperature, with triethylborane as the radical initiator, the spirocycle **182** was afforded as the major product (Scheme 37 - path A). The group carried out computational modelling to explore these cyclisation pathways, finding the spirocyclisation transition state (Scheme 37 - path A) is 4.64 kcal mol⁻¹ lower compared to the direct *ortho* cyclisation (Scheme 37 - path B). This method was then successfully applied to several other examples, including a naphthalene derivative and even substrates with electron-withdrawing bromo substituents at both *ortho* and *meta* positions of the arene, thus showcasing a wide scope for this reaction.

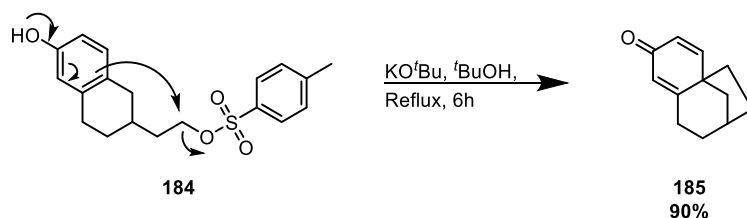


Scheme 37 - Proposed mechanism to give spirocycles and N-t-butyl-dihydroisoquinolones Miranda *et al.*

1.4.6 Electrophilic dearomatising spirocyclisations

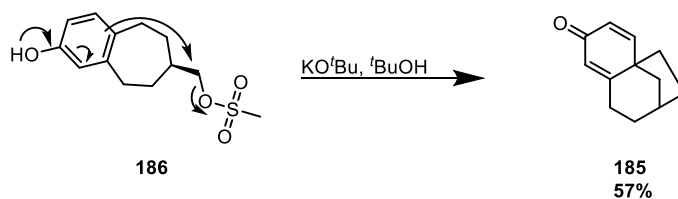
There are numerous examples of electrophilic dearomatising spirocyclisations in the literature. These reactions employ a variety of leaving groups including sulfonates and halides as well as electrophilic tethers such as alkenes/alkynes, allenes, epoxides and nitriles.

An early example of an electrophilic spirocyclisation by Masamune utilised a tethered sulfonate leaving group **184** to produce a spirodienone **185** in a 90% yield (Scheme 38).⁸²



Scheme 38 - Masamune spirocyclisation using a tosyl tether.

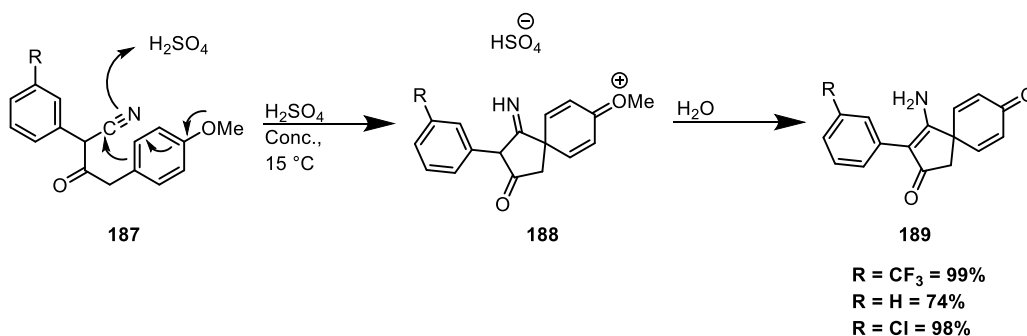
To explore whether this spirocyclisation could occur with a less conformationally flexible starting material, Swanson *et al.* performed a similar reaction with the tetrahydrobenzocycloheptene substrate **186**, generating the corresponding product **185** in the process (Scheme 39).⁸³



Scheme 39 - Spirocyclisation using a tosyl leaving group reported by Swanson *et al.*

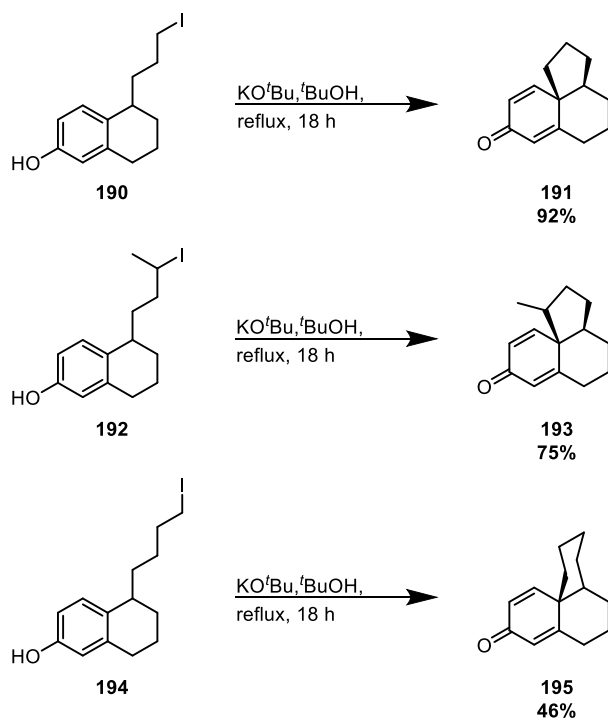
Although in a much lower yield of 57%, the reaction did still proceed, demonstrating the versatility of this spirocyclisation.⁸³ In addition to these examples, the use of a tethered sulfonate for a spirocyclisation has also been exploited in a concise total synthesis of platensimycin by Njardarson *et al* in 2009.⁵⁶

Gajewski reported a spirocyclisation reaction to **189** involving the electrophilic attack of a nitrilium ion (Scheme 40).⁸⁴ Upon heating **189** in DMSO, these products could then undergo a rearrangement to rearomatise and give γ -(4-hydroxyphenyl)- α -phenylacetonitrile, thus showing the mild instability of these spirocycles.



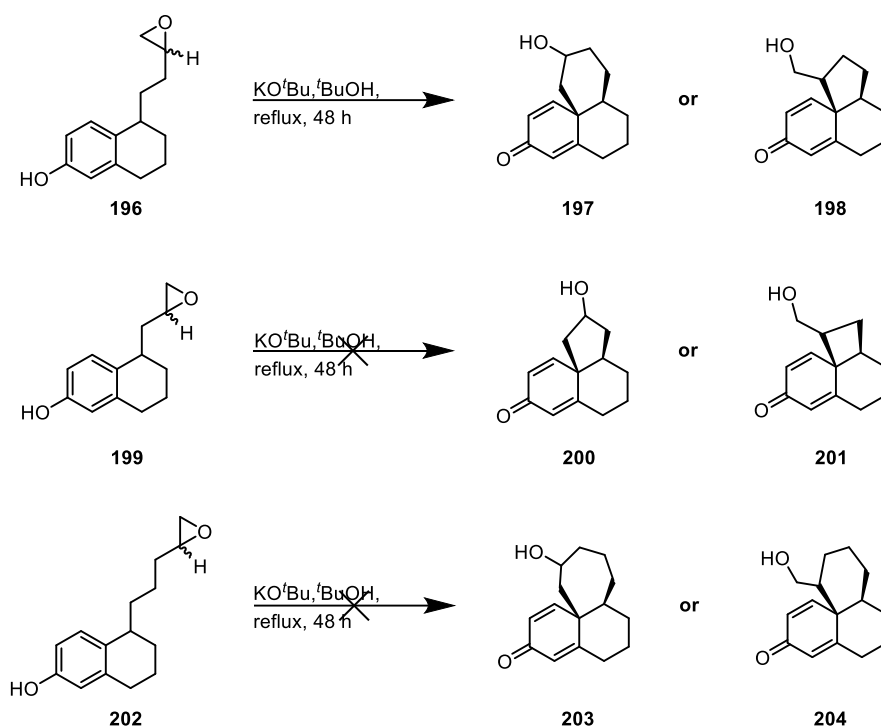
Scheme 40 - Gajewski spirocyclisation using a nitrile tether.

Halogens have also been exploited as a leaving group in dearomatising electrophilic spirocyclisations. An excellent example of this was demonstrated in a paper by Whiting *et al.* describing a variety of spirocyclisations using an iodine tether. This allowed for the production of tricyclospirodienones, which are valuable synthetic precursors to steroid mimics, following further manipulations (Scheme 41).^{85,86}



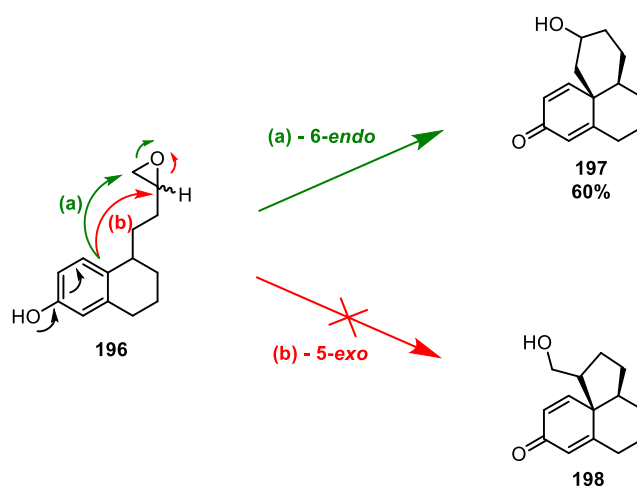
Scheme 41 - Spirocyclisations using an iodide leaving group reported by Whiting *et al.*

As seen with other electrophilic spirocyclisations, the use of potassium *t*-butoxide in refluxing *t*-butyl alcohol gave the desired spirocyclisation products in moderate to excellent yields. Whiting *et al.* expanded this protocol to spirocyclisations with epoxides tethers (Scheme 42).⁸⁵



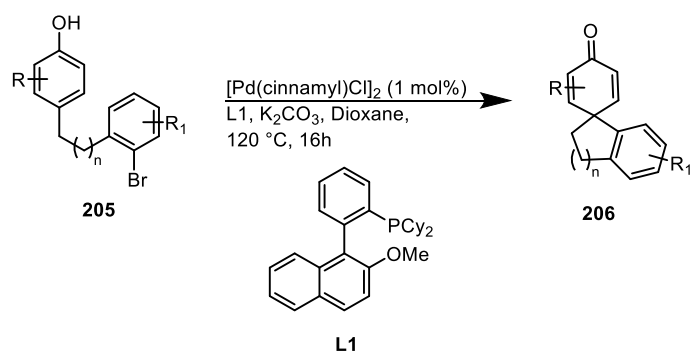
Scheme 42 - Spirocyclisations with a tethered epoxide reported by Whiting *et al.*

Applying the same conditions used for the iodide tether, only the C₂ chain epoxide **196** was successful in undergoing cyclisation. The **199** and **202** epoxides failed to react in either an 7- or 5-*endo* fashion at the primary carbon, or a 4- or 6-*exo* cyclisation at the secondary carbon. The phenolic epoxide **196**, with a two carbon tether, afforded the 6-*endo* stereoisomer **197** only (60% - Scheme 43 - green) with no evidence of a competing 5-*exo* cyclisation to **198** (Scheme 43 - red) – indicating that the cyclisations of epoxides are more constrained.^{85,86}



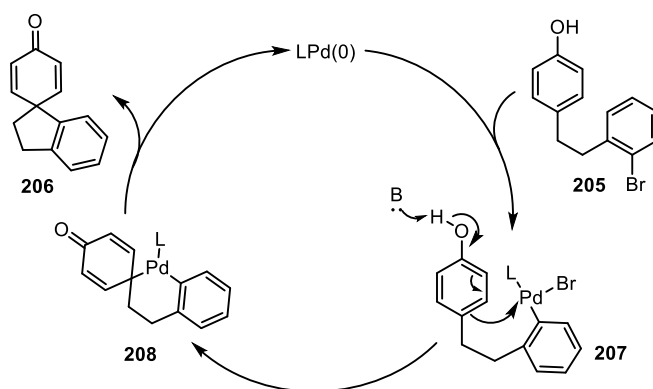
Scheme 43 - Whiting *et al.* possible regioisomers and their mechanisms.

A palladium(0)-catalysed spirocyclisation reaction was developed by Buchwald *et al.* which utilised ‘activated’ electrophilic aryl halides (Scheme 44).⁸⁷



Scheme 44 - Spirocyclisation utilising an activate aryl halide tether reported by Buchwald *et al.*

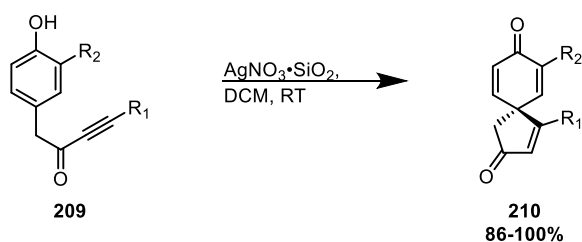
They proposed a catalytic cycle beginning with oxidative addition into the carbon-bromine bond, followed by the electrophilic attack and finally reductive elimination (Scheme 45).



Scheme 45 - Buchwald *et al.* proposed spirocyclisation mechanism.

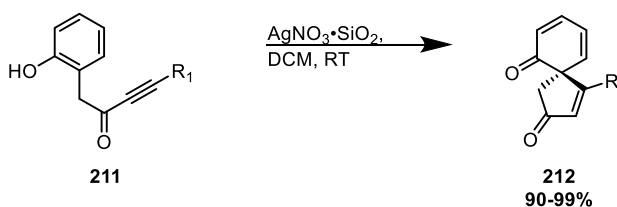
The scope of the reaction was explored with 14 aryl halides which cyclised in yields ranging between 44-91%. They investigated various ring substitutions, naphthalene derivatives and a longer tether chain length ($n = 2$). Electron donating groups were well tolerated on both rings. However, electron withdrawing substituents proved more challenging. When electron withdrawing groups were incorporated into the aryl halide, the reaction required either reduced concentrations or increased catalyst loading to proceed. Electron withdrawing substituents on the phenol ring reduced the electron density of the arene leading to complete shutdown of the spirocyclisation reaction.

Activated alkynes have been reported in the literature to undergo spirocyclisation reactions when tethered to a phenol group.⁸⁸⁻⁹¹ For example, Unsworth *et al.* reported an efficient synthesis of spirodienones utilising an ynone tether **209** (Scheme 46).⁹²



Scheme 46 - Spirocyclisation with a tethered activated alkyne reported by Unsworth *et al.*

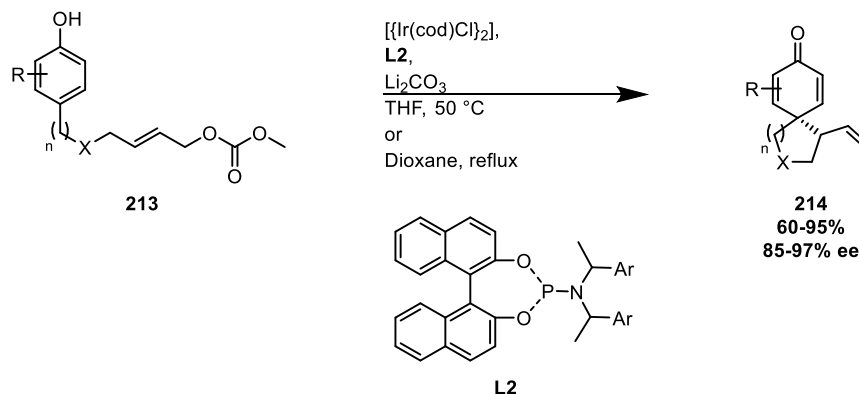
Using these conditions, they produced eight spirodienone products **210** in high yields. Examples included a simple butyl chain, phenyl, 4-methoxyphenyl, protected amines and alcohols, along with cyclopropane and cyclopentane in the R_1 position and a methoxy substituent in the R_2 position. Most interestingly, the authors reported that *ortho*-spirocyclisations, to give **212**, were viable using this method in yields between 90-99% (Scheme 47).⁹²



Scheme 47 - Unsworth *et al.* *ortho*-spirocyclisation.

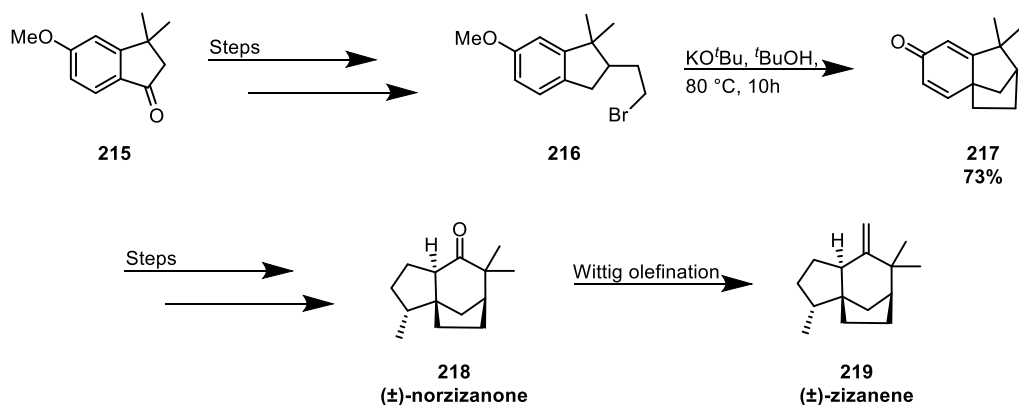
They also demonstrated the versatility of the *ortho* spirocyclisation reaction conditions with 4 examples, R_1 = Cyclopropane, phenyl, 4-methoxy phenyl and 4-fluorophenyl (Scheme 47).

Alkenes are another well utilised tether for electrophilic spirocyclisations of phenols.^{93,94} You *et al.* reported an iridium catalysed asymmetric spirocyclisation using an allylic carbonate tether **213** (Scheme 48).⁹⁵ They produced 11 examples with moderate to excellent yields and reasonable enantioselectivity. Examples included a variety of substitutions on both the phenol ring and chain, chain lengths ($n = 1$ and 2) and both carbon and nitrogen linkers (X).



Scheme 48 - Spirocyclisation using an allylic carbonate reported by You *et al.*

Mukherjee *et al.* utilised electrophilic spirocyclisations of phenols in total syntheses of the sesquiterpenes (\pm)-norzizanone and (\pm)-zizanene, demonstrating the usefulness of this reaction in the synthesis of complex natural products.^{96,97} In both syntheses, a halogen tethered spirocyclisation is exploited with a final functional group interconversion step allowing the synthesis of (\pm)-zizanene from (\pm)-norzizanone (Scheme 49).

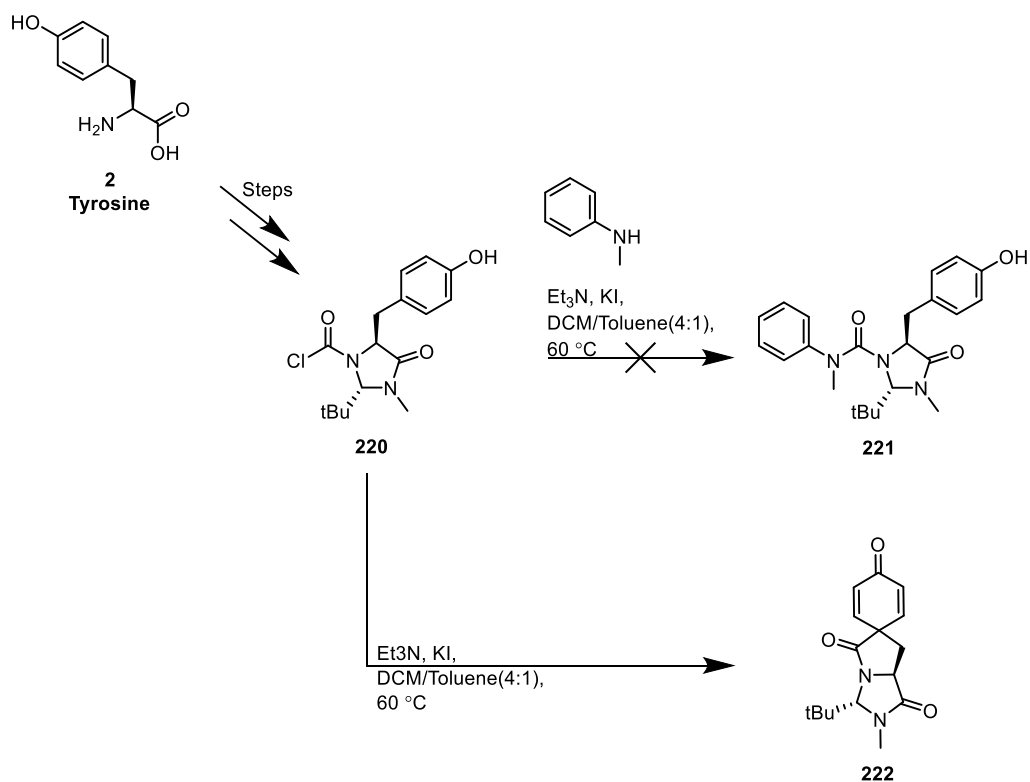


Scheme 49 - Use of a phenol ether spirocyclisation in natural product synthesis by Mukherjee *et al.*

Other electrophilic spirocyclisation examples include nucleophile tethers, propargyl bromides/carbonates,⁹⁸ activated allenes,⁹⁹ along with other reports of sulfonates,¹⁰⁰ activated alkynes,^{101,102} activated alkenes^{103,104} and allylic carbonates¹⁰⁵. To the best of our knowledge, no electrophilic spirocyclisations that yield dienones have utilised a carbamoyl chloride tether.

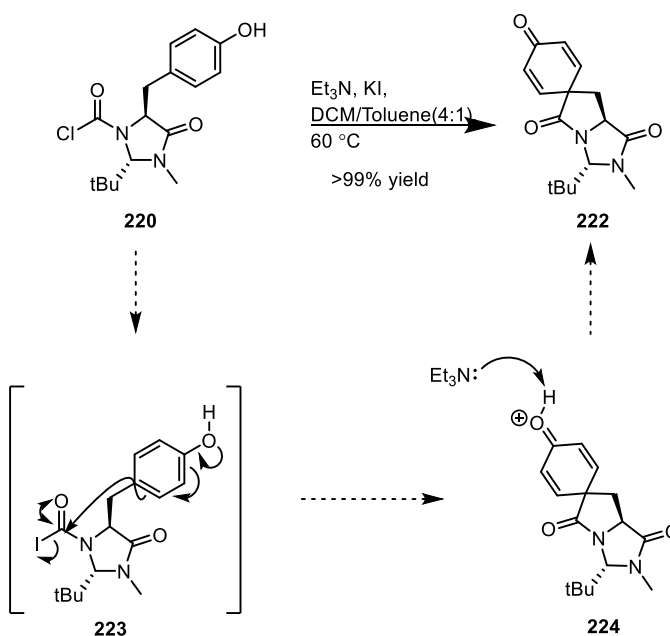
1.5 Previous work

Previous work in the group focused on producing imidazolidinone-derived carbamoyl chlorides to couple with nucleophiles to be utilised in synthesis of amino acids.¹⁰⁶ Attempted coupling of the tyrosine derived carbamoyl chloride **220** with *N*-methylaniline to produce the corresponding urea **220** led to the discovery of an alternative spirocyclisation reaction to the dienone **222** (Scheme 50).



Scheme 50 - Alternative spirocyclisation reaction discovery

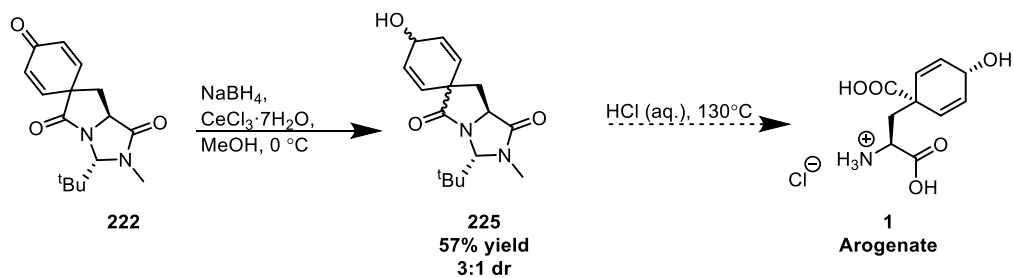
It was proposed that the reaction proceeded via a more reactive, transient carbamoyl iodide generated in situ from potassium iodide (Scheme 51).



Scheme 51 - Proposed mechanism of the alternative spirocyclisation reaction.

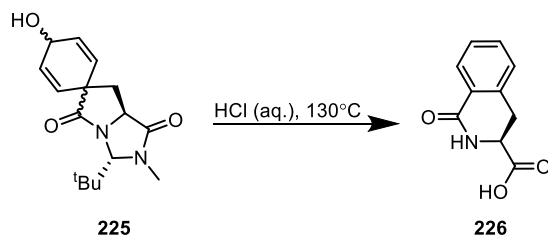
The group postulated that this spirocyclic intermediate **222** could function as a precursor to the natural product arogenate **1** through diastereoselective reduction of the dienone, followed by

hydrolysis (Scheme 52). The diastereoselective reduction of **222** proceeded in moderate yield to **225** and reasonable diastereoselectivity in favour of the desired stereoisomer.



Scheme 52 - Proposed route to arogenate.

However, the hydrolysis of the reduced imidazolidinone did not proceed as expected, instead resulting in undesired products, one of which was identified as the dihydroisoquinolinone **226** (Scheme 53).

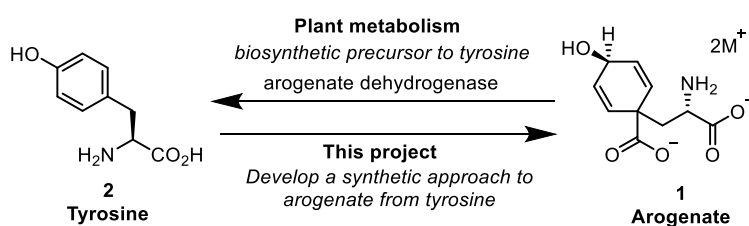


Scheme 53 - Hydrolysis undesired product.

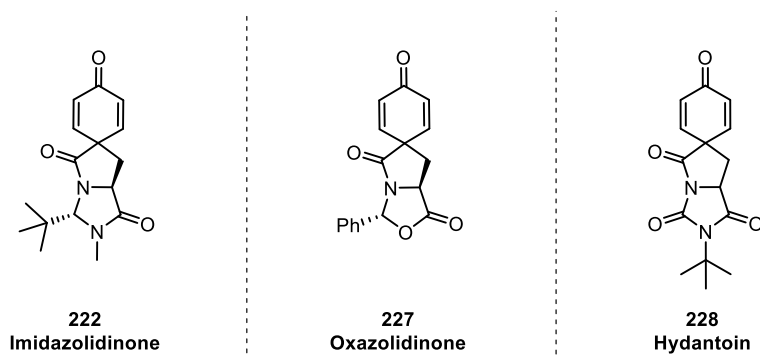
2. Results and discussion

2.1 Aims of the project

This project aimed to exploit a somewhat unconventional and previously unexplored starting material in the synthesis of arogenate, its own biosynthetic end product L-tyrosine, to give a process which is effectively the inverse of plant metabolism. We hoped that this ‘reverse-biomimetic’ approach starting from an inexpensive, chiral amino acid would provide an efficient route to arogenate that would also provide an opportunity to generate analogues (Scheme 54).

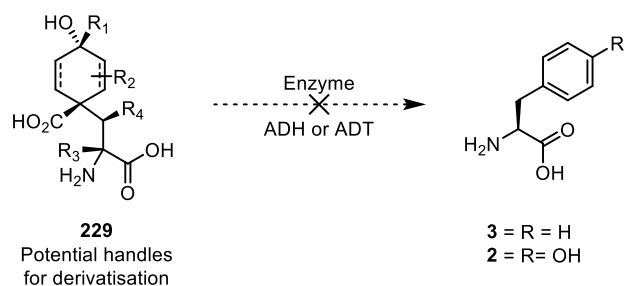


The project set out to investigate three interlinked routes, the original imidazolidinone route, an oxazolidinone route and a hydantoin route, and their feasibility to produce arogenate (Figure 7).



Since the imidazolidinone hydrolysis proved problematic, analogous oxazolidinone route was exploited as a means of overcoming this issue. It had been reported in the literature that the hydrolysis of oxazolidinones requires much milder conditions than their imidazolidinone counterparts.¹⁰⁷ The use of an analogous hydantoin moiety was also investigated as the group has previously demonstrated their ease of synthesis and use in producing amino acids upon hydrolysis.¹⁰⁸

The second part of the project focused upon producing a variety of arogenate analogues as potential competitive inhibitors of ADH or ADT thereby interrupting aromatic amino acid biosynthesis (Scheme 55).



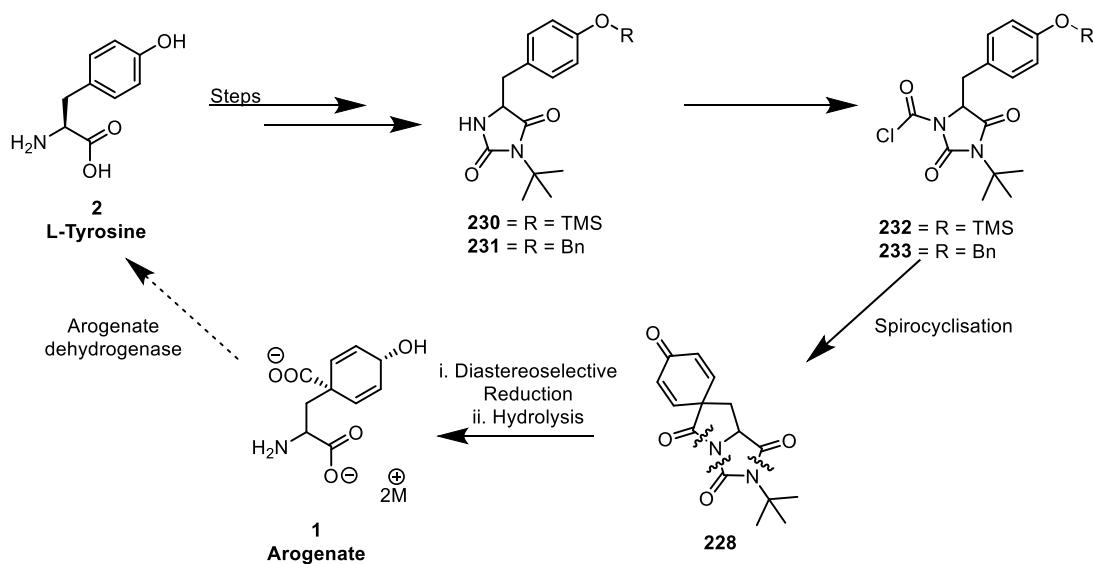
Scheme 55 - Enzyme inhibition by arogenate derivatives.

In particular, we intended to generate analogues which either remove or reduce the possibility of rearomatisation, as these would represent ideal candidates for agrochemical enzyme inhibition studies.^{4,10}

2.2 Unsuccessful routes

2.2.1 Hydantoin route

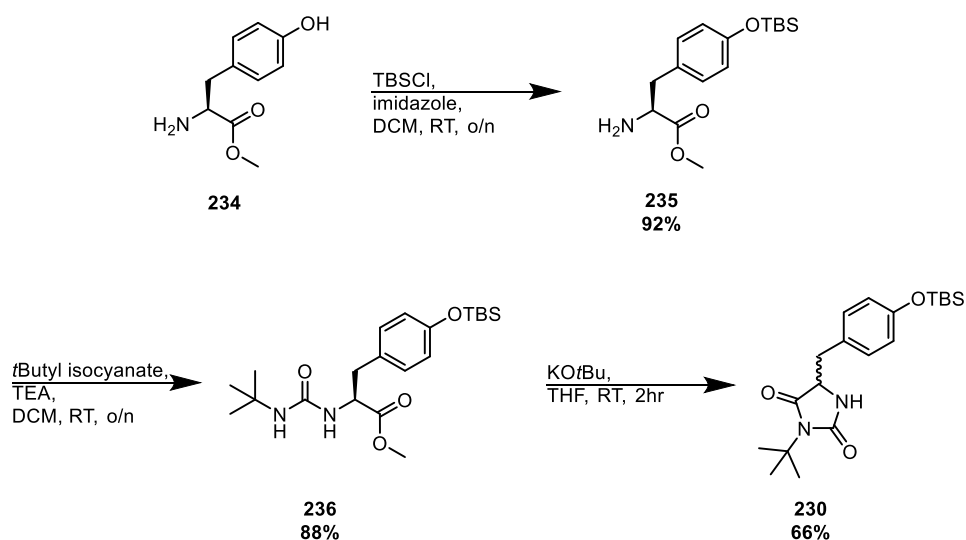
The hydantoins, **230** & **231**, were synthesised from the methyl ester of tyrosine using a route which has been previously optimised within the group. From this species, phosgenation was performed to install the carbamoyl chloride unit, giving the potential precursor to the spirocycle **228** (Scheme 56).



Scheme 56 - Hydantoin route - synthetic concept.

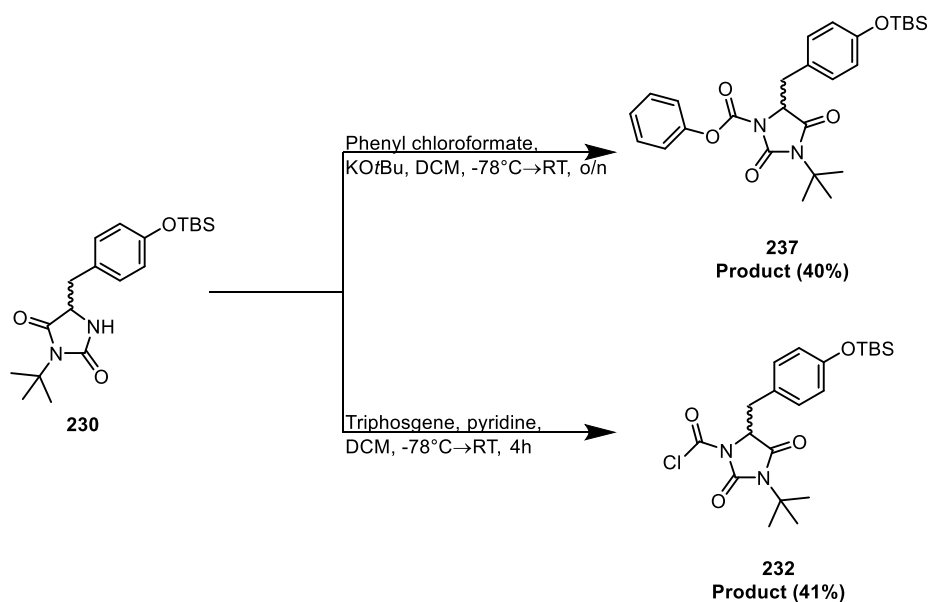
2.2.1.1 Silyl route

The first route explored the use of a silyl protecting group on the alcohol which was easily installed by reaction of L-tyrosine methyl ester **234** with TBSCl and imidazole to produce **235** in excellent yield. The heterocyclic core was then generated by firstly forming the urea **236** in a good yield using *t*-butyl isocyanate, followed by cyclisation using potassium *t*-butoxide to give the hydantoin **230** in a moderate yield (Scheme 57).



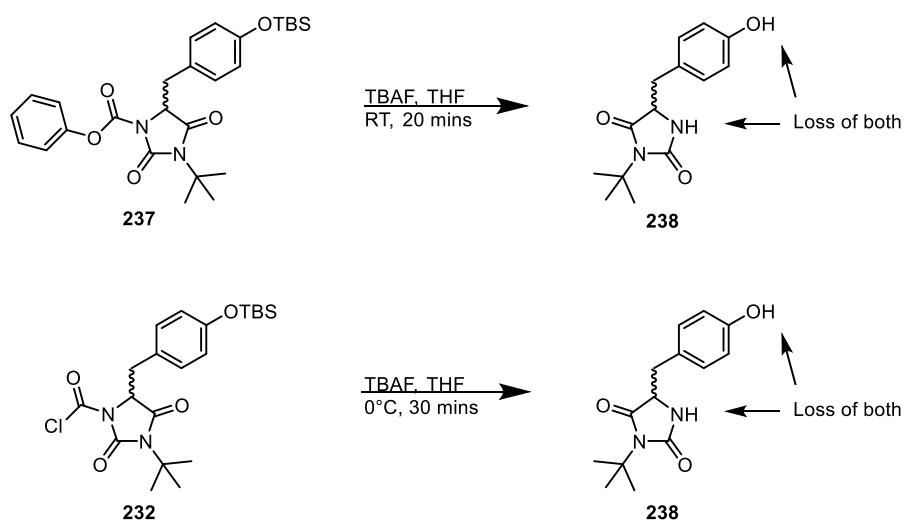
Scheme 57 - Synthesis of hydantoin, 230, from amino acid ester, 234.

Acylation was performed with either triphosgene or phenyl chloroformate in modest yields of 40 and 41% respectively (Scheme 58).



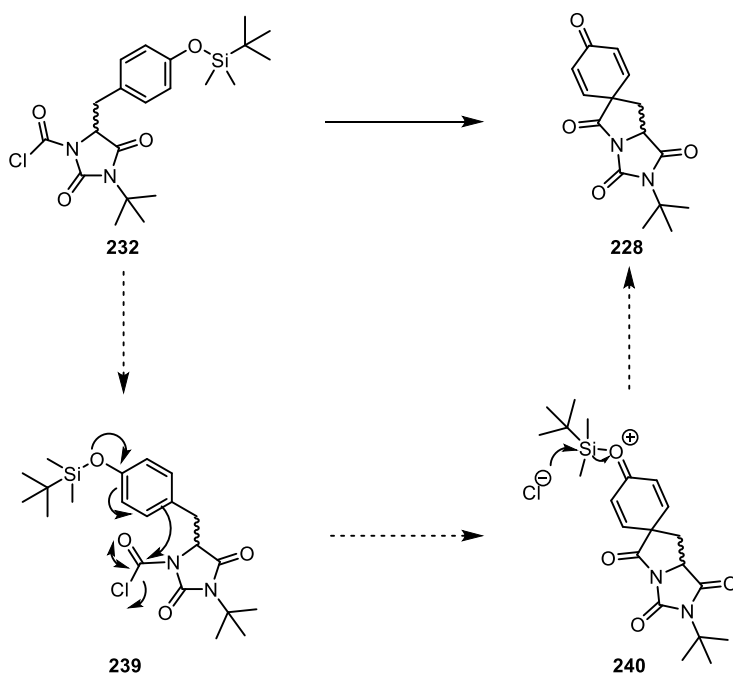
Scheme 58 - Acylation of hydantoin, 230.

Unfortunately, desilylation of the phenol caused unforeseen issues. In both cases, the carbamate and carbamoyl chloride functionalities were removed as well as the silyl group, giving undesired hydantoins **238** (Scheme 59).



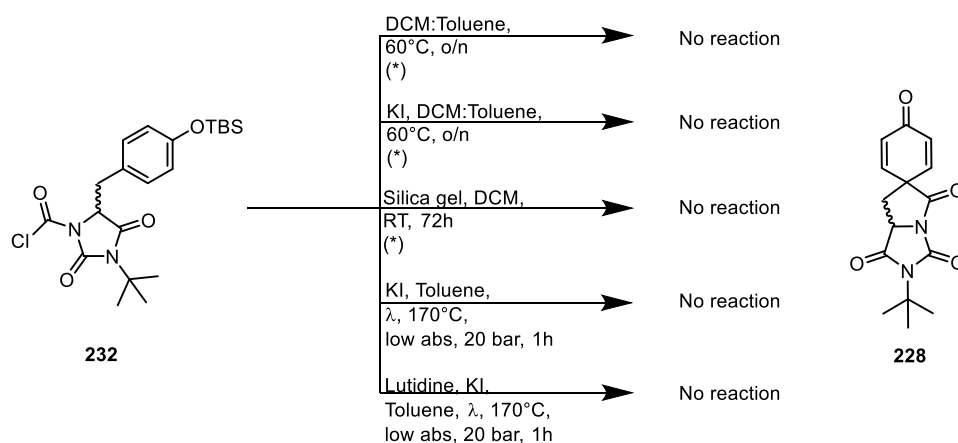
Scheme 59 - Attempted removal of the silyl group.

Silyl ethers have been reported to undergo spirocyclisation directly,⁹⁹ so the possibility that **232** may be capable of undergoing an in situ spirocyclisation/deprotection was proposed. In this case, the proposed spirocyclisation would first occur to give **240** followed by silyl deprotection by the chloride ion to give the desired spirocycle **228** (Scheme 60).



Scheme 60 - Proposed in situ deprotection/spirocyclisation.

A variety of conditions were trialled for this tandem reaction (Scheme 61); however, in all cases only starting material was recovered. As a result, this route was abandoned and a new approach was proposed.

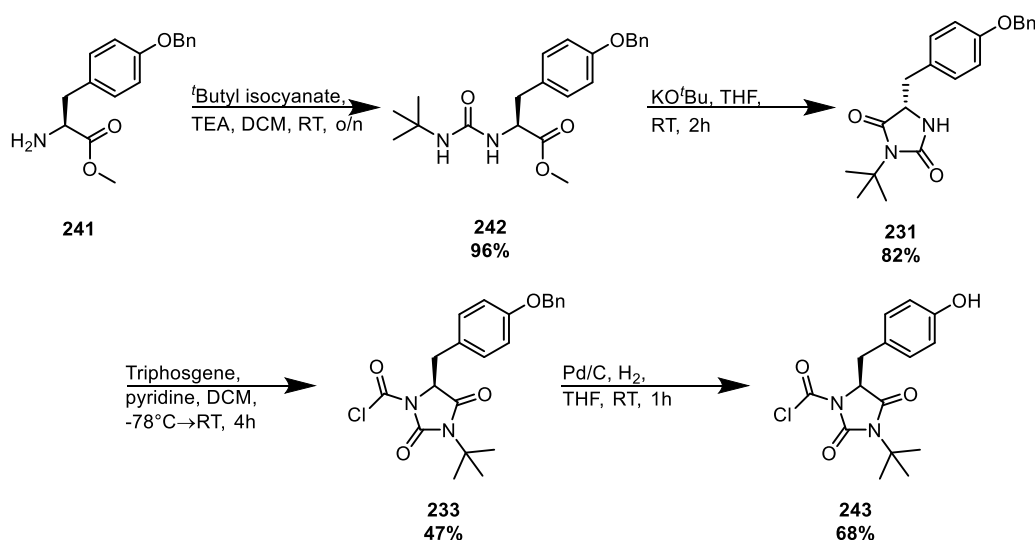


Scheme 61 - Attempted spirocyclisation of protected carbamoyl chloride, 232.*

2.2.1.2 Benzyl route

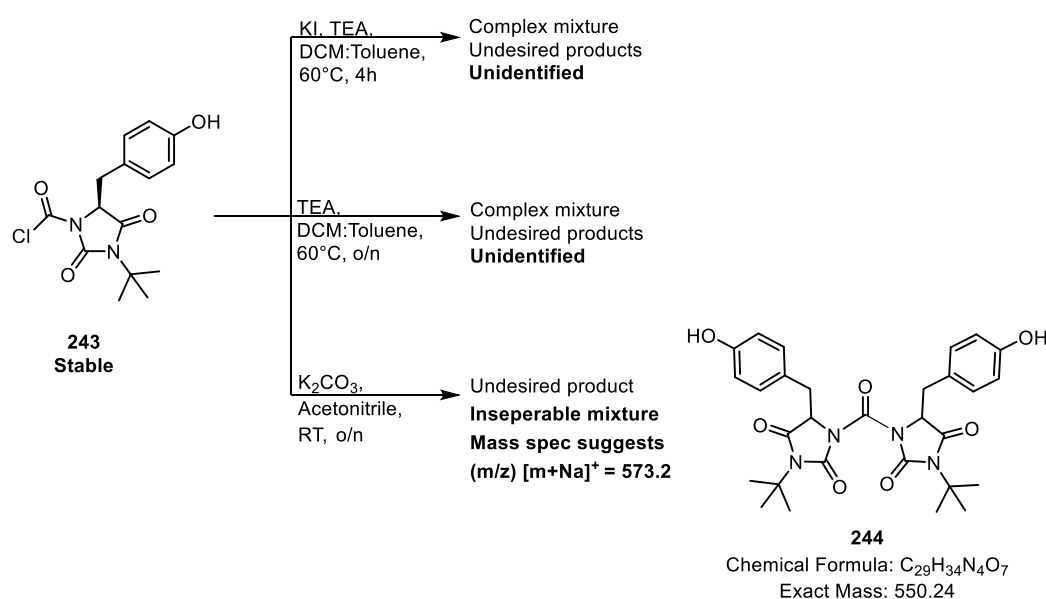
Since it appeared that the silyl group could not be removed without compromising the acyl group, a new method was developed based on the benzyl protecting group strategy which had proved successful in the imidazolidinone route (Section 2.3). The unprotected carbamoyl chloride **243** could be produced in four steps. The first three steps of coupling with *t*-butyl isocyanate, cyclisation with potassium *t*-butoxide and acylation with triphosgene to give the protected carbamoyl chloride **233** followed the same procedures as the silyl route (Section 2.2.1.1). The carbamoyl chloride **233** was then debenzylated by hydrogenolysis to yield the precursor to spirocyclisation **243** (Scheme 62).

* With thanks to Iñaki Urruzuno for conducting part of these preliminary studies



Scheme 62 - Synthesis of the unprotected carbamoyl chloride, 243.

With this in hand, several conditions for spirocyclisation were explored (Scheme 63). Unfortunately, no evidence of spirocyclisation products was observed. The first conditions trialled mirrored the conditions used in the imidazolidinone route (Section 2.3). However, a complex mix of undesired products was observed. Repeating these conditions without the use of potassium iodide was also explored as it was thought that any transient carbamoyl iodide formed may simply be too unstable to cyclise; however, this also gave a complex mixture of products. A final reaction with an alternative base, potassium carbonate, was attempted but again proved unsuccessful. From this reaction, a major ion peak was observed by mass spectrometry which suggested formation of the dimer **244**; however, the mixture was inseparable by chromatography and was not explored further (Scheme 63).

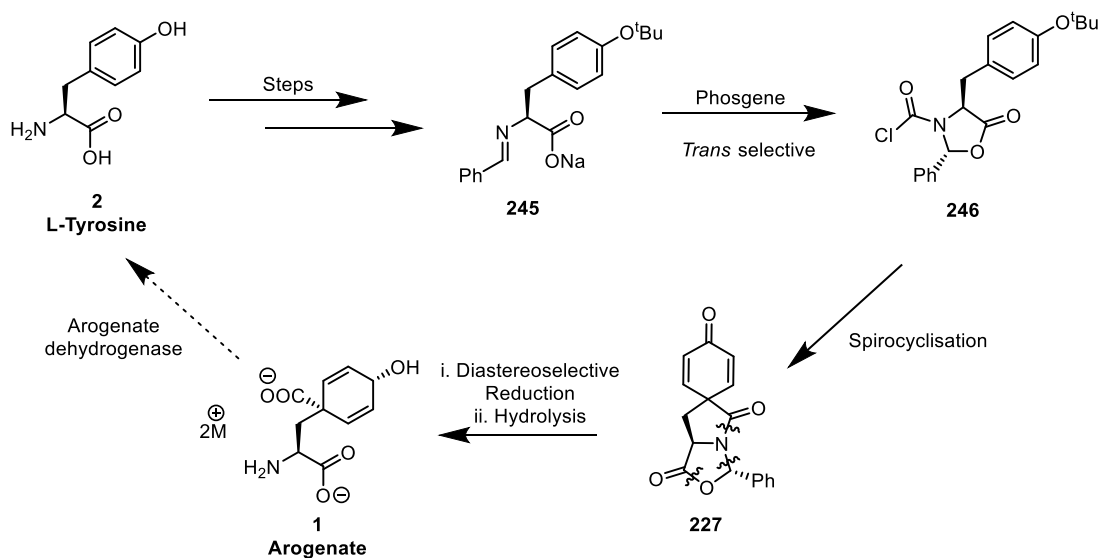


Scheme 63 – Attempted spirocyclisation of 243.

Accordingly, this route was suspended in favour of more productive avenues, with the conclusion that the conformation of the hydantoin is likely not oriented in such a way that it is in close enough proximity to facilitate the spirocyclisation. Computational modelling and crystal structures of these compounds may help determine if this is the case but this was not probed further due to success obtained in other routes (Section 2.3).

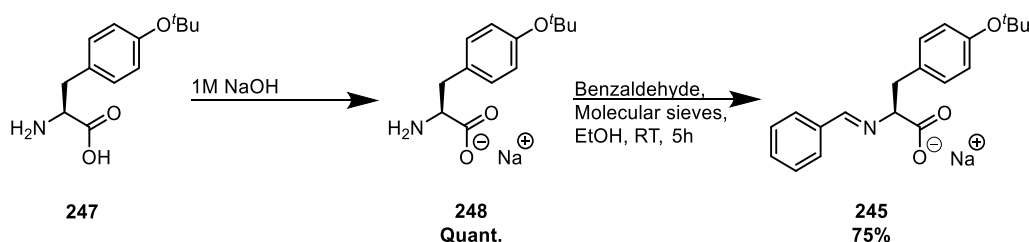
2.2.2 Oxazolidinone route

Similarly to the imidazolidinone route, an amino-acid-derived imine can be produced which can undergo cyclisation on treatment with an acylating agent.¹⁰⁷ However, in this work, benzaldehyde was used instead of pivaldehyde to produce the imine. This was due to reports in the literature that the major product diastereoisomer formed in the cyclisation could be skewed by variation of the aminal substituent.¹⁰⁹ The use of pivaldehyde resulted in *cis* selectivity, whereas benzaldehyde offered *trans* selectivity. It was then hoped that this oxazolidinone analogue would be susceptible to the same spirocyclisation reaction observed with imidazolidinones and generate a variant which would be more easily hydrolysable (Scheme 64).¹⁰⁷



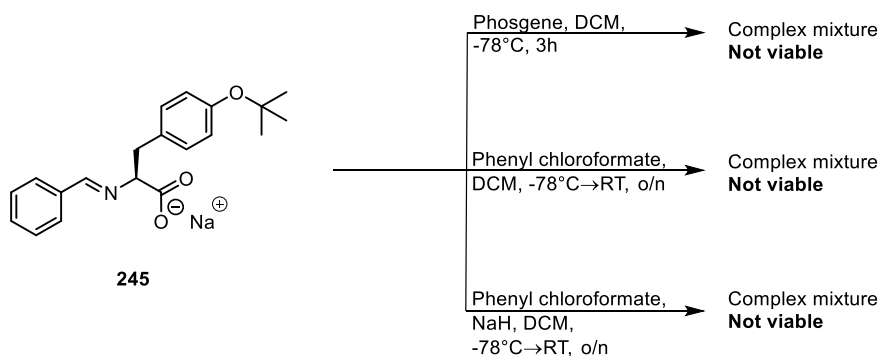
Scheme 64 - Oxazolidinone - synthetic concept.

The Schiff base **245** was synthesised according to a protocol reported by Davies *et al.*¹¹⁰ *O*-*tert*-Butyl-L-tyrosine **247** was dissolved in sodium hydroxide and concentrated to produce the salt quantitatively. Reaction with benzaldehyde in ethanol then furnished the imine **245** in 75% yield (Scheme 65).



Scheme 65 - Method for producing imine.

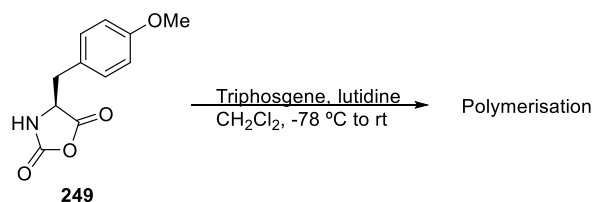
With the imine in hand, cyclisations were then attempted (Scheme 66). Initially the conditions of phosgene addition at -78°C were tested as low temperatures had been reported to favour the kinetic *trans* oxazolidinone.¹¹⁰ However, this approach gave a complex mixture in which the desired product could not be discerned. The less reactive phenyl chloroformate was then employed as the acylating agent but once again a complex mixture was produced. A final attempt was made using phenyl chloroformate in the presence of sodium hydride, to ensure the carboxylate of the starting material was fully deprotonated; however, this gave only a complex mixture. Possible traces of the desired product were observed following purification but in such small quantity as to be impractical for further exploitation.



Scheme 66 - Attempts at tandem acylation/cyclisation.

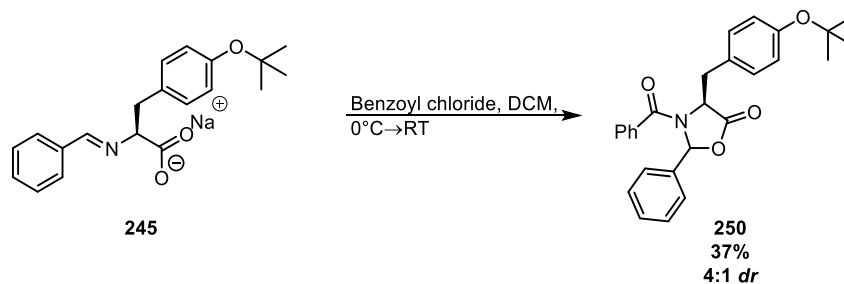
Previous work found the reaction of *O*-methyl protected tyrosine with phosgene resulted in formation of the *N*-carboxyanhydride **249**. It was thought that this heterocycle could possibly be used in the synthesis of aroenate; however, attempts at phosgenation of this species resulted in polymerisation (Scheme 67).*

* With thanks to Iñaki Urruzuno for conducting these preliminary studies



Scheme 67 - An attempted phosgenation of *N*-carboxyanhydride 249.

To ensure there were no issues with the starting material, a control reaction with benzoyl chloride, the acylating agent of choice as reported by Seebach *et al.* for producing oxazolidinones,¹⁰⁹ was carried out (Scheme 68). The reaction proceeded in a modest yield of 37% and 4:1 *dr*. The same reaction was also previously performed using the equivalent *O*-methoxy tyrosine derivative which proceeded with a good yield of 70% and 2:1 *dr*.^{*} This reaction showed that there was no issue with starting material and that instead problems were occurring due to the alternative acylating agent used.



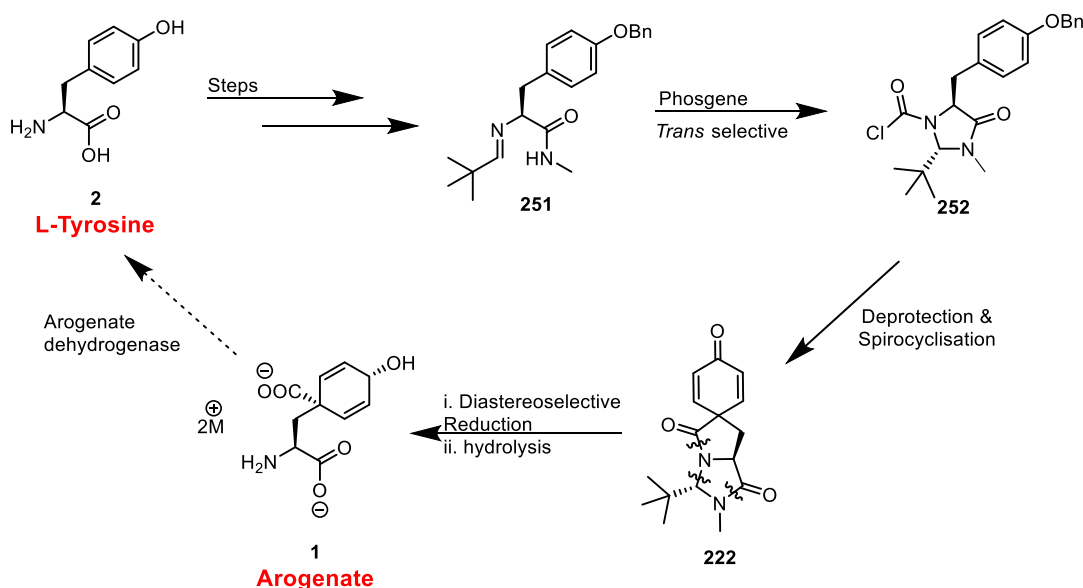
Scheme 68 - Benzoyl chloride cyclisation.

^{*} With thanks to Iñaki Urruzuno for conducting these preliminary studies

2.3 Total synthesis of aroenate & its analogues

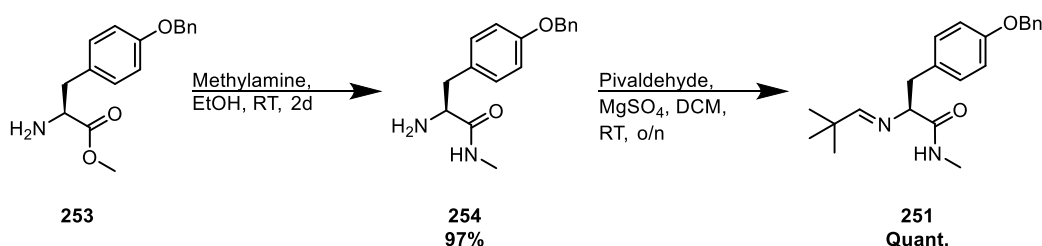
2.3.1 Aroenate synthesis via an imidazolidinone route

Since it appeared that the *trans* imidazolidinone was key to spirocyclisation, and the desired oxazolidinone could not be produced, attention returned to the imidazolidinone route. The original imidazolidinone route started from the *O*-benzyl-protected methyl ester of L-tyrosine which is commercially available (Scheme 69).



Scheme 69 - Imidazolidinone route – overall synthetic concept.

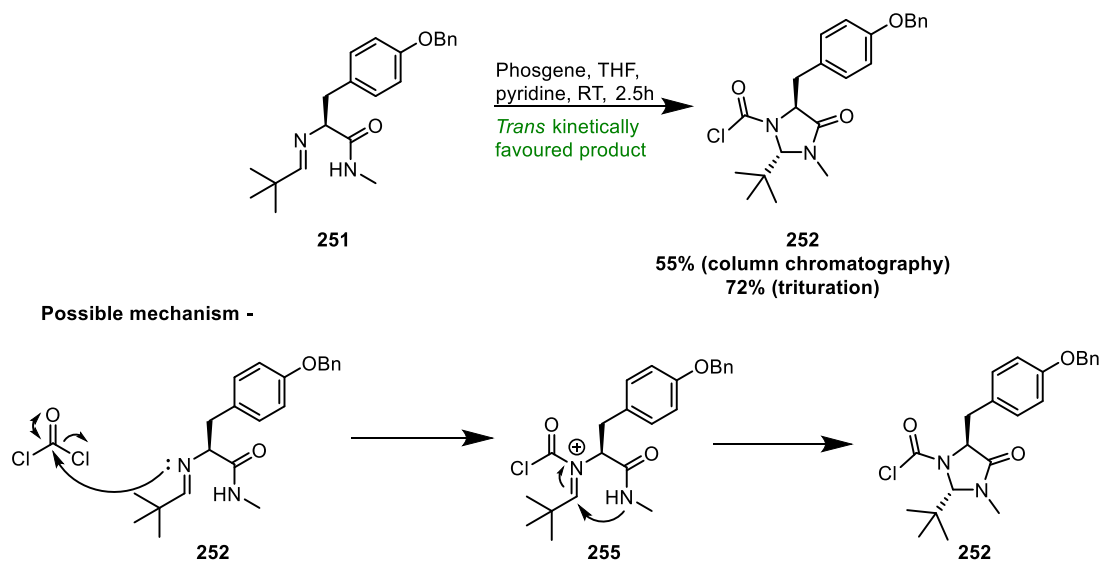
The Schiff base **251** was easily produced in two steps from the commercial ester **253**. Firstly, **253** was reacted with methylamine to generate the *N*-methylamide **254** in excellent yield. Condensation of **254** with pivaldehyde afforded the imine **251** in quantitative yield (Scheme 70).



Scheme 70 - Synthesis of the Schiff base, 251.

Tandem cyclisation/phosgenation of the imine **251** was then performed to yield the imidazolidinone, **252**. Seebach *et al.* reported that, under kinetic control, intermediate acyliminiums (e.g **255**) cyclise to give *trans* imidazolidinones preferentially so as to avoid clashing of the sterically demanding *t*-butyl and α -substituents (Scheme 71).¹¹¹ The cyclisation conditions have been optimised previously in the group to offer complete *trans* selectivity.¹¹² The

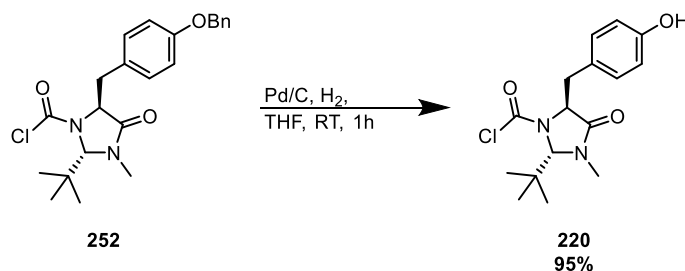
trans imidazolidinone was desired as previous work found the *cis* isomer to be unreactive in the subsequent spirocyclisation.



Scheme 71 - Phosgene cyclisation to 252 and possible mechanism.

Unfortunately, a moderate yield of 55% was recovered in this step which may be attributed to poor solubility of the product in the purification step. Various solvent systems were trialed to help overcome this issue, but all proved unsuccessful; attempts at recrystallisation also proved futile resulting only in lower yields. Trituration with ether or 1:1 ether:pentane proved more effective than chromatographic purification giving an increase in yield to 72%.

To enable the spirocyclisation reaction to occur, it was necessary for **252** to undergo hydrogenolysis to remove the benzyl protecting group, generating the phenol **220** in 95% yield. It should be noted that this debenzylolation was carried out in THF in lieu of the more typical alcoholic solvents to avoid compromising the carbamoyl chloride moiety (Scheme 72).

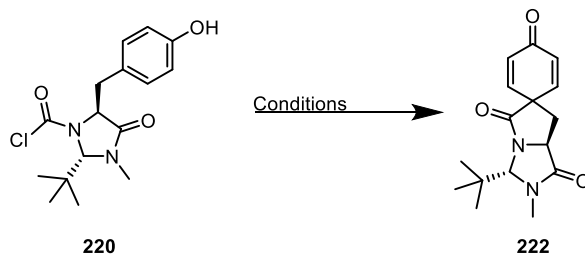


Scheme 72 - Hydrogenolysis of the benzyl protecting group.

Previously, the spirocyclisation reaction of **220** had been performed using a mixture of triethylamine and stoichiometric potassium iodide at 60 °C for 72 hours. It was proposed that the reaction went via a transient carbamoyl iodide, (Section 1.5 - Scheme 51). It was hoped the reaction could be transferred to the microwave reactor to allow shorter reaction times. A variety

of conditions were screened in the microwave reactor, starting with conditions (Table 1– entry b) used previously in the group to perform a related Friedel-Crafts acylation.¹¹³

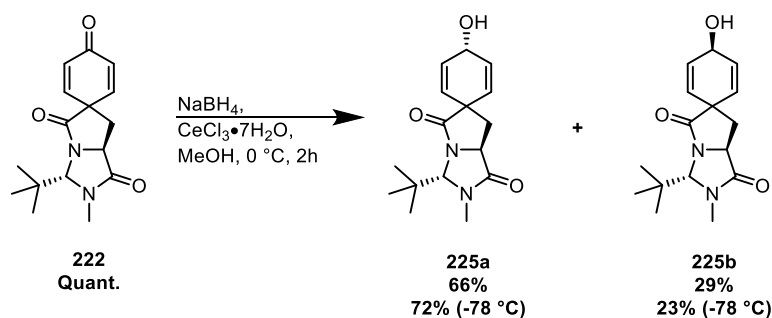
Table 1 - Conditions for transferring the spirocyclisation reaction to the microwave.



	Solvent	Time	Temp (°C)	Base	KI (eq.)	Yield (%)	Comments
a	DCM:toluene (4:1) ^a	72 h	60	TEA	1.1	82	Conventional heating
b	Acetonitrile ^b	5 min	150	Lutidine	1.1	NMR - full conversion	Microwave (test)
c	Acetonitrile ^b	5 min	150	TEA	1.1	NMR - full conversion	Microwave (test)
d	Acetonitrile ^b	5 min	150	TEA	0	NMR - full conversion	Microwave (test)
e	Acetonitrile ^b	5 min	150	TEA	1.1	79	Microwave (100mg)

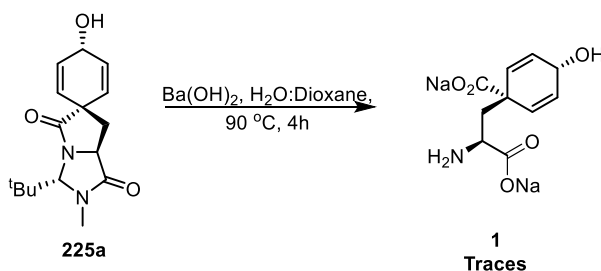
^a 0.5M ^b 0.15M

Using microwave irradiation, full conversion was observed after only 5 minutes. Substituting 2,6-lutidine for the original base, triethylamine, gave no adverse effects (Table 1 - entry c). The reaction was also attempted without potassium iodide to determine whether pre-activation of the carbamoyl unit was necessary (Table 1 - entry e). The positive results showed that potassium iodide was not required for the spirocyclisation to proceed. Upon scaling up the reaction, a yield comparable to that obtained with conventional heating was obtained after purification (Table 1 - entry d). Interestingly, it was found that even at room temperature, starting material dissolved in DCM or CDCl₃ showed signs of conversion to the spirocycle, **222**, after 1 week – highlighting the favourable nature of this reaction. It was found that the reaction could be scaled up easily using concentrations up to 1 M, extending the reaction time to 10 minutes ensured full conversion in these larger reactions. Following work-up, the product appeared clean by NMR and required no further purification, providing quantitative yield.



Scheme 73 - Luche reduction of the dienone 222.

The spirocyclisation product **222** was reduced under Luche conditions to give a separable mixture of diastereomeric alcohols **225a** and **225b** (2.3:1 *dr*) in excellent yield (Scheme 73). It was found lowering the reaction temperature to -78 °C increased the diastereoselectivity to 3.1:1. With these products in hand, a variety of hydrolysis conditions to give aroenate, **1**, could be explored. Provisional work suggested that barium hydroxide gave traces of the desired product in the basic hydrolysis of **225a** (Scheme 74).*



Scheme 74 - Preliminary hydrolysis result.

Performing this reaction at lower temperature (30 °C) for extended time (16-18 h) resulted in fewer aromatic impurities; however, reduced conversion of the starting material was also observed. It was found that by simply washing the crude hydrolysis mixture with DCM, this unreacted starting material could be completely recovered. Hence, at this stage, it was deemed more of a priority to limit formation of unwanted aromatic impurities.

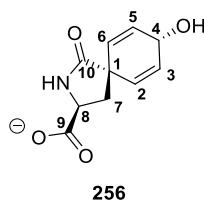


Figure 8 - Structure of spiroarogenate 256.

* With thanks to Iñaki Urruzuno for conducting these preliminary studies

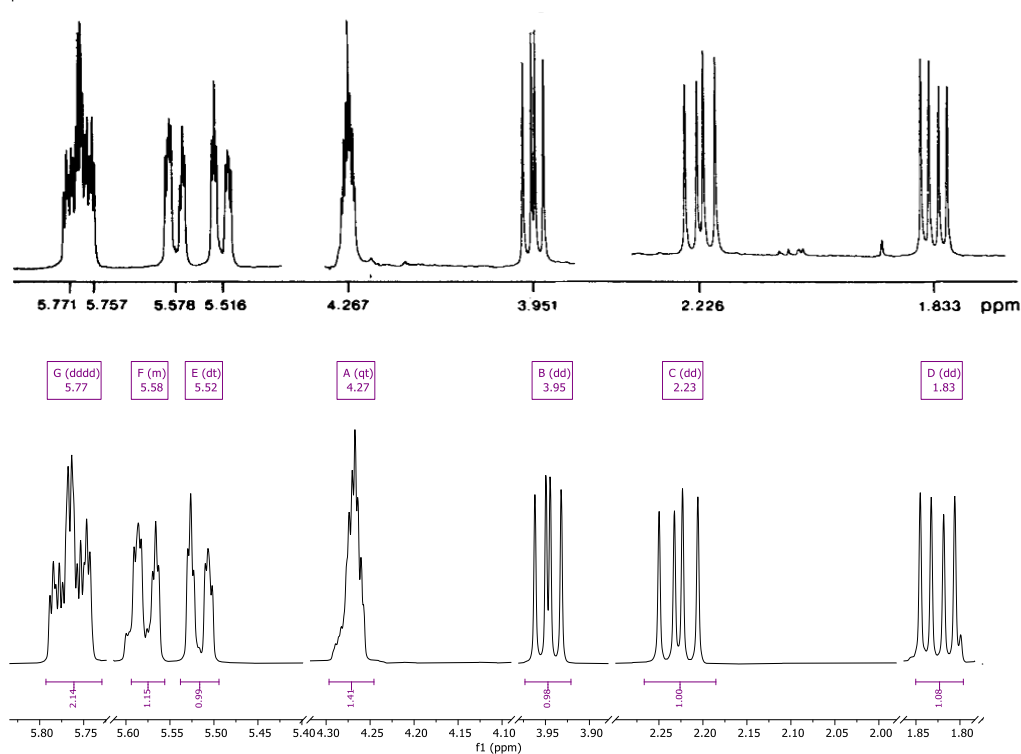


Figure 9 - Comparison of Zamir *et al.* isolated spiroarogenate (top) and synthetic spiroarogenate (bottom).

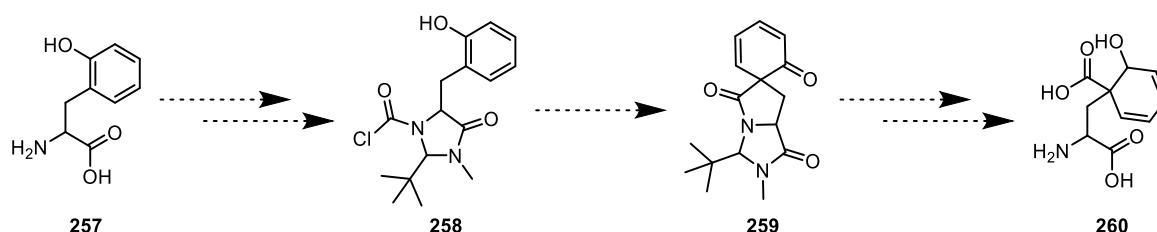
Curiously, it was found that the major product produced was not in fact aroenate but another species bearing a remarkable similarity. Upon consulting the literature, it was discovered this species was most likely spiroarogenate, **256**, itself a natural product previously reported by Zamir *et al.* upon isolation from red bread mould (Figure 8).¹¹⁴ **256** is coincidentally also the product from the penultimate step in Danishefsky's synthesis of aroenate.³⁶

2.3.2 Synthesis of analogues

As previously mentioned, it has long been thought that analogues of aroenate may inhibit the aroenate enzymes and in turn produce herbicides or antibiotics.^{8,9} The natural products, aroenate and spiroaroenate, proved difficult to handle due to their small polar nature and inherent desire to rearomatise. Due to this, the project explored the application of this synthesis for the production of analogues, with particular interest in more stable analogues.

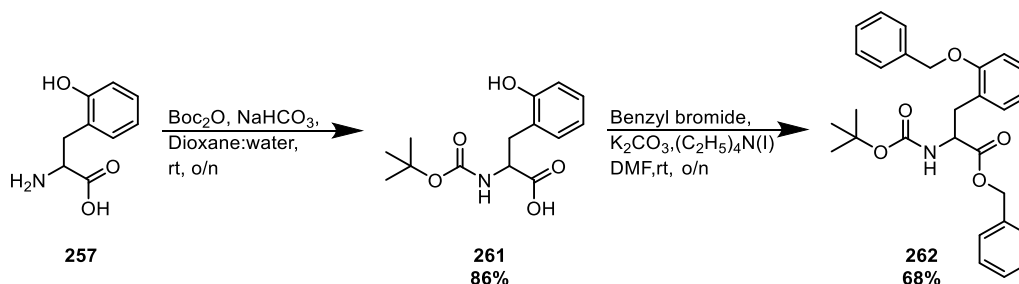
2.3.2.1 *ortho*-Aroenate

It was envisaged that the use of *ortho*-tyrosine **257** in the same synthetic pathway may lead to an alternative spirocyclisation reaction to give **259**, which could potentially undergo hydrolysis to give a novel regioisomer of aroenate **260** (Scheme 75).



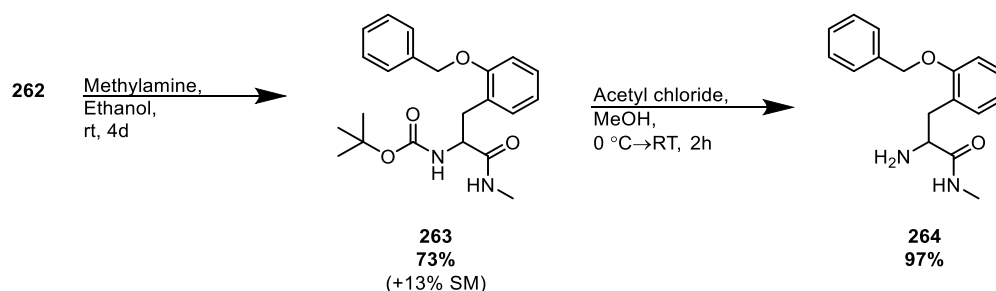
Scheme 75 - *Ortho* spirocyclisation pathway to aroenate regioisomer **260**.

DL-*o*-tyrosine, **257**, was commercially available and following a protecting group strategy using Boc anhydride and benzyl bromide, it was anticipated that the optimised method used to synthesise the *para*-tyrosine imidazolidinone could be employed. The protection strategy first involved installing a *tert*-butoxycarbonyl group on the free amine to prevent *N*-benzylation in the next step. Using Boc anhydride and sodium hydrogen carbonate in a mixture of dioxane and water, the reaction proceeded to give **261** in good yield. Subsequent benzylation of both the acid and alcohol moieties was carried out using a mixture of benzyl bromide, potassium carbonate and tetraethylammonium iodide in DMF to give the protected species **262** in reasonable yield (Scheme 76).



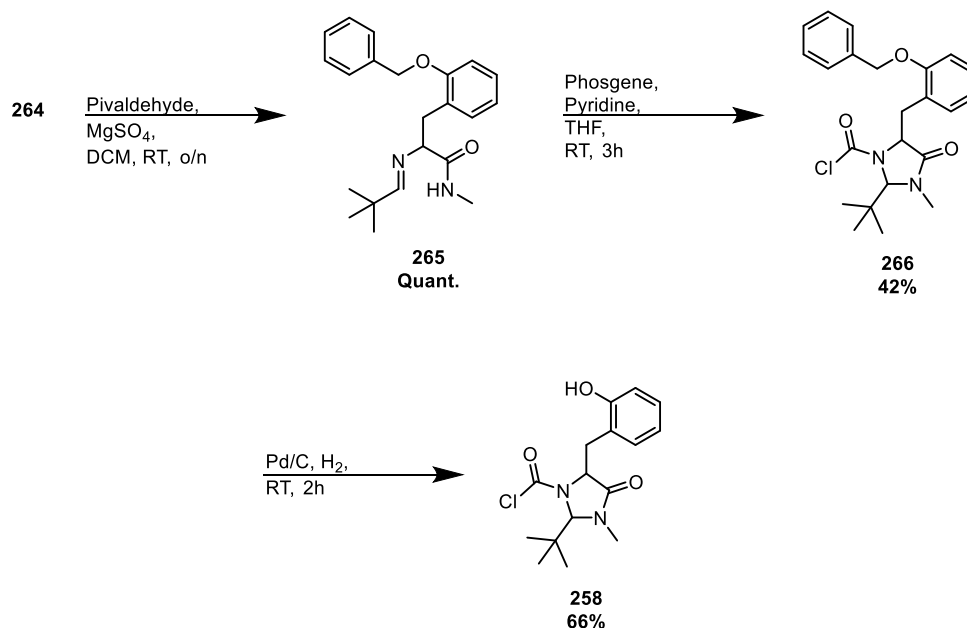
Scheme 76 - Protecting group strategy – synthesis of **262** from **257**.

Reaction of **262** with methylamine was performed using the standard conditions affording a good yield of 73% and 13% starting material recovery. Boc deprotection of **263** with acetyl chloride in methanol gave the desired product **264** in virtually quantitative yields (Scheme 77).



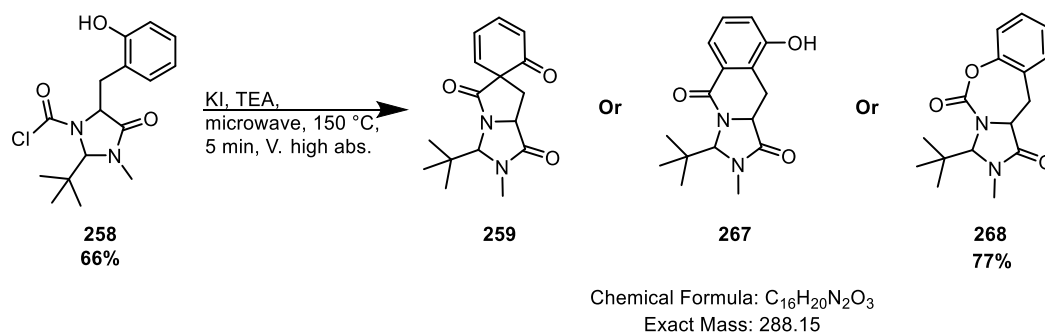
Scheme 77 - Coupling with methyl amine and deprotection to 264.

The debenzylated carbamoyl chloride **258** was obtained using previously applied procedures (Scheme 78 & Section 2.3).



Scheme 78 - Synthesis of deprotected carbamoyl chloride 258.

With this material in hand, the *ortho* spirocyclisation was attempted (Scheme 79). Using the same conditions optimised for the *para* derivative, complete consumption of the starting material was observed; however, the chemical shifts in the crude NMR spectrum appeared to be more characteristic of aromatic protons than vinylic.

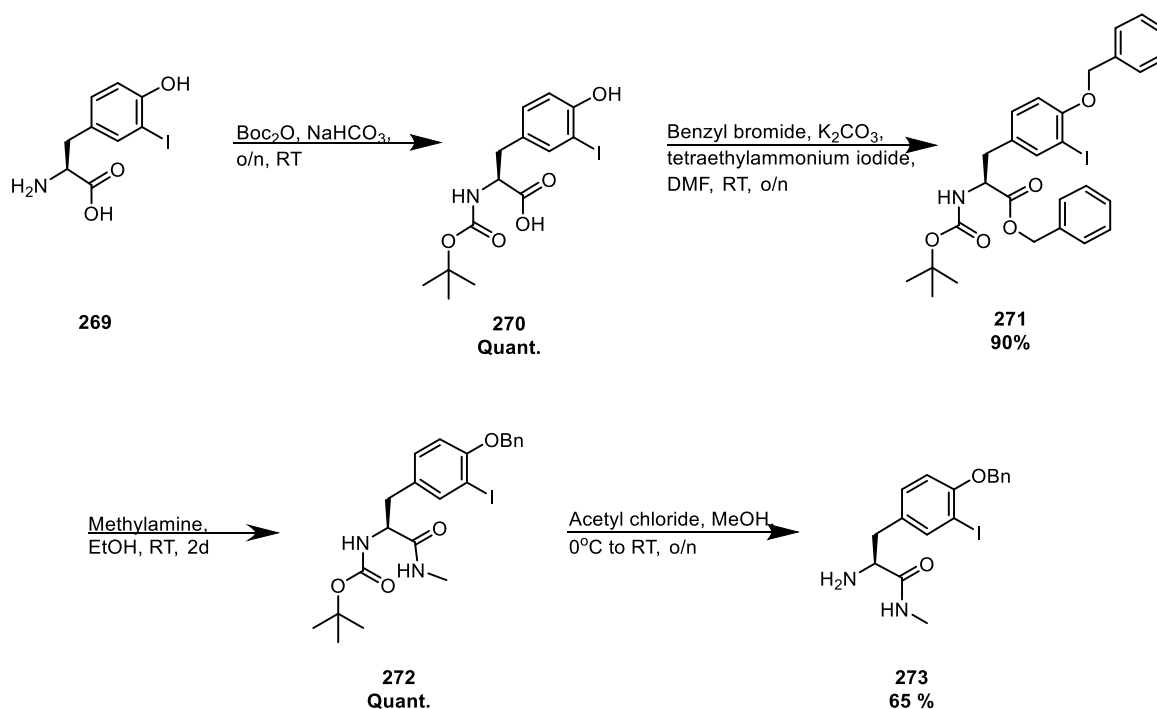


Scheme 79 - Possible cyclisation products.

Three plausible products were proposed; the expected spirocyclisation product **259**, the Friedel-Crafts acylation product **267** and the product of phenolic attack on the carbamoyl chloride to give a 7-membered ring **268**. As each of these possible products had the same molecular weight, mass spectrometry could not aid us in distinguishing which product had been obtained. IR analysis showed no distinctive O-H stretch which would indicate product **267**, hence this species could be ruled out. Based on the NMR spectra obtained, the number of chemical shifts in the aromatic region, six signals rather than four, suggest product **268** had formed. The lack of an additional peak in the carbonyl range (>160 ppm) in the ^{13}C NMR spectra expected for product **259** further suggested product **268** had been produced instead. Even when the reaction was performed in DCM with TEA at room temperature the reaction went to full conversion of **268** – demonstrating how favourable this alternative cyclisation reaction is.

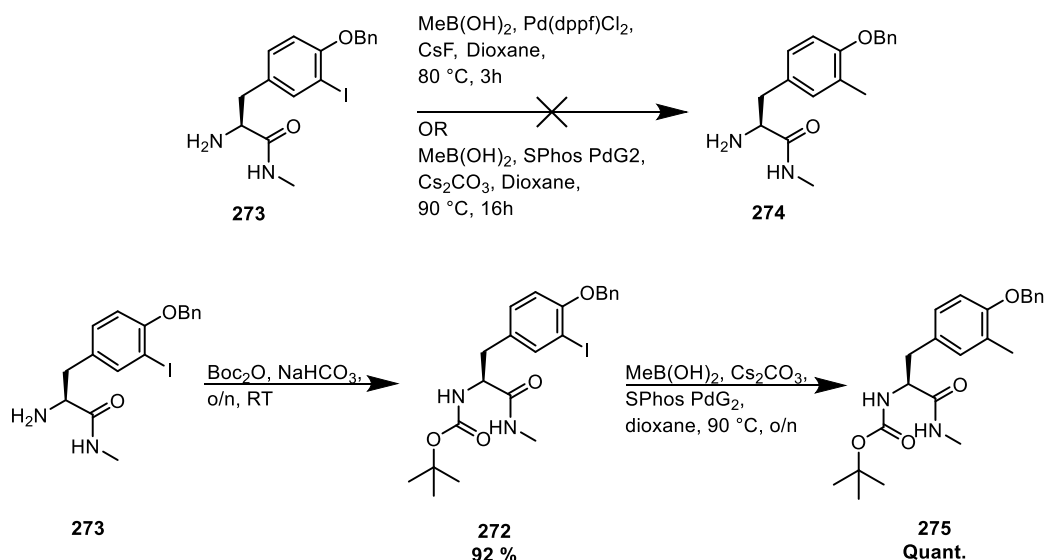
2.3.2.2 3-Methyl Aroenate

To assess the robustness of the method substitution on the ring was carried out; an alternative starting material was utilised to install a methyl group at the aryl *meta* position. Starting from 3-iodo-L-tyrosine, **269**, a Boc protection followed by benzylation was carried out to produce **271**. Amination with methylamine gave **272** in quantitative yield which was then followed by a Boc deprotection to give the free amine **273** (Scheme 80).



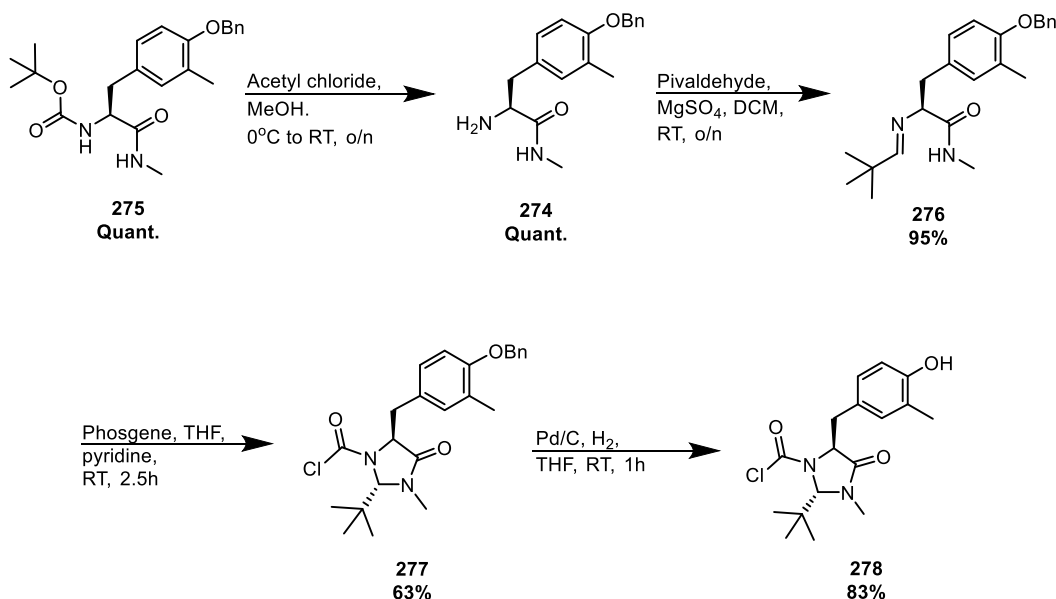
Scheme 80 – Initial protection steps in the synthesis towards 3-Methyl aroenate.

Two conditions for the Suzuki coupling using methylboronic acid were trialed to install the methyl group, **274**. However, only starting material was recovered which may be due to the free amine coordinating to the palladium and preventing the reaction from occurring. In an attempt to circumvent this the Boc group was reinstalled to return to product **272**. Gratifyingly, use of this species allowed the Suzuki coupling to be employed successfully in quantitative yield giving **275** (Scheme 81).



Scheme 81 – Attempted Suzuki couplings.

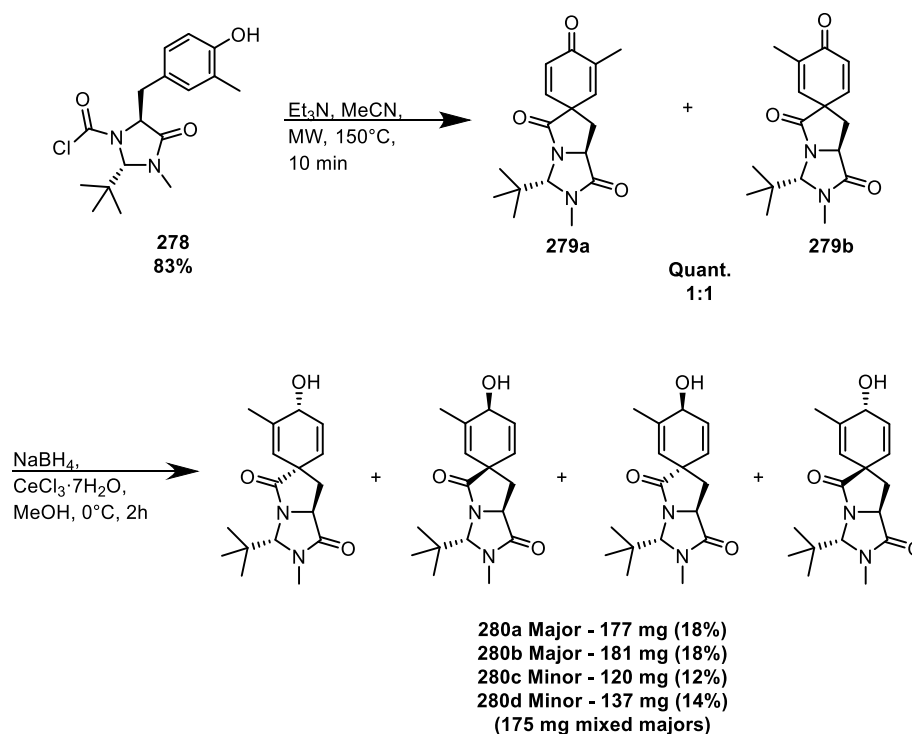
With this installed, Boc deprotection was performed to produce **276**. The original method could then be performed to produce the benzyl deprotected imidazolidinone carbamoyl chloride **278** ready to undergo the spirocyclisation reaction (Scheme 82).



Scheme 82 – Continued synthesis of 3-Methyl derivative starting from 3-iodo-L-tyrosine, 269.

Upon attempting the spirocyclisation reaction it was found that two diastereomers had formed in a 1:1 ratio due to the methyl group producing a chiral spirocyclic centre. These were taken through to the Luche reduction, without prior separation, giving four different diastereomers which could be separated using standard column chromatography (Scheme 83). Upon repeating these reactions, the two diastereomeric dienones were separated beforehand in the hopes of offering easier purification. However, following the two separate Luche reductions the respective

diastereomers nonetheless gave tight chromatographic separation and provided similar overall yields.



Scheme 83 – Spirocyclisation and Luche reduction of 3-Methyl derivative.

2D NOESY and X-ray crystallography were used to determine the configuration of the four diastereomers. Due to the perpendicular geometry of the rings in the spirocycle, **280**, a 2D NOE correlation was used to aid in determination of the configuration. Depending on the relationship between the carbonyl, oriented either up or down, and the methyl group; either the singlet peak (position **1**) or the doublet peak (position **2**) will observe the alpha proton. This was further confirmed by the crystal structure (Figure 10).

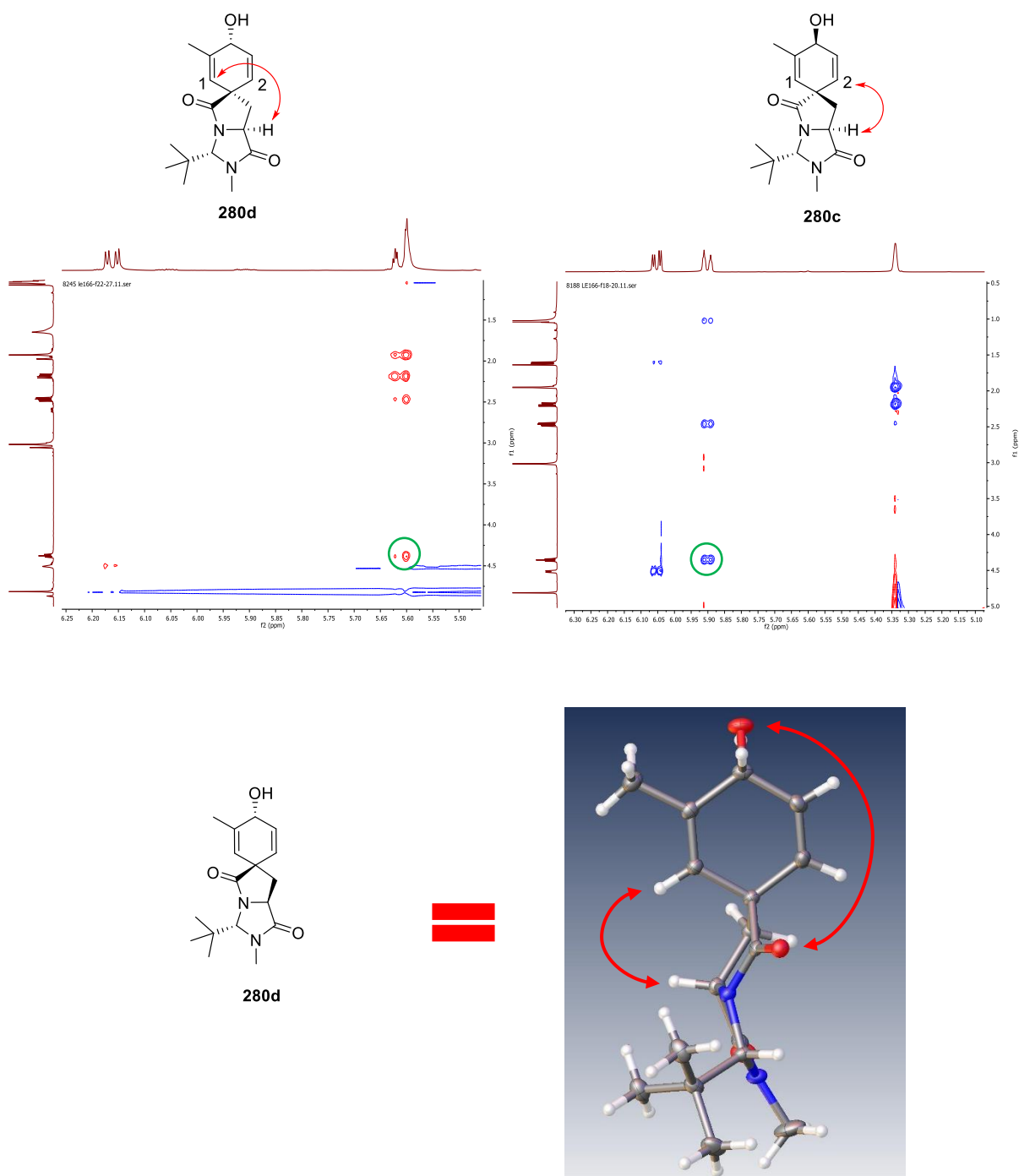


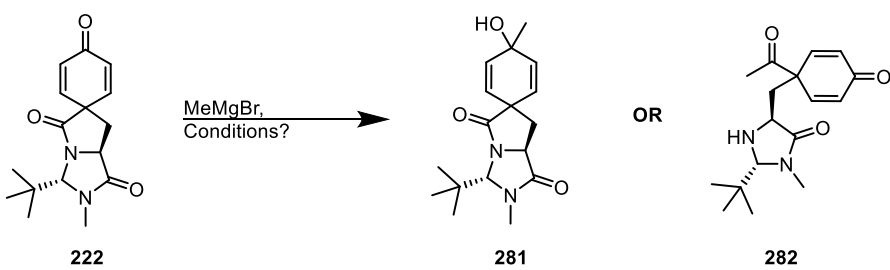
Figure 10 – Determination of configuration for 3-Methyl derivative.

The *trans* relationship between the hydroxyl and amide groups (Figure 10) was found to be the minor diastereomer **280d**, which corresponds with what is observed in the original synthesis. It was therefore assumed the other minor product, **280c**, was also *trans* and the major diastereomers **280a** and **280b** are of a *cis* relationship.

2.3.2.3 Grignard additions

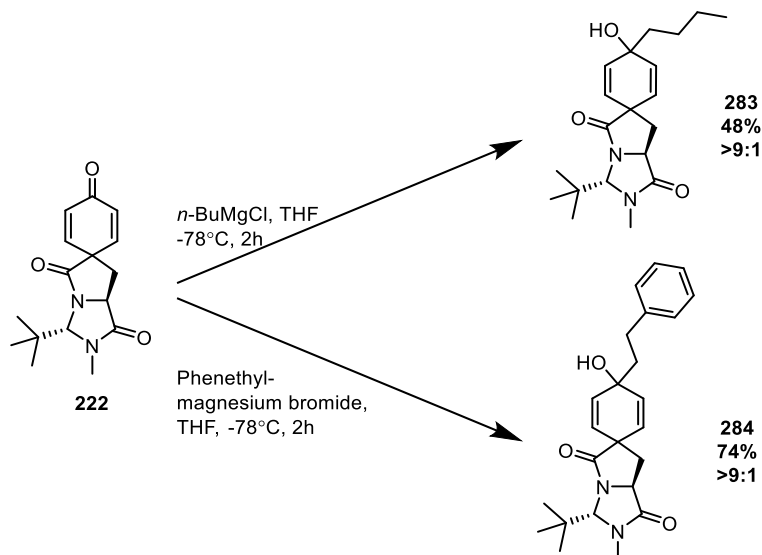
1,2-Additions were an attractive avenue for derivatisation as it is thought they could provide stability towards rearomatisation by removing the hydrogen adjacent to the hydroxyl group. Methylmagnesium bromide was the first Grignard reagent explored. Although the reaction did proceed, complete conversion could not be achieved causing difficulties in purification due to co-elution of the product and starting material. A brief optimisation was carried out with the aim of obtaining complete consumption of starting material (Table 2).

Table 2 – MeMgBr Grignard addition optimisation.

 <p>The reaction scheme shows compound 222 (a bicyclic amide with a cyclohexenone ring) reacting with MeMgBr under various conditions to produce either compound 281 (a bicyclic amide with a cyclohexenol ring) or compound 282 (a bicyclic amide with a cyclohexenone ring and a methyl group).</p>						
Entry	Conc. (M) (THF)	Eq.	Temp	Time (h)	Conversion by NMR (%)	
					281	282
a	0.1	1.5	-78→RT	16-18	93	-
b	0.2	1.5	-78→RT	16-18	81	-
c	0.02	1.5	-78→RT	16-18	69	-
d	0.2	1.5	-78	1	84	-
e	0.1	3	-78→RT	16-18	-	83
f	0.1	1.5 x 2	-78→RT	3	-	100

However, at least >7% starting material always remained which could not be separated from the major diastereomer. Increasing concentration (Table 2 – entry b) or decreasing concentration (Table 2 - entry c) both resulted in a decrease in yield. A similar yield was obtained when the reaction was left for only one hour at a 0.2 M concentration (Table 2 – entry d) suggesting no further reaction occurred with extended reaction times. Increasing the number of equivalents used resulted in Grignard attack of the amide resulting in **282** (Table 2). Thus, the use of methylmagnesium bromide was abandoned.

Alkylation with an alternative Grignard reagent was proposed in the hope of generating a product with better chromatographic separation. Gratifyingly, *N*-butylmagnesium chloride successfully yielded a product, with high diastereoselectivity (>9:1 *dr*), which could be easily isolated (Scheme 84).



Scheme 84 – Synthesis of *n*-butyl and phenethyl derivatives.

Phenethylmagnesium bromide was also trialed in the hope of synthesising an analogue which could mimic NADP in the enzyme binding site pocket, based upon computational docking models of aroenate in aroenate dehydrogenase (2F1K)(Figure 11).¹¹⁵

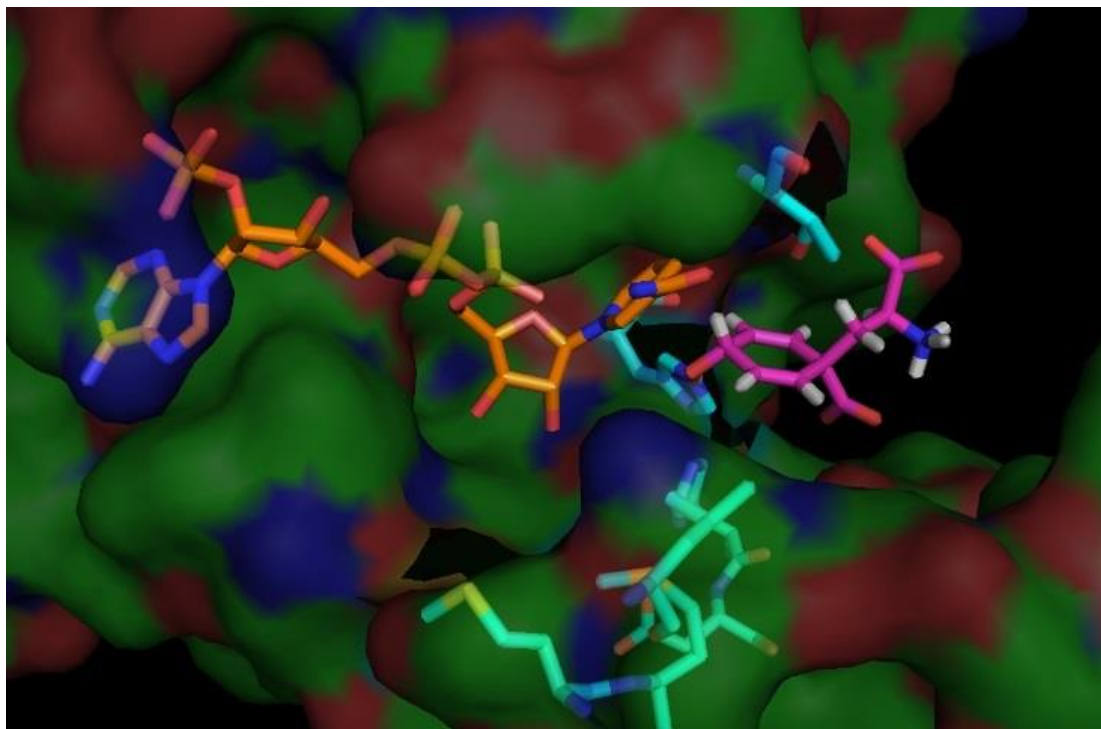
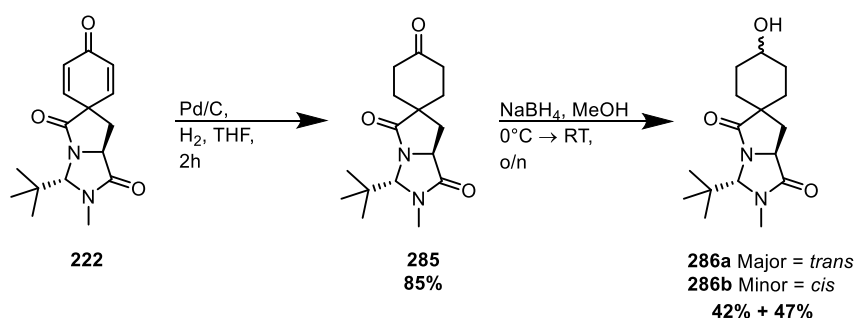


Figure 11 - Computational docking of aroenate (pink) in the crystal structure of aroenate dehydrogenase (2F1K) with key residues (blue) and NADP (orange) highlighted.

2.3.2.4 Double bond reductions

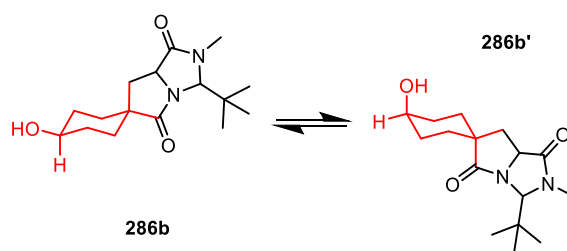
2.3.2.4.1 Fully saturated derivative

To produce a derivative which was not susceptible to rearomatisation, reduction of the unsaturated ring was carried out. Hydrogenation in THF gave access to the fully saturated carbocycle **285** in good yield; ethanol was initially used as the solvent, but this resulted in the acetal by attack into the ketone. **285** was then reduced using NaBH₄ to give the alcohol **286a** and **286b** in a 1:1.1 *dr*. The use of cerium chloride in this reaction gave no change in diastereoselectivity.



Scheme 85 – Synthesis of saturated spiroarogenate.

Attempts to identify the configuration of **286** using 1D and 2D NOE along with basic computational modelling proved difficult. We believe this is due to ring flipping giving two conformations in different populations resulting in NOEs of averaged intensities (Scheme 86). This likely could have been solved by computational calculations for the various populations and applying these to the interproton distances calculated by 1D NOE data.¹¹⁶ However, a crystal structure of **286a** was obtained in the meantime showing a *trans* configuration (Figure 12).



Scheme 86 – Ring flipping of the *trans* hydrogenated spirocycle.

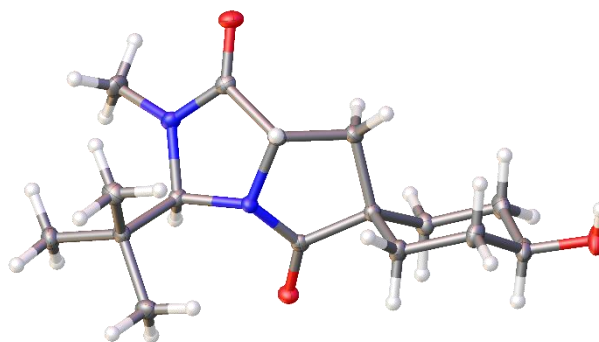
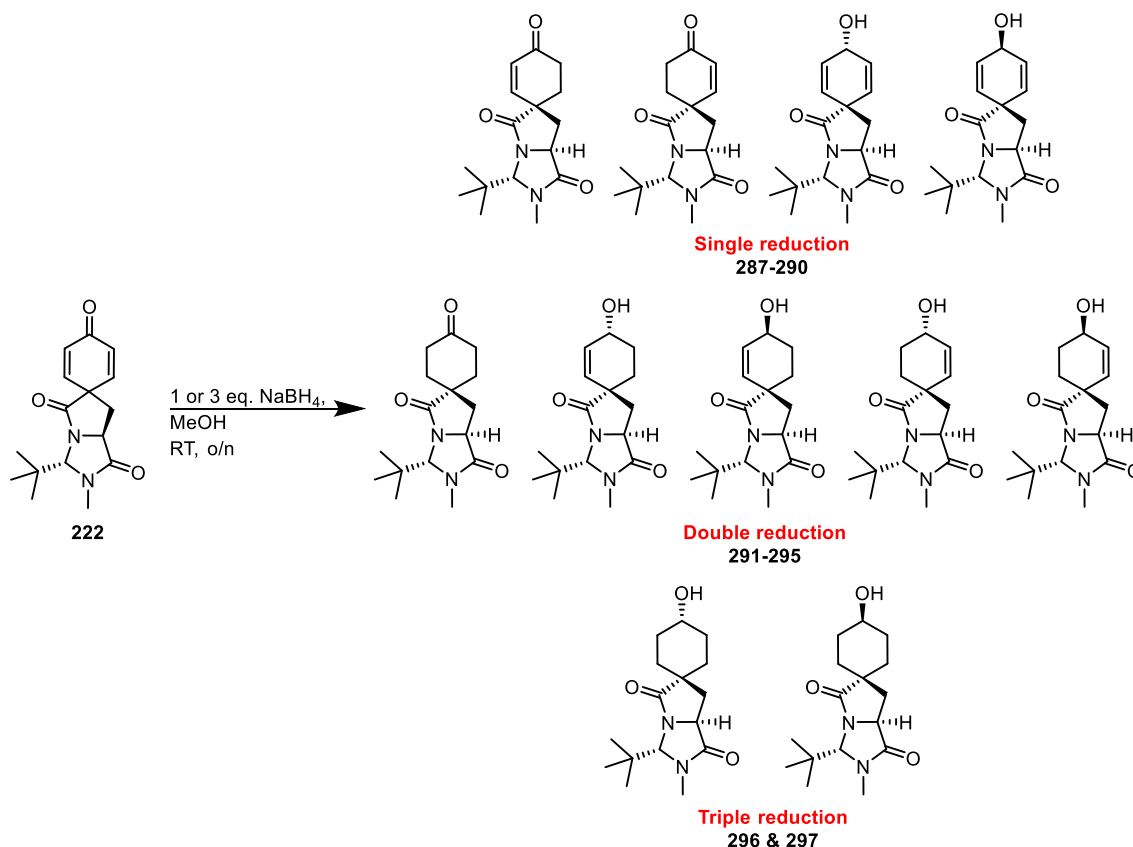


Figure 12 – Crystal structure of *trans* hydrogenated spirocycle.

2.3.2.4.2 Partially reduced derivative

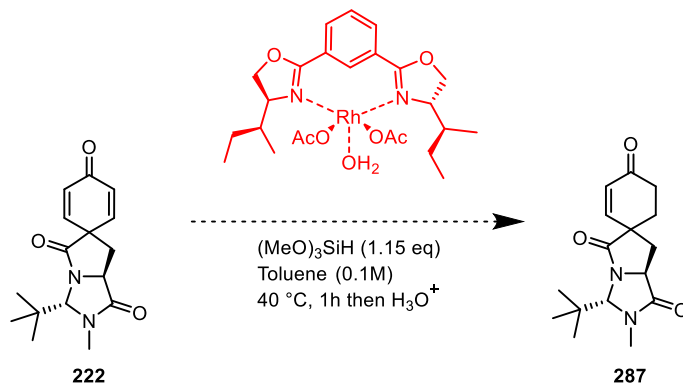
It was initially hoped reduction with NaBH_4 would allow access to partially saturated intermediates, however, the initial experiment produced a complex mixture of at least 8 species. This may be due to use of excess NaBH_4 allowing multiple reductions with the possibility of 11 different products (Scheme 87).



Scheme 87 – Plausible products from the NaBH_4 reduction.

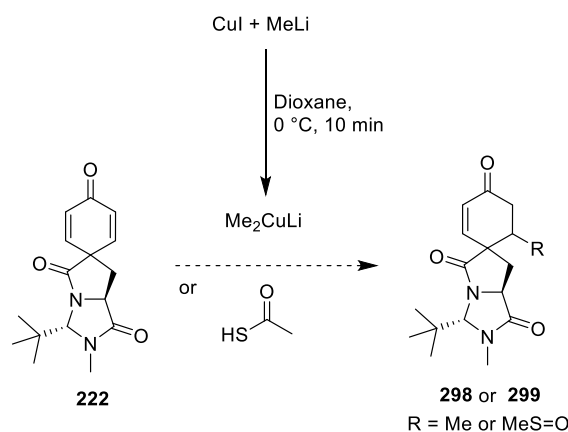
Reducing the equivalents of NaBH_4 to one in the hopes of limiting the number of products formed still resulted in a complex mixture with numerous spots by TLC. A rhodium catalyst has

previously been reported in the literature for use in the asymmetric desymmetrisation of a dienone.¹¹⁷ Although initial results with this reagent appeared promising, with only a single product formed, the conversion was only 23% by NMR and the product could not be successfully isolated and characterised; it is hoped through further optimisation this route can be made viable.*



Scheme 88 – Diastereoselective reductive of the dienone **222 with [Rh(Phebox-sBu)].**

An alternative approach which would result in removal of the alkene(s) would be to carry out 1,4-additions. Gilman reagents, with and without TMSCl, and thioacetic acid were utilised as soft nucleophiles. However, this approach also proved difficult with the best example giving only 23% conversion by NMR.[†] Further optimisation will hopefully allow conversion to be maximised, along with investigation of the diastereoselectivity, which would allow for easier purification.



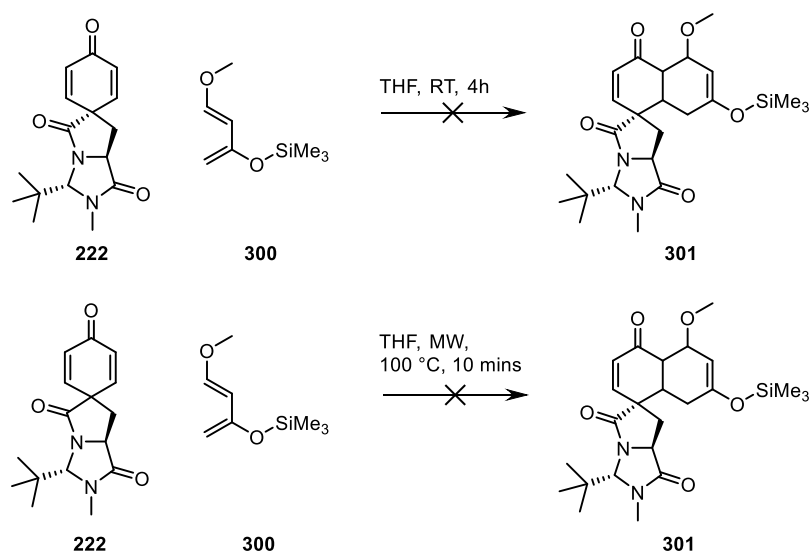
Scheme 89 – 1,4-Additions to **222 with soft nucleophiles.**

* With thanks to Rachel Pankhurst for carrying out these reactions.

† With thanks to Rachel Pankhurst for carrying out these reactions.

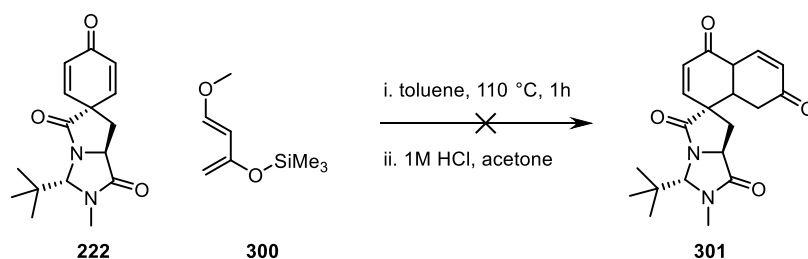
2.3.2.5 Diels-Alder

An attempt was made to carry out a Diels-Alder reaction between spirocycle **222** and the reactive and regioselective Danishefsky's diene **300**. However, attempts at both room temperature and 100 °C under microwave irradiation yielded only starting material by LCMS. It was thought the lack of reaction may be due to steric hindrance, reaction with cyclopentadiene may be worth exploration in the future.



Scheme 90 – Diels-Alder reaction with **222**.

A further attempt of the Diels-Alder reaction (Scheme 91), replicated the conditions reported for a hindered cyclic enone and Danishefsky's diene reported by Tang *et al.*¹¹⁸ The crude reaction mixture appeared promising by TLC-MS and NMR, however, purification proved problematic and the major isolated spot did not show any signs of product by NMR or mass spec.*

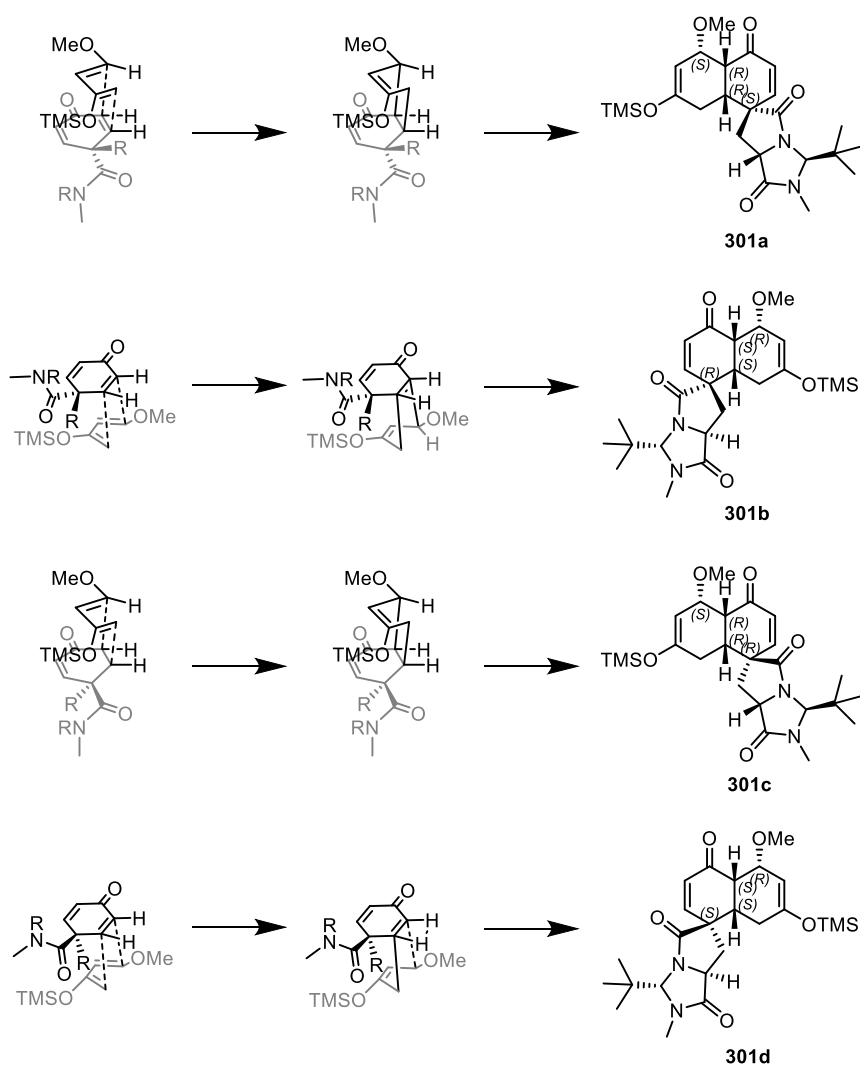


Scheme 91 – Diels-Alder reaction following Tang *et al.* conditions.

Although Danishefsky's diene was selected for its excellent regioselectivity, due to the various stereogenic centres within the spirodienone there would still be eight possible diastereomeric products from this reaction. It was assumed four of these could be ruled out as the reaction was expected to follow the *endo* rule, in which there is favourable secondary orbital interaction

* With thanks to Rachel Pankhurst for this result.

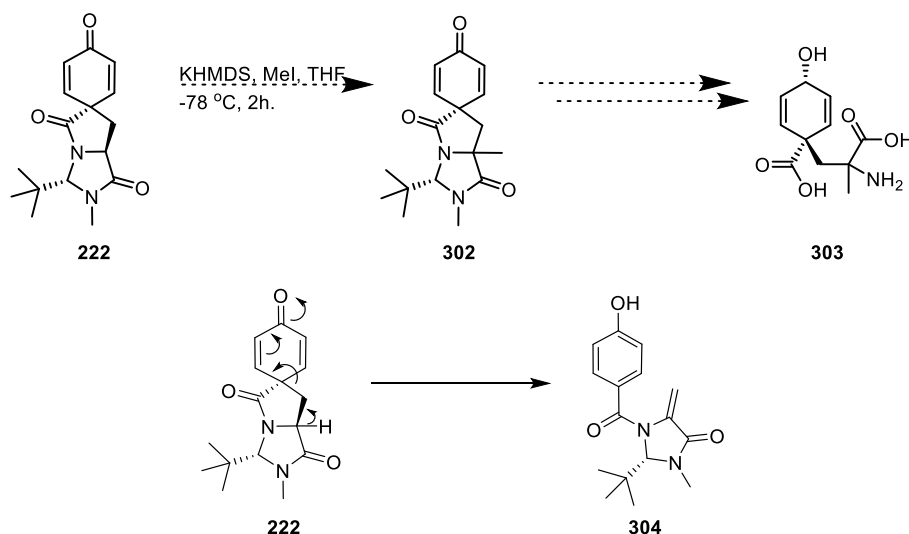
between the diene and ketone.¹¹⁹ It was also hoped that selectivity, similar to that observed in the Luche reduction, may be observed due to the methylene group sterically disfavoured products **301a** and **301d** (Scheme 92).



Scheme 92 – Endo selective product outcomes from reaction of Danishesky's diene with 222.

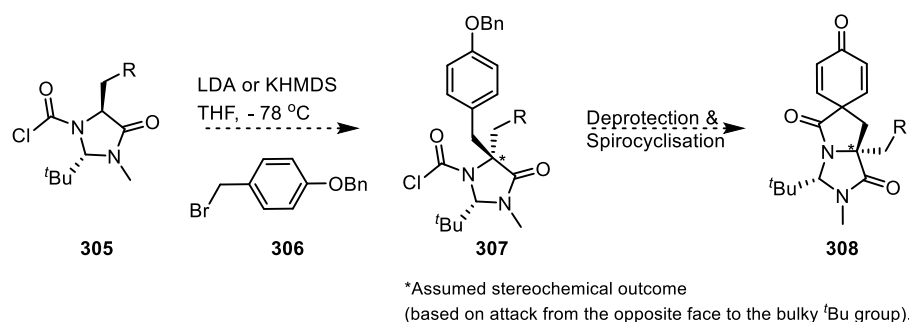
2.3.2.6 Alkylation to produce aroenate-based quaternary amino acids

Alpha-alkylations of the spirocycle **222** would allow access to a library of aroenate based quaternary amino acids. Previous work in the group found enolisation with KHMDS followed by alkylation with methyl iodide gave good results with similar imidazolidinones.¹¹³ Unfortunately, likely due to the unstable nature of the dienone and its tendency to rearomatise, applying these conditions to **222** proved unsuccessful resulting only in formation of an undesired product. By NMR, this side product showed two peaks which each integrated for 1H in the alkene region and phenolic aromatic protons. This, along with the loss of the α -proton suggests KHMDS caused elimination and rearomatisation to give the exocyclic alkene **304** (Scheme 93).



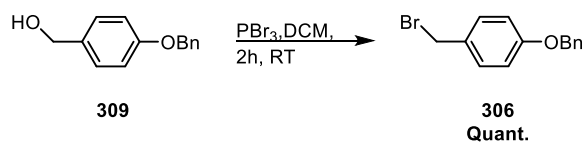
Scheme 93 – Attempted alpha-alkylation of spirocycle **222**.

An alternative route was explored in which, to prevent the risk of rearomatisation, alkylation of a library of imidazolidinones **305** was carried out with the electrophile 1-(benzyloxy)-4-(bromomethyl)benzene **306** to install the tyrosine motif in **307**. These products could then undergo deprotection and spirocyclisation to give **308** (Scheme 94).



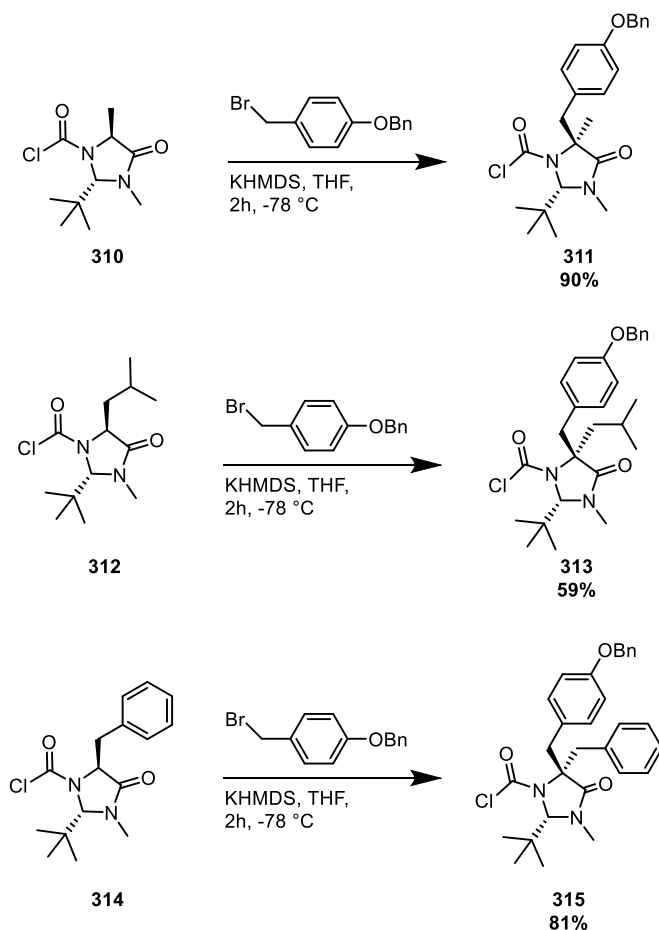
Scheme 94 – Alternative route to alpha-alkylations.

The electrophile **306** could be produced in quantitative yield by conversion of the alcohol **309** using PBr₃ (Scheme 95). Using this electrophile initial conditions were trialled using similar conditions to those previously used in the group to alkylate *N*-chloroformylimidazolidinones.¹²⁰



Scheme 95 – Synthesis of electrophile 306 using PBr₃.

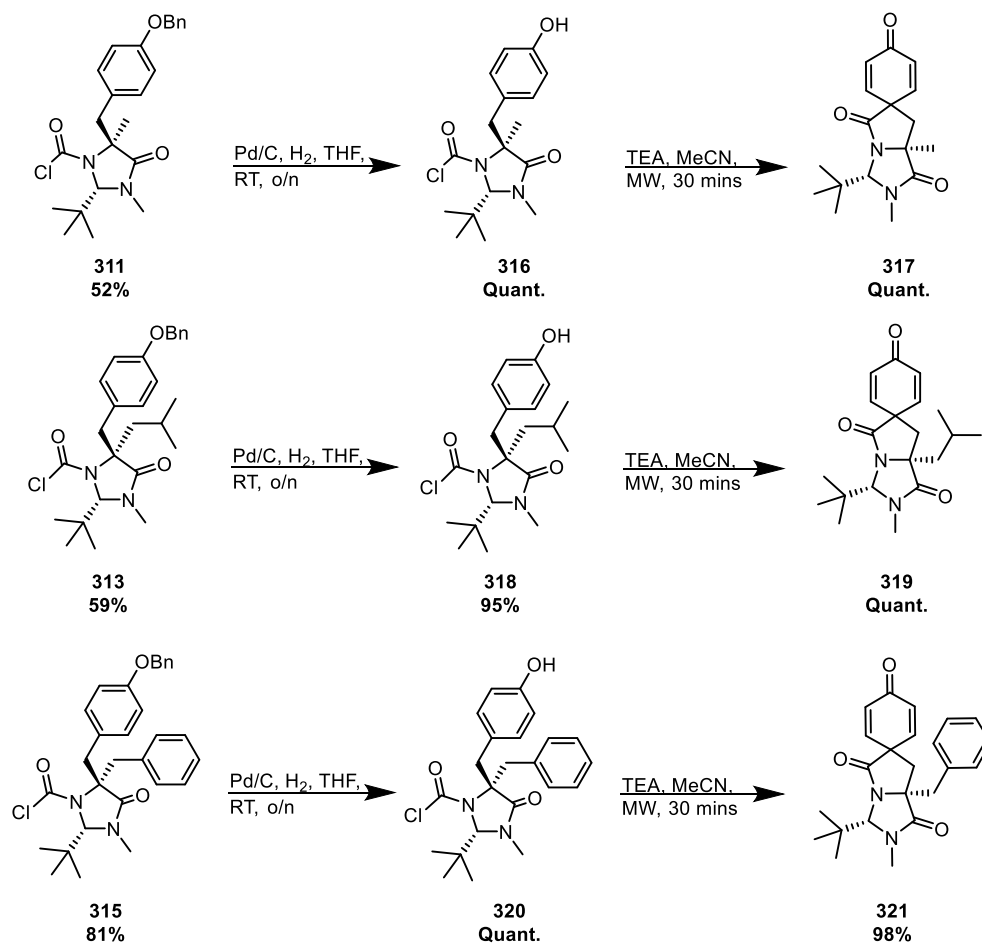
Initial alkylations were carried out by addition of KHMDS to the imidazolidinone in dry THF at -78 °C, followed by addition of the electrophile immediately afterwards. This gave a yield of 47% for the alanine imidazolidinone derivative **311**, however, using these conditions with leucine, phenylalanine and tryptophan (later abandoned due to lack of starting material) derivatives gave complex mixtures with little to no product; which may be due to decomposition of the starting material by the base prior to alkylation. Adding KHMDS to a solution of imidazolidinone and electrophile in dry THF, degassed by nitrogen gas sparging, at -78 °C resulted in a great improvement in yields; this optimisation was particularly marked for the alanine derivative **311** which showed a 43% increase in yield (Scheme 96).



Scheme 96 – Alkylations of various natural amino acid derived imidazolidinones with 1-(Benzyloxy)-4-(bromomethyl)benzene.

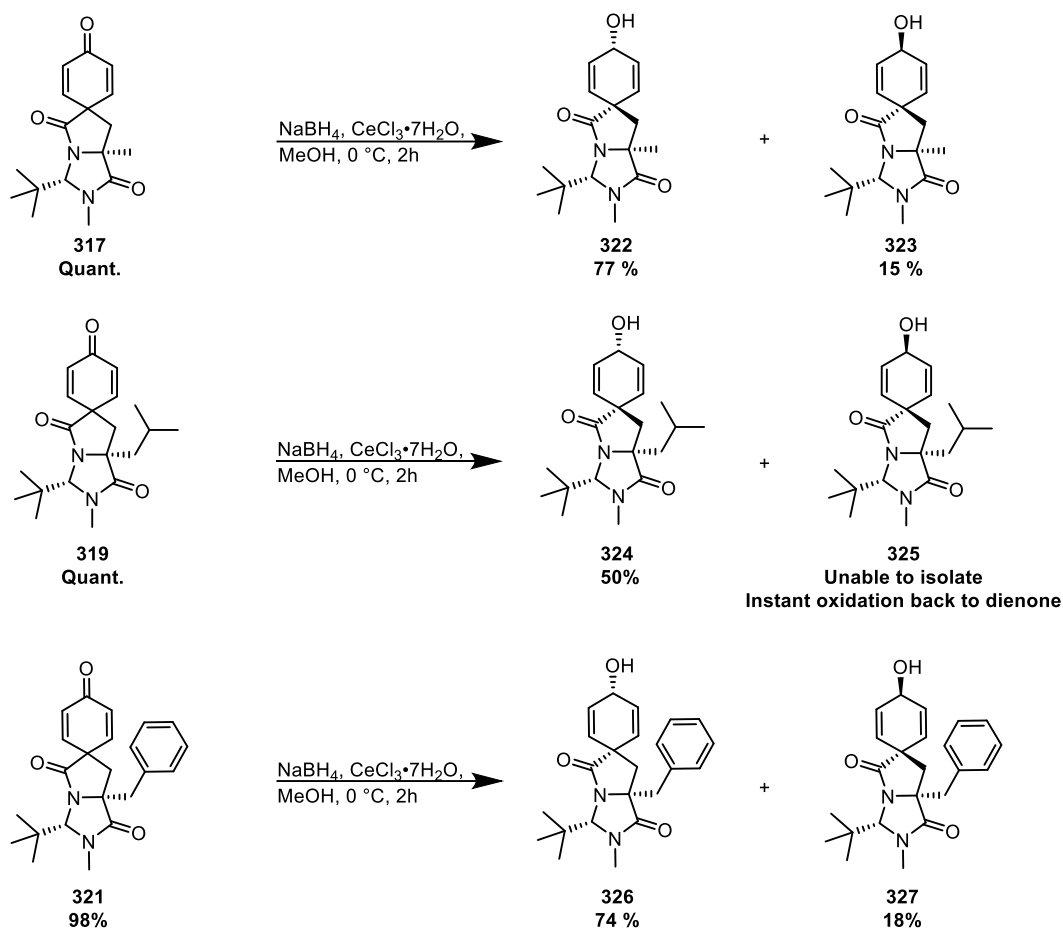
These alkylated products could then be debenzylated using reductive cleavage conditions, which proved successful in the previous syntheses, and subjected to the spirocyclisation conditions. It

was found that, with a substituent in the alpha position, extended times were required in the spirocyclisation to allow for full conversion to the products **317**, **319** and **321** (Scheme 97).



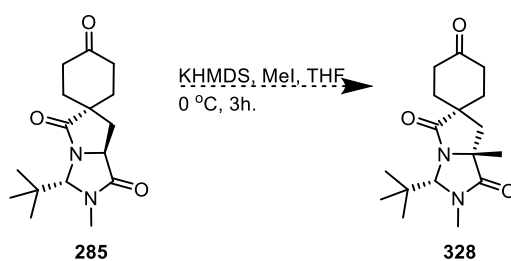
Scheme 97 – Debenzylation and spirocyclisation of alpha-alkylated imidazolidinones.

The dienones produced were subjected to Luche reduction conditions to give the dienols **322-327** (Scheme 98). It was assumed diastereoselectivity obeyed that seen in the original synthesis to give the *cis* conformation (Scheme 73); introduction of a substituent in the alpha-position appeared to give a slight increase in diastereoselectivity in the Luche reduction (Scheme 98).



Scheme 98 – Luche reductions of alpha-alkylated derivatives.

A final attempt at alkylation was attempted with the more stable analogue **285** using the original alkylation method in the hopes rearomatisation would be excluded in this route (Scheme 99). Alas, the crude reaction mixture contained many components and proved impossible to purify. With additional time, optimisation could be carried to explore the viability of this method. Alternatively, the route described in scheme 98 could be used, followed by hydrogenation of the alkenes to achieve product **328**.

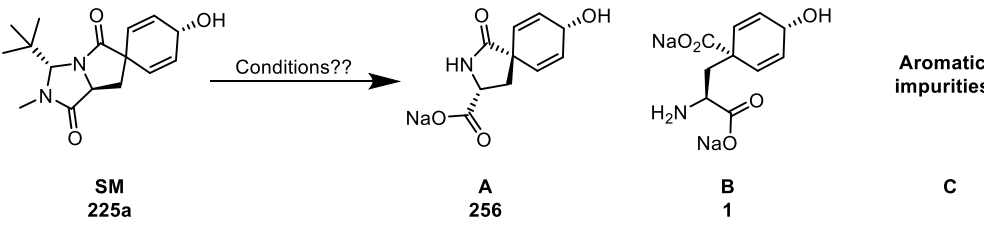


Scheme 99 – Attempted alkylation of stable dienone analogue.

2.3.3 Hydrolysis of arogenate and its analogues

Having explored several methods for the synthesis of analogues, we returned to the challenge of the final step. Since initial attempts at hydrolysis and subsequent purification proved difficult, optimising the conditions was the first task undertaken. Initially this work focused upon production of spiroarogenate **256** due to it being the more stable and thus the easier to handle substrate.

Table 3 - Exploring various bases for the hydrolysis of 9.

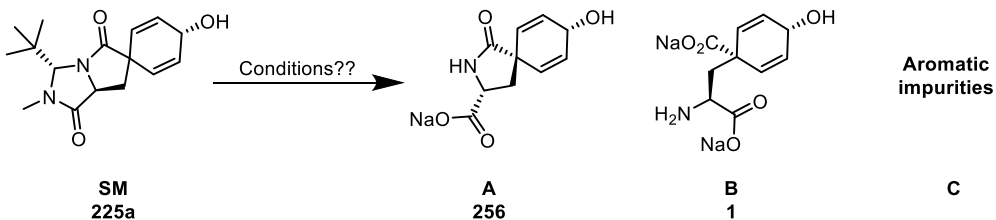
									
	Base (eq.)	Eq.	Solvent	Conc. (M)	Ratio				Comment
					SM	A	B	C	
a	Ba(OH) ₂	3	D ₂ O	0.2	52	39	-	9	Base added last
b	BaO	3	H ₂ O	0.2	63	31	-	6	Sonicated & Concentrated
c	NaOH	3	H ₂ O	0.2	27	40	-	33	Sonicated & Concentrated
d	LiOH	3	D ₂ O	0.2	-	-	-	-	Sonicated. Complex mixture
e	KOH	3	D ₂ O	0.2	50	23	-	27	Sonicated
f	Ca(OH) ₂	3	D ₂ O	0.2	94	-	-	6	Sonicated
g	NaOH/NaCO ₃	3	D ₂ O	0.2	42	22	-	36	Sonicated

All reactions performed at 30 °C, overnight.

A variety of inorganic bases were trialled to explore conversion to spiroarogenate **256** (Table 3). Barium oxide was investigated as a means of generating barium hydroxide in solution to see if this aided the reaction; however, this approach gave only similar ratios of starting material, spiroarogenate and aromatic impurities to using barium hydroxide itself (Table 3 - entries a&b). The reaction with sodium hydroxide showed reasonable conversion to spiroarogenate; however,

it also gave high levels of unwanted aromatic side products (Table 3 - entry c). Danishefsky *et al.* reported that the use of 1 equivalent of sodium carbonate in the hydrolysis of spiroarogenate increased the rate of hydrolysis. However, in our reaction, addition of this reagent resulted in a diminished yield of spiroarogenate and increased levels of aromatic impurities (Table 3 - entry g). Lithium hydroxide gave a complex product mixture which did not look particularly encouraging (Table 3 - entry d). Potassium hydroxide also appeared to increase rearomatisation whilst reducing levels of spiroarogenate (Table 3 - entry e). Calcium hydroxide gave a disappointing result with no conversion to spiroarogenate observed as well as small amounts of aromatic side products (Table 3 - entry g).

Table 4 - Exploring various solvents, equivalents & concentrations for the barium hydroxide hydrolysis of 9.

									
	Base (eq.)	Eq.	Solvent	Conc. (M)	Ratio				Comment
					SM	A	B	C	
a	Ba(OH) ₂	3	D ₂ O	0.2	52	39	-	9	Base added last.
b	Ba(OH) ₂	3	D ₂ O:dioxane	0.2	99	t	-	t	Base added last.
c	Ba(OH) ₂	3	D ₂ O:MeOD	0.2	83	14	-	3	Base added last.
d	Ba(OH) ₂	3	D ₂ O	0.4	62	32	-	6	Base added last.
e	Ba(OH) ₂	3	H ₂ O	0.1	40	47	-	13	Sonicated & Concentrated.
f	Ba(OH) ₂	12	H ₂ O	0.1	22	57	t	21	Sonicated & Concentrated.
g	Ba(OH) ₂	3	H ₂ O	0.05	61	32	-	7	Sonicated & Concentrated.
h	Ba(OH) ₂	12	D ₂ O	0.05	44	40	t	16	Sonicated & Concentrated.

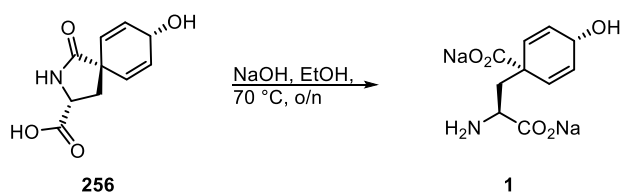
All reactions performed at 30 °C, overnight. t – trace (<1%).

Confident in the knowledge that barium hydroxide was the most efficient base for the hydrolysis, the effect of solvents, reagent equivalents and concentrations were explored. Comparing to the best conditions so far (Table 4 - entry a), it was hoped the investigations would result in an increase of conversion to spiroarogenate whilst reducing conversion to aromatic impurities (Table 4). It was thought that the addition of organic solvent in the hydrolysis could aid solubility of the starting material and therefore allow the reaction to proceed more efficiently; however, the addition of dioxane (Table 4 - entry b) severely inhibited the reaction with only traces of conversion observed. The addition of methanol, which is more similar in polarity to water, also hindered the hydrolysis (Table 4 - entry c); nevertheless, some conversion was observed. It was concluded that the addition of organic solvents was detrimental to the hydrolysis and that future reactions would focus on aqueous systems only.

Increasing the concentration of the reaction (Table 4 - entry d) resulted in only minor changes in the product ratio and if anything impeded the reaction slightly. On the other hand, decreasing the concentration (half compared to the original conditions) promoted conversion of the starting material (Table 4 - entry e & f). Increasing the number of equivalents of base from 3 to 12 (Table 4 - entry f) gave higher levels of spiroarogenate but also undesired aromatics. However, further dilution (fourfold compared to the original conditions) did not further increase conversion as anticipated. Instead, the product to starting material ratio began to deteriorate again (Table 4 - entry g & h).

Presently, the optimum hydrolysis conditions are barium hydroxide (3 or 12 eq.) in water (0.1 M) at 30 °C. During the above investigations, it was found that the solubility of barium hydroxide in the reaction medium was poor and thus sonication of the base suspension was carried out to increase dispersion prior to addition of **225a** which appeared to aid the reaction.

As mentioned earlier, spiroarogenate was hydrolysed to aroenate by Danishefsky *et al.* in the final step of their aroenate synthesis. Therefore, repeating their conditions of sodium hydroxide in ethanol at 70 °C was initially attempted on crude spiroarogenate material obtained from hydrolysis of the imidazolidinone (Table 5 - entry a).³⁶

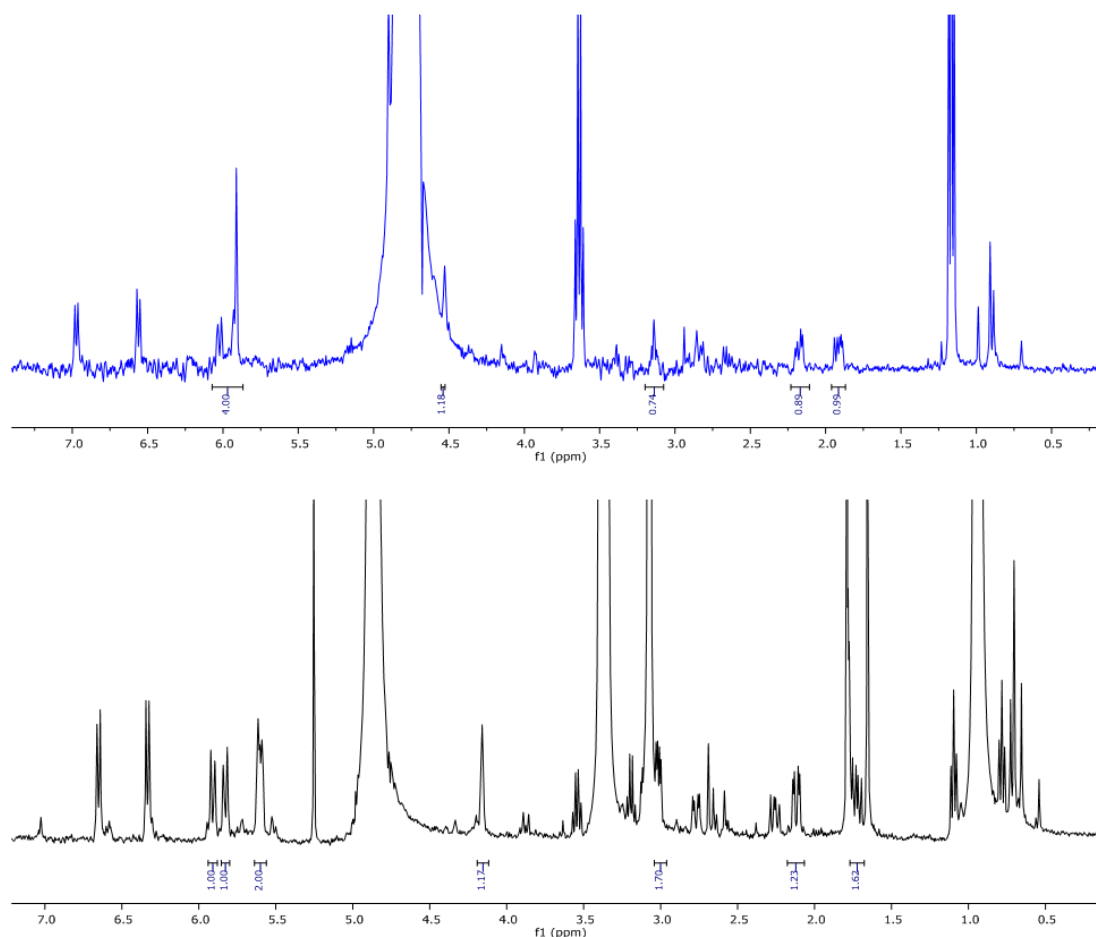


Scheme 100 - Hydrolysis of spiroarogenate to aroenate.

The crude NMR spectrum from this reaction in D₂O matched very closely to the NMR of synthetic arogenate produced by Danishefky *et al.* (**Error! Reference source not found.**):³⁶

¹H NMR (400 MHz, Deuterium Oxide) δ 6.07 – 5.87 (m, 4H), 4.53 (m, 1H), 3.14 (m, 1H), 2.18 (dd, *J* = 14.2, 5.3 Hz, 1H), 1.96 – 1.87 (m, 1H). – **this work.**

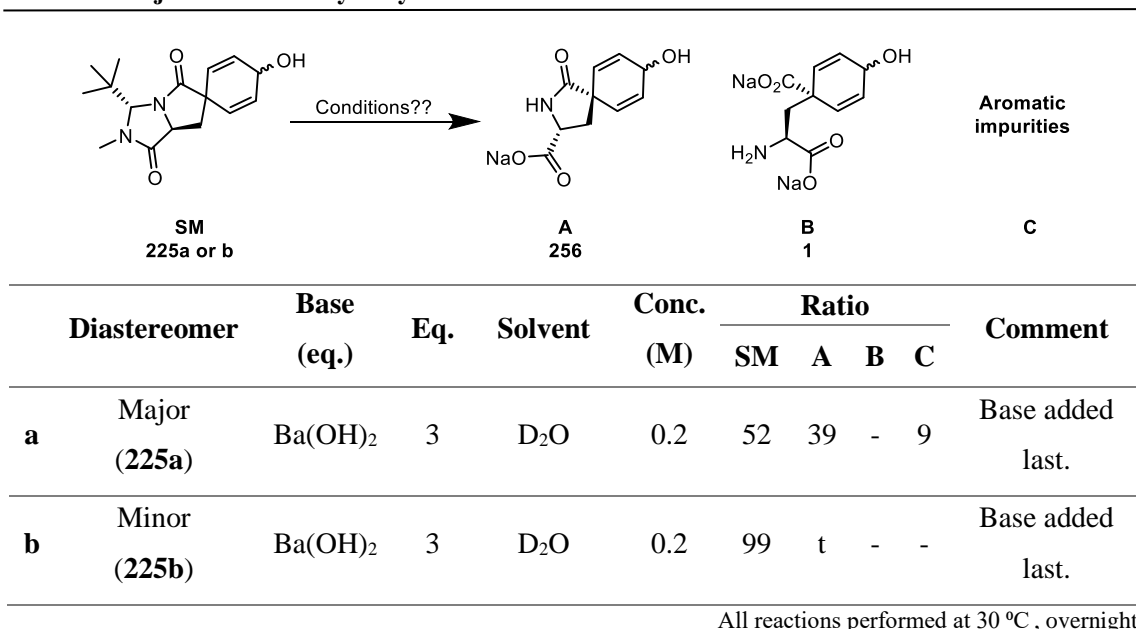
¹H NMR (270 MHz, Deuterium Oxide) δ 6.05 (d, 1H), 5.96 (d, 1H), 5.94 (br s, 2H), 4.55 (m, 1H), 3.07 (dd, 1H), 2.15 (dd, 1H), 1.88 (dd, 1H). – **Danishefky *et al.***³⁶



carbonyl - Arogenate in D₂O (blue) and CD₃OD (black).

Upon repeating the reaction on a small amount of >90% pure spiroarogenate (20 mg), isolated from purification by reverse phase chromatography (0-60% acetonitrile in water), no formation of arogenate was observed after 48h at 70 °C. A further equivalent of base was added in the hope of aiding arogenate production; however, only aromatic side products were observed. Interestingly, after the addition of a small amount of water (10% by volume with respect to ethanol) and stirring for a further 16h, near complete conversion of starting material was observed, suggesting that water was essential to this process.

Hydrolysis of the minor spirocycle **225b** was also attempted to determine whether use of a particular diastereomer would affect the rate of hydrolysis (Table 5). Hydrolysis of **225b** would potentially allow access to *epi*-spiroarogenate/arogenate.



Only minute traces of *epi*-spiroarogenate were observed after subjecting the minor diastereomer to the hydrolysis conditions previously optimised for the major, suggesting that the rate of hydrolysis for the **225b** is significantly slower.

A large amount of time was spent developing methods for purification as the small, polar and unstable properties of spiroarogenate and arogenate, along with the large amount of salts present and the lack of solubility in organic solvents rendered this a difficult task. Since normal phase column chromatography was not possible, four other techniques for purification were explored.

Use of C18-reversed phase silica gel as a stationary phase was the first method explored. This allowed us to gain a better understanding of what exactly was present in the crude mixture but there were several issues that rendered the technique inadequate for purification. Carrying out the purification with a gradient of 0-100% H₂O in methanol or acetonitrile gave little retention and caused extremely quick elution of a mixture of products. In reverse phase chromatography the solvent system is often spiked with an acid, such as TFA, acetic or formic acid, to aid with retention and peak shape for ionisable or strongly polar analytes. This retention is achieved by the formation of an ion pair which increases the hydrophobicity and in turn provides increased

retention. Several attempts were carried out using these various ion-pairing agents.* However, due to the acidity of these additives, major issues with rearomatisation were observed; both aroenate and spiroaroenate are known to convert to phenylalanine under mild acid conditions.^{6,121}

Purification carried out with a gradient of 0-100% H₂O in MeOH (spiked with 0.1% NH₄OAc [w/w]) gave the most promising results. Traces of aroenate were identified in one fraction, alongside several other co-eluted species. Among the compounds isolated were the imidazolidinone protected aroenate derivative **329**, which may be of interest as a semi-stable source of aroenate, as well as the imidazolidinone protected tyrosine derivative **330** and the amine **331** (Figure 13).

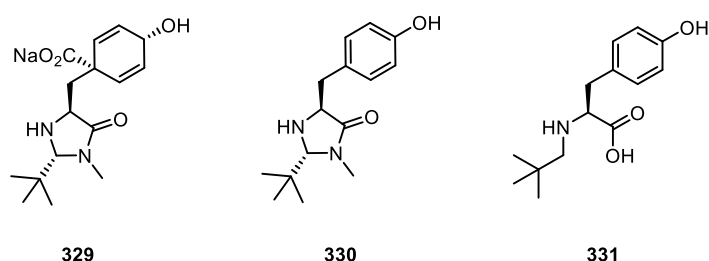
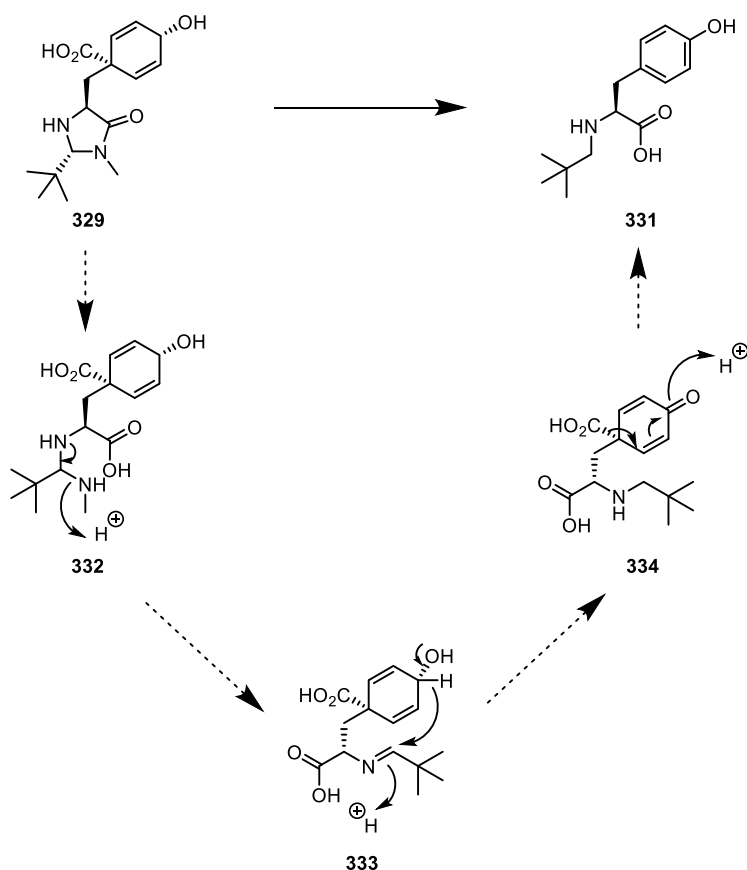


Figure 13 - Other products isolated from the hydrolysis purification.

Hydrolysis of only the lactam ring and not the imidazolidinone accounted for the observation of **329** and **330**. From **329**, a mechanism of imidazolidinone hydrolysis followed by disproportionation may explain product **331** (Scheme 101).

* With thanks to Derick McCormack (Syngenta) and Daniel Leonard (UoB) for their guidance and assistance in these protocols.



Scheme 101 - Possible mechanism for formation of 331 from 329.

Attempts using several reverse-phase HPLC columns also proved fruitless; with several columns being damaged by the basic nature of the crude sample as any acid for neutralisation or retention on the column caused rearomatisation issues.

Ion exchange chromatography –

The next method trialled was ion exchange chromatography; this technique had been used to purify aroenate in both the two previously reported syntheses and the natural product isolation.^{6,36,37,122} Efforts to purify using Dowex-chloride or Sephadex A-25, using methods set out in the literature, proved ineffective. All attempts resulted in little to no retention with elution of all products collectively. This may be due to the large salt concentration present in the crude mixture preventing effective binding of the negatively charged free acid. To obtain viable levels of retention, a very large dilution of the crude material was required which is impractical for our purposes. Another major disadvantage of ion exchange chromatography is the need for low eluent flow rates resulting in purification being a lengthy process and a large number of fractions to collect.

Further exploration of ion exchange methods was carried out using a Dionex 3000 system to carry out automated ion exchange chromatography. An IonPac AS11 (250 x 4.0 mm) column showed

retention and optimisation focused upon the pH of the buffer system to optimise separation. Samples of phenylalanine, tyrosine, pure spiroarogenate and crude spiroarogenate were all run independently for comparison. A crude arogenate sample was also tested but this was found to contain multiple components, so work focused on achieving purification of spiroarogenate before attempting the more complex arogenate mixtures.

A 10 µl injection of each sample was run at a gradient of 10-90% buffer in water over 10 minutes. Using ammonium bicarbonate (0.1M) buffered at pH 9.0 gave the best separation however the separation proved inadequate. As can be seen below both phenylalanine and tyrosine have a longer retention time but streak off the column. The pure spiroarogenate produces a sharp peak at 2.42 minutes but on attempting purification of the crude reaction mixture another component overlaps with spiroarogenate preventing a clean separation from being achieved (Figure 14).^{*} Due to the lack of separation seen here and the inability to replicate the literature findings, ion exchange chromatography was deemed ineffective for purification.

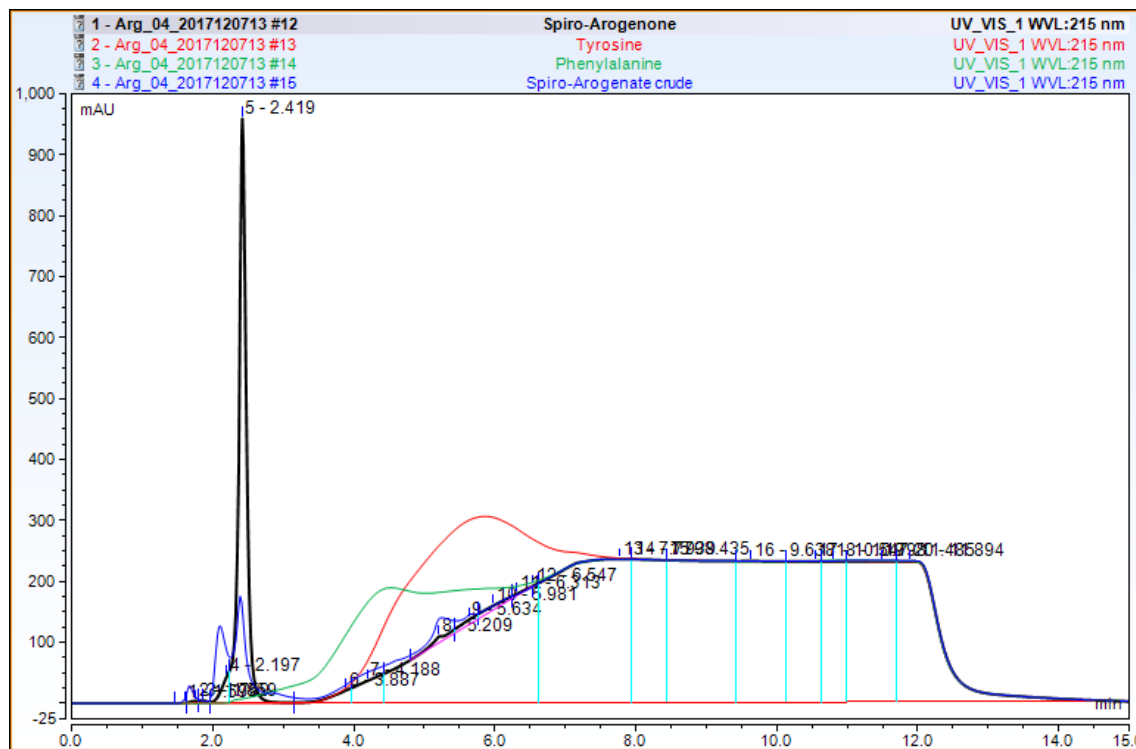


Figure 14 – Ion exchange trace using ammonium bicarbonate (0.1M) buffered at pH 9.0.

HILIC (Hydrophilic interaction liquid chromatography) –

HILIC is a variant of normal phase chromatography in which a hydrophilic stationary phase with reverse-phase type eluents. Despite using reversed-phase eluents the gradient begins with the organic solvent, typically acetonitrile. It is known to be particularly useful in separations of amino acids; hence it was thought that it may be suitable for this situation. It is also known to be an

^{*} With thanks to Mark Brittin and Loretta Bradbury (Syngenta) for their help with this work.

alternative method for purification of analytes which elute in the void volume in reserved-phase chromatography, as was experienced in this project.^{123,124} A Waters XBridge BEH Amide column was used with a gradient of 20-50% ammonium bicarbonate, buffered to pH 7.5 with glacial acetic acid, in acetonitrile as the optimised method. The various peaks were identified by running separate injections with pure spiroarogenate, phenylalanine and tyrosine. This technique gave some separation though very tight and unsatisfactory for purification; particularly on a larger scale (Figure 15).*

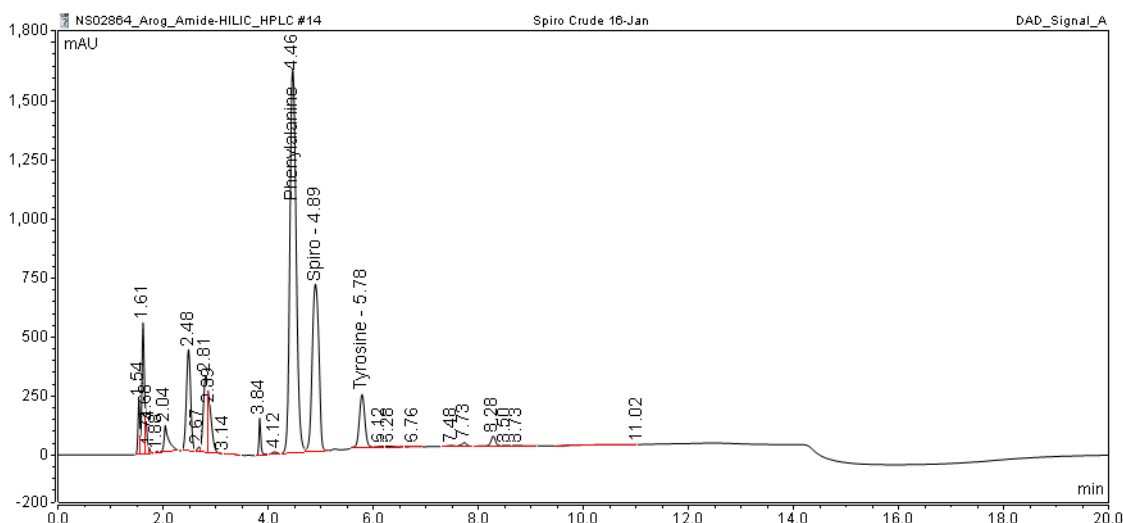


Figure 15 – HPLC trace using HILIC conditions.

Hypercarb –

A Hypercarb column is a stationary phase of porous graphitic carbon (PGC) and is usually used under reverse phase conditions. Separation occurs based on hydrophobicity along with two other interlinked mechanisms of interactions. The first of which is the induction of a charge on polarisable surface of graphitic carbon. The second works on how close a fit the molecule has with the graphitic carbon. The more planar the molecule the more it can interact and induce a charge across the PGC surface providing an increase in retention.¹²⁵ For example a planar molecule would allow for more interactions between the analyte and graphite surface in comparison to a molecule with more 3D structure.

* With thanks to Mark Brittin and Loretta Bradbury (Syngenta) for their help with this work.

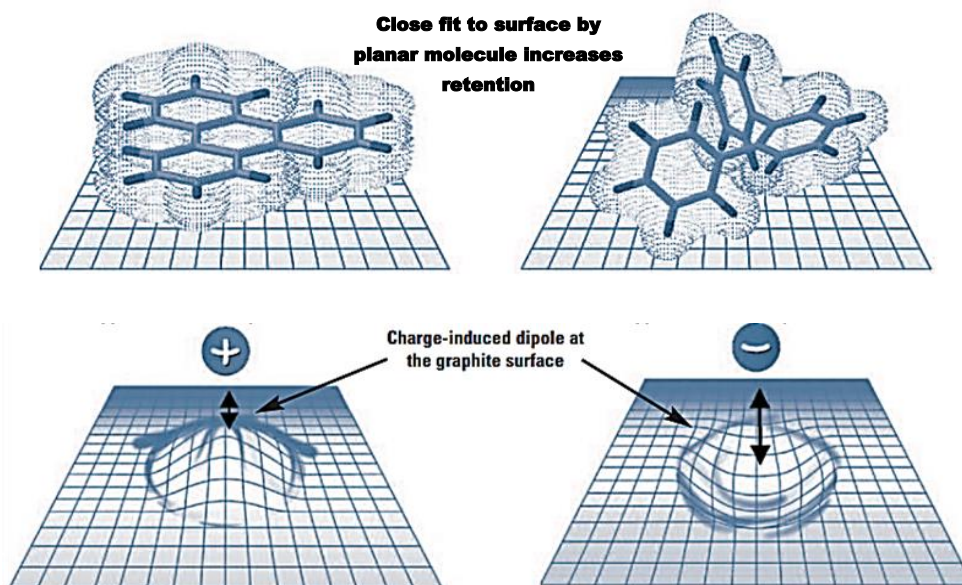


Figure 16 – Hypercarb mechanism of interaction.¹²⁶

Due to the unique surface of the PGC, the Hypercarb column user guide states its benefits include¹²⁷ –

- Excellent for the separation of highly polar compounds
- Stability across the entire pH range 0-14, due to unreactive surface (Figure 17)
- Excellent batch-to-batch reproducibility
- Homogeneous crystalline surface (Figure 17)
- Enhanced selectivity for closely related compounds, including geometric isomers and diastereoisomers (Figure 18)

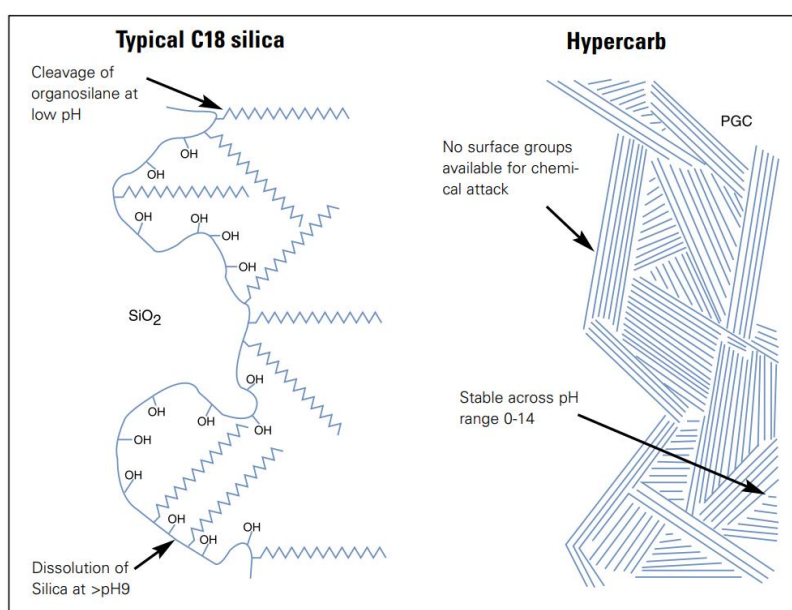


Figure 17 – Comparison of Silica surface to PGC.¹²⁵

An excellent example of the Hypercarb capabilities is demonstrated in the Hypercarb user guide in which the separation of a mixture of 20 underivatised amino acids is carried out (Figure 18). This highlights both the ability of PGC to retain polar molecules and also separate out several closely related compounds.¹²⁵

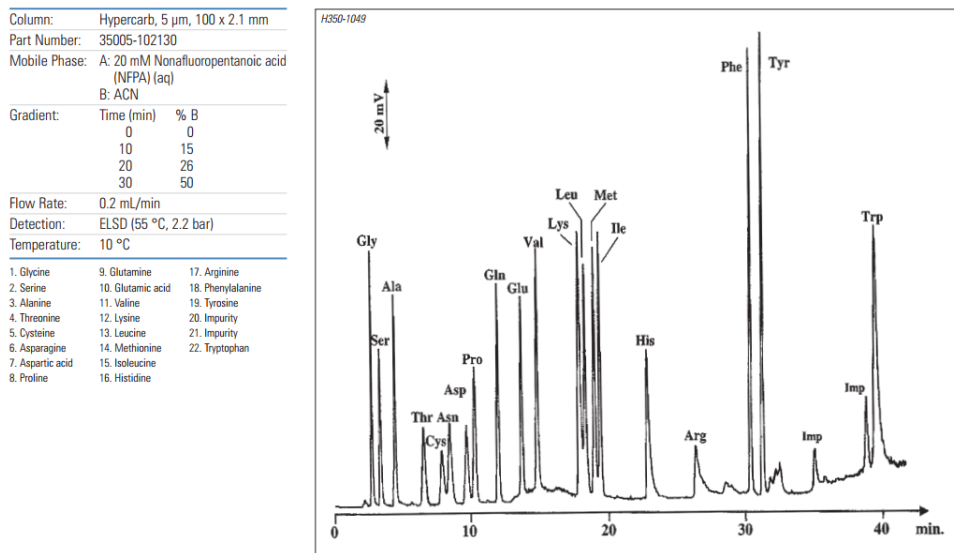


Figure 18 – Separation of 20 underivatised amino acids on a Hypercarb column.¹²⁵

Encouragingly, the initial runs carried out on the Hypercarb column, with a gradient of 0-100% MeCN in 100 mM ammonium bicarbonate buffer, provided excellent retention and separation. A mass ion for spiroarogenate was observed for the peak around 18 minutes (Figure 19).*

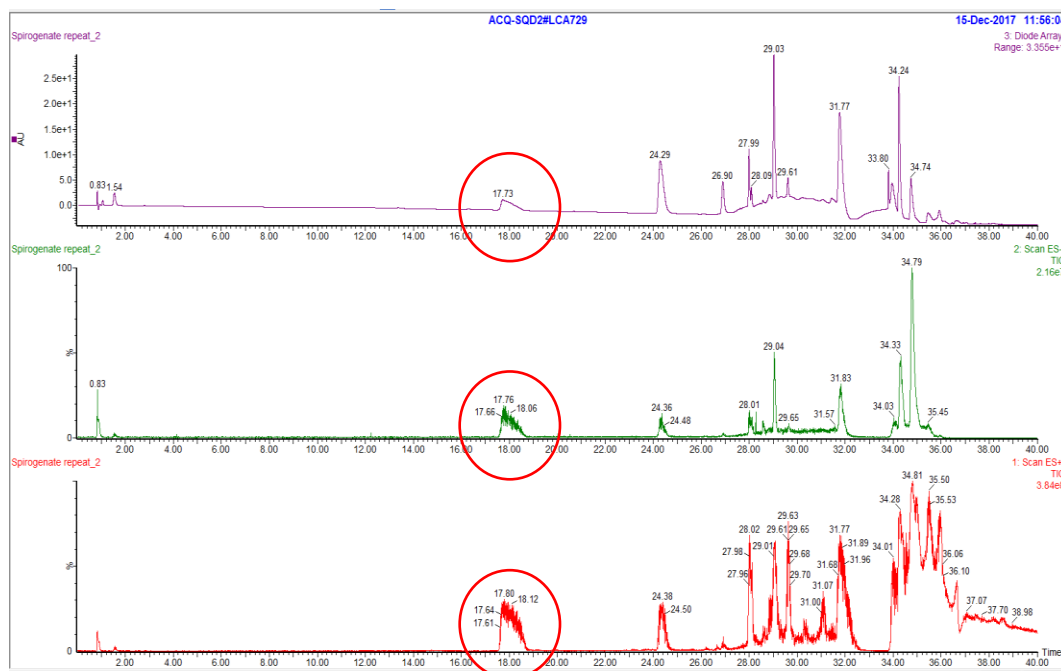


Figure 19 – initial Hypercarb HPLC trace.

* With thanks to Dianne Irwin for her help with this work.

Upon moving to a semi-preparative scale column and increasing loading, to lessen the number of runs, the retention time dramatically reduced and streaking occurred. Optimisation of conditions found that increasing the rate of the eluent gradient provided sharper peaks and allowed for the isolation of 4 major peaks which were found to be arogenate **1**, spiroarogenate **256**, arogenate imidazolidinone **329** and a tyrosine side product **331** (Figure 20).

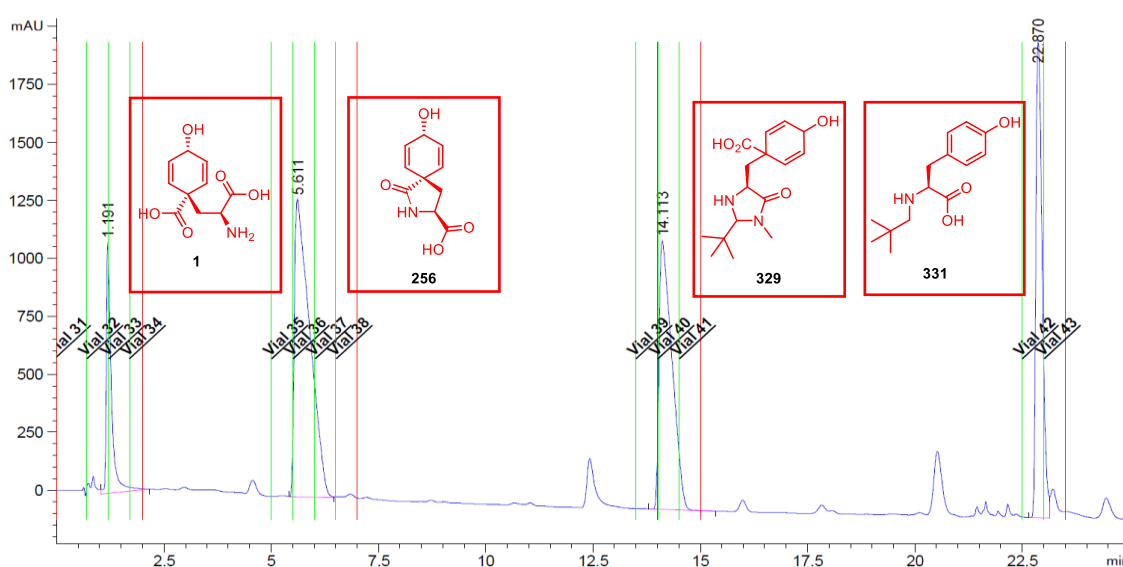


Figure 20 – Semi-preparative HPLC showing relevant peaks and corresponding compounds.

A large problem in the isolation of these types of compounds is the sensitivity to pH. This was demonstrated during the isolation of spiroarogenate, where upon obtaining NMRs at several points in time decomposition could be seen. It was determined that the NMR sample was around pH 5, which was thought to be caused by contamination with acid during use of a communal freeze dryer. This slight pH change led to a 60:40 ratio of spiroarogenate to phenylalanine in only two hours (Figure 21).

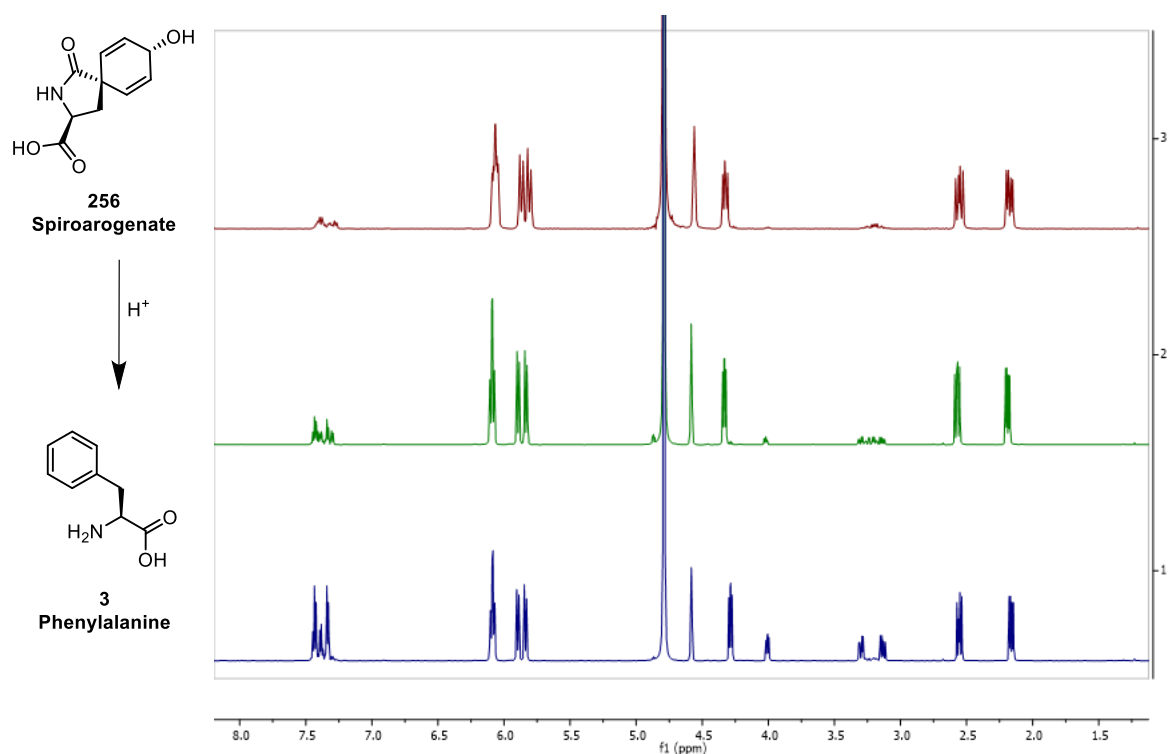
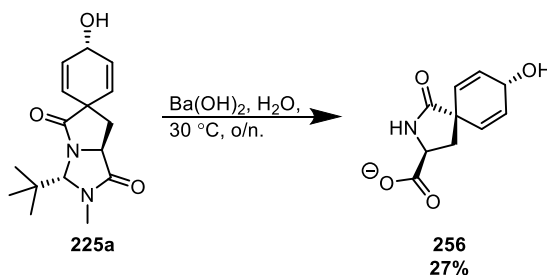


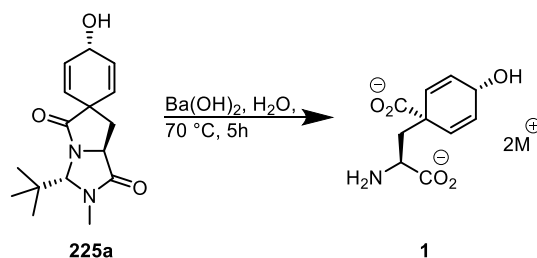
Figure 21 – Decomposition of spiroarogenate, 256, to phenylalanine, 3, over two hours.

To remove any issues of contamination an otherwise empty, clean freeze dryer was used for all future purifications. The reaction was then repeated using the optimised conditions and spiroarogenate was isolated in 27% yield with no sign of instability over the course of a month exposed to air (Scheme 102). Full NMR data, high resolution nanospray mass spectrometry, specific rotation and circular dichroism data have been obtained for spiroarogenate, **256**.



Scheme 102 – Hydrolysis to spiroarogenate, 256, using optimised conditions.

During the HPLC runs it became obvious arogenate, **1**, was also being produced directly from the spirocycle, **225a**, rather than stepwise via spiroarogenate, **256**. A quick optimisation found using an increased heat, 70 °C, with a reduced time of 5 hours gave the largest conversion to arogenate, **1** (Scheme 103). A noteworthy observation is that following the repeated use of barium hydroxide reaction conversion began to reduce. It was proposed the top layer of barium hydroxide may have reacted with the air to produce traces of barium carbonate which catalysed the reaction. This may have been the reasoning behind the addition of sodium carbonate in the Danishefsky *et al.* arogenate synthesis where it was found to also catalyse their hydrolysis conditions.³⁶



Scheme 103 – Optimised hydrolysis of arogenate, 1, from spirocycle, 225a.

During several attempts at purification of arogenate another issue of rearomatisation arose. The initial test purification produced stable arogenate, however, all further attempts resulted in moderate levels of rearomatisation, around 50% (Figure 22 – circled in red). It was discovered that collection of the product fraction without a minor peak observed slightly before the arogenate peak resulted in instability. By ^{13}C NMR this peak corresponded to carbonate salts which appear to stabilise arogenate.

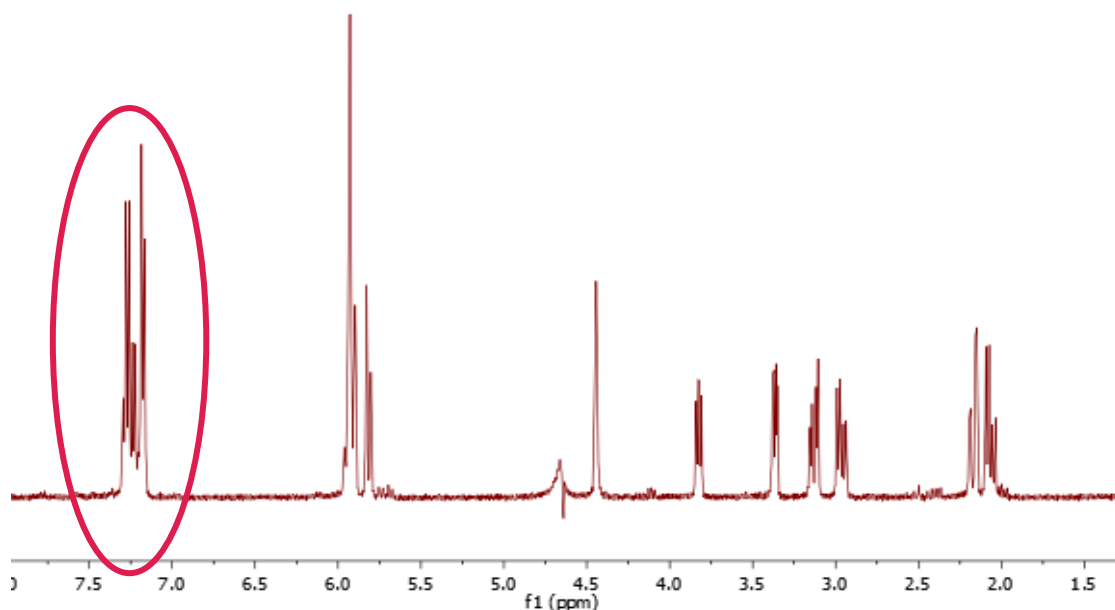


Figure 22 – Rearomatisation of purified arogenate.

Since arogenate is unstable as the free acid it was decided collection with these salts would be preferable. Both barium and sodium carbonate salt additives were trialled to compare product stability. Sodium carbonate, most likely the salt eluting with arogenate, was easier to handle due to better solubility and also resulted in minimal rearomatisation following standing in solution for 2 days.

With the knowledge that sodium carbonate provided product stabilisation, 1 mL of 1M sodium carbonate was added to each collected HPLC fraction to ensure saturation. However, upon reviewing the ^1H -NMR, splitting of all of the peaks was observed as though two components were

present. It was proposed these were two different salt forms as arogenate is known to provide very different NMRs based upon the counterion and pH.⁶ As an ammonium bicarbonate buffer was used there was the possibility of three different salt forms; ammonium, barium or sodium. It was decided to switch to a 10 mM sodium bicarbonate/carbonate buffer (pH = 9) to remove the possibility of the ammonium salt formation, whilst also providing an easier method for addition and control of the salt present. Unfortunately, switching to this sodium salt buffer did not remove the splitting seen by NMR suggesting the two components were the barium and sodium forms of arogenate. This observation of multiple salt forms was also noted in the hydrolysis of arogenate analogues (Chapter 2.3.2). To confirm this theory approximately 10 equivalents of sodium carbonate was added to the available purified 3-methyl arogenate in solution in an attempt to observe a shift in the equilibrium to the sodium salt. This resulted in a change of NMR ratio from a 60:40 to a 80:20 mixture of the salts (Figure 23).

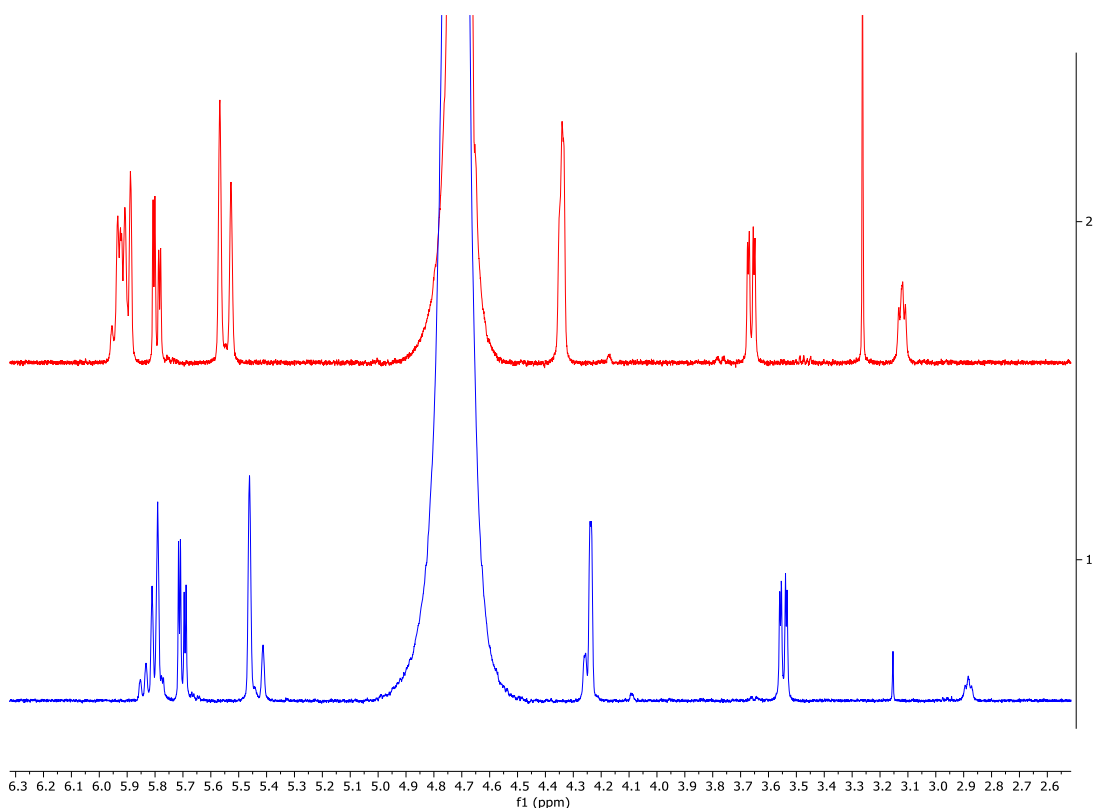


Figure 23 – Addition of sodium carbonate to produce a shift in salt ratios.

Due to the inclusion of sodium carbonate needed for stabilisation a weight-based yield could not be established. The instability of arogenate, particularly in the presence of acid, meant that most common D₂O soluble quantitative NMR standards could not be used. A standard that could be easily removed from the arogenate which is only completely soluble in water was also desired. For these reasons, ethanol was chosen as a standard for these compounds as it posed no issue of incompatibility with arogenate, would be water soluble, easy to handle and could be easily removed *in vacuo*. A 5% ethanol standard was checked against a known amount of maleic acid

and gave an error of >2%. The accuracy in the use of an ethanol standard was also confirmed by comparing the use of a 5% ethanol stock by Gilson pipette solution against the common standard of dimethyl sulfone with an accurate balance. This was carried out with reference to the fully saturated and therefore stable spiroarogenate analogue (Section 2.3.2.4.1). During purification the sample had become contaminated with an unknown salt resulting in being unable to calculate a yield based on weight. From the known total weight, a 20 mg amount was taken and to it was added the standard assuming 100% purity. Both the ethanol stock solution (0.5 eq.) and the dimethyl sulfone (1 eq.) showed the same 42% ($\pm 1\%$) concentration of product, showing consistency in the method.

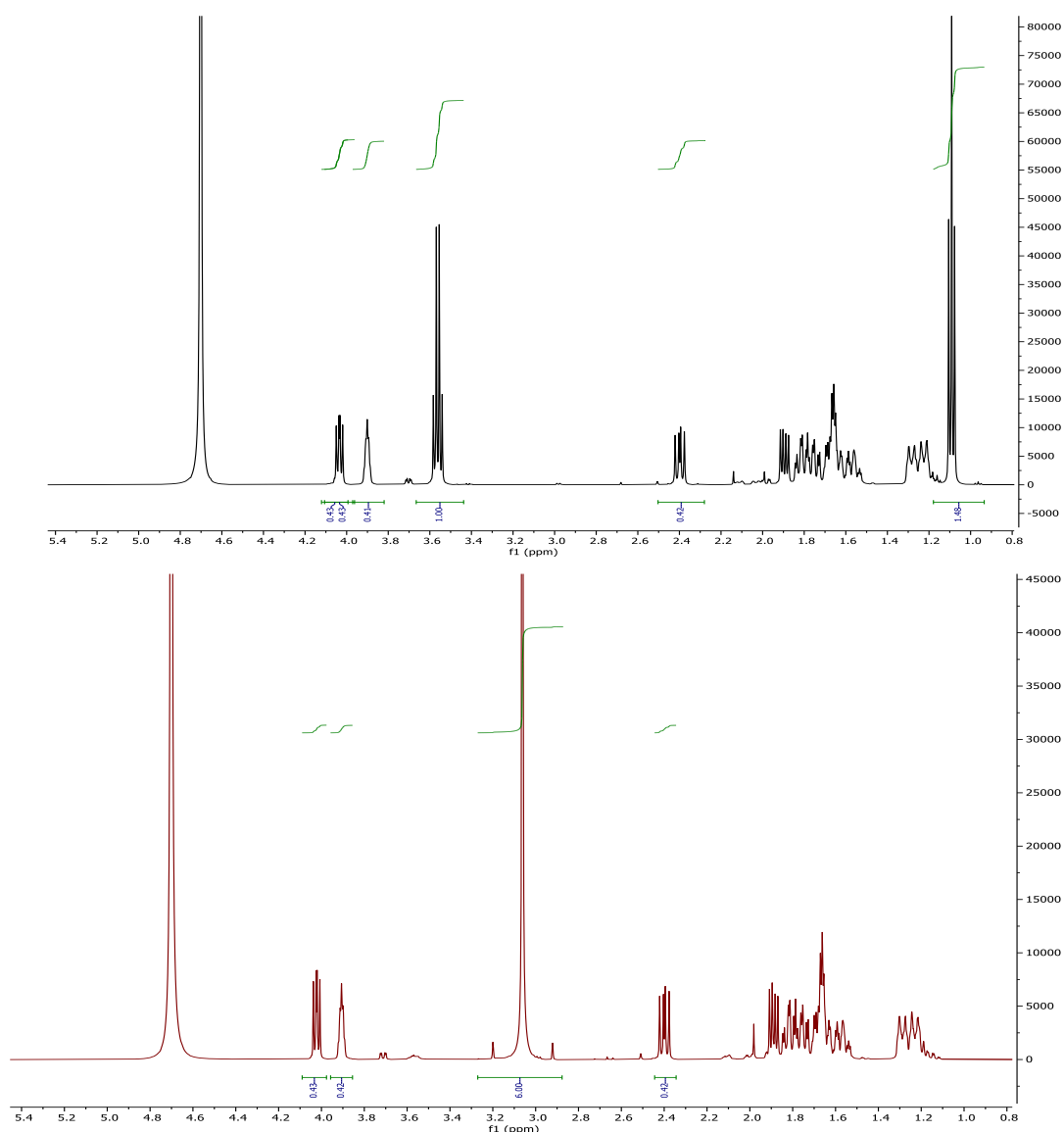


Figure 24 – Comparison of Ethanol standard (black – top) to dimethyl sulfone standard (red – bottom) on a stable spiroarogenate analogue.

Analysis of the crude reaction mixture with an ethanol standard showed around 55% conversion to arogenate and initial purifications, before stabilisation was achieved, gave yields calculated by

qNMR of around 35%; however, several further hydrolysis attempts with sodium carbonate stabilisation gave yields in the range of 12-15%. Investigation into this drop in yield found that the starting material appeared to have undergone partial oxidation back to the dienone (Figure 25).

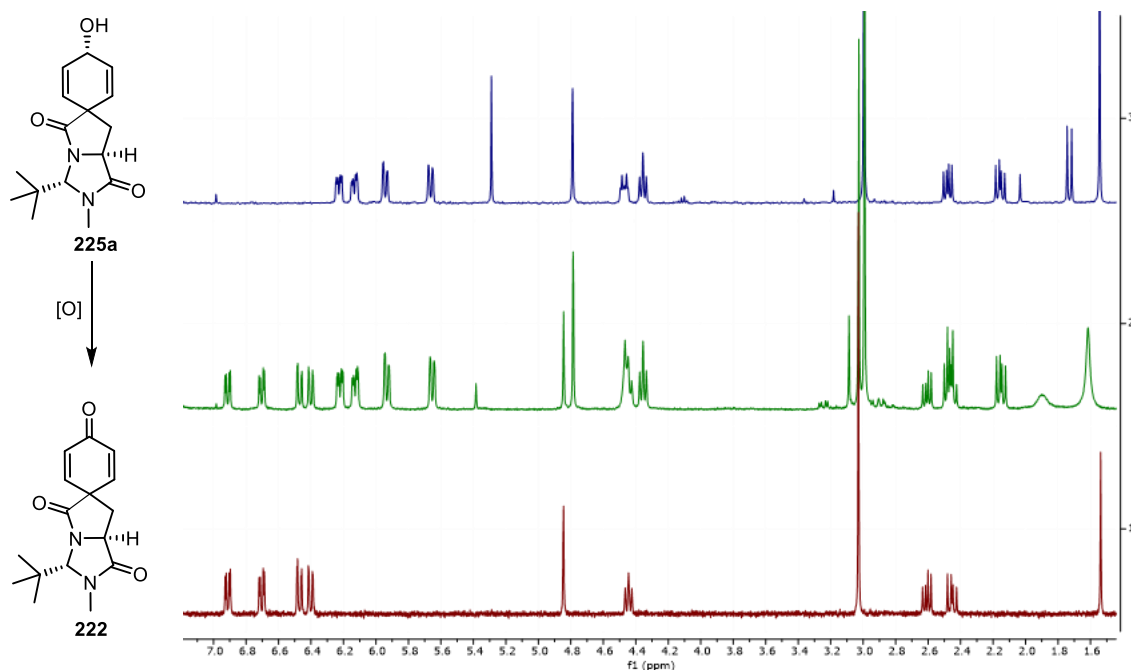
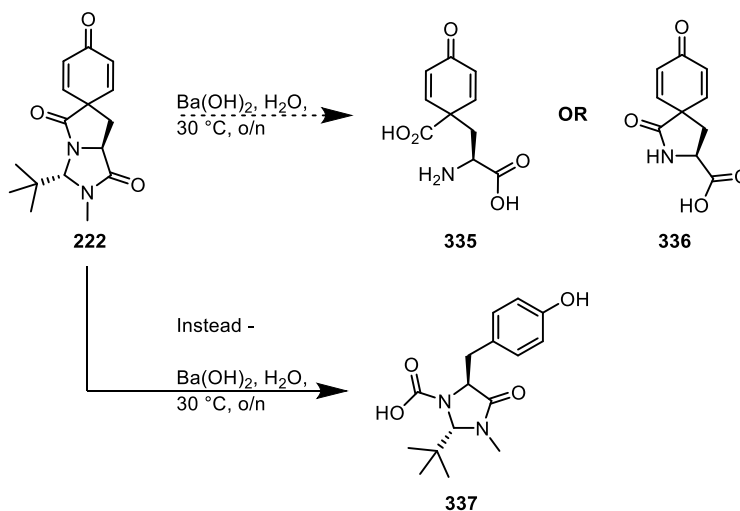


Figure 25 – Dienol conversion to dienone following months of exposure to air.

An attempt was made to hydrolyse the dienone **222** to arogenate or spiroarogenate derivatives **335** or **336**. However, the rearomatised carbamate **337** was formed, most likely due to attack of the lactam ring by a hydroxide anion followed by rearomatisation (Scheme 104). This may be the cause behind the drop in yield of arogenate during later hydrolyses; as more rearomatised side products would be produced when the dienol material contaminated with dienone **222** was hydrolysed.



Scheme 104 – Attempted hydrolysis of dienone **222**.

Upon obtaining a fresh batch of starting material **225a** and using the sodium carbonate buffer stabilisation method following hydrolysis, a 41% yield of **1** was calculated by qNMR using a 5% standard stock solution of ethanol. Full NMR data, high resolution nanospray mass spectrometry, specific rotation and circular dichroism data have been obtained for aroenate, **1** (Figure 26). The total synthesis of aroenate has been realised in seven steps with an overall yield of 19.6%.

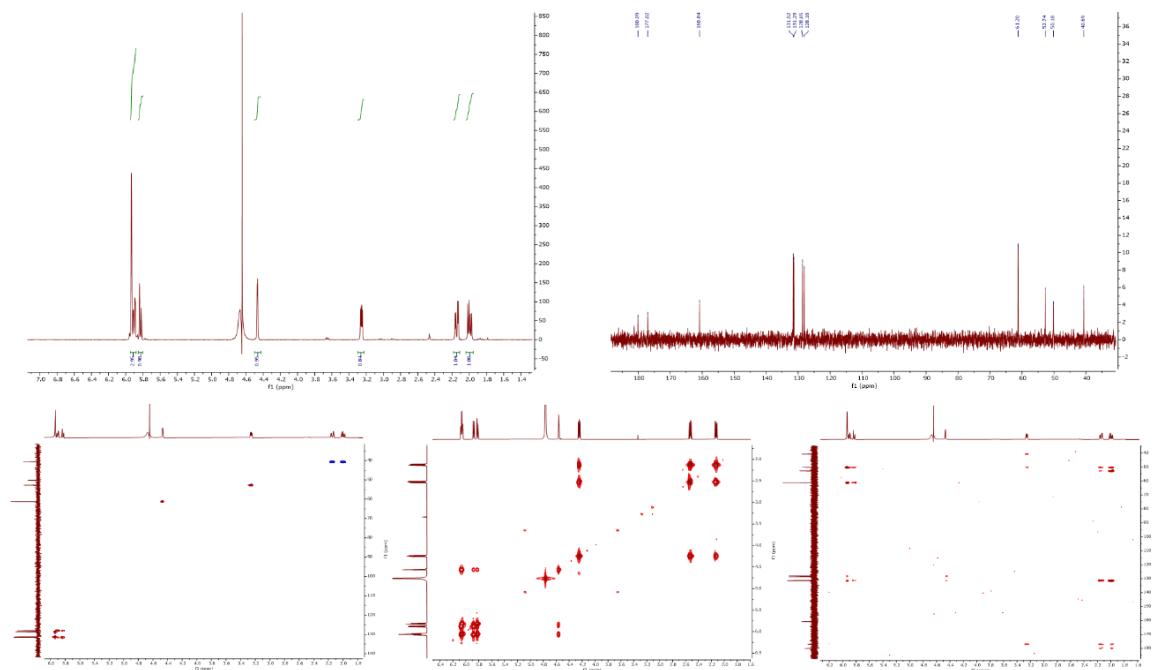
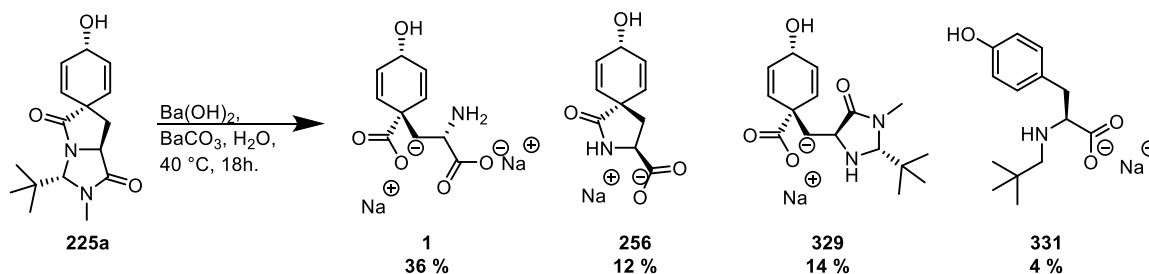


Figure 26 – Full NMR data for aroenate, 1.

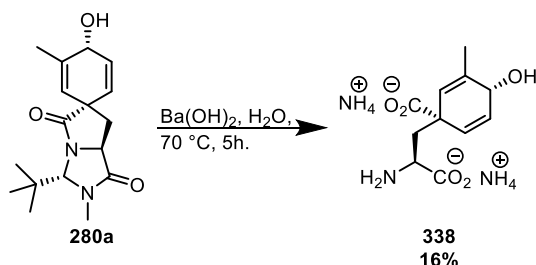
Using a compromise in temperature and time conditions in the hydrolysis, 40 °C for 18 hours, reasonable amounts of both aroenate **1** and spiroaroenate **256**, along with some of the imidazolidinone protected aroenate **329**, could be generated in the same reaction with only minimal amounts of the rearomatised side product **331** (Scheme 105). These conditions would be used for future analogues to provide both derivatised natural products from a single reaction.



Scheme 105 – Yield of aroenate 1, spiroaroenate 256, imidazolidinone protected aroenate 329 and aromatic side product 331 from the hydrolysis reaction at 40 °C for 18 hours calculated using an ethanol standard for qNMR.

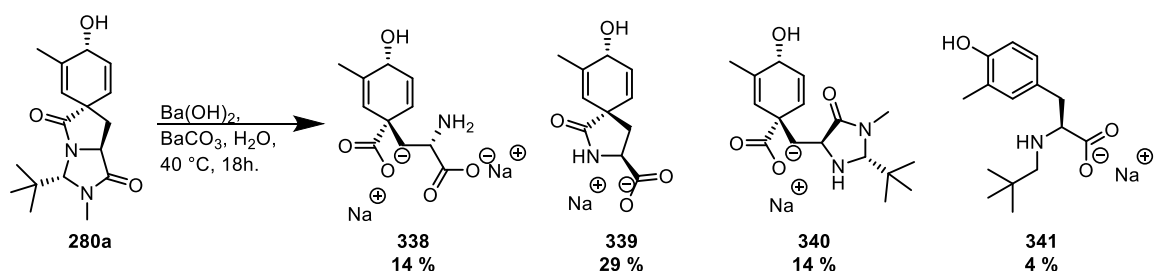
2.3.3.2 Hydrolysis of 3-Methyl Derivative

Hydrolysis produced 3-methyl aroenate, **338**, in 16% isolated yield. The product appeared to have improved stability compared to aroenate with <10% rearomatisation in the isolated product NMR.



Scheme 106 – Hydrolysis to 3-methyl aroenate.

The reaction was then repeated with the addition of sodium carbonate to prevent decomposition. The 40 °C barium hydroxide hydrolysis conditions were used to produce both natural product analogues in the same reaction (Scheme 107).

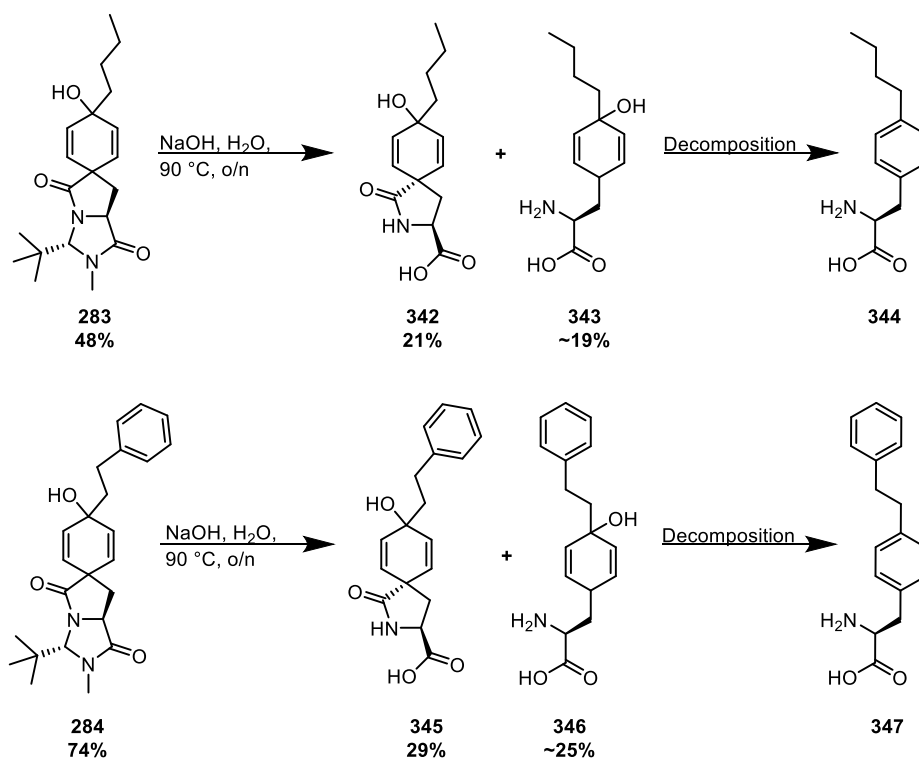


Scheme 107 - Yield of 3-methyl aroenate 338, spiroaroenate 339, imidazolidinone protected aroenate 340 and aromatic side product 341 from the hydrolysis reaction at 40 °C for 18 hours calculated using an ethanol standard for qNMR.

Had time permitted, further optimisation of the hydrolysis conditions would likely allow for each natural product to be favoured over the other, as seen in the original synthesis.

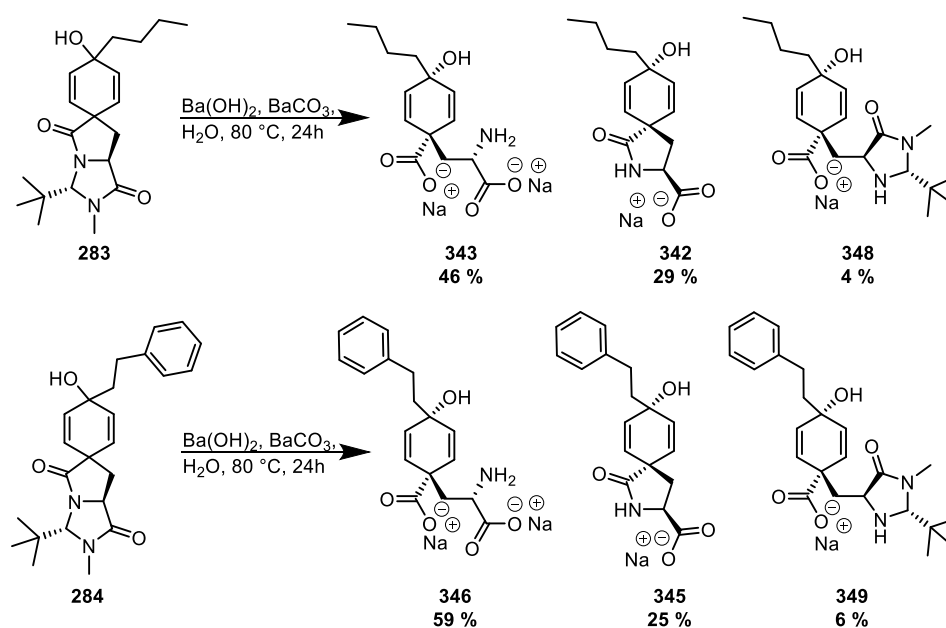
2.3.3.3 Hydrolysis of Grignard Derivatives

The initial attempts at hydrolysis of **283** and **284** were carried out with sodium hydroxide and harsher heating conditions; initial test reactions showed lower temperatures provided little conversion. Despite requiring these harsher conditions to hydrolyse, suggesting increased substrate stability, following purification the aroenate derivatives still rearomatised by loss of the hydroxyl group to give **344** and **347** (Scheme 108). The hydrolyses were therefore repeated using the addition of sodium carbonate/bicarbonate salts to hopefully prevent this.



Scheme 108 – Initial hydrolysis attempt of the Grignard derivatives.

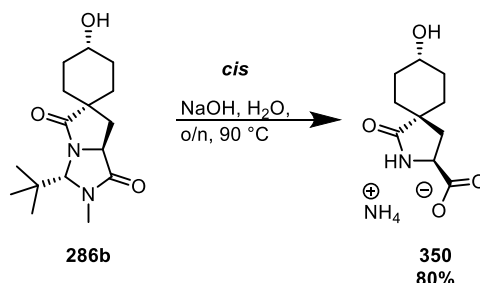
Switching to the barium hydroxide conditions and use of sodium bicarbonate buffer in purification resulted in good yields of both aroenate **343/346** and spiroarogenate **342/345** derivatives. No rearomatised side product was isolated and only small amounts of the imidazolidnone protected aroenate **348/349** were observed.



Scheme 109 –Yield of grignard analogues of aroenate 342/245, spiroarogenate 343/346 and imidazolidinone protected aroenate 348/349 from the hydrolysis reaction at 80 °C for 24 hours calculated using an ethanol standard for qNMR.

2.3.3.4 Hydrolysis of a Fully Saturated Derivative

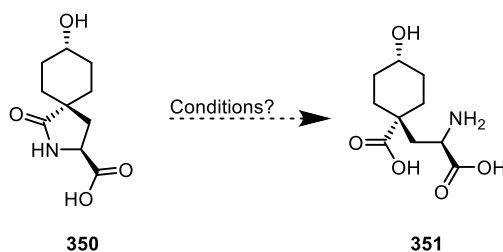
The hydrogenated spirocycle **286b** proved more stable under hydrolysis conditions requiring a higher reaction temperature. The increased stability of the hydrogenated analogue is reflected in the yield of 80% (Scheme 85).



Scheme 110 – Synthesis of saturated spiroarogenate.

The *trans* derivative **286a** was also hydrolysed in a 79% yield. Repeating the *cis* **286b** reaction with barium hydroxide as the base gave an almost identical yield. Thus far, hydrolysis has only produced the spiroarogenate derivative **350** with no sign of the fully hydrolysed arogenate derivative. Various conditions, using barium hydroxide or HCl, were trialled in an attempt to convert **350** to the arogenate form **351** however the 5-membered lactam ring proved difficult to hydrolyse (Table 6).*

Table 6 – Attempted hydrolysis conditions.



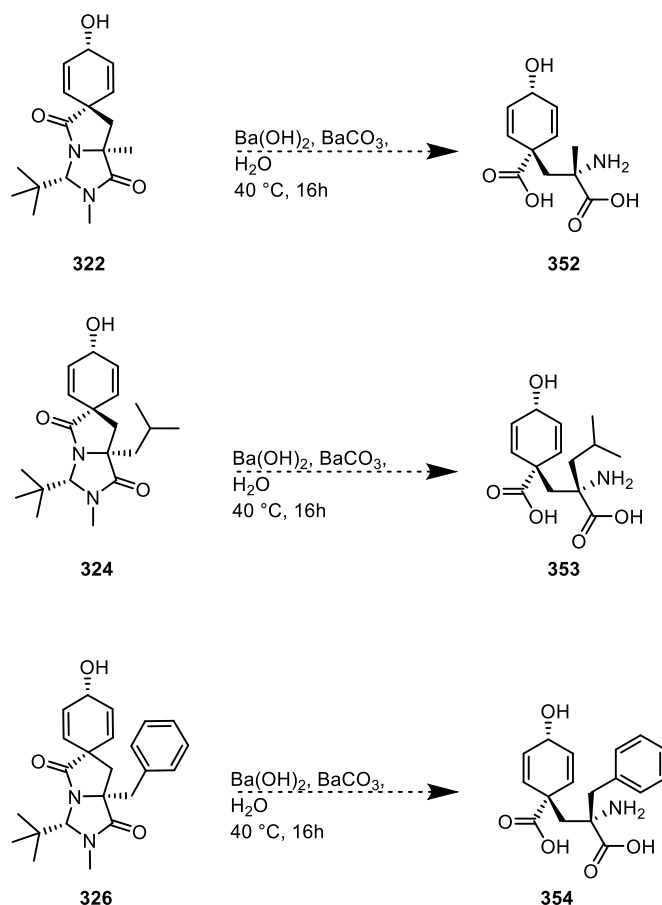
	Reagent	Eq.	Solvent	Temp. / °C	Time / h	NMR Ratio	
						350	351
a	Ba(OH) ₂ / BaCO ₃	3/1	H ₂ O	100	72	100	-
b	HCl	6	H ₂ O	80	24	98	2
c	HCl	10	H ₂ O	80	24	78	22
d	HCl	10	H ₂ O	160 (MW)	19	Decomposed	

All reactions performed on a 10 mg scale.

* With thanks to Rachel Pankhurst for hydrolysis of the *trans* derivative, hydrolysis with barium hydroxide and further exploration of hydrolysis of the lactam.

2.3.3.5 Hydrolysis of Alkylation Derivatives

Attempts were made to hydrolyse the major diastereomer from each Luche reduction, **322**, **324** and **326**, using the milder hydrolysis conditions; 3 eq. Ba(OH)₂, 1 eq. BaCO₃ at 40 °C for 18 hours (Scheme 111). However, the crude reaction mixtures proved very complex and despite weeks of trialling purification conditions using the HyperCarb column little separation of products could be achieved. Some separation was achieved for the alanine derivative **352**, however the only components recovered were 12% starting material and >5% of a species with characteristics of the desired aroenate/spiroaroenate derivative. Attempts at purification of the leucine analogue **353** proved futile and whilst moderate separation was achieved with the crude reaction mixture from hydrolysis of the phenylalanine derivative **354**, only starting material or rearomatised product were detected.



Scheme 111 – Attempted hydrolyses of alkylation derivatives 352-354.

3. Conclusions

A novel synthesis of aroenate in seven steps with an overall yield of 19.6% has been attained; this is a marked improvement on the 2.1% overall yield of the previous reported synthesis.³⁷ Spiroaroenate, which is itself a natural product, has also been produced by this route and it has been discovered that altering the final hydrolysis conditions can favour conversion to either one of these natural products. Aroenate's inherent instability has proved challenging but purification and stabilisation has been realised through the use of a HyperCarb column and the use of a sodium carbonate/bicarbonate buffer. With this knowledge in hand, it is hoped that this route will provide ample opportunity to derivatise aroenate, particularly with respect to improved stability, and open an avenue to explore the potential of such analogues in both agrochemicals and pharmaceuticals.

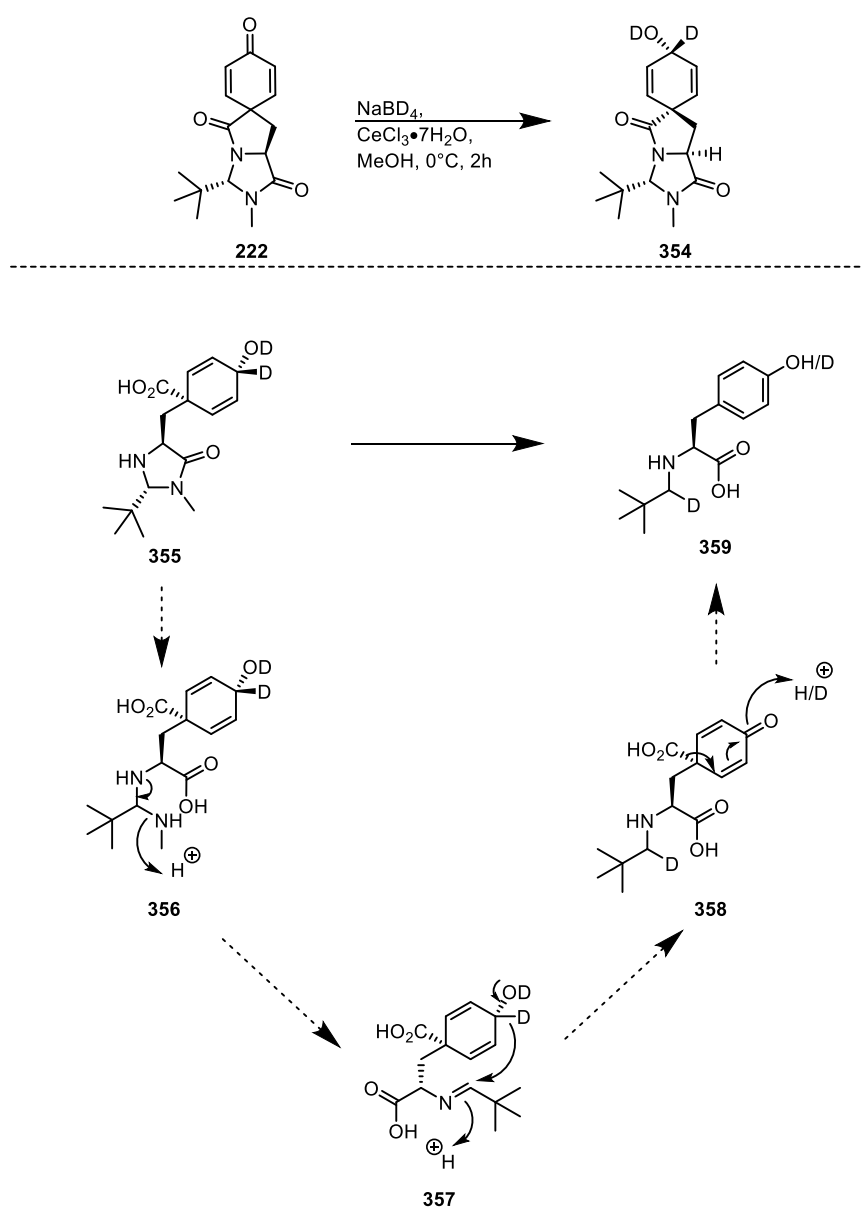
The first derivatised analogues of both aroenate and spiroaroenate have been produced using this synthesis. Several successful functionalisations have been accomplished including producing a stable spiroaroenate analogue as well as introducing substituents in the 3- and 4- position of the carbocycle. These analogues are now available for testing purposes as potential herbicides as part of a collaboration with Syngenta. A collaboration with Professor Hiroshi Maeda at the University of Wisconsin has also been discussed to test their effect directly on aroenate dehydrogenase/dehydratase enzymes and other enzymes earlier in the shikimate pathway.

Strides have also been made in the synthesis of partially reduced stable analogues of aroenate using asymmetric desymmetrisation using a rhodium catalyst, the use of soft nucleophiles for 1,4 additions and Diels-Alder reactions. Hopefully, with further optimisation these will soon be realised.

An alternative route has been established for the alpha-alkylation of amino acid derived *N*-chloroformylimidazolidinones using a benzylic electrophile to install the tyrosine motif, opening up the possibility of accessing alpha-substituted aroenate analogues. This will hopefully allow a compound library to be produced for probing chemical space in the α -position.

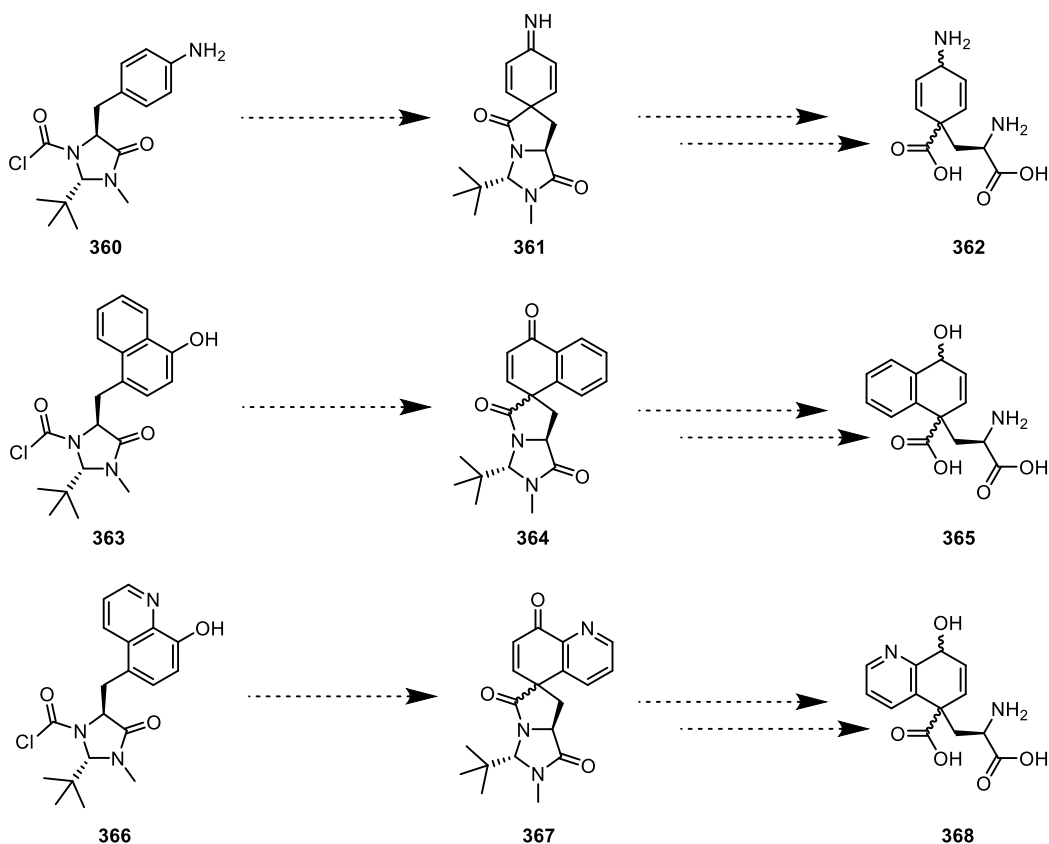
4. Future Directions

Further investigations into the mechanism for the production of rearomatised side product **331/359** would be of great interest as this would provide insight into potential avenues for blocking this rearomatisation pathway. It is hoped carrying out the Luche reduction using sodium borodeuteride would allow for deuterium incorporation in the position alpha to the hydroxyl group **354** (Scheme 112). If the proposed mechanism is operating this could be seen in the proton NMR for the rearomatisation side product **359** (Scheme 112). This would also further explain the lack of rearomatised products seen with the 1,2-addition derivatisation products (Section 2.3.2.3), where no proton is available for abstraction.



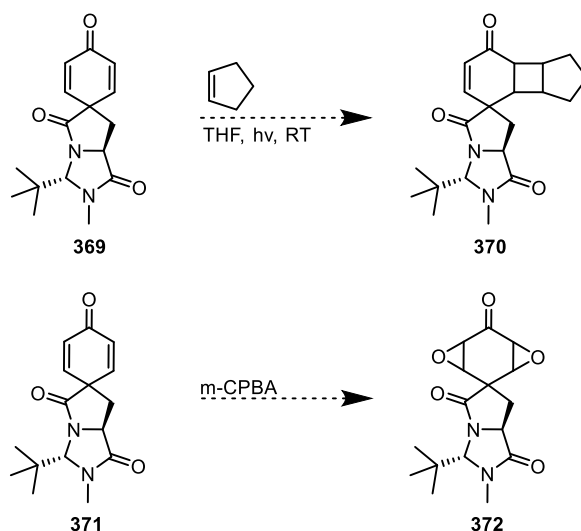
Scheme 112 – NaBD_4 reduction for mechanistic insight into rearomatisation pathway.

Converting the phenol in **220** to an aniline to give **360** would provide a potential alternative substrate for spirocyclisation. The product imine **361**, could then undergo reduction and hydrolysis to yield the amino arogenate derivative **362** (Scheme 113). The amine **362** could act as both a hydrogen bond donor and acceptor in the enzyme active site which may alter its binding and activity. This could also allow for production of further analogues with secondary and tertiary amines to explore their effect on the arogenate enzymes. Alternatively, bicyclic structures could potentially be produced using this spirocyclisation method. Naphthol¹²⁸ and hydroxyquinoline¹²⁹ rings have been known to undergo spirocyclisation reactions and may be a sensible starting point for this investigation in the hopes of producing **365** and **368** (Scheme 113).



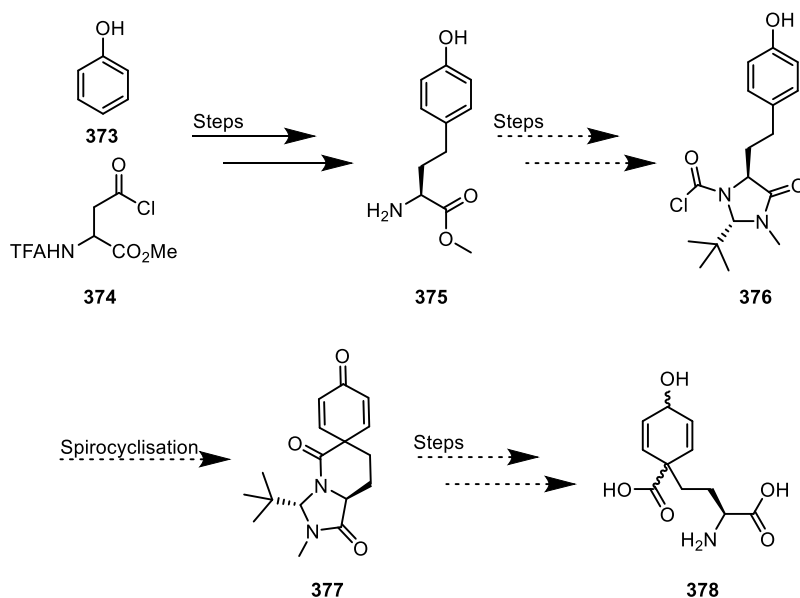
Scheme 113 – Alternative ring systems for spirocyclisations.

Thus far Diels-Alder reactions have proved unsuccessful; as an alternative [2+2] cycloadditions may be trialled for their potential in producing alternative polycyclic ring structures such as **370** (Scheme 114). Epoxidation of the double bonds in tyrosine-based spirocycles has been previously reported in the literature and may provide an opportunity for further derivatisation whilst affording stable arogenate analogue **372**.^{75,76}



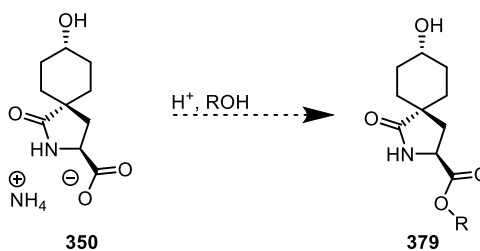
Scheme 114 – [2+2] cycloaddition or epoxidation to produce polycyclic ring structures.

It would also be of interest to attempt the spirocyclisation from a homotyrosine derivative. The homotyrosine starting material **375** can be produced from phenol and N-TFA-Asp(Cl)-OMe via a Friedel-Crafts acylation followed by a reduction using Pd/C.¹³⁰ **375** could then be protected and converted to the carbamoyl chloride **376** allowing attempts at spirocyclisation to give the six-membered aroenate analogue **377** (Section 2.3.2.1).



Scheme 115 – Potential homoarogenate derivative from homotyrosine.

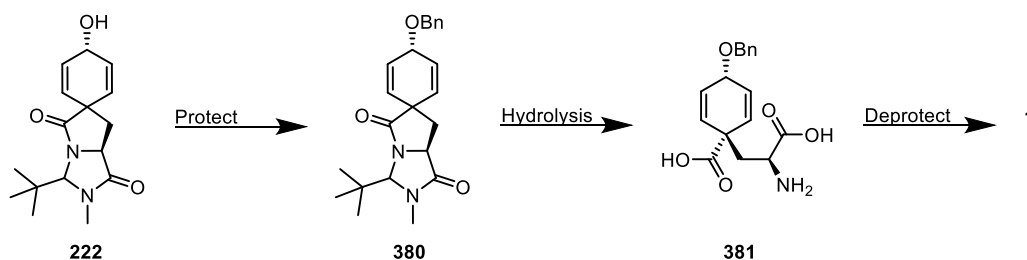
With a stable analogue of spiroarogenate in hand, we hope that further derivatisations could be carried out on **350** itself. For example, it may be of interest to produce ester derivatives for use as pro-drugs or pro-cides (Scheme 116). Esterification should allow facile modification of physical properties, such as logP, which may aid in absorption and distribution of these molecules.



Scheme 116 – Esterification of a stable analogues of spiroarogenate.

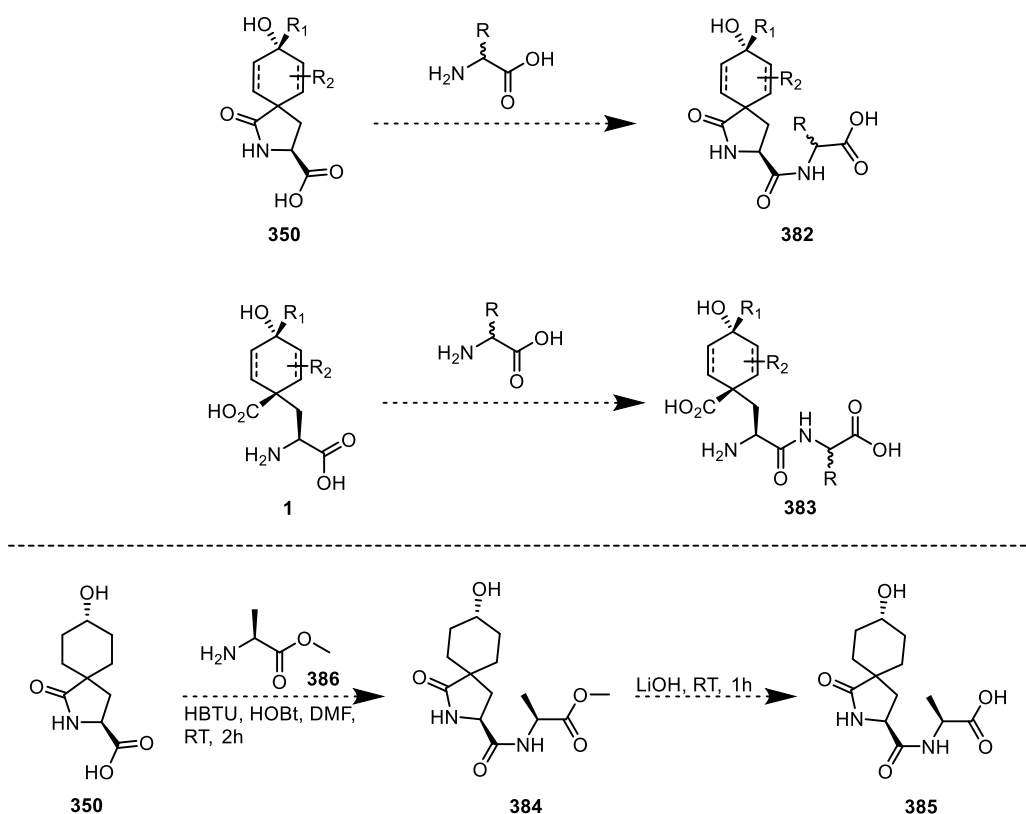
Further work, particularly in the 1,4-addition and partial reduction derivatisations, will concentrate on optimisation of these reactions. Focus will also be paid to whether any selectivity is observed in these reactions and exploration of whether temperature, solvents, chiral catalysts or ligands could be used to bias formation of particular diastereomers.

Another transformation to be explored as a method of preventing rearomatisation would be the addition of a base-stable protecting group at the phenolic position (Scheme 117). This investigation would help to determine whether the hydrolytic rearomatisation side reaction proceeds via a stepwise or concerted mechanism as identified in previous arogenate dehydrogenase studies.¹³ For example, if the hydroxy group is alkylated, i.e. with a benzyl group, this should prevent a stepwise rearomatisation as the dienone could no longer form (Scheme 117).



Scheme 117 - Derivatisation strategies to explore stepwise or concerted mechanism.

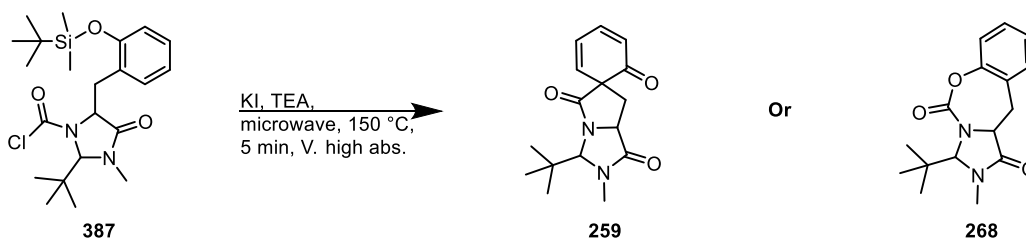
An alternative avenue to be explored would involve carrying out peptide couplings with stable arogenate or spiroarogenate analogues (Scheme 118). A preliminary reaction could utilise tetrahydrospiroarogenate **350** due to its known stability. The spiroarogenate analogues are not expected to require any additional protection due to the N-terminus being involved in the lactam ring which reduces its reactivity. This could then be coupled with L-alanine methyl ester **386**, using conditions employed in coupling of pyroglutamate amino acids,¹³¹ followed by deprotection of the ester using lithium hydroxide to give **385** (Scheme 118). Such compounds may be of interest for incorporation into peptides for SAR studies or as pro-drugs/pro-cides.



Scheme 118 – Peptide coupling reactions with stable arogenate or spiroarogenate derivatives.

A collaboration is in the process of being established which will allow derivatives to be tested against arogenate dehydrogenase and dehydratase assays to explore mode of action. Any positive testing of analogues could be explored further by co-crystallisation with arogenate dehydrogenase/dehydratase. This may give further information about substrate binding and offer further assistance in computational aided drug/herbicide discovery.

As mentioned previously (Section 2.2.1.1), silyl ethers have been used in spirocyclisation reactions.⁹⁹ Therefore, it was proposed that the use of a silyl ether in the *ortho*-tyrosine spirocyclisation may aid in promoting the desired spirocyclisation to **259** over the unwanted cyclisation to the carbamate **268** (Scheme 119).



Scheme 119 - Proposed silyl ether ortho-spirocyclisation.

Future efforts could also include revisiting the oxazolidinone and hydantoin routes with the aim of achieving spirocyclisation which could generate more readily hydrolysable species for the synthesis of aroenate and its derivatives.

5. Experimental

Unless stated otherwise, all reagents and chemicals were bought from commercial suppliers and used without further purification.

When anhydrous conditions were necessary, reactions were carried out under nitrogen in flame-dried glassware using standard Schlenk syringe-septa techniques.

Anhydrous dichloromethane, THF, MeCN and toluene were dried by passing through a modified Grubbs system of alumina columns, manufactured by Anhydrous Engineering. Petrol Ether indicates fractions of petroleum ether boiling at 40-60 °C.

Thin layer chromatography (TLC) was performed with aluminium backed silica TLC plates (Merck-Kieselgel 60 F254) with a suitable solvent system. Visualisation was via UV light (at 254 nm) or by staining with potassium permanganate solution or 'Seebach' dip and heat.

Flash column chromatography was performed on a Biotage Isolera™ four system using 10, 25, 50 or 100 g silica Biotage® SNAP columns and a variable 200-400 nm wavelength detector scanning all wavelengths.

Infrared spectra were recorded on a Perkin Elmer Spectrum (Spectrum One) FT-IR with an ATR accessory and frequencies are reported in wavenumbers (cm⁻¹).

¹H and ¹³C NMR spectra were recorded in CDCl₃ solutions (unless otherwise stated) on Jeol-ECS 400, Varian 400/500, Bruker 400 and Bruker 500 (cryo-enhanced ¹³C probe) spectrometers at ambient temperature, and were referenced to the residual deuterated solvent peak for CDCl₃ (7.26 ppm for ¹H and 77.16 ppm for ¹³C) or D₂O (4.79 ppm for ¹H). Chemical shifts (δ) are reported in parts per million (ppm) and coupling constants (*J*) in hertz (Hz). Multiplicities are denoted as singlet (s), doublet (d), triplet (t), quartet (q) or multiplet (m). COSY, HMBC and HSQC NMR spectra were routinely used to definitively assign the signals of ¹H and ¹³C NMR spectra.

Electrospray (ESI) mass spectra were recorded on a Bruker Daltronics MicroTOF 2 mass spectrometer. Nanospray mass spectra were recorded on a UHPLC-MS (Dionex RS3000 LC system). Unless stated otherwise, mass spectrometry measurements are recorded for the isotope ³⁵Cl.

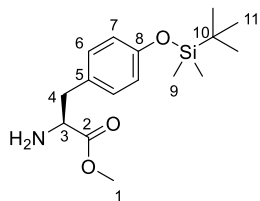
Melting points were measured on a Stuart Scientific melting point SMP 10 apparatus and are uncorrected.

Specific rotations ($[\alpha]_D^T$) were measured on a Bellingham and Stanley Ltd. ADP220 polarimeter where *c* is given in g/100 mL.

Suitable X-ray crystallography samples were grown by slow diffusion technique.

5.1 Hydantoin route

5.1.1 Silyl route



Methyl (S)-2-amino-3-(4-((tert-butyldimethylsilyl)oxy)phenyl)propanoate (**235**)¹³²

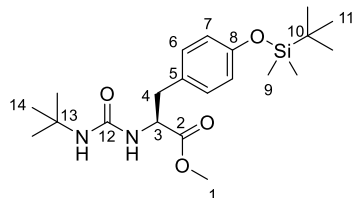
L-tyrosine methyl ester (3.00 g, 15.3 mmol) was dissolved in DCM (150 mL) under N₂. To this imidazole (2.79 g, 18.3 mmol) and TBSCl (1.26 g, 18.3 mmol) were added. The mixture was stirred at room temperature overnight. A further equivalent of imidazole and TBSCl was added and the reaction mixture was stirred for a further 2 hours. The mixture was then quenched with saturated aqueous NH₄Cl (100 mL) solution. Phases were separated and the aqueous layer was extracted with DCM (3 x 100 mL). The organic phase was dried over MgSO₄, filtered and concentrated *in vacuo*. Purification was carried out by column chromatography on silica gel eluting with a gradient of 25-100% ethyl acetate in petroleum ether to yield **235** (4.15 g, 92%) as a colourless oil.

¹H NMR (400 MHz, Chloroform-*d*) δ 7.07 – 6.97 (m, 2H, H₇), 6.80 – 6.73 (m, 2H, H₆), 3.70 (m, 4H, H₁ & H₃), 3.00 (dd, *J* = 13.6, 5.3 Hz, 1H, H₄), 2.80 (dd, *J* = 13.6, 7.7 Hz, 1H, H₄), 0.97 (s, 9H, H₁₁), 0.18 (s, 6H, H₉).

HRMS-ESI (*m/z*) [M+H]⁺ calc. for C₁₆H₂₈NO₃Si 310.1833, found 310.1833.

R_f - 0.14 in 50% EtOAc in Petroleum ether

Consistent with literature data.



Methyl (S)-2-(3-(tert-butyl)ureido)-3-(4-((tert-butyldimethylsilyl)oxy)phenyl)propanoate (**236**)

To a solution of **235** (4.15 g, 13.5 mmol) in DCM (55.0 mL) under N₂, *tert*-butyl isocyanate (1.85 mL, 16.2 mmol) and triethylamine (3.76 mL, 27.0 mmol) were added. The resultant mixture was stirred at room temperature overnight. The mixture was then washed with ammonium chloride (3

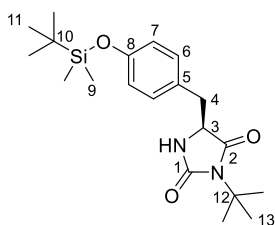
x 100 mL), sodium hydrogen carbonate (100 mL) and brine (100 mL). The organic phase was dried over MgSO₄, filtered and concentrated *in vacuo* to yield **236** (4.87 g, 88%) as a pale-yellow oil.

¹H NMR (400 MHz, Chloroform-*d*) δ 6.96 (d, *J* = 8.4 Hz, 2H), 6.80 – 6.67 (m, 2H), 4.67 (dt, *J* = 7.7, 5.8 Hz, 1H, H₃), 4.54 (d, *J* = 7.7 Hz, 1H, NH), 4.24 (s, 1H, NH), 3.69 (s, 3H, H₁), 3.00 (m, 2H, H₄), 1.29 (s, 9H), 0.97 (s, 9H), 0.17 (s, 6H, H₉).

¹³C NMR (100 MHz, Chloroform-*d*) δ 173.35 (C₂), 156.23 (C₁₂), 154.61 (C₈), 130.28 (C₆), 128.87 (C₅), 120.03 (C₇), 53.80 (C₃), 52.05 (C₁), 50.51 (C₁₃), 37.74 (C₄), 29.59 (C₁₀), 29.42 (C₁₄), 25.64 (C₁₁), -4.44 (C₉).

HRMS-ESI (*m/z*) [M+H]⁺ calc. for C₂₁H₃₇N₂O₄Si 409.2517, found 409.2517.

R_f - 0.46 in 50% EtOAc in Petroleum ether



(S)-3-(tert-butyl)-5-(4-((tert-butyl)dimethylsilyloxy)benzyl)imidazolidine-2,4-dione (230)

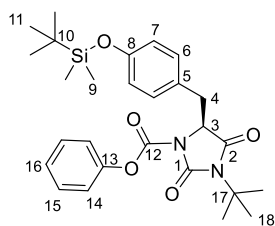
To a solution of **236** (4.86 g, 11.9 mmol) in THF (40.0 mL) under N₂, potassium *tert*-butoxide (1.47 g, 13.1 mmol) was added. The resultant mixture was stirred at room temperature for two hours. The mixture was then washed with water (3 x 100 mL), sodium hydrogen carbonate (100 mL) and brine (50 mL). The organic phase was dried over MgSO₄, filtered and concentrated *in vacuo*. Purification was carried out by column chromatography on silica gel eluting with a gradient of 2-100% ethyl acetate in petroleum ether to yield **230** (2.97 g, 66%) as a white solid.

¹H NMR (400 MHz, Chloroform-*d*) δ 7.04 (d, *J* = 8.4 Hz, 2H), 6.83 – 6.63 (m, 2H), 5.51 (s, 1H, NH), 4.02 (ddd, *J* = 7.6, 3.7, 1.3 Hz, 1H, H₃), 3.08 (dd, *J* = 14.0, 3.7 Hz, 1H, H₄), 2.81 (dd, *J* = 14.0, 7.6 Hz, 1H, H₄), 1.49 (s, 9H), 0.97 (s, 9H), 0.16 (s, 6H, H₉).

¹³C NMR (100 MHz, Chloroform-*d*) δ 174.04 (C₂), 158.02 (C₁), 154.94 (C₈), 130.43 (C₇), 127.68 (C₅), 120.26 (C₆), 57.61 (C₁₂), 57.33 (C₃), 37.32 (C₄), 28.47 (C₁₃), 25.65 (C₁₁), 18.18 (C₁₀), -4.45 (C₉).

HRMS-ESI (*m/z*) [M+Na]⁺ calc. for C₂₀H₃₂N₂O₃SiNa 399.2074, found 399.2084.

R_f - 0.40 in 50% EtOAc in Petroleum ether



Phenyl (S)-3-(tert-butyl)-5-(4-((tert-butyldimethylsilyl)oxy)benzyl)-2,4-dioxoimidazolidine-1-carboxylate (237)

To a solution of **230** (200 mg, 0.53 mmol) in THF (5.00 mL) under N₂ at 0 °C, potassium *tert*-butoxide (65.0 mg, 0.58 mmol) was added and the reaction mixture was stirred for 5 minutes. Phenyl chloroformate (0.08 mL, 0.64 mmol) was then added and the mixture was warmed to room temperature and stirred for 2 hours. The mixture was then diluted with EtOAc (50 mL), washed with water (3 x 30 mL) and brine (30 mL). The organic phase was dried over MgSO₄, filtered and concentrated *in vacuo*. Purification was carried out by column chromatography on silica gel eluting with 100% dichloromethane to yield **237** (106 mg, 40%) as a pale-yellow oil.

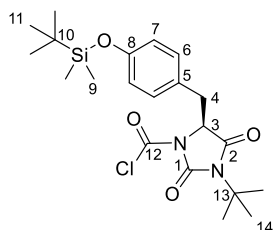
¹H NMR (400 MHz, Chloroform-*d*) δ 7.48 – 7.40 (m, 2H, H₁₅), 7.33 – 7.27 (m, 1H, H₁₆), 7.27 – 7.22 (m, 2H, H₁₄), 7.02 – 6.96 (m, 2H, H₆), 6.80 – 6.75 (m, 2H, H₇), 4.60 (dd, *J* = 4.8, 2.8 Hz, 1H, H₃), 3.49 (dd, *J* = 14.2, 4.8 Hz, 1H, H₄), 3.24 (dd, *J* = 14.2, 2.8 Hz, 1H, H₄), 1.41 (s, 9H, H₁₈), 0.97 (s, 9H, H₁₁), 0.17 (s, 6H, H₉).

¹³C NMR (100 MHz, Chloroform-*d*) δ 170.82 (C₂), 155.32 (C₁), 151.68 (C₈), 150.02 (C₁₂), 148.82 (C₁₃), 130.91 (C₆), 129.61 (C₁₅), 126.49 (C₁₆), 125.74 (C₅), 121.36 (C₁₄), 120.31 (C₇), 59.46 (C₃), 59.16 (C₁₇), 34.43 (C₄), 28.20 (C₁₈), 25.66 (C₁₁), 18.19 (C₁₀), -4.45 (C₉).

HRMS-ESI (*m/z*) [M+Na]⁺ calc. for C₂₇H₃₆N₂O₅SiNa 519.2286, found 519.2272.

R_f - 0.51 in 100% DCM

IR ν_{max} - 2961, 2935, 2855 (C–H), 1728 (C=O)



(S)-3-(tert-butyl)-5-(4-((tert-butyldimethylsilyl)oxy)benzyl)-2,4-dioxoimidazolidine-1-carbonyl chloride (232)

Pyridine (64 μL, 0.80 mmol) was added to a triphosgene (80.0 mg, 0.27 mmol) solution in dry dichloromethane (3.00 mL) in a flame-dried round bottom flask at -78 °C and the resulting solution was stirred at the same temperature for 10 min before adding **230** (200 mg, 1.53 mmol)

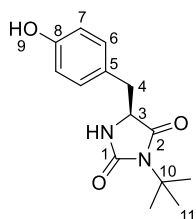
in dichloromethane (2 mL). The resulting mixture was slowly warmed to room temperature and was stirred at that temperature for 5 h. The solvent was partially eliminated under reduced pressure and purification was carried out by column chromatography on silica gel eluting with a gradient of 0-100% ethyl acetate in petroleum ether to yield **232** (5 mg, 4.5%) as a colourless oil.

¹H NMR (500 MHz, Chloroform-*d*) δ 6.98 – 6.94 (m, 2H, H₆), 6.81 – 6.76 (m, 2H, H₇), 4.62 (dd, J = 4.8, 2.6 Hz, 1H, H₃), 3.49 (dd, J = 14.4, 4.8 Hz, 1H, H₄), 3.24 (dd, J = 14.4, 2.6 Hz, 1H, H₄), 1.39 (s, 9H, H₁₄), 0.98 (s, 9H, C₁₁), 0.18 (s, 6H, H₉).

¹³C NMR (100 MHz, Chloroform-*d*) δ 169.54 (C₂), 155.56 (C₁), 150.71 (C₈), 143.63 (C₁₂), 130.89 (C₆), 124.91 (C₅), 120.47 (C₇), 61.09 (C₃), 59.87 (C₁₃), 34.28 (C₄), 28.07 (C₁₄), 25.66 (C₁₁), 18.21 (C₁₀), -4.45 (C₉).

HRMS-ESI (m/z) [$M + Na^+$] calculated for C₂₁H₃₁ClN₂NaO₄Si, 461.1639, found 461.1634.

R_f = 0.64 in 30% EtOAc in Petroleum ether



(S)-3-(tert-butyl)-5-(4-hydroxybenzyl)imidazolidine-2,4-dione (238)

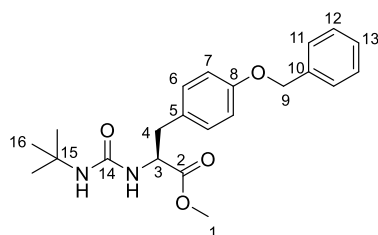
To a solution of **237** (45 mg, 0.09 mmol) in dry THF (1.00 mL), tetrabutylammonium fluoride (1 M in THF) (0.10 mL, 0.09 mmol) was added at 0 °C. The resulting solution was stirred at the same temperature for 30 min. The reaction was quenched with brine (10 mL) and extracted with DCM (3 x 10 mL). The organic phase was dried over MgSO₄ and concentrated *in vacuo*. Purification was carried out by column chromatography on silica gel eluting with a gradient of 0-100% ethyl acetate in petroleum ether to yield **238** (14 mg, 60 %) as a white solid.

¹H NMR (500 MHz, Methanol-*d*₄) δ 7.00 (d, J = 8.4 Hz, 2H), 6.68 (d, J = 8.4 Hz, 2H), 4.07 (t, J = 4.3 Hz, 1H), 3.00 – 2.84 (m, 2H), 1.34 (s, 9H).

¹³C NMR (126 MHz, Methanol-*d*₄) δ 176.62, 173.04, 157.73, 132.28, 126.59, 116.07, 58.46, 37.44, 28.82, 20.98.

HRMS-ESI (m/s) [$M + Na^+$] calc. for C₁₄H₁₈NNaO₃ 285.1215, found 285.12.

5.1.2 Benzyl route

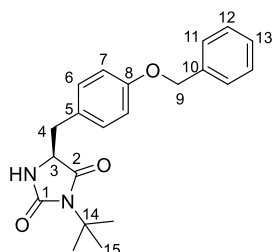


Methyl (S)-3-(4-(benzyloxy)phenyl)-2-(3-(tert-butyl)ureido)propanoate (**242**)

To a solution of *O*-benzyl methyltyrosinate hydrochloride (2.84 g, 8.82 mmol) and triethylamine (2.60 mL, 18.6 mmol) in dichloromethane (40.0 mL) under N₂, *tert*-Butyl isocyanate (1.20 mL, 10.3 mmol) was added. The reaction mixture was stirred at room temperature overnight. The organic phase was washed with a saturated aqueous solution of NH₄Cl (3 x 30 mL), a saturated aqueous solution of NaHCO₃ (3 x 30 mL) and brine (30 mL), dried over MgSO₄ and concentrated in *vacuo* to yield **242** (3.25 g, 96 %) as a white solid.

¹H NMR (400 MHz, Chloroform-*d*) δ 7.46 – 7.29 (m, 5H, H_{11,12&13}), 7.03 (d, *J* = 8.5 Hz, 2H, H₆), 6.90 (d, *J* = 8.5 Hz, 2H, H₇), 5.04 (s, 2H, H₉), 4.72 – 4.65 (m, 1H, H₃), 4.47 (d, *J* = 7.8 Hz, 1H, NH), 4.16 (s, 1H, NH), 3.72 (s, 3H, H₁), 3.04 (m, H₄), 1.30 (s, 9H, H₁₆).

R_f - 0.52 in 50% EtOAc in petroleum ether



(S)-5-(4-(Benzyloxy)benzyl)-3-(tert-butyl)imidazolidine-2,4-dione (**231**)

To a solution of **242** (3.25 g, 8.46 mmol) in THF (30.0 mL) under N₂, potassium *tert*-butoxide (1.04 g, 9.31 mmol) was added. The reaction mixture was stirred at room temperature for 2 h. The reaction was then quenched with saturated aqueous solution of NH₄Cl (30 mL). The organic phase was separated and washed with a saturated aqueous solution of NaHCO₃ (30 mL) and brine (30 mL), dried over MgSO₄ and concentrated in *vacuo*. Purification was carried out by column chromatography on silica gel eluting with a gradient of 0-70% ethyl acetate in petroleum ether to yield **231** (2.44 g, 82%) as a white solid.

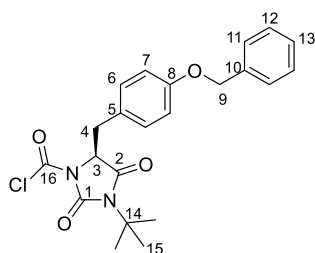
¹H NMR (400 MHz, Chloroform-*d*) δ 7.45 – 7.28 (m, 5H, H_{11,12&13}), 7.14 – 7.06 (m, 2H, H₆), 6.96 – 6.86 (m, 2H, H₇), 5.34 – 5.16 (m, 1H, NH) 5.05 (s, 2H, H₉), 4.01 (ddd, *J* = 8.0, 3.7, 1.3 Hz, 1H, H₃), 3.10 (dd, *J* = 14.0, 3.7 Hz, 1H, H₄), 2.80 (dd, *J* = 14.0, 8.0 Hz, 1H, H₄), 1.49 (s, 9H, H₁₅)

¹³C NMR (100 MHz, Chloroform-*d*) δ 174.14 (C₂), 158.22 (C₁), 158.03 (C₈), 137.02 (C₁₀), 130.60 (C₆), 128.75 (C₁₂), 128.13 (C₁₃), 127.58 (C₅), 127.54 (C₁₁), 115.29 (C₇), 70.16 (C₉), 57.81 (C₃), 57.49 (C₁₄), 37.52 (C₄), 28.62 (C₁₅)

HRMS-ESI (*m/z*) [M+Na]⁺ calc. for C₂₁H₂₄N₂NaO₃ 375.1679, found 375.1689

R_f - 0.24 in 50% EtOAc in petroleum ether

IR ν_{max} – 3266 (N-H), 2974, 2935 (C-H), 1700 (C=O)



(S)-5-(4-(Benzyloxy)benzyl)-3-(tert-butyl)-2,4-dioximidazolidine-1-carbonyl chloride (233)

To a solution of triphosgene (295 mg, 0.99 mmol) solution in dry dichloromethane (10.0 mL) under N₂ at -78 °C, pyridine (0.24 mL, 2.98 mmol) was added. The resulting solution was stirred at the same temperature for 10 min before adding **231** (689 mg, 1.99 mmol) in dichloromethane (3.00 mL). The resulting mixture was slowly warmed to room temperature and stirred for 4 h. The mixture was concentrated in *vacuo* and purification was carried out by column chromatography on silica gel eluting with a gradient of 0-100% ethyl acetate in petroleum ether to yield **233** (378 mg, 47%) as a colourless oil.

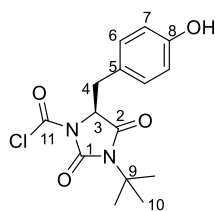
¹H NMR (400 MHz, Chloroform-*d*) δ 7.43 – 7.29 (m, 5H, H_{11,12&13}), 6.99 (d, *J* = 8.7 Hz, 2H, H₆), 6.90 (d, *J* = 8.7 Hz, 2H, H₇), 5.04 (s, 2H, H₉), 4.60 (dd, *J* = 4.8, 2.6 Hz, 1H, H₃), 3.47 (dd, *J* = 14.4, 4.8 Hz, 1H, H₄), 3.23 (dd, *J* = 14.4, 2.6 Hz, 1H, H₄), 1.34 (s, 9H, H₁₅)

¹³C NMR (100 MHz, Chloroform-*d*) δ 169.64 (C₂), 158.63 (C₁), 150.86 (C₈), 143.73 (C₁₀), 136.87 (C₁₆), 131.03 (C₆), 128.73 (C_{11/12}), 128.13 (C₁₃), 127.50 (C_{11/12}), 124.67 (C₅), 115.38 (C₇), 70.09 (C₉), 61.23 (C₃), 60.00, 34.38 (C₄), 28.14 (C₁₅)

HRMS-ESI (*m/z*) [M+Na]⁺ calc. for C₂₂H₂₃ClN₂NaO₄ 437.1239, found 437.1243

R_f - 0.63 in 50% EtOAc in petroleum ether

IR ν_{max} – 2923, 2851 (C-H), 1704 (C=O)



(S)-3-(*tert*-Butyl)-5-(4-hydroxybenzyl)-2,4-dioximidazolidine-1-carbonyl chloride (243**)**

To a solution of **233** (378 mg, 0.91 mmol) in THF (9.00 mL) under N₂, palladium on active carbon (20 wt. %) (76.0 mg, 20 % wt.) was added. The mixture was then stirred at room temperature for 1 hour under hydrogen atmosphere. The reaction mixture was filtered over a pad of celite and concentrated in *vacuo*. Purification was carried out by column chromatography on silica gel eluting with a gradient of 0-100% ethyl acetate in petroleum ether to yield **243** (200 mg, 68 %) as a white solid.

¹H NMR (400 MHz, Chloroform-*d*) δ 6.99 – 6.90 (m, 2H, H₆), 6.78 – 6.71 (m, 2H, H₇), 4.67 (s, 1H, OH), 4.59 (dd, *J* = 4.8, 2.7 Hz, 1H, H₃), 3.45 (dd, *J* = 14.4, 4.8 Hz, 1H, H₄), 3.22 (dd, *J* = 14.4, 2.7 Hz, 1H, H₄), 1.36 (s, 9H, H₁₀)

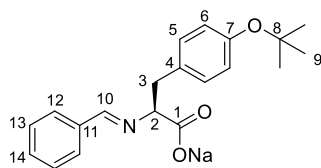
¹³C NMR (100 MHz, Chloroform-*d*) δ 169.68 (C₂), 155.53 (C₁), 150.91 (C₈), 131.24 (C_{6,11}), 124.55 (C₅), 115.83 (C₇), 61.26 (C₃), 60.11 (C₉), 34.39 (C₄), 28.19 (C₁₀)

HRMS-ESI (*m/z*) [M+H]⁺ calc. for C₁₅H₁₇ClN₂O₄Na 347.0769, found 347.0774

R_f - 0.55 in 50% EtOAc in petroleum ether

IR ν_{max} – 3421 (O-H), 2979, 2945 (C-H), 1758, 1704 (C=O)

5.2 Oxazolidinone route



Sodium (*S,E*)-2-(benzylideneamino)-3-(4-(*tert*-butoxy)phenyl)propanoate (**245**)

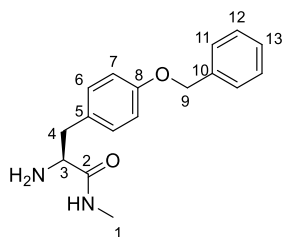
O-*tert*-Butyl-L-tyrosine (600 mg, 2.53 mmol) was dissolved in NaOH (1M, 2.53 mL). The mixture was stirred at room temperature for 2 hours. The solution was then concentrated *in vacuo* and dried at 70 °C *in vacuo* overnight. To the amino acid salt, molecular sieves, benzaldehyde (0.19 mL, 2.52 mmol) and absolute EtOH (4.50 mL) were added and the resultant mixture was stirred at room temperature for 5 hours. The mixture was then filtered and concentrated *in vacuo*. The residue was suspended in pentane, filtered, washed with pentane and dried at 70 °C *in vacuo* overnight to give **245** as a white solid (665.9 mg, 80%).

¹H NMR (400 MHz, Methanol-*d*₄) δ 7.80 (s, 1H, H₁₀), 7.66 (dd, *J* = 7.6, 2.0 Hz, 2H, H_{12/13}), 7.41 – 7.32 (m, 3H, H_{12/13&14}), 7.08 (dd, *J* = 8.4 Hz, 2H, H₅), 6.85 – 6.76 (m, 2H, H₆), 3.99-3.92 (m, 1H, H₂), 3.38 – 3.33 (m, 1H, H₃), 3.04 (dd, *J* = 13.5, 9.8 Hz, 1H, H₃), 1.23 (s, 9H, H₉)

¹³C NMR (100 MHz, Methanol-*d*₄) δ 179.57 (C₁), 163.61 (C₁₀), 154.48 (C₇), 137.40 (C₁₁), 135.97 (C₄), 131.63 (C₁₄), 131.26 (C₅), 129.45 (C₁₃), 129.43 (C₁₂), 125.00 (C₆), 80.32 (C₂), 79.36 (C₈), 41.03 (C₃), 29.10 (C₉)

HRMS-ESI (*m/z*) [M+Na]⁺ calc. for C₂₀H₂₃NO₃Na 348.1570, found 348.1560

5.3 Synthesis of arogenate



(*S*)-2-Amino-3-(4-(benzyloxy)phenyl)-*N*-methylpropanamide (**254**)¹³³

To a solution of *O*-Benzyl-L-tyrosine methyl ester hydrochloride (10.0 g, 31.1 mmol) in EtOH (60.0 mL), methylamine (33 % wt. in EtOH)(54.0 mL, 435.1 mmol) was added. The mixture was stirred at room temperature for 2 days. The solution was concentrated *in vacuo*, redissolved in dichloromethane (100 mL) and washed with a saturated aqueous solution of NaHCO₃ (50 mL). The aqueous phase was extracted with dichloromethane (3 x 30 mL). The combined organics were washed with brine (30 mL), dried over MgSO₄ and concentrated in *vacuo* to yield **254** (8.59 g, 97 %) as a white powder.

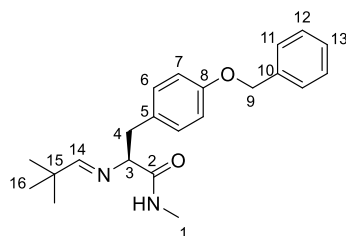
¹H NMR (400 MHz, Chloroform-*d*) δ 7.46 – 7.27 (m, 5H, H_{11,12&13}), 7.12 (d, *J* = 8.6 Hz, 2H, H₆), 6.92 (d, *J* = 8.6 Hz, 2H, H₇), 5.04 (s, 2H, H₉), 3.55 (dd, *J* = 9.3, 4.0 Hz, 1H, H₃), 3.19 (dd, *J* = 13.9, 4.0 Hz, 1H, H₄), 2.80 (d, *J* = 5.0 Hz, 3H, H₁), 2.63 (dd, *J* = 13.9, 9.3 Hz, 1H, H₄)

¹³C NMR (100 MHz, Chloroform-*d*) δ 174.86 (C₂), 157.74 (C₈), 137.01 (C₁₀), 130.28 (C₆), 130.21 (C₅), 128.59 (C₁₂), 127.97 (C₁₃), 127.45 (C₁₁), 115.07 (C₇), 70.06 (C₉), 56.57 (C₃), 40.19 (C₄), 25.81 (C₁)

HRMS-ESI (*m/z*) [M+H]⁺ calc. for C₁₇H₂₁N₂O₂ 285.1597, found 285.1584

R_f - 0.13 in 2% MeOH in EtOAc

Consistent with literature data.



(*S,E*)-3-(4-(Benzyloxy)phenyl)-2-((2,2-dimethylpropylidene)amino)-*N*-methylpropanamide (**251**)¹³³

To a solution of **254** (4.06 g, 14.3 mmol) in dichloromethane (14.0 mL), MgSO₄ (4 g, 100% wt.) and pivaldehyde (1.87 mL, 17.2 mmol) were added. The mixture was stirred at room temperature

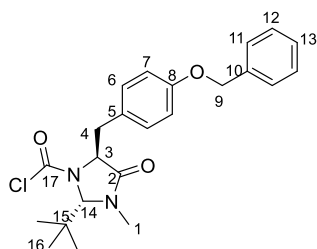
overnight. The solution was filtered and washed with dichloromethane (10 mL). The filtrate was concentrated *in vacuo* to yield **251** (4.62 g, Quant.) as a white powder.

¹H NMR (400 MHz, Chloroform-*d*) δ 7.45 – 7.29 (m, 5H, H_{11,12&13}), 6.98 (d, *J* = 8.5 Hz, 2H, H₆), 6.88 – 6.83 (m, 3H, H₁₄, H₇), 5.04 (s, 2H, H₉), 3.65 (dd, *J* = 10.4, 3.1 Hz, 1H, H₃), 3.28 (dd, *J* = 13.5, 3.1 Hz, 1H, H₄), 2.86 (d, *J* = 5.0 Hz, 3H, H₁), 2.69 (dd, *J* = 13.5, 10.4 Hz, 1H, H₄), 0.89 (s, 9H, H₁₆)

¹³C NMR (100 MHz, Chloroform-*d*) δ 174.24 (C₁₄), 173.44 (C₂), 157.31 (C₈), 137.07 (C₁₀), 131.01 (C₆), 130.00 (C₅), 128.52 (C₁₂), 127.85 (C₁₃), 127.32 (C₁₁), 114.58 (C₇), 74.49 (C₃), 69.95 (C₉), 40.06 (C₄), 36.21 (C₁₅), 26.63 (C₁₆), 25.86 (C₁)

HRMS-ESI (*m/z*) [*M*+H]⁺ calc. for C₂₂H₂₉N₂O₂ 353.2224, found 353.2225

Consistent with literature data.



(2*S*,5*S*)-5-(4-(Benzyloxy)benzyl)-2-(tert-butyl)-3-methyl-4-oxoimidazolidine-1-carbonyl chloride (252**)**¹³³

To a solution of **251** (3.10 g, 9.45 mmol) in THF (19.0 mL), phosgene (10.2 mL, 15% in toluene, 14.2 mmol) was added. The mixture was stirred at room temperature for 2 hours. Pyridine (1.50 mL, 18.9 mmol) was then added and the mixture stirred for a further 1 hour. The solution was concentrated *in vacuo* and redissolved in dichloromethane (30 mL). The organic phase was washed with HCl (1M, 50 mL) and extracted with dichloromethane (3 x 30 mL). The combined organics were washed with brine (20 mL), dried over MgSO₄ and concentrated *in vacuo*. Purification was carried out by trituration using diethyl ether to yield **252** (2.85 g, 72 %) as a pale-yellow powder.

¹H NMR (500 MHz, Chloroform-*d*) δ 7.45 – 7.36 (m, 5H, H_{11,12&13}), 7.09 (d, *J* = 8.2 Hz, 2H, H₆), 6.86 (d, *J* = 8.2 Hz, 2H, H₇), 5.03 (s, 2H, H₉), 4.73 (s, 0.55H, H₁₄), 4.62 (s, 0.45H, H₁₄), 4.42 (s, 0.55H, H₃), 4.39 (s, 0.45H, H₃), 3.80 (d, *J* = 14.6 Hz, 0.45H, H₄), 3.69 (d, *J* = 14.6 Hz, 0.55H, H₄), 3.29 (d, *J* = 14.5 Hz, 0.45H, H₄), 3.21 (d, *J* = 14.5 Hz, 0.55H, H₄), 2.87 (s, 1.65H, H₁), 2.73 (s, 1.35H, H₁), 1.01 (s, 4.65H, H₁₆), 0.94 (s, 4.35H, H₁₆) – rotameric mixture

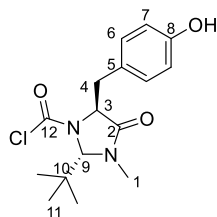
¹³C NMR (125 MHz, Chloroform-*d*) δ 169.82 (C₂), 169.32 (C₂), 158.07 (C₈), 157.88 (C₈), 147.30 (C₁₇), 146.06 (C₁₇), 136.97 (C₁₀), 136.89 (C₁₀), 131.21 (C₆), 131.05 (C₆), 128.55 (C₁₂), 127.96

(C₁₃), 127.56 (C₁₁), 126.50 (C₅), 126.10 (C₅), 114.75 (C₇), 114.58 (C₇), 83.40 (C₁₄), 82.79 (C₁₄), 69.92 (C₉), 63.71 (C₃), 62.79 (C₃), 41.71 (C₁₅), 41.57 (C₁₅), 35.77 (C₄), 32.05 (C₁), 31.93 (C₄), 26.70 (C₁₆), 26.44 (C₁₆) – rotameric mixture

HRMS-ESI (m/z) [$M+H$]⁺ calc. for C₂₃H₂₈ClN₂O₃ 415.1783, found 415.1782

R_f - 0.36 in 100% dichloromethane

Consistent with literature data.



(2S,5S)-2-(tert-Butyl)-5-(4-hydroxybenzyl)-3-methyl-4-oxoimidazolidine-1-carbonyl chloride (220)

To a solution of **252** (1.25 g, 3.02 mmol) in THF (30.0 mL) under N₂, palladium on active carbon (10 wt. %) (250 mg, 20 % wt.) was added. The mixture was then stirred at room temperature for 4 hours under hydrogen atmosphere. The reaction mixture was filtered over a pad of celite and concentrated in *vacuo* to yield **220** (978 mg, 95 %) as a white powder.

¹H NMR (400 MHz, Chloroform-d) δ 7.04 (d, J = 8.0 Hz, 2H, H₆), 6.72 (m, 2H, H₇), 4.75 (s, 0.53H, H₉), 4.64 (s, 0.47H, H₉), 4.40 (d, J = 11.9 Hz, 1H, H₃), 3.81 (d, J = 14.6 Hz, 0.47H, H₄), 3.68 (d, J = 14.6 Hz, 0.53H, H₄), 3.29 (d, J = 14.6 Hz, 0.47H, H₄), 3.20 (d, J = 14.6 Hz, 0.53H, H₄), 2.89 (s, 1.61H, H₁), 2.76 (s, 1.38H, H₁), 1.01 (s, 4.82H, H₁₁), 0.94 (s, 4.18H, H₁₁). – rotameric mixture

¹³C NMR (126 MHz, Chloroform-d) δ 170.13 (C₂), 169.61 (C₂), 155.33 (C₈), 154.99 (C₈), 147.56 (C₁₂), 146.23 (C₁₂), 131.50 (C₆), 131.33 (C₆), 126.23 (C₅), 125.79 (C₅), 115.47 (C₇), 115.28 (C₇), 83.62 (C₉), 83.02 (C₉), 63.88 (C₃), 62.99 (C₃), 41.84 (C₁₀), 41.70 (C₁₀), 35.84 (C₄), 32.23 (C₁), 32.00 (C₄), 26.83 (C₁₁), 26.56 (C₁₁). – rotameric mixture

HRMS-ESI (m/z) [$M+H$]⁺ calc. for C₁₆H₂₂ClN₂O₃ 325.1313, found 325.1311

R_f - 0.63 in 100% EtOAc

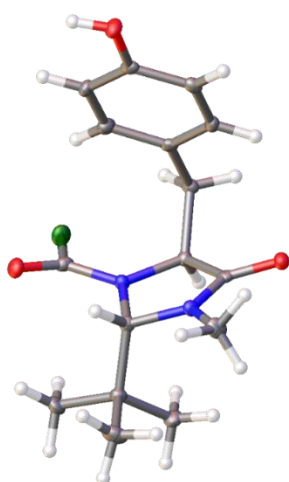
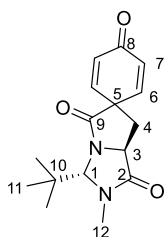


Table 1 Crystal data and structure refinement for 220.	
Empirical formula	C ₁₆ H ₂₁ ClN ₂ O ₃
Formula weight	324.80
Temperature/K	100(2)
Crystal system	orthorhombic
Space group	P2 ₁ 2 ₁ 2 ₁
a/Å	10.8233(2)
b/Å	11.9161(3)
c/Å	12.3076(3)
α/°	90
β/°	90
γ/°	90
Volume/Å ³	1587.33(6)
Z	4
ρ _{calc} /cm ³	1.359
μ/mm ⁻¹	0.255
F(000)	688.0
Crystal size/mm ³	0.426 × 0.396 × 0.166
Radiation	MoKα (λ = 0.71073)
2θ range for data collection/°	4.758 to 55.812
Index ranges	-8 ≤ h ≤ 14, -15 ≤ k ≤ 15, -16 ≤ l ≤ 16
Reflections collected	14647
Independent reflections	3800 [R _{int} = 0.0395, R _{sigma} = 0.0362]
Data/restraints/parameters	3800/0/207
Goodness-of-fit on F ²	1.023
Final R indexes [I ≥ 2σ (I)]	R ₁ = 0.0298, wR ₂ = 0.0669
Final R indexes [all data]	R ₁ = 0.0347, wR ₂ = 0.0691
Largest diff. peak/hole / e Å ⁻³	0.22/-0.21
Flack parameter	0.01(3)



(3'S,7a'S)-3'-(tert-Butyl)-2'-methyl-2',3',7',7a'-tetrahydro-1'H,5'H-spiro[cyclohexane-1,6'-pyrrolo[1,2-c]imidazole]-2,5-diene-1',4,5'-trione (222)

To a solution of **220** (5.20 g, 15.2 mmol) in MeCN (24.0 mL), triethylamine (2.70 mL, 19.1 mmol) was added. The mixture was then heated under microwave irradiation at 150 °C for 10 minutes. The reaction mixture was concentrated *in vacuo*, redissolved in dichloromethane (40 mL) and washed with water (20 mL). The aqueous phase was extracted with dichloromethane (3 x 30 mL).

The combined organics were washed with brine (30 mL), dried over MgSO₄, filtered and concentrated *in vacuo* to yield **222** (4.37 g, Quant.) as a yellow powder.

¹H NMR (400 MHz, Chloroform-*d*) δ 6.92 (dd, *J* = 10.1, 3.0 Hz, 1H, H₆), 6.71 (dd, *J* = 10.1, 3.0 Hz, 1H, H₆), 6.47 (dd, *J* = 10.1, 1.8 Hz, 1H, H₇), 6.40 (dd, *J* = 10.1, 1.8 Hz, 1H, H₇), 4.85 (d, *J* = 1.1 Hz, 1H, H₁), 4.45 (t, *J* = 8.2 Hz, 1H, H₃), 3.03 (s, 3H, H₁₂), 2.61 (dd, *J* = 13.3, 7.4 Hz, 1H, H₄), 2.46 (dd, *J* = 13.3, 9.0 Hz, 1H, H₄), 1.04 (s, 9H, H₁₁)

¹³C NMR (100 MHz, Chloroform-*d*) δ 184.63 (C₈), 173.86 (C₂), 171.32 (C₉), 146.11 (C₆), 143.51 (C₆), 132.24 (C₇), 130.86 (C₇), 81.87 (C₁), 56.85 (C₃), 53.89 (C₅), 38.35 (C₁₀), 37.29 (C₄), 31.44 (C₁₂), 25.77 (C₁₁)

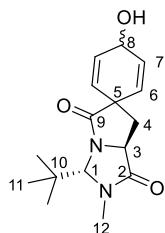
HRMS-ESI (*m/z*) [M+Na]⁺ calc. for C₁₆H₂₁N₂NaO₃ 311.1366, found 311.1365

IR ν_{max} – 2966 (C–H), 1698 (C=O)

R_f - 0.31 in 100% EtOAc

mp 193–195 °C

[α]_D²⁶ = 8 (*c* = 1 in CHCl₃)



(3'*S*,7a'*S*)-3'-(tert-Butyl)-4-hydroxy-2'-methyl-2',3',7',7a'-tetrahydro-1'H,5'H-spiro[cyclohexane-1,6'-pyrrolo[1,2-*c*]imidazole]-2,5-diene-1',5'-dione (225)

To a solution of **220** (480 mg, 1.67 mmol) in dry methanol (17.0 mL) under N₂, cerium(III) chloride heptahydrate (95.0 mg, 2.50 mmol) was added and stirred for 15 minutes at room temperature. The reaction mixture was then cooled to -78 °C and sodium borohydride (930 mg, 2.50 mmol) was added. The resultant mixture was left to stir at -78 °C for a further 30 minutes and then quenched with water (10 mL). The mixture was then diluted with EtOAc (50 mL) and washed with water (30 mL). The aqueous phase was extracted with EtOAc (3 x 30 mL) and brine (30 mL). The organic phase was dried over MgSO₄, filtered and concentrated *in vacuo*. Purification was carried out by column chromatography on silica gel eluting with 0–10% MeOH in dichloromethane to yield **225** (463 mg, 95 %, d.r. = 3.1:1) as white powders.

Major - 225a

¹H NMR (400 MHz, Chloroform-*d*) δ 6.23 (ddd, *J* = 9.9, 3.9, 1.7 Hz, 1H, H₆), 6.14 (ddd, *J* = 9.9, 3.9, 1.7 Hz, 1H, H₇), 5.95 (ddd, *J* = 9.9, 2.3, 1.1 Hz, 1H, H₇), 5.66 (ddd, *J* = 9.9, 2.3, 1.1 Hz, 1H, H₆), 4.80 (d, *J* = 1.1 Hz, 1H, H₁), 4.48 (dtt, *J* = 11.0, 3.9, 1.1 Hz, 1H, H₈), 4.41 – 4.32 (m, 1H,

H₃), 3.00 (s, 3H, H₁₂), 2.49 (dd, *J* = 13.2, 7.7 Hz, 1H, H₄), 2.16 (dd, *J* = 13.2, 8.7 Hz, 1H, H₄), 1.03 (s, 9H, H₁₁)

¹³C NMR (100 MHz, Chloroform-*d*) δ 177.84 (C₂), 172.27 (C₉), 131.56 (C₆), 130.72 (C₆), 129.74 (C₇), 128.50 (C₇), 81.82 (C₁), 61.45 (C₈), 56.78 (C₃), 50.62 (C₅), 38.90 (C₄), 38.38 (C₁₀), 31.37 (C₁₂), 25.85 (C₁₁)

HRMS-ESI (*m/z*) [M+Na]⁺ calc. for C₁₆H₂₂N₂NaO₃ 313.1522, found 313.1521

IR ν_{max} – 3392 (O-H), 3029, 2964, 2871 (C-H), 1695 (C=O)

R_f - 0.23 in 5% MeOH in dichloromethane

mp 58-59 °C

[α]_D²⁶ = -4 (*c* = 1 in CHCl₃)

Minor – 225b

¹H NMR (400 MHz, Chloroform-*d*) δ 6.19 (ddd, *J* = 9.9, 3.1, 2.0 Hz, 1H, H₆), 6.07 (ddd, *J* = 9.9, 3.1, 2.0 Hz, 1H, H₆), 5.92 (dt, *J* = 9.9, 2.0 Hz, 1H, H₇), 5.63 (dt, *J* = 9.9, 2.0 Hz, 1H, H₇), 4.82 (d, *J* = 1.2 Hz, 1H, H₁), 4.71 (dtt, *J* = 8.9, 3.2, 1.7 Hz, 1H, H₈), 4.38 (t, *J* = 8.2 Hz, 1H, H₃), 3.03 (d, *J* = 0.6 Hz, 3H, H₁₂), 2.51 (dd, *J* = 13.2, 7.5 Hz, 1H, H₄), 2.23 (dd, *J* = 13.2, 8.9 Hz, 1H, H₄), 1.04 (s, 9H, H₁₁)

HRMS-ESI (*m/z*) [M+Na]⁺ calc. for C₁₆H₂₂N₂NaO₃ 313.1522, found 313.1522

IR ν_{max} – 3335 (O-H), 2922, 2851 (C-H), 1692 (C=O)

R_f - 0.15 in 5% MeOH in dichloromethane

mp >220 °C decomposition

[α]_D²⁶ = 8 (*c* = 1 in CHCl₃)

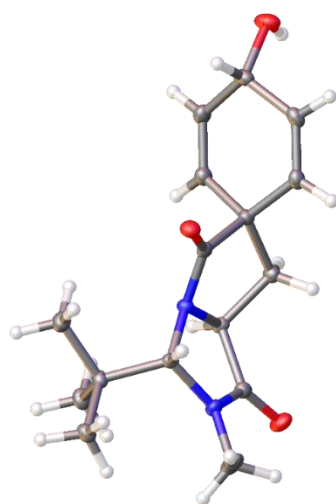
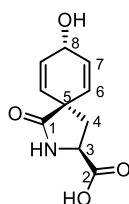


Table 1 Crystal data and structure refinement for 225b.	
Empirical formula	C ₁₆ H ₂₂ N ₂ O ₃
Formula weight	290.35
Temperature/K	100(2)
Crystal system	monoclinic
Space group	P2 ₁
<i>a</i> /Å	5.7583(3)
<i>b</i> /Å	13.5711(6)
<i>c</i> /Å	9.6541(5)
α/°	90
β/°	95.964(3)
γ/°	90
Volume/Å ³	750.35(6)
<i>Z</i>	2
ρ _{calc} /g/cm ³	1.285
μ/mm ⁻¹	0.089
<i>F</i> (000)	312.0

Crystal size/mm ³	0.534 × 0.23 × 0.136
Radiation	MoK α (λ = 0.71073)
2 Θ range for data collection/°	4.242 to 55.984
Index ranges	-7 ≤ h ≤ 7, -17 ≤ k ≤ 15, -12 ≤ l ≤ 12
Reflections collected	10338
Independent reflections	3447 [R _{int} = 0.0447, R _{sigma} = 0.0519]
Data/restraints/parameters	3447/1/198
Goodness-of-fit on F ²	1.025
Final R indexes [I ≥ 2 σ (I)]	R ₁ = 0.0411, wR ₂ = 0.0824
Final R indexes [all data]	R ₁ = 0.0519, wR ₂ = 0.0867
Largest diff. peak/hole / e Å ⁻³	0.23/-0.21
Flack parameter	-0.6(7)



(3*S*,5*r*,8*S*)-8-Hydroxy-1-oxo-2-azaspiro[4.5]deca-6,9-diene-3-carboxylic acid (Spiroarogenate) (256)¹¹⁴

To a solution of **225a** (120 mg, 0.41 mmol) in water (2.00 mL), barium hydroxide (213 mg, 1.24 mmol) was added. The mixture was stirred at 30 °C overnight, and then sodium carbonate anhydrous (263 mg, 2.48 mmol) and water (5 mL) were added. The resulting barium carbonate salt was separated by filtration and the aqueous layer was washed with dichloromethane (15 mL). The aqueous phase was then neutralised (approx. pH = 8) and lyophilised. The mixture was redissolved in ethanol and filtered to remove excess salt. The product was purified by Hypercarb HPLC with a gradient of 0-100% acetonitrile in 100 mM ammonium bicarbonate buffer to yield **256** (21 mg, 27 %) as a white powder.

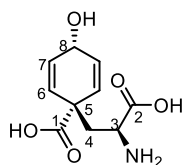
¹H NMR (600 MHz, Deuterium Oxide) δ 6.12 – 6.06 (m, 2H, H₇), 5.90 (dt, J = 10.1, 2.0 Hz, 1H, H₆), 5.84 (dt, J = 10.1, 2.0 Hz, 1H, H₆), 4.59 (tt, J = 3.4, 1.5 Hz, 1H, H₈), 4.27 (dd, J = 8.7, 6.3 Hz, 1H, H₃), 2.55 (dd, J = 13.3, 8.7 Hz, 1H, H₄), 2.15 (dd, J = 13.3, 6.3 Hz, 1H, H₄)

¹³C NMR (150 MHz, Deuterium Oxide) δ 180.49 (C₁), 180.16 (Br, C₂), 129.97 (C₆), 129.92 (C₇), 129.85 (C₇), 129.37 (C₆), 61.32 (C₈), 55.83 (Br, C₃) 48.54 (C₅), 40.26 (C₄)

HRMS-Nanospray (m/z) [M-H]⁻ calc. for C₁₁H₁₄NO₅, 208.0610; found 208.0612

CD spectra – Positive Cotton effect below 230 nm (**consistent with literature**)

$[\alpha]_D^{23}$ = -40 (c = 0.1 in H₂O)



(1*s*,4*R*)-1-((*S*)-2-Amino-2-carboxyethyl)-4-hydroxycyclohexa-2,5-diene-1-carboxylic acid (Arogenate) (1)¹

To a solution of **225a** (32.2 mg, 0.11 mmol) in water (0.52 mL), barium hydroxide (52.0 mg, 0.32 mmol) and barium carbonate (20.0 mg, 0.11 mmol) were added. The mixture was stirred at 80 °C for 5 hours, and then sodium carbonate anhydrous (70.0 mg, 0.63 mmol) and water (5 mL) were added. The resulting barium carbonate salt was filtered through a Whatman 0.45 µm Nylon syringe filter. The aqueous phase was lyophilised. The solid was redissolved in water (3 mL), filtered through a Millipore Millex-HN 0.45 µm Nylon syringe filter and purified by Hypercarb HPLC with a gradient of 0-80% acetonitrile in 10 mM sodium carbonate-bicarbonate buffer (pH 9.2) to yield **1 as the disodium salt** (41 % by quantitative NMR using a stock solution of EtOH) as a white powder.

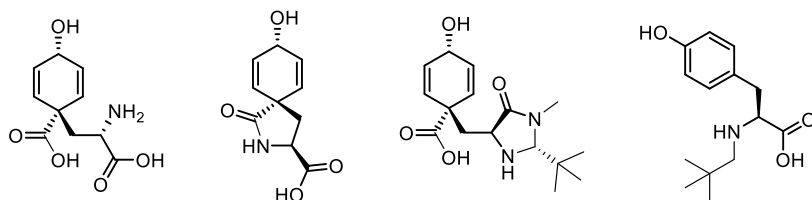
¹H NMR (500 MHz, Deuterium Oxide) δ 5.93 – 5.86 (m, 3H, H_{6&7}), 5.82 – 5.76 (m, 1H, H_{6&7}), 4.47 (d, *J* = 3.6 Hz, 1H, H₈), 3.66 (dd, *J* = 10.5, 3.0 Hz, 1H, H₃), 1.98 (dd, *J* = 14.3, 3.0 Hz, 1H, H₄), 1.89 (dd, *J* = 14.3, 10.5 Hz, 1H, H₄) (**consistent with literature**)

¹³C NMR (126 MHz, Deuterium Oxide) δ 188.13 (C₁), 186.94 (C₂), 168.88 (Na₂CO₃), 138.06 (C₇), 137.81 (C₆), 133.68 (C₆), 132.19 (C₇), 67.36 (C₈), 60.57 (C₃), 56.12 (C₅), 46.94 (C₄) (**consistent with literature**)

CD spectra – Positive Cotton effect below 230 nm (**consistent with literature**)

HRMS-Nanospray (*m/z*) [M-H]⁻ calc. for C₁₀H₁₂NO₅, 226.0715; found 226.0717

[α]_D²³ = -8 (*c* = 0.5 in H₂O)



Arogenate (1), Spiroarogenate (256), Imidazolidinone-protected arogenate (329) and rearomatised side product (331)

To a solution of **225a** (30.5 mg, 0.11 mmol) in water (0.52 mL), barium hydroxide (52.0 mg, 0.32 mmol) and barium carbonate (20.0 mg, 0.11 mmol) were added. The mixture was stirred at 40 °C for 16 hours, and then sodium carbonate anhydrous (70.0 mg, 0.66 mmol) and water (5 mL) were added. The resulting barium carbonate salt was filtered through a Whatman 0.45 µm Nylon

syringe filter. The aqueous phase was lyophilised. The solid was redissolved in water (3 mL), filtered through a Millipore Millex-HN 0.45 µm Nylon syringe filter and purified by Hypercarb HPLC with a gradient of 0-80% acetonitrile in 10 mM sodium carbonate-bicarbonate buffer (pH 9.2) to yield:

1 as the disodium salt (36 % by quantitative NMR using a stock solution of EtOH) as a white powder.

256 as the sodium salt (12 % by quantitative NMR using a stock solution of EtOH) as a white powder.

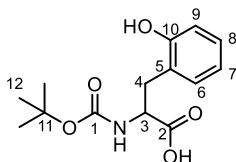
329 as the disodium salt (14% by quantitative NMR using a stock solution of EtOH) as a white powder.

331 as the sodium salt* (4 % by quantitative NMR using a stock solution of EtOH) as a white powder

* contains trace amount of starting material

5.4 Aroenate derivatives

5.4.1 *Ortho*-tyrosine



2-((*tert*-Butoxycarbonyl)amino)-3-(2-hydroxyphenyl)propanoic acid (**261**)

To a solution of DL-*o*-tyrosine (1.06 g, 5.85 mmol) in dioxane:water (30.0 mL, 1:1) sodium hydrogen carbonate (1.47 g, 17.53 mmol) was added portionwise. To this mixture boc anhydride (1.53 g, 7.02 mmol) was added and the reaction mixture was stirred at room temperature overnight. The resulting mixture was concentrated *in vacuo* to approx. 10 mL and the residue was acidified with 2M HCl to pH 2. The aqueous was then extracted with ethyl acetate (3 x 20 mL). The combined organic phases were washed with brine (20 mL), dried over MgSO₄, and concentrated *in vacuo* to yield **261** (1.45 g, 88 %) as a white foam.

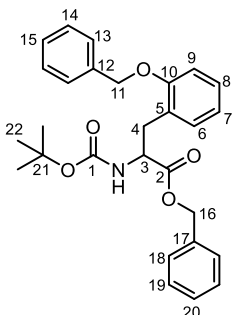
¹H NMR (500 MHz, Methanol-*d*₄) δ 7.12 – 7.03 (m, 2H, H_{6&8}), 6.82 – 6.73 (m, 2H, H_{7&9}), 4.39 (m, 1H, H₃), 3.18 (m, 1H, H₄), 2.95 – 2.80 (m, 1H, H₄), 1.39 (s, 6.74H, H₁₂), 1.34 (s, 2.26H, H₁₂)

¹³C NMR (125 MHz, Methanol-*d*₄) δ 174.03 (C₂), 157.82 (C₁), 156.65 (C₁₀), 132.24 (C₆), 129.07 (C₈), 124.86 (C₅), 120.54 (C₇), 115.84 (C₉), 80.40 (C₁₁), 55.70 (C₃), 33.37 (C₄), 28.66 (C₁₂)

HRMS-ESI (*m/z*) [M+Na]⁺ calc. for C₁₄H₁₉NNaO₅ 304.1155, found 304.1153

IR ν_{max} – 3346 (O-H), 2978, 2933 (C-H), 1678 (C=O)

R_f - 0.41 in 25% EtOAc in petroleum ether



Benzyl 3-(2-(benzyloxy)phenyl)-2-((*tert*-butoxycarbonyl)amino)propanoate (**262**)

To a solution of **261** (1.40 g, 4.98 mmol) in dry DMF (20.0 mL) under N₂, potassium carbonate (1.72 g, 12.5 mmol), benzyl bromide (1.50 mL, 12.5 mmol), and tetraethylammonium iodide (160 mg, 0.62 mmol) were added. The reaction mixture was stirred at room temperature overnight. The

resultant mixture was diluted with ether (40 mL) and washed with water (30 mL). The aqueous phase was extracted with ether (3 x 30 mL) and the combined organics were washed with 1M HCl (20 mL) and brine (20 mL), dried over MgSO₄, and concentrated *in vacuo*. Purification was carried out by column chromatography on silica gel eluting with a gradient of 2-50% ethyl acetate in petroleum ether to yield **262** (1.57 g, 68 %) as a white solid.

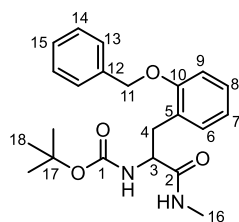
¹H NMR (500 MHz, Chloroform-*d*) δ 7.47 – 7.42 (m, 2H, H₁₃), 7.37 – 7.29 (m, , 6H, H_{14,15,19&20}), 7.26 – 7.22 (m, 2H, H₁₈), 7.20 (t, *J* = 7.5 Hz, 1H, H₈), 7.11 – 7.04 (m, 1H, H₆), 6.94 – 6.84 (m, 2H, H₉), 5.34 (d, *J* = 7.9 Hz, 1H, NH), 5.13 – 5.04 (m, 4H, H_{11&16}), 4.60 (td, *J* = 8.0, 5.2 Hz, 1H, H₃), 3.19 (dd, *J* = 13.7, 5.2 Hz, 1H, H₄), 3.07 (dd, *J* = 13.7, 8.0 Hz, 1H, H₄), 1.37 (s, 9H, H₂₂)

¹³C NMR (125 MHz, Chloroform-*d*) δ 172.37 (C₂), 156.91 (C₁), 155.40 (C₁₀), 136.98 (C₁₂), 135.70 (C₁₇), 131.46 (C₆), 128.60 (Ar), 128.75 (C₈), 128.54 (Ar), 128.30 (Ar), 128.03 (C₁₃), 127.34 (C₁₄), 125.23 (C₅), 121.15 (C₇), 112.01 (C₉), 79.68 (C₂₁), 70.35 (C₁₁), 66.89 (C₁₆), 54.59 (C₃), 33.01 (C₄), 28.43 (C₂₂)

HRMS-ESI (*m/z*) [M+Na]⁺ calc. for C₂₈H₃₁NNaO₅ 484.2094, found 484.2093

IR ν_{max} – 3415 (N-H), 3032, 2977, 2930 (C-H), 1742, 1713 (C=O)

R_f - 0.48 in 25% EtOAc in petroleum ether



***tert*-Butyl (3-(2-(benzyloxy)phenyl)-1-(methylamino)-1-oxopropan-2-yl)carbamate (**263**)**

To a solution of **262** (1.67 g, 3.62 mmol) in EtOH (22 mL), methylamine (9.8 mL, 50.69 mmol) was added. The mixture was stirred at room temperature for 2 days. The solution was concentrated *in vacuo*, redissolved in dichloromethane (30 mL) and washed with a saturated aqueous solution of NaHCO₃ (30 mL). The aqueous phase was extracted with dichloromethane (3 x 20 mL). The combined organics were washed with brine (20 mL), dried over MgSO₄ and concentrated *in vacuo*. Purification was carried out by column chromatography on silica gel eluting with a gradient of 2-100% ethyl acetate in petroleum ether to yield **263** (1.02 g, 73 %) as a white solid.

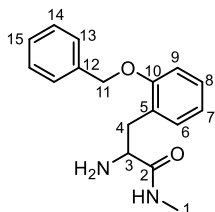
¹H NMR (500 MHz, Chloroform-*d*) δ 7.51 – 7.45 (m, 2H, H₁₃), 7.45 – 7.39 (m, 2H, H₁₄), 7.39 – 7.33 (m, 1H, H₁₅), 7.25 – 7.16 (m, 2H, H_{6&8}), 6.98 – 6.88 (m, 2H, H_{7&9}), 5.82 (s, 1H, NH), 5.40 (s, 1H, NH), 5.10 (d, *J* = 3.0 Hz, 2H, H₁₁), 4.28 (s, 1H, H₃), 3.16 (dd, *J* = 13.7, 4.8 Hz, 1H, H₄), 3.02 - 2.94 (m, 1H, H₄), 2.66 (d, *J* = 4.8 Hz, 3H, H₁₆), 1.34 (s, 9H, H₁₈)

¹³C NMR (125 MHz, Chloroform-*d*) δ 172.42 (C₂), 156.69 (C_{1&10}), 136.88 (C₁₂), 131.55 (C₆), 128.90 (C₁₄), 128.38 (C₈), 128.33 (C₁₅), 127.78 (C₁₃), 126.19 (C₅), 121.39 (C₇), 111.84 (C₉), 79.93 (C₁₇), 70.52 (C₁₁), 56.12 (C₃), 33.40 (C₄), 28.37 (C₁₈), 26.17 (C₁₆)

HRMS-ESI (*m/z*) [M+Na]⁺ calc. for C₂₂H₂₉N₂NaO₄ 407.1941, found 407.1954

IR ν_{max} – 3314 (N-H), 3064, 2976, 2932 (C-H), 1703, 1659 (C=O)

R_f - 0.23 in 50% EtOAc in petroleum ether



2-Amino-3-(2-(benzyloxy)phenyl)-N-methylpropanamide (**264**)

To a solution of **263** (1.00 g, 2.60 mmol) in MeOH (10.0 mL) at 0 °C, acetyl chloride (1.00 mL, 14.0 mmol) was added dropwise. The solution was warmed to room temperature and left to stir overnight. The resultant mixture was diluted with dichloromethane (50 mL) and washed with a saturated aqueous solution of NaHCO₃ (20 mL) and brine (20 mL), dried over MgSO₄ and concentrated *in vacuo* to yield **264** (733 mg, 97%) as a clear oil.

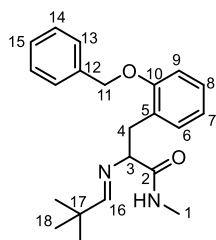
¹H NMR (400 MHz, Chloroform-*d*) δ 7.48 – 7.30 (m, 5H, H_{12,13,14&15}), 7.24 – 7.16 (m, 2H, H_{6&8}), 7.09 (s, 1H, NH), 6.99 – 6.90 (m, 2H, H_{7&9}), 5.10 (s, 2H, H₁₁), 3.64 (dd, *J* = 9.3, 3.9 Hz, 1H, H₃), 3.36 (dd, *J* = 13.6, 3.9 Hz, 1H, H₄), 2.81 – 2.72 (m, 4H, H_{1&4})

¹³C NMR (125 MHz, Chloroform-*d*) δ 175.39 (C₂), 156.98 (C₁₀), 137.10 (C₁₂), 131.42 (C₆), 128.81 (C₁₄), 128.13 (C₁₅), 128.10 (C₈), 127.41 (C₅), 127.39 (C₁₃), 121.24 (C₇), 112.04 (C₉), 70.24 (C₁₁), 56.09 (C₃), 35.80 (C₄), 25.90 (C₁)

HRMS-ESI (*m/z*) [M+Na]⁺ calc. for C₁₇H₂₀N₂NaO₂ 307.1416, found 307.1412

IR ν_{max} – 3367, 3321 (N-H), 3066, 3032, 2932 (C-H), 1659 (C=O)

R_f - 0.10 in 5 % MeOH in EtOAc



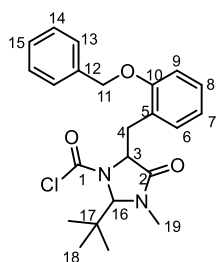
(E)-3-(2-(Benzyloxy)phenyl)-2-((2,2-dimethylpropylidene)amino)-N-methylpropanamide (265)

To a solution of **264** (700 mg, 2.46 mmol) in dichloromethane (5.00 mL) under N₂, MgSO₄ (700 mg, 100% wt.) and pivaldehyde (0.32 mL, 2.96 mmol) were added. The mixture was stirred at room temperature overnight. The solution was filtered and washed with dichloromethane (10 mL). The filtrate was concentrated *in vacuo* to yield **265** (855 mg, Quant.) as a pale-yellow powder.

¹H NMR (500 MHz, Chloroform-*d*) δ 7.52 (d, J = 8.3 Hz, 2H, H₁₃), 7.44 – 7.36 (m, 2H, H₁₄), 7.34 – 7.27 (m, 1H, H₁₅), 7.18 – 7.10 (m, 1H, H₈), 7.00 – 6.92 (m, 2H, H₆ & NH), 6.88 (d, J = 8.3 Hz, 1H, H₉), 6.83 (t, J = 7.4 Hz, 1H, H₇), 6.76 (s, 1H, H₁₆), 5.12 (s, 2H, H₁₁), 3.93 (dd, J = 10.8, 3.4 Hz, 1H, H₃), 3.58 (dd, J = 13.2, 3.4 Hz, 1H, H₄), 2.88 (d, J = 4.9 Hz, 3H, H₁), 2.80 – 2.72 (m, 1H, H₄), 0.81 (s, 9H, H₁₈)

¹³C NMR (125 MHz, Chloroform-*d*) δ 174.01 (C₁₆), 173.97 (C₂), 156.86 (C₁₀), 137.43 (C₅), 132.47 (C₆), 128.67 (C₁₄), 127.87 (C₈), 127.80 (C₁₃), 127.05 (C₁₅), 126.63 (C₁₂), 120.53 (C₇), 111.90 (C₉), 72.06 (C₃), 69.79 (C₁₁), 36.18 (C₁₇), 35.99 (C₄), 26.65 (C₁₈), 26.01 (C₁)

HRMS-ESI (m/z) [M+Na]⁺ calc. for C₂₂H₂₈N₂NaO₂ 375.2042, found 375.2051



5-(2-(Benzyloxy)benzyl)-2-(tert-butyl)-3-methyl-4-oxoimidazolidine-1-carbonyl chloride (266)

To a solution of **265** (800 mg, 2.46 mmol) in THF (5.00 mL) under N₂, phosgene (2.30 mL, 15% in toluene, 3.20 mmol) was added dropwise. The mixture was stirred at room temperature for 30 minutes. Pyridine (0.40 mL, 4.92 mmol) was then added and the mixture stirred for a further 2 hours. The solution was concentrated *in vacuo* and redissolved in dichloromethane (30 mL). The

organic phase was washed with HCl (1M, 3 x 20 mL) and brine (20 mL), then dried over MgSO₄ and concentrated *in vacuo*. Purification was carried out by column chromatography on silica gel eluting with 100% dichloromethane to yield **266** (432 mg, 42 %) as a white solid.

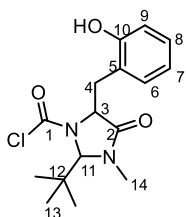
¹H NMR (500 MHz, Chloroform-*d*) δ 7.34 (d, J = 7.5 Hz, 2H, H₁₃), 7.29 – 7.22 (m, 2H, H₁₄), 7.19 (t, J = 7.3 Hz, 1H, H₁₅), 7.09 – 6.98 (m, 2H, H_{6&8}), 6.81 – 6.70 (m, 2H, H_{7&9}), 5.06 – 4.94 (m, 2H, H₁₁), 4.77 (s, 1H, H₁₆), 4.40 (s, 1H, H₃), 3.72 (s, 1H, H₄), 3.29 (d, J = 14.5 Hz, 1H, H₄), 2.71 (s, 3H, H₁₉), 0.89 (s, 9H, H₁₈). – rotameric mixture – VT @ 50 °C

¹³C NMR (125 MHz, Chloroform-*d*) δ 169.98 (C₂), 157.31 (C₁₀), 137.46 (C₁), 131.37 (C₆), 128.71 (C₁₂), 128.57 (C₁₄), 128.40 (C₈), 127.89 (C₁₅), 127.69 (C₁₃), 127.12 (C₅), 120.54 (C₇), 112.28 (C₉), 83.20 (C₁₆), 70.39 (C₁₁), 62.29 (C₃), 42.04 (C₄), 32.18 (C₁₉), 26.89 (C₁₈). – rotameric mixture – VT @ 50 °C

HRMS-ESI (m/z) [M+H]⁺ calc. for C₂₃H₂₈ClN₂O₃ 415.1782, found 415.1785

IR ν_{max} – 3070, 3033, 2966, 2876 (C-H), 1744, 1713 (C=O)

R_f - 0.57 in 50% EtOAc in petroleum ether



2-(*tert*-Butyl)-5-(2-hydroxybenzyl)-3-methyl-4-oxoimidazolidine-1-carbonyl chloride (**258**)

To a solution of **266** (400 mg, 0.97 mmol) in THF (9.00 mL) under N₂, palladium on active carbon (10 wt. %) (80 mg, 20 % wt.) was added. The mixture was then stirred at room temperature for 2 hours under hydrogen atmosphere. The reaction mixture was filtered over a pad of celite and concentrated *in vacuo*. Purification was carried out by column chromatography on silica gel eluting with a gradient of 0-100% ethyl acetate in petroleum ether to yield **258** (220 mg, 66 %) as a white solid.

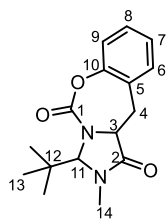
¹H NMR (500 MHz, Chloroform-*d*) δ 7.54 (s, br, 1H, OH), 7.17 – 7.09 (m, 2H, H_{6&8}), 6.91 (d, J = 8.1 Hz, 1H, H₉), 6.84 (t, J = 7.5 Hz, 1H, H₇), 5.00 (s, 1H, H₁₁), 4.46 (s, 1H, H₃), 3.57 (s, 1H, H₄), 3.40 (d, J = 15.1 Hz, 1H, H₄), 2.91 (s, 3H, H₁₄), 1.03 (s, 9H, H₁₃). – rotameric mixture – VT @ 50 °C

¹³C NMR (125 MHz, Chloroform-*d*) δ 172.69 (C₂), 155.33 (C_{1&10}), 131.71 (C₆), 129.12 (C₈), 122.09 (C₅), 120.83 (C₇), 118.54 (C₉), 84.13 (C₁₁), 63.59 (C₃), 41.76 (C₄), 32.50 (C₁₄), 29.78 (C₁₂), 26.86 (C₁₃). – rotameric mixture – VT @ 50 °C

HRMS-ESI (m/z) [M+Na]⁺ calc. for C₁₆H₂₁ClN₂NaO₃ 347.1132, found 347.1134

IR ν_{max} – 3301 (O-H), 2968 (C-H), 1739, 1686 (C=O)

R_f - 0.45 in 50% EtOAc in petroleum ether



3-(*tert*-Butyl)-2-methyl-2,3,11,11a-tetrahydro-1H,5H-benzo[f]imidazo[1,5-c][1,3]oxazepine-1,5-dione (268)

To a solution of **258** (30.0 mg, 0.09 mmol) in dry acetonitrile (0.60 mL) under N₂, potassium iodide (16.9 mg, 0.10 mmol) and triethylamine (14 μ L, 0.10 mmol) were added. The mixture was subjected to the microwave at 150 °C for 5 minutes at very high absorption. The reaction mixture was concentrated *in vacuo*, redissolved in dichloromethane (20 mL) and washed with water (10 mL). The aqueous phase was extracted with dichloromethane (3 x 30 mL). The combined organics were washed with brine (30 mL), dried over MgSO₄, filtered and concentrated *in vacuo* to yield **268** (19.0 mg, 77 %) as a white solid.

¹H NMR (500 MHz, Chloroform-*d*) δ 7.35 – 7.26 (m, 1H, H₈), 7.28 – 7.22 (m, 1H, H₆), 7.21 – 7.14 (m, 2H, H_{7&9}), 5.45 (d, *J* = 0.8 Hz, 1H, H₁₁), 4.06 (dd, *J* = 12.0, 2.2 Hz, 1H, H₃), 3.29 (dd, *J* = 14.5, 2.2 Hz, 1H, H₄), 3.15 – 3.05 (m, 4H, H_{4&14}), 0.97 (s, 9H, H₁₃)

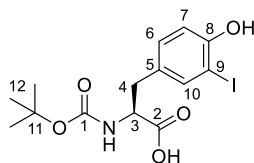
¹³C NMR (125 MHz, Chloroform-*d*) δ 169.76 (C₁), 151.30 (C₂), 151.05 (C₁₀), 129.51 (C₅), 129.05 (C₈), 128.70 (C₆), 126.18 (C₇), 120.21 (C₉), 83.22 (C₁₁), 63.52 (C₃), 39.40 (C₁₂), 32.00 (C₁₄), 31.88 (C₄), 26.20 (C₁₃)

HRMS-ESI (*m/z*) [M+H]⁺ calc. for C₁₆H₂₁N₂O₃ 289.1546, found 289.1551

IR ν_{max} – 2962, 2922, 2852 (C-H), 1699 (C=O)

R_f - 0.38 in 50% EtOAc in petroleum ether

5.4.2 3-Methyl Arogenate

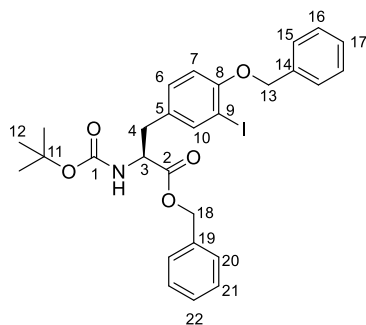


(S)-2-((tert-Butoxycarbonyl)amino)-3-(4-hydroxy-3-iodophenyl)propanoic acid (**270**)¹³⁴

To a solution of 3-iodo-L-tyrosine (5.00 g, 16.3 mmol) in dioxane:water (80.0 mL, 1:1) sodium hydrogen carbonate (4.10 g, 48.9 mmol) was added portionwise. To this mixture boc anhydride (4.30 g, 19.6 mmol) was added and stirred at room temperature overnight. The resulting mixture was concentrated *in vacuo* to approx. 40 mL and the residue was acidified with 2M HCl to pH 2. The aqueous was then extracted with ethyl acetate (3 x 50 mL) and the organics was washed with brine (30 mL), dried over MgSO₄, and concentrated *in vacuo* to yield **270** (6.63 g, quant.) as a white powder.

¹H NMR (400 MHz, Chloroform-d) δ 7.48 (s, 1H, H₁₀), 7.06 (dd, J = 8.3, 2.1 Hz, 1H, H₆), 6.91 (d, J = 8.3 Hz, 1H, H₇), 4.95 (d, J = 7.9 Hz, 1H, NH), 4.53 (d, J = 7.3 Hz, 1H, H₃), 3.19 – 2.91 (m, 2H, H₄), 1.44 (s, 9H, H₁₂)

Consistent with literature data.



Benzyl (S)-3-(4-(benzyloxy)-3-iodophenyl)-2-((tert-butoxycarbonyl)amino)propanoate (**271**)¹³⁵

To a solution of **270** (6.30 g, 16.3 mmol) in DMF (65.0 mL), potassium carbonate (5.60 g, 40.8 mmol), benzyl bromide (4.85 mL, 40.8 mmol), and tetraethylammonium iodide (523 mg, 2.04 mmol) were added. The reaction mixture was stirred at room temperature overnight. The resultant mixture was diluted with ether (150 mL) and washed with water (50 mL). The aqueous phase was extracted with ether (3 x 50 mL). The combined organics were washed with 1M HCl (50 mL) and brine (30 mL), dried over MgSO₄, and concentrated *in vacuo*. Purification was carried out by

column chromatography on silica gel eluting with a gradient of 0-50% ethyl acetate in hexane to yield **271** (8.89 g, 92 %) as a white powder.

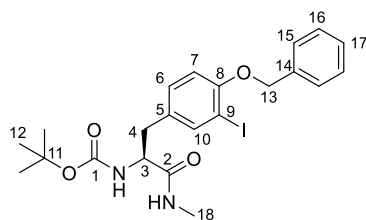
¹H NMR (500 MHz, Chloroform-d) δ 7.55 (s, 1H, H₁₀), 7.49 (d, J = 7.1 Hz, 2H, H₁₅), 7.42 – 7.29 (m, 8H, H_{16,17,20,21&22}), 6.93 (d, J = 8.3 Hz, 1H, H₆), 6.68 (d, J = 8.3 Hz, 1H, H₇), 5.20 – 5.07 (m, 4H, H_{13,18}), 5.00 (d, J = 8.0 Hz, 1H, NH), 4.57 (m, 1H, H₃), 2.99 (m, 2H, H₄), 1.43 (s, 9H, H₁₂)
¹³C NMR (125 MHz, Chloroform-d) δ 171.64 (C₂), 156.47 (C₈), 155.12 (C₁), 140.42 (C₁₀), 136.63 (C₁₄), 135.19 (C₁₉), 130.57 (C₆), 130.38 (C₅), 128.78 (C₁₆), 128.70 (C_{20&21}), 128.66 (C₁₇), 128.03 (C₂₂), 127.09 (C₁₅), 112.63 (C₇), 86.89 (C₉), 80.19 (C₁₁), 71.03 (C₁₈), 67.37 (C₁₃), 54.63 (C₃), 37.06 (C₄), 28.46 (C₁₂)

HRMS-ESI (m/z) [M+Na⁺] calc. for C₂₈H₃₀INO₅Na, 610.1061; found 610.1053

IR ν_{max} – 3363 (N-H), 2975, 2931 (C-H), 1740, 1711 (C=O)

R_f - 0.54 in 25% EtOAc in Hexane

Consistent with literature data.



***tert*-Butyl (S)-(3-(4-(benzyloxy)-3-iodophenyl)-1-(methylamino)-1-oxopropan-2-yl)carbamate (**272**)**

To a solution of **271** (8.70 g, 14.8 mmol) in EtOH (30.0 mL), methylamine (33 % wt. in EtOH)(12.9 mL, 104 mmol) was added. The mixture was stirred at room temperature for 2 days. The solution was concentrated *in vacuo*, redissolved in dichloromethane (80 mL) and washed with a saturated aqueous solution of NaHCO₃ (50 mL). The aqueous phase was extracted with dichloromethane (3 x 30 mL). The combined organics were washed with brine (30 mL), dried over MgSO₄ and concentrated *in vacuo* to yield **272** (7.75 g, Quant.) as a white powder.

¹H NMR (500 MHz, Chloroform-d) δ 7.63 (d, J = 2.2 Hz, 1H, H₁₀), 7.51 – 7.44 (m, 2H, H₁₅), 7.39 (t, J = 7.4 Hz, 2H, H₁₆), 7.32 (t, J = 7.4 Hz, 1H, H₁₇), 7.10 (dd, J = 8.4, 2.2 Hz, 1H, H₆), 6.77 (d, J = 8.4 Hz, 1H, H₇), 5.78 (s, 1H, NH), 5.12 (s, 2H, H₁₃), 5.07 – 4.96 (m, 1H, NH), 4.21 (m, 1H, H₃), 2.95 (m, 2H, H₄), 2.74 (d, J = 4.8 Hz, 3H, H₁₈), 1.41 (s, 9H, H₁₂)

¹³C NMR (125 MHz, Chloroform-d) δ 171.63 (C₁), 156.38 (C₂), 155.50 (C₈), 140.29 (C₁₀), 136.57 (C₁₄), 131.45 (C₅), 130.41 (C₆), 128.70 (C₁₆), 128.06 (C₁₇), 127.13 (C₁₅), 112.76 (C₇), 86.99 (C₉), 71.05 (C₁₃), 56.15 (C₃), 37.51 (C₄), 28.44 (C₁₂), 26.32 (C₁₈)

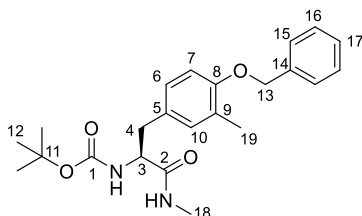
HRMS-ESI (m/z) [M+Na]⁺ calc. for C₂₂H₂₇IN₂O₄Na, 533.0908; found 533.0888

IR ν_{max} – 3325 (NH), 2970, 2921, 2851 (C-H), 1683, 1649 (C=O)

R_f - 0.51 in 10% MeOH in dichloromethane

mp 114-116 °C

[α]_D²⁶ = 12 (*c* = 1 in CHCl₃)



***tert*-Butyl(*S*)-(3-(4-(benzyloxy)-3-methylphenyl)-1-(methylamino)-1-oxopropan-2-yl)carbamate (275)**

To a solution of **272** (7.75 g, 15.2 mmol) in Dry degassed dioxane (100 mL), cesium carbonate (24.9 g, 76.4 mmol), SPhos Pd G₂ (1.01 g, 1.52 mmol) and Methyl boronic acid (4.60 g, 76.4 mmol) were added. The mixture was stirred at 90 °C overnight. The solution was diluted with dichloromethane (100 mL) and water (100 mL). The aqueous phase was extracted with dichloromethane (3 x 50 mL). The combined organic phases dried over MgSO₄ and concentrated *in vacuo*. Purification was carried out by column chromatography on silica gel eluting with 0-100% EtOAc in petroleum ether to yield **275** (4.43 g, 73 %) as a yellow powder.

¹H NMR (500 MHz, Chloroform-*d*) δ 7.45 – 7.41 (m, 2H, H₁₅), 7.38 (t, *J* = 7.5 Hz, 2H, H₁₆), 7.35 – 7.28 (m, 1H, H₁₇), 7.11 (d, *J* = 8.3 Hz, 0.25H, H₆), 6.99 (s, 1H, H₁₀), 6.95 (d, *J* = 8.3 Hz, 0.75H, H₆), 6.91 (m, 0.25H, H₇), 6.80 (d, *J* = 8.3 Hz, 0.75H, H₇), 5.66 (s, 1H, NH), 5.05 (s, 2H, H₁₃), 4.21 (m, 1H, H₃), 3.03 – 2.97 (m, 1H, H₄), 2.91 (m, 1H, H₄), 2.72 (d, *J* = 4.9 Hz, 3H, H₁₈), 2.25 (s, 3H, H₁₉), 1.41 (s, 9H, H₁₂) – rotameric mixture

¹³C NMR (125 MHz, Chloroform-*d*) δ 172.02 (C₂), 156.01 (C₈), 155.54 (C₁), 137.51 (C₁₄), 131.79 (C₁₀), 130.46 (C₆), 128.72 (C₅), 128.65 (C₁₆), 127.92 (C₁₇), 127.61 (C₉), 127.58 (C₆), 127.23 (C₁₅), 115.16 (C₇), 111.66 (C₇), 80.24 (C₁₁), 70.03 (C₁₃), 56.37 (C₃), 38.11 (C₄), 28.44 (C₁₂), 26.26 (C₁₈), 16.49 (C₁₉) – rotameric mixture

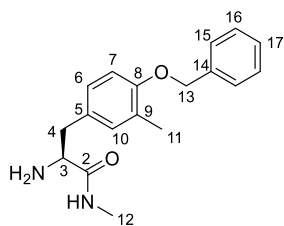
HRMS-ESI (*m/z*) [*M*+Na]⁺ calc. for C₂₃H₃₀N₂O₄Na, 421.2098; found 421.2101

IR ν_{max} – 3317 (N-H), 3063, 3032 (Ar-H), 2973, 2929, 2856 (C-H), 1704, 1658 (C=O)

R_f - 0.65 in dichloromethane

mp 134-135 °C

[α]_D²⁶ = 16 (*c* = 1 in CHCl₃)



(S)-2-Amino-3-(4-(benzyloxy)-3-methylphenyl)-N-methylpropanamide (274)

To a solution of **275** (4.30 g, 10.8 mmol) in MeOH (43.0 mL) at 0 °C, acetyl chloride (4.15 mL, 58.3 mmol) was slowly added. The mixture was warmed to room temperature and stirred overnight. The solution was diluted with dichloromethane (200 mL) and washed with saturated NaHCO₃ (50 mL) and brine (30 mL). The organic phase was dried over MgSO₄ and concentrated *in vacuo*. Purification was carried out by column chromatography on silica gel eluting with a gradient of 0-10% methanol in dichloromethane to yield **274** (3.11 g, 97%) as a yellow powder.

¹H NMR (500 MHz, Chloroform-d) δ 7.46 – 7.41 (m, 2H, H₁₅), 7.41 – 7.36 (m, 2H, H₁₆), 7.34 – 7.29 (m, 1H, H₁₇), 7.02 (d, *J* = 2.2 Hz, 1H, H₁₀), 6.98 (dd, *J* = 8.2, 2.2 Hz, 1H, H₆), 6.82 (d, *J* = 8.2 Hz, 1H, H₇), 5.06 (s, 2H, H₁₃), 3.57 (dd, *J* = 9.4, 4.1 Hz, 1H, H₃), 3.19 (dd, *J* = 13.8, 4.1 Hz, 1H, H₃), 2.82 (d, *J* = 5.0 Hz, 3H, H₁₂), 2.60 (dd, *J* = 13.8, 9.4 Hz, 1H, H₄), 2.27 (s, 3H, H₁₁)

¹³C NMR (125 MHz, Chloroform-d) δ 175.01 (C₂), 155.97 (C₈), 137.56 (C₁₀), 131.79 (C₁₄), 129.86 (C₅), 128.65 (C₁₆), 127.90 (C₁₇), 127.55 (C₆), 127.53 (C₉), 127.21 (C₁₅), 111.69 (C₇), 70.05 (C₁₃), 56.72 (C₃), 40.26 (C₄), 25.95 (C₁₂), 16.55 (C₁₁)

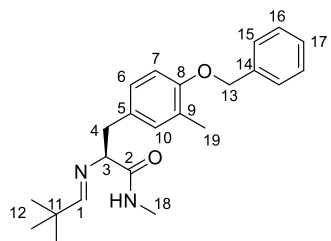
HRMS-ESI (*m/z*) [M+H]⁺ calc. for C₁₈H₂₃N₂O₂, 299.1754; found 299.1747

IR ν_{max} – 3366, 3299 (N-H), 3064, 3032 (Ar-H), 2921 (C-H), 1654 (C=O)

R_f - 0.25 in 10% MeOH in dichloromethane

mp 78-80 °C

[α]_D²⁶ = -64 (*c* = 1 in CHCl₃)



(S,E)-3-(4-(Benzyloxy)-3-methylphenyl)-2-((2,2-dimethylpropylidene)amino)-N-methylpropanamide (276)

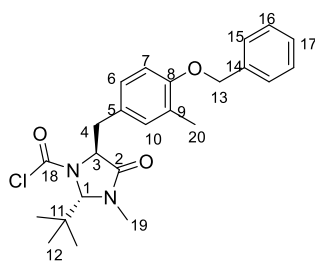
To a solution of **274** (3.00 g, 10.1 mmol) in dichloromethane (10.0 mL), MgSO₄ (3.00 g, 100% wt.) and pivaldehyde (1.31 mL, 12.1 mmol) were added. The mixture was stirred at room

temperature overnight. The solution was filtered and washed with dichloromethane (3 x 30 mL). The filtrate was concentrated *in vacuo* to yield **276** (3.68 g, Quant.) as a white powder.

¹H NMR (400 MHz, Chloroform-d) δ 7.45 – 7.40 (m, 2H, H₁₅), 7.40 – 7.34 (m, 2H, H₁₆), 7.33 – 7.28 (m, 1H, H₁₇), 6.91 (d, J = 5.0 Hz, 1H, NH), 6.86–6.79 (m, 3H, H_{1,7&10}), 6.75 (d, J = 8.0 Hz, 1H, H₆), 5.05 (s, 2H, H₁₃), 3.63 (dd, J = 10.5, 3.0 Hz, 1H, H₃), 3.26 (dd, J = 13.5, 3.0 Hz, 1H, H₄), 2.84 (d, J = 5.0 Hz, 3H, H₁₈), 2.64 (dd, J = 13.5, 10.5 Hz, 1H, H₄), 2.23 (s, 3H, H₁₉), 0.89 (s, 9H, H₁₂)

¹³C NMR (100 MHz, Chloroform-d) δ 174.26 (C₁), 173.72 (C₂), 155.52 (C₈), 137.64 (C₁₄), 132.76 (C₁₀), 129.73 (C₅), 128.60 (C₁₆), 128.23 (C_{7&1}), 127.81 (C₁₇), 127.12 (C₁₅), 126.71 (C₉), 111.44 (C₆), 74.67 (C₃), 70.00 (C₁₃), 40.23 (C₄), 36.38 (C₁₁), 26.79 (C₁₂), 26.01 (C₁₈), 16.49 (C₁₉)

HRMS-ESI (m/z) [M+H]⁺ calc. for C₂₃H₃₁N₂O₂, 367.2380; found 367.2396



(5S)-5-(4-(Benzyloxy)-3-methylbenzyl)-2-(tert-butyl)-3-methyl-4-oxoimidazolidine-1-carbonyl chloride (277)

To a solution of **276** (3.68 g, 10.1 mmol) in THF (20.0 mL), phosgene (10.8 mL, 15% in toluene, 15.1 mmol) was added. The mixture was stirred at room temperature for 2 hours. Pyridine (1.63 mL, 20.1 mmol) was then added and the mixture stirred for a further 2 hours. The solution was concentrated *in vacuo* and redissolved in dichloromethane (50 mL). The organic phase was washed with HCl (1M, 3 x 30 mL) and brine (20 mL), then dried over MgSO₄ and concentrated *in vacuo*. Purification was carried out by column chromatography on silica gel eluting with a gradient of 0–100% EtOAc in hexane to yield **277** (3.46 g, 80 %) as a pale yellow powder.

¹H NMR (400 MHz, Chloroform-d) δ 7.43 (d, J = 7.0 Hz, 2H, H₁₅), 7.41 – 7.35 (m, 2H, H₁₆), 7.33 – 7.29 (m, 1H, H₁₇), 7.00–6.90 (m, 2H, H_{6&10}), 6.76 (d, J = 8.3 Hz, 1H, H₇), 5.04 (s, 2H, H₁₃), 4.72 (s, 0.54H, H₁), 4.60 (s, 0.46H, H₁), 4.41 (m, 0.54H, H₃), 4.37 (m, 0.46H, H₃), 3.78 (m, 0.46H, H₄), 3.65 (m, 0.54H, H₄), 3.27 (m, 0.46H, H₄), 3.18 (m, 0.54H, H₄), 2.86 (s, 1.62H, H₁₉), 2.75 (s, 1.38H, H₁₉), 2.23 (s, 3H, H₂₀), 1.00 (s, 4.86H, H₁₂), 0.93 (s, 4.14H, H₁₂) – rotameric mixture

¹³C NMR (125 MHz, Chloroform-d) δ 170.05 (C₂), 169.64 (C₂), 156.24 (C₈), 156.02 (C₈), 147.42 (C₁₈), 146.24 (C₁₈), 137.55 (C₁₄), 137.46 (C₁₄), 132.48 (C₁₀), 132.26 (C₁₀), 128.58 (C_{16&6}), 127.85 (C₁₇), 127.27 (C₁₅), 126.19 (C₅), 125.80 (C₅), 111.31 (C₇), 83.49 (C₁), 82.90 (C₁), 69.89 (C₁₃),

63.89 (C₃), 62.87 (C₃), 41.80 (C₁₁), 41.70 (C₁₁), 35.92 (C₄), 32.14 (C₁₉), 32.09 (C₄), 26.79 (C₁₂), 26.54 (C₁₂), 16.34 (C₂₀) – rotameric mixture

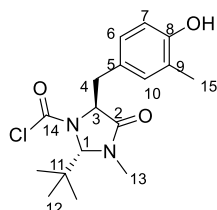
HRMS-ESI (m/z) [$M+H$]⁺ calc. for C₂₄H₂₉N₂O₃Cl, 429.1939; found 429.1924

IR ν_{\max} – 2963, 2931 (C-H), 1739, 1708 (C=O)

R_f - 0.59 in 50% EtOAc in Hexane

mp 92-94 °C

[α]_D²⁶ = 4 (c = 1 in CHCl₃)



(5S)-2-(tert-Butyl)-5-(4-hydroxy-3-methylbenzyl)-3-methyl-4-oxoimidazolidine-1-carbonyl chloride (278)

To a solution of **277** (3.35 g, 7.82 mmol) in THF (39.0 mL) under N₂, palladium on active carbon (10 wt. %) (670 mg, 20 % wt.) was added. The mixture was then stirred at room temperature for 2 hours under hydrogen atmosphere. The reaction mixture was filtered over a pad of celite and concentrated in *vacuo* to yield **278** (2.61 g, 94 %) as a white powder.

¹H NMR (500 MHz, Chloroform-d) δ 6.93 (s, 1H, H₁₀), 6.87 (d, J = 8.2 Hz, 1H, H_{6/7}), 6.65 (t, J = 8.6 Hz, 1H, H_{6/7}), 4.73 (s, 0.55H, H₁), 4.62 (s, 0.45H, H₁) 4.44 – 4.34 (m, 1H, H₃), 3.84 – 3.72 (m, 0.55H, H₄), 3.64 (m, 0.45H, H₄) 3.26 (m, 0.45H, H₄), 3.15 (m, 0.55H, H₄), 2.88 (s, 1.65H, H₁₃), 2.77 (s, 1.35H, H₁₃), 2.19 (s, 3H, H₁₅), 1.00 (s, 4.95H, H₁₂), 0.93 (s, 4.05H, H₁₂) – rotameric mixture

¹³C NMR (126 MHz, Chloroform-d) δ 170.19 (C₂), 169.77 (C₂), 153.47 (C₈), 153.14 (C₈), 147.54 (C₁₄), 146.31 (C₁₄), 132.83 (C₁₀), 132.61 (C₁₀), 128.88 (C_{6/7}), 128.73 (C_{6/7}), 126.16 (C₅), 125.77 (C₅), 124.02 (C₉), 123.71 (C₉), 114.95 (C_{6/7}), 114.82 (C_{6/7}), 83.59 (C₁), 82.99 (C₁), 63.95 (C₃), 62.95 (C₃), 41.83 (C₁₁), 41.71 (C₁₁), 35.87 (C₄), 32.19 (C₄), 32.04 (C₁₃), 26.80 (C₁₂), 26.55 (C₁₂), 15.75 (C₁₅) – rotameric mixture

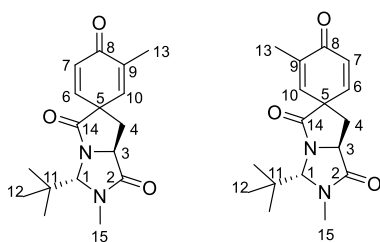
HRMS-ESI (m/z) [$M+H-H_2O$]⁺ calc. for C₁₇H₂₃N₂O₃, 303.1703; found 303.1703

IR ν_{\max} – 3363 (O-H), 2968, 2875 (C-H), 1738, 1691 (C=O)

R_f - 0.46 in 10% MeOH in Dichloromethane

mp 134-135 °C

[α]_D²⁶ = -12 (c = 1 in CHCl₃)



(3'*S*,7a'*S*)-3'-(tert-Butyl)-2',3-dimethyl-2',3',7',7a'-tetrahydro-1'H,5'H-spiro[cyclohexane-1,6'-pyrrolo[1,2-c]imidazole]-2,5-diene-1',4,5'-trione (279**)**

To a solution of **278** (1.1 g, 3.08 mmol) in MeCN (4.4 mL), triethylamine (0.46 mL, 3.39 mmol) was added. The mixture was then heated under microwave irradiation at 150 °C for 10 minutes. The reaction mixture was concentrated *in vacuo*, redissolved in dichloromethane (20 mL) and washed with water (20 mL). The aqueous phase was extracted with dichloromethane (3 x 20 mL). The organic layer was washed with brine (10 mL), dried over MgSO₄ and concentrated *in vacuo* to yield **279** (926 mg, Quant., 1:1) as a white powder.

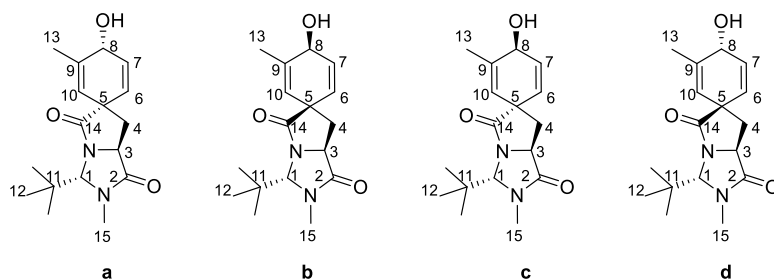
¹H NMR (400 MHz, Chloroform-*d*) δ 6.90 (dd, *J* = 9.8, 3.0 Hz, 0.5H, H₆), 6.71 – 6.65 (m, 1H, H_{6&10}), 6.52 – 6.44 (m, 1H, H_{7&10}), 6.40 (d, *J* = 9.8 Hz, 0.5H, H₇), 4.85 (t, *J* = 1.4 Hz, 1H, H₁), 4.45 (m, 1H, H₃), 3.04 (d, *J* = 1.2 Hz, 3H, H₁₅), 2.59 (m, 1H, H₄), 2.44 (m, 1H, H₄), 1.96 (t, *J* = 1.4 Hz, 3H, H₁₃), 1.05 (s, 4.5H, H₁₂), 1.04 (s, 4.5H, H₁₂) - as 1:1 mix of diastereomers

¹³C NMR (100 MHz, Chloroform-*d*) δ 185.60 (C₈), 185.50 (C₈), 174.87 (C₂), 174.72 (C₂), 171.70 (C₁₄), 171.68 (C₄), 146.08 (C_{6/10}), 143.37 (C₆), 141.70 (C_{7/10}), 139.22 (C₉), 138.81 (C_{6/10}), 137.97 (C₉), 132.08 (C_{7/10}), 130.73 (C₇), 82.03 (C₁), 82.01 (C₁), 57.13 (C₃), 56.94 (C₃), 54.16 (C₅), 54.05 (C₅), 38.53 (C₁₁), 37.65 (C₄), 37.58 (C₄), 31.61 (C₁₅), 31.60 (C₁₅), 25.98 (C₁₂), 25.95 (C₁₂), 16.34 (C₁₃), 16.31 (C₁₃)

HRMS-ESI (*m/z*) [M+Na]⁺ calc. for C₁₇H₂₂N₂O₃Na, 325.1523; found 325.1515.

R_f – 0.28/0.34 in 5% MeOH in dichloromethane.

The diastereomers could be separated by column chromatography on silica gel eluting with a gradient of 0-30% Acetone in dichloromethane for testing purposes, otherwise material was taken through crude.



(1*S*,3'*S*,4*R*,7*a*'*S*)-3'-(*tert*-Butyl)-4-hydroxy-2',3-dimethyl-2',3',7',7*a*'-tetrahydro-1*H*,5'*H*-spiro[cyclohexane-1,6'-pyrrolo[1,2-*c*]imidazole]-2,5-diene-1',5'-dione & diastereomers (280)

To a solution of **279** (0.93 g, 3.08 mmol) in dry methanol (30 mL) under N₂, cerium(III) chloride heptahydrate (175 mg, 4.62 mmol) was added and the reaction mixture was stirred for 15 minutes at room temperature. The reaction mixture was then cooled to -78 °C and sodium borohydride (1.72 g, 4.62 mmol) was added. The resultant mixture was left to stir for a further 30 minutes at -78 °C and then quenched with water (10 mL). The mixture was then diluted with EtOAc (50 mL) and washed with water (30 mL). The aqueous phase was extracted with EtOAc (3 x 30 mL). The combined organics were washed with brine (30 mL), dried over MgSO₄, filtered and concentrated *in vacuo*. Purification was carried out by column chromatography on silica gel eluting with 0-10% MeOH in dichloromethane to yield **280** (615 mg, 66 %, d.r. = 1.5:1.5:1.2:1) as clear oils.

280a

(177 mg, 18%)

¹H NMR (500 MHz, Chloroform-*d*) δ 6.12 (dd, *J* = 9.7, 4.2 Hz, 1H, H₇), 5.92 (dd, *J* = 9.7, 1.6 Hz, 1H, H₆), 5.34-5.30 (m, 1H, H₁₀), 4.77 (d, *J* = 1.1 Hz, 1H, H₁), 4.34 (m, 1H, H₃), 4.27 (dd, *J* = 11.1, 4.2 Hz, 1H, H₈), 3.00 (s, 3H, H₁₅), 2.47 (dd, *J* = 13.2, 7.8 Hz, 1H, H₄), 2.13 (dd, *J* = 13.2, 8.6 Hz, 1H, H₄), 1.97 (d, *J* = 11.2 Hz, 3H, O-H), 1.93 (d, *J* = 1.5 Hz, 1H, H₁₃), 1.01 (s, 9H, H₁₂)
¹³C NMR (125 MHz, Chloroform-*d*) δ 178.52 (C₂), 172.58 (C₁₄), 139.69 (C₉), 130.70 (C₇), 128.86 (C₆), 125.25 (C₁₀), 82.05 (C₁), 65.29 (C₈), 56.92 (C₃), 51.71 (C₅), 38.98 (C₄), 38.50 (C₁₁), 31.49 (C₁₅), 25.99 (C₁₂), 20.43 (C₁₃)

IR ν_{max} – 3416 (O-H), 2965 (C-H), 1700 (C=O)

HRMS-ESI (*m/z*) [M+Na]⁺ calc. for C₁₇H₂₄N₂O₃Na, 327.1679; found 327.1680

R_f – 0.38 in 10% MeOH in dichloromethane

mp 173-175 °C

[α]_D²⁶ = -4 (*c* = 1 in CHCl₃)

Carbonyl 'down' confirmed by NOE (Figure 10)

Major isomer assumed as *cis*

280b

(181 mg, 18%)

¹H NMR (500 MHz, Chloroform-d) δ 6.23 (dd, J = 9.7, 4.2 Hz, 1H, H₇), 5.66 – 5.57 (m, 2H, H_{6&9}), 4.78 (d, J = 1.1 Hz, 1H, H₁), 4.36 (m, 1H, H₃), 4.27 (dd, J = 11.2, 4.2 Hz, 1H, H₈), 3.00 (d, J = 0.4 Hz, 3H, H₁₅), 2.46 (dd, J = 13.2, 7.8 Hz, 1H, H₄), 2.16 (dd, J = 13.2, 8.6 Hz, 1H, H₄), 1.92 (d, J = 1.2 Hz, 3H, H₁₃), 1.80 (d, J = 11.2 Hz, 1H, OH) 1.03 (s, 9H, H₁₂)

¹³C NMR (125 MHz, Chloroform-d) δ 178.66 (C₂), 172.59 (C₁₄), 138.65 (C₉), 131.71 (C₇), 129.86 (C₆), 123.34 (C₁₀), 82.00 (C₁), 65.24 (C₈), 56.97 (C₃), 51.46 (C₅), 38.94 (C₄), 38.49 (C₁₁), 31.51 (C₁₅), 26.01 (C₁₂), 20.42 (C₁₃)

IR ν_{max} – 3416 (O-H), 2966 (C-H), 1698 (C=O)

HRMS-ESI (m/z) [M+Na]⁺ calc. for C₁₇H₂₄N₂O₃Na, 327.1679; found 327.1683

R_f – 0.35 in 10% MeOH in dichloromethane

mp 56-58 °C

[α]_D²⁶ = -8 (c = 1 in CHCl₃)

Carbonyl ‘up’ confirmed by NOE (Figure 10)

Major isomer assumed as *cis*

280c

(137 mg, 14%)

¹H NMR (500 MHz, Chloroform-d) δ 6.03 (dd, J = 9.8, 3.2 Hz, 1H, H₇), 5.88 (dt, J = 9.8, 1.9 Hz, 1H, H₆), 5.34 – 5.29 (m, 1H, H₁₀), 4.79 (d, J = 1.1 Hz, 1H, H₁), 4.49 (d, J = 8.5 Hz, 1H, H₈), 4.33 (m, 1H, H₃), 2.99 (s, 3H, H₁₅), 2.45 (dd, J = 13.1, 7.5 Hz, 1H, H₄), 2.17 (dd, J = 13.1, 9.0 Hz, 1H, H₄), 1.93 (s, 3H, H₁₃), 1.56 (d, J = 9.1 Hz, 1H, OH), 1.01 (s, 9H, H₁₂)

¹³C NMR (125 MHz, Chloroform-d) δ 178.31 (C₂), 172.59 (C₁₄), 138.27 (C₉), 129.98 (C₇), 126.70 (C₆), 123.73 (C₁₀), 81.73 (C₁), 65.31 (C₈), 56.81 (C₃), 51.32 (C₅), 38.95 (C₄), 38.49 (C₁₁), 31.48 (C₁₅), 25.96 (C₁₂), 20.15 (C₁₃)

IR ν_{max} – 3417 (O-H), 2966 (C-H), 1697 (C=O)

HRMS-ESI (m/z) [M+Na]⁺ calc. for C₁₇H₂₄N₂O₃Na, 327.1679; found 327.1690

R_f – 0.32 in 10% MeOH in dichloromethane

mp >200 °C decomposition

[α]_D²⁶ = 20 (c = 1 in CHCl₃)

Carbonyl ‘down’ confirmed by NOE (Figure 10)

Minor isomer assumed as *trans*

280d

(120 mg, 12%)

¹H NMR (500 MHz, Chloroform-d) δ 6.14 (dd, J = 9.6, 3.3 Hz, 1H, H₇), 5.61 – 5.54 (m, 2H, H_{6&10}), 4.79 (d, J = 1.2 Hz, 1H, H₁), 4.48 (s, br, 1H, H₈), 4.35 (m, 1H, H₃), 3.00 (s, 3H, H₁₅), 2.45 (dd, J = 13.0, 7.5 Hz, 1H, H₄), 2.16 (dd, J = 13.0, 8.9 Hz, 1H, H₄), 1.90 (s, 3H, H₁₃), 1.55 (s, 1H, OH), 1.02 (s, 9H, H₁₂)

¹³C NMR (125 MHz, Chloroform-d) δ 178.42 (C₂), 172.62 (C₁₄), 136.82 (C₉), 131.55 (C₇), 128.42 (C₆), 121.92 (C₁₀), 81.72 (C₁), 65.26 (C₈), 57.05 (C₃), 51.35 (C₅), 39.09 (C₄), 38.48 (C₁₁), 31.50 (C₁₅), 25.99 (C₁₂), 20.17 (C₁₃)

IR ν_{max} – 3425 (O-H), 2967 (C-H), 1698 (C=O)

HRMS-ESI (m/z) [M+Na]⁺ calc. for C₁₇H₂₄N₂O₃Na, 327.1679; found 327.1676

R_f – 0.30 in 10% MeOH in dichloromethane

mp 160-162 °C

[α]_D²⁶ = -20 (c = 1 in CHCl₃)

Carbonyl ‘up’ confirmed by NOE (Figure 10)

Minor isomer assumed as *trans* & confirmed by crystal below

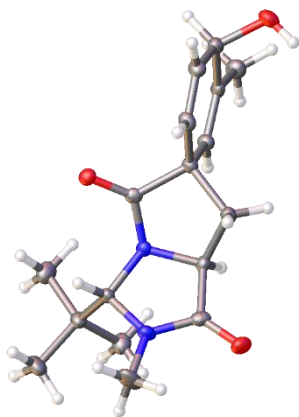
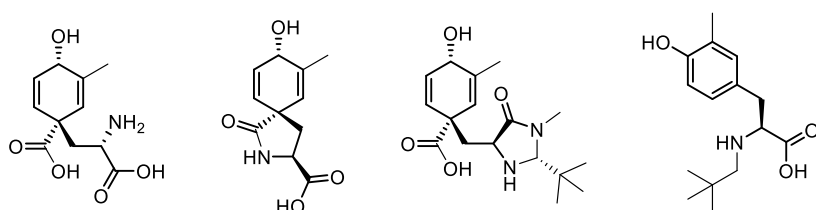


Table 1 Crystal data and structure refinement for 280d.

Empirical formula	C ₁₇ H ₂₄ N ₂ O ₃
Formula weight	304.38
Temperature/K	100(2)
Crystal system	monoclinic
Space group	P2 ₁
a/Å	5.7444(2)
b/Å	12.0901(5)
c/Å	12.1546(6)
α /°	90
β /°	95.471(3)
γ /°	90
Volume/Å ³	840.30(6)
Z	2
ρ_{calc} /cm ³	1.203
μ /mm ⁻¹	0.083
F(000)	328.0
Crystal size/mm ³	0.32 × 0.24 × 0.2
Radiation	MoK α (λ = 0.71073)
2 θ range for data collection/°	4.762 to 54.164
Index ranges	-7 ≤ h ≤ 7, -8 ≤ k ≤ 15, -15 ≤ l ≤ 15

Reflections collected	6822
Independent reflections	3061 [$R_{\text{int}} = 0.0355$, $R_{\text{sigma}} = 0.0476$]
Data/restraints/parameters	3061/1/205
Goodness-of-fit on F^2	1.021
Final R indexes [$I \geq 2\sigma(I)$]	$R_1 = 0.0417$, $wR_2 = 0.0841$
Final R indexes [all data]	$R_1 = 0.0544$, $wR_2 = 0.0903$
Largest diff. peak/hole / $e \text{ \AA}^{-3}$	0.21/-0.21



3-Methyl Arogenate (338), Spiroarogenate (339), Imidazolidinone protected arogenate (340) and rearomatised side product (341)

To a solution of **280a** (151 mg, 0.50 mmol) in water (2.50 mL), barium hydroxide (255 mg, 1.49 mmol) and barium carbonate (98.0 mg, 0.50 mmol) were added. The mixture was stirred at 40 °C for 16 hours, and then sodium carbonate anhydrous (315 mg, 2.98 mmol) and water (15 mL) were added. The resulting barium carbonate salt was filtered through a Whatman 0.45 μm Nylon syringe filter. The aqueous phase was lyophilised. The solid was redissolved in water (15 mL), filtered through a Millipore Millex-HN 0.45 μm Nylon syringe filter and purified by Hypercarb HPLC with a gradient of 0-80% acetonitrile in 10 mM sodium carbonate-bicarbonate buffer (pH 9.2) to yield:

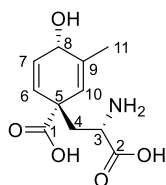
338 as the disodium salt (14 % by quantitative NMR using a stock solution of EtOH) as a white powder.

339 as the sodium salt (29 % by quantitative NMR using a stock solution of EtOH) as a white powder.

340 as the disodium salt (14% by quantitative NMR using a stock solution of EtOH) as a white powder.

341 as the sodium salt (4 % by quantitative NMR using a stock solution of EtOH) + **19% recovered starting material*** as a white powder

* poor conversion may be due to a larger sample requiring longer reaction times to reach completion.



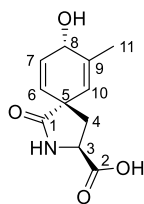
^1H NMR (500 MHz, Deuterium Oxide) δ 5.86 – 5.63 (m, 2H, $\text{H}_{6\&7}$), 5.46 (s, 0.8H, H_{10}), 5.41 (s, 0.2H, H_{10}), 4.27 – 4.25 (m, 0.2H, H_8), 4.25 – 4.21 (m, 0.8H, H_8), 3.55 (m, 0.8H, H_3), 2.88 (m, 0.2H, H_3), 1.89 – 1.70 (m, 2H, H_4), 1.67 (s, 2.4H, H_{11}), 1.64 (s, 0.6H, H_{11}) – 80:20 mixture of sodium:barium salts

^{13}C NMR (126 MHz, Deuterium Oxide) δ 188.83 (C_1), 188.09 (C_2), 141.15 (C_8), 138.52 ($\text{C}_{6/7}$), 133.68 ($\text{C}_{6/7}$), 132.91 (C_{10}), 71.43 (C_8), 61.21 (C_3), 57.54 (C_5), 47.79 (C_4), 25.85 (C_{11})

HRMS-Nanospray (m/z) [$\text{M}-\text{H}$] $^-$ calc. for $\text{C}_{11}\text{H}_{14}\text{NO}_5$, 240.0872; found 240.0879

$[\alpha]_D^{23} = -80$ ($c = 0.1$ in H_2O)

CD spectra – Positive Cotton effect below 230 nm



^1H NMR (500 MHz, Deuterium Oxide) δ 5.98 (dd, $J = 9.9, 3.3$ Hz, 1H, H_7), 5.79 (m, 1H, H_6), 5.48 – 5.41 (m, 1H, H_{10}), 4.34 (d, $J = 3.3$ Hz, 1H, H_8), 4.17 (dd, $J = 8.6, 6.5$ Hz, 1H, H_3), 2.43 (dd, $J = 13.3, 8.6$ Hz, 1H, H_4), 2.01 (dd, $J = 13.3, 6.5$ Hz, 1H, H_4), 1.82 – 1.69 (m, 3H, H_{11})

^{13}C NMR (126 MHz, Deuterium Oxide) δ 188.31 ($\text{C}_{1/2}$), 187.72 ($\text{C}_{1/2}$), 145.06 (C_9), 137.33 (C_7), 136.60 (C_6), 132.74 (C_{10}), 72.24 (C_8), 63.11 (C_3), 56.94 (C_5), 47.79 (C_4), 27.22 (C_{11})

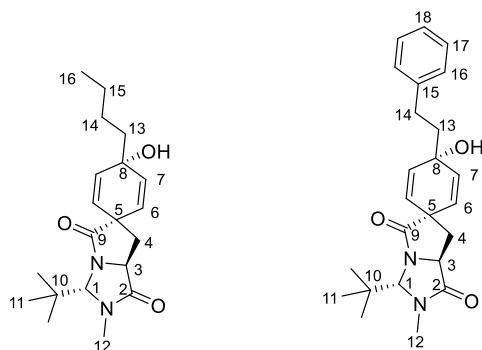
HRMS-ESI (m/z) [$\text{M}+\text{Na}+\text{H}$] $^+$ calc. for $\text{C}_{11}\text{H}_{13}\text{NO}_4$, 246.0737; found 246.0739

$[\alpha]_D^{23} = 40$ ($c = 0.1$ in H_2O)

CD spectra – Positive Cotton effect below 230 nm

5.4.3 Grignard addition derivatives

General procedure for Grignard addition



To a solution of **222** (1 eq.) in dry THF (0.10 M) under N₂ at -78 °C, the relevant Grignard reagent (2M in THF, 1.5 eq.) was slowly added and the reaction mixture was stirred for 2 hours at room temperature. The reaction mixture was then cooled to 0 °C and quenched slowly with water. The mixture was concentrated *in vacuo*, diluted with water and extracted with ether. Purification was carried out by column chromatography on silica gel eluting with 0-100% EtOAc in Hexane to yield the corresponding alkylated product.

(1*s*,3'*S*,4*R*,7*a*'*S*)-3'-(*tert*-Butyl)-4-butyl-4-hydroxy-2'-methyl-2',3',7',7*a*'-tetrahydro-1'H,5'H-spiro[cyclohexane-1,6'-pyrrolo[1,2-*c*]imidazole]-2,5-diene-1',5'-dione (**283**)

Only one diastereomer isolated (crude NMR d.r. = >9:1)

Major isolated diastereomer (441 mg, 75 %) as a pale-yellow oil

¹H NMR (400 MHz, Chloroform-*d*) δ 6.00 (dd, *J* = 10.0, 1.5 Hz, 1H, H₆), 5.94 – 5.85 (m, 2H, H₇), 5.62 (dd, *J* = 10.0, 1.5 Hz, 1H, H₆), 4.79 (d, *J* = 1.1 Hz, 1H, H₁), 4.35 (m, 1H, H₃), 3.00 (s, 3H, H₁₂), 2.42 (dd, *J* = 13.2, 7.7 Hz, 1H, H₄), 2.25 – 2.13 (m, 2H, H₄ & OH), 1.66 – 1.56 (m, 2H, H₁₃), 1.36 – 1.24 (m, 2H, H₁₅), 1.15 – 1.05 (m, 2H, H₁₄), 1.02 (s, 9H, H₁₁), 0.87 (t, *J* = 7.3 Hz, 3H, H₁₆)

¹³C NMR (100 MHz, Chloroform-*d*) δ 178.21 (C₂), 172.46 (C₉), 135.63 (C₆), 134.79 (C₇), 128.70 (C₆), 127.33 (C₇), 81.90 (C₁), 67.69 (C₈), 56.99 (C₃), 50.86 (C₅), 39.93 (C₁₃), 38.97 (C₄), 38.52 (C₁₀), 31.51 (C₁₂), 26.69 (C₁₄), 25.99 (C₁₁), 23.09 (C₁₅), 14.16 (C₁₆)

HRMS-ESI (*m/z*) [M+Na⁺] calc. for C₂₀H₃₀N₂O₃Na, 369.2149; found 369.2164

IR ν_{max} – 3416 (O-H), 2957, 2931 (C-H), 1697 (C=O)

R_f - 0.47 in 10% MeOH in dichloromethane

[α]_D²⁵ = 8 (*c* = 1 in CHCl₃)

(1*s*,3'*s*,4*R*,7*a*'*S*)-3'-(*tert*-Butyl)-4-hydroxy-2'-methyl-4-phenethyl-2',3',7',7*a*'-tetrahydro-1'H,5'H-spiro[cyclohexane-1,6'-pyrrolo[1,2-*c*]imidazole]-2,5-diene-1',5'-dione (284)

Only one diastereomer isolated (crude NMR d.r. = >9:1)

Major isolated diastereomer (202 mg, 74 %) as a clear oil

¹H NMR (500 MHz, Chloroform-*d*) δ 7.31 – 7.23 (m, 2H, H₁₇), 7.20 – 7.13 (m, 3H, H_{16&18}), 6.09 (dd, *J* = 9.9, 1.9 Hz, 1H, H₇), 6.00 (dd, *J* = 9.8, 1.9 Hz, 1H, H₇), 5.94 (dd, *J* = 9.8, 2.2 Hz, 1H, H₆), 5.68 (dd, *J* = 9.9, 2.2 Hz, 1H, H₆), 4.80 (s, 1H, H₁), 4.38 (m, 1H, H₃), 3.01 (s, 3H, H₁₂), 2.54 – 2.38 (m, 4H, H_{4,14} & O-H), 2.21 (m, 1H, H₄), 1.99 – 1.91 (m, 2H, H₁₃), 1.03 (s, 9H, H₁₁)

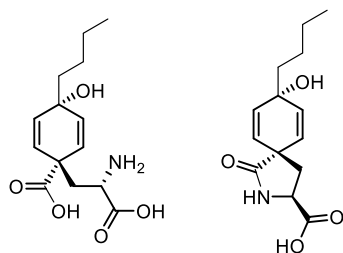
¹³C NMR (100 MHz, Chloroform-*d*) δ 178.01 (C₂), 172.40 (C₉), 141.84 (C₁₅), 135.26 (C₇), 134.37 (C₇), 129.35 (C₆), 128.53 (C₁₇), 128.40 (C₁₆), 127.92 (C₆), 126.02 (C₁₈), 81.97 (C₁), 67.46 (C₈), 57.00 (C₃), 50.99 (C₅), 41.79 (C₁₃), 38.81 (C₄), 38.81 (C₁₀), 31.53 (C₁₂), 30.77 (C₁₄), 26.01 (C₁₁)

HRMS-ESI (*m/z*) [*M*+Na⁺] calc. for C₂₄H₃₀N₂O₃Na, 417.2149; found 417.2152

IR ν_{max} – 3405 (O-H), 2964, 2931 (C-H), 1693 (C=O)

R_f - 0.53 in 10% MeOH in dichloromethane

[α]_D²⁵ = 16 (*c* = 1 in CHCl₃)



n-Butyl Arogenate (343) and Spiroarogenate (342)

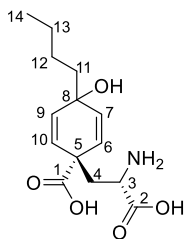
To a solution of **283** (31.3 mg, 0.09 mmol) in water (0.45 mL), barium hydroxide (46.3 mg, 0.27 mmol) and barium carbonate (17.8 mg, 0.09 mmol) were added. The mixture was stirred at 80 °C for 24 hours, and then sodium carbonate anhydrous (57.0 mg, 0.54 mmol) and water (5.00 mL) were added. The resulting barium carbonate salt was filtered through a Whatman 0.45 μ m Nylon syringe filter. The aqueous phase was lyophilised. The solid was redissolved in water (3 mL), filtered through a Millipore Millex-HN 0.45 μ m Nylon syringe filter and purified by Hypercarb HPLC with a gradient of 0-80% acetonitrile in 10 mM sodium carbonate-bicarbonate buffer (pH 9.2) to yield:

343 as the disodium salt* (46 % by quantitative NMR using a stock solution of EtOH) as a white powder.

348 as the sodium salt (29 % by quantitative NMR using a stock solution of EtOH) as a white powder.

Starting material (4 % by quantitative NMR using a stock solution of EtOH).

* <4% rearomatisation



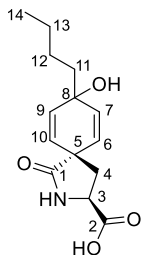
¹H NMR (500 MHz, Deuterium Oxide) δ 5.97 (dd, J = 10.1, 2.3 Hz, 0.3H, H_{7/9}), 5.91 (dd, J = 10.1, 2.3 Hz, 0.7H, H_{7/9}), 5.82 (dd, J = 10.1, 2.3 Hz, 1H, H_{7/9}), 5.77 – 5.61 (m, 2H, H_{6&10}), 3.64 (m, 0.7H, H₃), 3.02 (m, 0.3H, H₃), 2.08 – 1.99 (m, 0.3H, H₄), 1.92 – 1.76 (m, 1.7H, H₄), 1.50 – 1.37 (m, 2H, H₁₁), 1.15 (m, 2H, H₁₃), 1.06 (m, 2H, H₁₂), 0.73 (q, J = 7.5 Hz, 3H, H₁₄) – Mixture of salts (30:70 sodium:barium)

¹³C NMR (126 MHz, Deuterium Oxide) δ 184.02 (C₂), 182.55 (C₁), 133.23 (C_{6/10}), 132.63 (C_{6/10}), 131.98 (C_{7/9}), 131.50 (C_{7/9}), 69.80 (C₈), 56.38 (C₃), 51.68 (C₅), 42.53 (C₄), 41.61 (C₁₁), 26.95 (C₁₂), 23.71 (C₁₃), 14.66 (C₁₄) – Major salt reported

HRMS-Nanospray (m/z) [M-H]⁻ calc. for C₁₄H₂₀NO₅, 282.1341; found 282.1336

[α]_D²⁴ = 80 (c = 0.1 in H₂O)

CD spectra – Positive Cotton effect below 230 nm



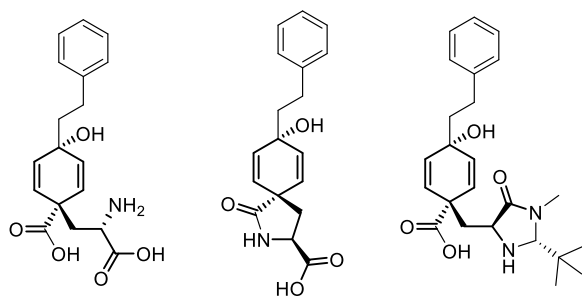
¹H NMR (500 MHz, Deuterium Oxide) δ 5.78 – 5.70 (m, 3H, H_{6/7/9/10}), 5.67 (dd, J = 10.2, 2.1 Hz, 1H, H_{6/7/9/10}), 4.13 (dd, J = 8.7, 6.2 Hz, 1H, H₃), 2.39 (dd, J = 13.3, 8.7 Hz, 1H, H₄), 1.99 (dd, J = 13.3, 6.2 Hz, 1H, H₄), 1.48 – 1.40 (m, 2H, H₁₁), 1.13 (m, 2H, H₁₃), 0.98 – 0.88 (m, 2H, H₁₂), 0.70 (q, J = 7.4 Hz, 3H, H₁₄)

¹³C NMR (126 MHz, Deuterium Oxide) δ 188.47 (C_{1/2}), 188.08 (C_{1/2}), 141.17 (C_{6/10}), 141.09 (C_{6/10}), 136.91 (C_{7/9}), 136.33 (C_{7/9}), 76.49 (C₈), 63.55 (C₃), 56.48 (C₅), 47.87 (C₁₁), 47.66 (C₄), 34.34 (C₁₂), 30.59 (C₁₂), 21.56 (C₁₃)

HRMS-Nanospray (m/z) [M-H]⁻ calc. for C₁₄H₁₈NO₄, 264.1236; found 264.1227

[α]_D²⁵ = 80 (c = 0.1 in H₂O)

CD spectra – Positive Cotton effect below 230 nm



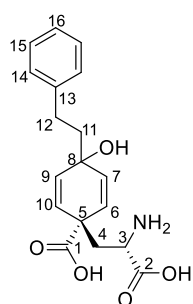
Phenethyl Arogenate (346), Spiroarogenate (345) and Imidazolidinone protected arogenate (349)

To a solution of **284** (30.3 mg, 0.08 mmol) in water (0.39 mL), barium hydroxide (40.2 mg, 0.23 mmol) and barium carbonate (15.7 mg, 0.08 mmol) were added. The mixture was stirred at 80 °C for 24 hours, and then sodium carbonate anhydrous (49.0 mg, 0.46 mmol) and water (5.00 mL) were added. The resulting barium carbonate salt was filtered through a Whatman 0.45 µm Nylon syringe filter. The aqueous phase was lyophilised. The solid was redissolved in water (3 mL), filtered through a Millipore Millex-HN 0.45 µm Nylon syringe filter and purified by Hypercarb HPLC with a gradient of 0-80% acetonitrile in 10 mM sodium carbonate-bicarbonate buffer (pH 9.2) to yield:

346 as the disodium salt (59 % by quantitative NMR using a stock solution of EtOH) as a white powder.

345 as the sodium salt (25 % by quantitative NMR using a stock solution of EtOH) as a white powder.

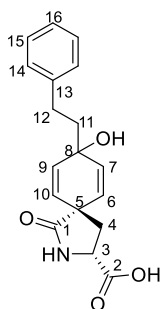
349 as the disodium salt (6 % by quantitative NMR using a stock solution of EtOH).



¹H NMR (500 MHz, Deuterium Oxide) δ 7.20 – 7.03 (m, 5H, H_{14,15&16}), 6.02 – 5.89 (m, 1H, H_{7/9}), 5.89 – 5.79 (m, 1H, H_{7/9}), 5.71 (m, 2H, H₁₄), 3.62 (m, 0.8H, H₃), 3.01 – 2.97 (m, 0.2H, H₃), 2.42 – 2.27 (m, 2H, H₁₂), 2.00 (m, 0.2H, H₄), 1.87 – 1.60 (m, 3.8H, H_{4&11})

¹³C NMR (126 MHz, Deuterium Oxide) δ 183.72 (C₂), 182.12 (C₁), 143.84 (C₁₃), 133.67 (C_{7/9}), 131.20 (C_{7/9}), 130.71 (C_{6/10}), 129.83 (C_{14/15&6/10}), 129.62 (C_{14/15}), 127.10 (C₁₆), 69.30 (C₈), 56.21 (C₃), 51.49 (C₅), 43.73 (C₁₁), 42.33 (C₄), 31.22 (C₁₂)

Unable to obtain HRMS despite several attempts.

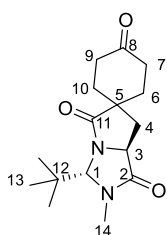


¹H NMR (500 MHz, Deuterium Oxide) δ 7.38 – 7.31 (m, 2H, H₁₅), 7.28 – 7.20 (m, 3H, H_{14&16}), 5.99 – 5.88 (m, 3H, H_{9,7&6/10}), 5.84 (dd, J = 10.0, 2.3 Hz, 1H, H_{6/10}), 4.27 (dd, J = 8.7, 6.1 Hz, 1H, H₃), 2.56 (dd, J = 13.4, 8.7 Hz, 1H, H₄), 2.51 – 2.39 (m, 2H, H₁₂), 2.16 (dd, J = 13.4, 6.1 Hz, 1H, H₄), 1.95 – 1.85 (m, 2H, H₁₁)

¹³C NMR (126 MHz, Deuterium Oxide) δ 188.06 (C₁), 187.79 (C₂), 150.38 (C₁₃), 140.47 (C_{7/9}), 140.40 (C_{7/9}), 137.19 (C_{6/10}), 136.74 (C₁₅), 136.62 (C_{6/10}), 136.57 (C₁₄), 134.12 (C₁₆), 75.99 (C₈), 63.31 (C₃), 56.28 (C₅), 49.74 (C₁₁), 47.35 (C₄), 38.37 (C₁₂)

HRMS-Nanospray (m/z) [M-H][−] calc. for C₁₈H₁₈NO₄, 312.1236; found 312.1227

5.4.4 Hydrogenation



(3'S,7a'S)-3'-(*tert*-Butyl)-2'-methyltetrahydro-1'H,5'H-spiro[cyclohexane-1,6'-pyrrolo[1,2-c]imidazole]-1',4,5'-trione (**285**)

To a solution of **222** (300 g, 1.04 mmol) in (10.0 mL) under N₂, palladium on active carbon (10 wt. %) (60.0 mg, 20 % wt.) was added. The mixture was then stirred at room temperature overnight under hydrogen atmosphere. The reaction mixture was filtered over a pad of celite and concentrated in *vacuo* to yield **285** (303 mg, Quant.) as a white powder.

¹H NMR (400 MHz, Chloroform-*d*) δ 4.82 (d, J = 1.1 Hz, 1H, H₁), 4.30 (t, J = 8.1 Hz, 1H, H₃), 3.03 (s, 3H, H₁₂), 2.96 – 2.85 (m, 1H, H_{7/9}), 2.61 – 2.48 (m, 2H, H_{4&7/9}), 2.48 – 2.35 (m, 1H, H_{7/9}), 2.35 – 2.15 (m, 3H, H_{6/10&7/9}), 2.10 – 1.93 (m, 2H, H_{4&6/10}), 1.82 – 1.72 (m, 1H, H_{6/10}), 1.03 (s, 9H, H₁₃)

¹³C NMR (100 MHz, Chloroform-*d*) δ 209.60 (C₈), 181.50 (C₂), 172.69 (C₁₁), 81.49 (C₁), 56.68 (C₃), 45.85 (C₅), 38.37 (C₁₂), 37.71 (C_{7/9}), 37.06 (C₄), 33.56 (C_{6/10}), 33.29 (C_{6/10}), 31.48 (C₁₂), 25.97 (C₁₄)

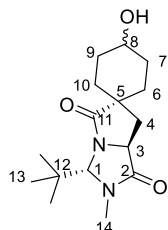
HRMS-ESI (m/z) [$M+Na^+$] calc. for $C_{16}H_{24}N_2O_3Na$, 315.1679; found 315.1689

IR ν_{max} – 2962, 2871 (C–H), 1697 (C=O)

R_f - 0.35 in 100% EtOAc

mp 177-178 °C

[α]_D²⁶ = 4 (c = 1 in $CHCl_3$)



(3'R,7a'S)-3'-(*tert*-Butyl)-4-hydroxy-2'-methyltetrahydro-1'H,5'H-spiro[cyclohexane-1,6'-pyrrolo[1,2-c]imidazole]-1',5'-dione (286)

To a solution of **285** (200 mg, 0.68 mmol) in dry methanol (7 mL) under N_2 at 0 °C, sodium borohydride (45 mg, 1.20 mmol) was slowly added. The resultant mixture was allowed to warm to room temperature and left to stir overnight. The reaction mixture was quenched with water (20 mL) and the mixture was then concentrated *in vacuo*. The crude product was then diluted with water (50 mL). The aqueous phase was extracted with dichloromethane (3 x 30 mL). The combined organic phases were dried over $MgSO_4$, filtered and concentrated *in vacuo*. Purification was carried out by column chromatography on silica gel eluting with 0-80% Acetone in dichloromethane to yield **286** (179 mg, 89 %, d.r. = 1.1:1) as white powders.

286b Minor (*cis* – desired)

¹H NMR (500 MHz, Chloroform- d) δ 4.77 (d, J = 1.1 Hz, 1H, H_1), 4.21 (m, 1H, H_3), 3.83 (dh, J = 7.1, 3.6 Hz, 1H, H_8), 2.96 (s, 3H, H_{14}), 2.40 (m, 1H, H_4), 2.11 – 1.95 (m, 3H, $H_{6/10\&7/9}$), 1.87 – 1.74 (m, 2H, $H_{4\&7/9}$), 1.71 – 1.60 (m, 2H, $H_{7/9}$), 1.54-1.44 (m, 2H, $H_{6/10}$ & OH), 1.32 – 1.23 (m, 1H, $H_{6/10}$), 1.00 (s, 9H, H_{13})

¹³C NMR (125 MHz, Chloroform- d) δ 182.66 (C_2), 173.29 (C_{11}), 81.31 (C_1), 67.48 (C_8), 56.77 (C_3), 46.18 (C_5), 38.39 (C_{12}), 37.59 (C_4), 31.45 (C_{14}), 30.40 ($C_{7/9}$), 30.40 ($C_{7/9}$), 30.08 ($C_{6/10}$), 29.32 ($C_{6/10}$), 25.97 (C_{13})

HRMS-ESI (m/z) [$M+Na^+$] calc. for $C_{16}H_{26}N_2O_3Na$, 317.1836; found 317.1842

IR ν_{max} – 3423 (O–H), 2955, 2929, 2870 (C–H), 1688 (C=O)

R_f - 0.35 in 10% MeOH in dichloromethane

mp 173-174 °C

[α]_D²⁶ = -20 (c = 1 in $CHCl_3$)

286a Major (*trans*)

¹H NMR (500 MHz, Chloroform-d) δ 4.76 (d, J = 1.2 Hz, 1H, H₁), 4.21 (m, 1H, H₃), 3.67 (ddt, J = 14.3, 9.9, 4.1 Hz, H₈), 2.96 (s, 3H, H₁₄), 2.59 (m, 1H, H₄), 2.06 - 1.92 (m, 2H, H_{6/10&7/9}), 1.91 - 1.70 (m, 3H, H_{4,6/10&7/9}), 1.70-1.59 (m, 2H, H_{6/10} & OH), 1.50 - 1.40 (m, 2H, H_{7/9}), 1.33 - 1.19 (m, 1H, H_{6/10}), 1.00 (s, 9H, H₁₃)

¹³C NMR (125 MHz, Chloroform-d) δ 182.97 (C₂), 173.21 (C₁₁), 81.59 (C₁), 69.39 (C₈), 56.85 (C₃), 46.62 (C₅), 38.37 (C₁₂), 35.77 (C₄), 31.57 (C_{7/9}), 31.45 (C₁₄), 31.36 (C_{7/9}), 31.32 (C_{6/10}), 30.78 (C_{6/10}), 26.00 (C₁₃)

HRMS-ESI (m/z) [$M+Na^+$] calc. for C₁₆H₂₆N₂O₃Na, 317.1836; found 317.1828

IR ν_{max} – 3405 (O-H), 2951, 2926, 2859 (C-H), 1685 (C=O)

R_f - 0.32 in 10% MeOH in dichloromethane

mp 197-198 °C

$[\alpha]_D^{26}$ = -4 (c = 1 in CHCl₃)

X-Ray data – shows *trans* OH group at C8 to carbonyl at C11.

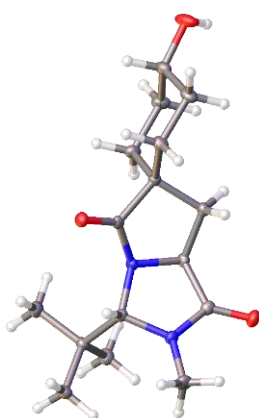
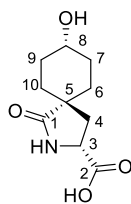


Table 1 Crystal data and structure refinement for 286a.	
Empirical formula	C ₁₆ H ₂₆ N ₂ O ₃
Formula weight	294.39
Temperature/K	99.97
Crystal system	monoclinic
Space group	P2 ₁
a/Å	5.94680(10)
b/Å	13.2423(3)
c/Å	10.0750(3)
α /°	90
β /°	97.9895(15)
γ /°	90
Volume/Å ³	785.70(3)
Z	2
ρ_{calc} /g/cm ³	1.244
μ /mm ⁻¹	0.086
F(000)	320.0
Crystal size/mm ³	0.424 × 0.266 × 0.074
Radiation	MoK α (λ = 0.71073)
2 θ range for data collection/°	4.082 to 55.932
Index ranges	-7 ≤ h ≤ 7, -17 ≤ k ≤ 17, -13 ≤ l ≤ 13
Reflections collected	18866
Independent reflections	3773 [R_{int} = 0.0301, R_{sigma} = 0.0227]
Data/restraints/parameters	3773/1/198
Goodness-of-fit on F ²	1.051
Final R indexes [$I \geq 2\sigma(I)$]	R_1 = 0.0318, wR_2 = 0.0801
Final R indexes [all data]	R_1 = 0.0339, wR_2 = 0.0812
Largest diff. peak/hole / e Å ⁻³	0.25/-0.17



(3R,5S,8S)-8-Hydroxy-1-oxo-2-azaspiro[4.5]decane-3-carboxylic acid (350)

To a solution of **286b** (30.0 mg, 0.10 mmol) in water (0.50 mL), sodium hydroxide (12.0 mg, 0.30 mmol) was added. The mixture was stirred at 90 °C for 16 hours in a sealed tube. The resulting mixture was then neutralised (approx. pH = 8) and lyophilised. The mixture was redissolved in ethanol and filtered to remove excess salt. The product was purified by Hypercarb HPLC with a gradient of 0-100% acetonitrile in 100 mM ammonium bicarbonate buffer to yield **350** (19.3 mg, 80%) as a white powder.

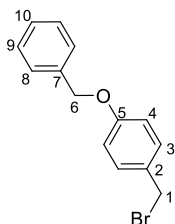
¹H NMR (500 MHz, Deuterium Oxide) δ 4.16 (m, 1H, H₃), 3.99 (s, 1H, H₈), 2.50 (m, 1H, H₄), 2.01 (m, 1H, H₄), 1.96 – 1.81 (m, 2H, H_{6&10}), 1.81 – 1.59 (m, 4H, H_{7&9}), 1.43 – 1.24 (m, 2H, H_{6&10})

¹³C NMR (125 MHz, Deuterium Oxide) δ 184.73 (C₁), 179.73 (C₂), 65.56 (C₈), 54.62 (C₃), 44.32 (C₅), 36.01 (C₄), 27.77 (C_{7/9}), 27.71 (C_{7/9}), 27.23 (C_{6/10}), 26.56 (C_{6/10})

HRMS-Nanospray (*m/z*) [M-H]⁻ calc. for C₁₀H₁₄NO₄, 212.0923; found 212.0928

CD spectra - showed end absorption only

5.5 Alpha alkylations

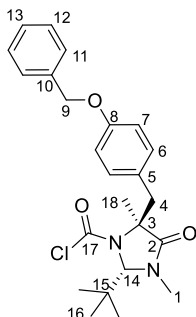


1-(Benzyloxy)-4-(bromomethyl)benzene (**306**)¹³⁶

To a solution of 4-Benzyloxybenzyl alcohol (2.00 g, 9.35 mmol) in dry, degassed DCM (45.0 mL) under N₂ at 0 °C, phosphorus tribromide (0.97 mL, 10.3 mmol) in DCM (45.0 mL) was added dropwise. The mixture stirred for 3 hours at 0 °C then warmed to room temperature and stirred for a further 2 hours. The reaction mixture was quenched with water (30 mL) and extracted with ethyl acetate (3 x 50 mL). The organic layer was washed with brine (30 mL), dried over MgSO₄, filtered and concentrated in *vacuo* to yield **306** (2.60 g, Quant.) as a white solid.

¹H NMR (400 MHz, Chloroform-d) δ 7.45 – 7.30 (m, 7H, H_{3,8,9&10}), 6.96 – 6.91 (m, 2H, H₄), 5.07 (s, 2H, H₆), 4.50 (s, 2H, H₁)

Consistent with literature data.



(2S,5S)-5-(4-(Benzyloxy)benzyl)-2-(tert-butyl)-3,5-dimethyl-4-oxoimidazolidine-1-carbonyl chloride (**311**)

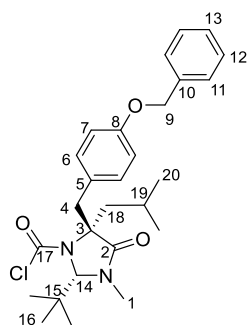
To a solution of **310** (50.0 mg, 0.18 mmol) and **306** (61.0 mg, 0.22 mmol) in dry, degassed THF (1.00 mL) under N₂ at -78 °C, KHMDS (1 M, 0.22 mL) was added. The mixture was warmed to room temperature and stirred for 2 hours. The reaction mixture was quenched with water (2 mL) and extracted with ethyl acetate (3 x 5 mL). The combined organics were washed with brine (5 mL), dried over MgSO₄, filtered and concentrated in *vacuo* to yield **311** (77.4 mg, 90 %) as a clear oil.

¹H NMR (400 MHz, Chloroform-d) δ 7.44 – 7.27 (m, 5H, H_{11,12&13}), 7.10 – 7.01 (m, 2H, H₆), 6.89 – 6.80 (m, 2H, H₇), 5.06 – 4.98 (m, 2H, H₉), 4.53 (s, 0.52H, H₁₄), 4.47 (s, 0.48H, H₁₄), 3.67 (m, H₄), 3.54 (m, 0.52H, H₄), 3.08 (m, 0.48H, H₄), 2.99 (m, 0.52H, H₄), 2.74 (s, 1.6H, H₁), 2.67

(s, 1.4H, H₁), 1.80 (s, 1.4H, H₁₈), 1.71 (s, 1.6H, H₁₈), 1.01 (s, 4.8H, H₁₆), 0.91 (s, 4.2H, H₁₆) – rotameric mixture

¹³C NMR (126 MHz, Chloroform-d) δ 171.72 (C₂), 171.68 (C₂), 158.05 (C₈), 157.88 (C₈), 148.38 (C₁₇), 146.82 (C₁₇), 136.95 (C₁₀), 136.87 (C₁₀), 131.15 (C₆), 130.94 (C₆), 128.57 (C_{11/12}), 128.55 (C_{11/12}), 127.99 (C₁₃), 127.96 (C₁₃), 127.59 (C_{11/12}), 127.56 (C_{11/12}), 127.45 (C₅), 127.22 (C₅), 114.63 (C₇), 114.56 (C₇), 82.69 (C₁₄), 82.58 (C₁₄), 70.70 (C₉), 69.94 (C₉), 69.89 (C₃), 68.50 (C₃), 42.57 (C₄), 40.00 (C₁₅), 39.79 (C₄), 39.35 (C₁₅), 31.78 (C₁), 31.40 (C₁), 27.54 (C₁₆), 26.84 (C₁₆), 23.41 (C₁₈), 22.44 (C₁₈) – rotameric mixture

HRMS-ESI (*m/z*) [M+Na]⁺ calc. for C₂₄H₂₉N₂O₃NaCl, 451.1758; found 451.1747



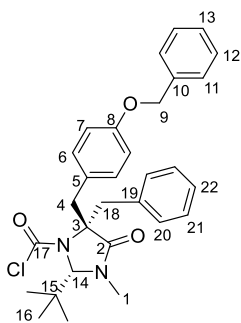
(2S,5S)-5-(4-(Benzyloxy)benzyl)-2-(tert-butyl)-5-isobutyl-3-methyl-4-oxoimidazolidine-1-carbonyl chloride (313)

To a solution of **312** (200 mg, 0.73 mmol) and **306** (244 mg, 0.89 mmol) in dry, degassed THF (3.60 mL) under N₂ at -78 °C, KHMDS (1 M, 0.89 mL) was added. The mixture was warmed to room temperature and stirred for 2 hours. The reaction mixture was quenched with water (5 mL) and extracted with ethyl acetate (3 x 10 mL). The combined organics were washed with brine (10 mL), dried over MgSO₄, filtered and concentrated in *vacuo* to yield **313** (201 mg, 59 %) as a clear oil.

¹H NMR (400 MHz, Chloroform-d) δ 7.48 – 7.27 (m, 5H, H_{11,12&13}), 7.06 (dd, *J* = 8.6, 6.2 Hz, 2H, H₆), 6.89 – 6.79 (m, 2H, H₇), 5.06 – 4.96 (m, 2H, H₉), 4.53 (s, 0.65H, H₁₄), 4.27 (s, 0.35H, H₁₄), 3.58 (m, 1H, H₄), 3.15 (m, 1H, H₄), 2.74 (s, 1.95H, H₁), 2.64 (s, 1.05H, H₁), 2.36 – 2.10 (m, 2.35H, H_{18&19}), 1.92 (dd, *J* = 14.6, 5.1 Hz, 0.65H, H₁₈), 1.10 – 0.96 (m, 11.85H, H_{16&20}), 0.93 (s, 3.15H, H₁₆) – rotameric mixture

¹³C NMR (101 MHz, Chloroform-d) δ 171.03 (C₂), 158.12 (C₈), 157.90 (C₈), 149.22 (C₁₇), 147.26 (C₁₇), 137.05 (C₁₀), 136.96 (C₁₀), 131.47 (C₆), 131.34 (C₆), 128.65 (C_{11/12}), 128.62 (C_{11/12}), 128.07 (C₁₃), 128.03 (C₁₃), 127.65 (C_{11/12}), 127.25 (C₅), 126.69 (C₅), 114.68 (C₇), 114.61 (C₇), 82.77 (C₁₄), 73.68 (C₃), 71.83 (C₃), 69.99 (C₉), 69.94 (C₉), 46.27 (C₁₈), 46.09 (C₁₈), 42.34 (C₄), 39.26 (C₁₅), 38.90 (C₁₅), 38.17 (C₄), 31.61 (C₁), 31.30 (C₁), 27.84 (C₁₆), 27.38 (C₁₆), 25.18 (C₂₀), 25.06 (C₂₀), 23.83 (C₁₉), 23.64 (C₁₉) – rotameric mixture

HRMS-ESI (m/z) [$M+Na$] $^+$ calc. for $C_{27}H_{35}N_2O_3NaCl$, 493.2228; found 293.2243



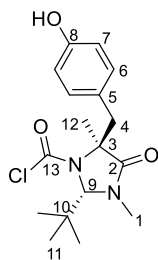
(2S,5S)-5-Benzyl-5-(4-(benzyloxy)benzyl)-2-(tert-butyl)-3-methyl-4-oxoimidazolidine-1-carbonyl chloride (315)

To a solution of **314** (200 mg, 0.65 mmol) and **306** (210 mg, 0.78 mmol) in dry, degassed THF (3.20 mL) under N_2 at $-78\text{ }^\circ\text{C}$, KHMDS (1 M, 0.78 mL) was added. The mixture was warmed to room temperature and stirred for 2 hours. The reaction mixture was quenched with water (5 mL) and extracted with ethyl acetate (3 x 10 mL). The combined organics were washed with brine (10 mL), dried over $MgSO_4$, filtered and concentrated in *vacuo* to yield **315** (323 mg, 81 %) as a clear oil.

1H NMR (500 MHz, Chloroform- d) δ 7.44 – 7.15 (m, 10H, $H_{11/12/13/20/21\&22}$), 7.06 (dd, $J = 11.1$, 8.6 Hz, 2H, H_6), 6.91 – 6.82 (m, 2H, H_7), 5.08 – 4.99 (m, 2H, H_9), 4.23 (s, 0.48H, H_{14}), 4.06 (s, 0.52H, H_{14}), 3.72 (m, 1H, $H_{4/18}$), 3.58 – 3.39 (m, 2H, $H_{4/18}$), 3.13 (m, 0.52H, $H_{4/18}$), 2.98 (m, 0.48H, $H_{4/18}$), 2.62 (s, 1.44H, H_1), 2.55 (s, 1.56H, H_1), 0.61 (s, 4.32H, H_{16}), 0.35 (s, 4.68H, H_{16}) – rotameric mixture

^{13}C NMR (126 MHz, Chloroform- d) δ 169.87 (C_2), 169.72 (C_2), 158.14 (C_8), 157.96 (C_8), 149.34 (C_{17}), 148.18 (C_{17}), 136.89 (C_{10}), 136.82 (C_{10}), 135.78 (C_{19}), 131.48 (C_6), 131.29 (C_{Phenyl}), 131.28 (C_{Phenyl}), 131.25 (C_6), 128.61 (C_{Phenyl}), 128.57 (C_{Phenyl}), 128.55 (C_{Phenyl}), 128.45 (C_{Phenyl}), 128.00 ($C_{13/22}$), 127.98 ($C_{13/22}$), 127.56 (C_{Phenyl}), 127.55 (C_{Phenyl}), 127.45 ($C_{13/22}$), 127.34 ($C_{13/22}$), 126.68 (C_5), 126.30 (C_5), 114.66 (C_7), 114.63 (C_7), 82.65 (C_{14}), 82.48 (C_{14}), 75.88 (C_3), 74.03 (C_3), 69.94 (C_9), 69.88 (C_9), 43.07 ($C_{4/18}$), 41.81 ($C_{4/18}$), 41.06 ($C_{4/18}$), 39.86 ($C_{4/18}$), 38.23 (C_{15}), 38.15 (C_{15}), 31.21 (C_1), 31.18 (C_1), 27.22 (C_{16}), 26.35 (C_{16}) – rotameric mixture

HRMS-ESI (m/z) [$M+Na$] $^+$ calc. for $C_{30}H_{33}N_2O_3NaCl$, 527.2072; found 527.2086



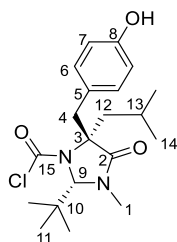
(2S,5S)-2-(tert-Butyl)-5-(4-hydroxybenzyl)-3,5-dimethyl-4-oxoimidazolidine-1-carbonyl chloride (316)

To a solution of **311** (280 mg, 0.60 mmol) in THF (6.00 mL) under N₂, palladium on active carbon (10 wt. %) (56.0 mg, 20 % wt.) was added. The mixture was then stirred at room temperature for 4 hours under hydrogen atmosphere. The reaction mixture was filtered over a pad of celite and concentrated in *vacuo* to yield **316** (203 mg, Quant.) as a clear oil.

¹H NMR (500 MHz, Chloroform-d) δ 7.07 – 7.01 (m, 2H, H₆), 6.78 – 6.72 (m, 2H, H₇), 4.61 (s, 0.52H, H₉), 4.53 (s, 0.48H, H₉), 3.70 (d, J = 14.3 Hz, 0.48H, H₄), 3.57 (d, J = 14.3 Hz, 0.52H, H₄), 3.15 – 3.06 (m, 0.52H, H₄), 3.02 (d, J = 14.3 Hz, 0.48H, H₄), 2.81 (s, 1.56H, H₁), 2.75 (s, 1.44H, H₁), 1.83 (s, 1.44H, H₁₂), 1.75 (s, 1.56H, H₁₂), 1.05 (s, 4.68H, H₁₁), 0.94 (s, 4.32H, H₁₁) – rotameric mixture

¹³C NMR (126 MHz, Chloroform-d) δ 171.83 (C₂), 171.80 (C₂), 155.10 (C₈), 154.84 (C₈), 148.45 (C₁₃), 146.83 (C₁₃), 131.33 (C₆), 131.11 (C₆), 126.93 (C₅), 126.59 (C₅), 115.16 (C₇), 115.02 (C₇), 82.77 (C₉), 82.65 (C₉), 70.72 (C₃), 68.54 (C₃), 42.54 (C₄), 39.96 (C₄), 39.79 (C₄), 39.34 (C₄), 31.82 (C₁), 31.44 (C₁), 27.54 (C₁₁), 26.84 (C₁₁), 23.40 (C₁₂), 22.43 (C₁₂) – rotameric mixture

HRMS-ESI (m/z) [M+Na]⁺ calc. for C₁₇H₂₃N₂O₃NaCl, 361.1289; found 361.1285



(2S,5S)-2-(tert-Butyl)-5-(4-hydroxybenzyl)-5-isobutyl-3-methyl-4-oxoimidazolidine-1-carbonyl chloride (318)

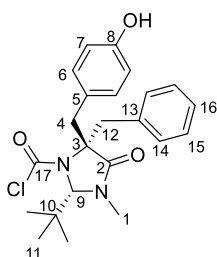
To a solution of **313** (250 mg, 0.53 mmol) in THF (6.00 mL) under N₂, palladium on active carbon (10 wt. %) (50.0 mg, 20 % wt.) was added. The mixture was then stirred at room temperature for 4 hours under hydrogen atmosphere. The reaction mixture was filtered over a pad of celite and concentrated in *vacuo* to yield **318** (203 mg, 95 %) as a clear oil.

¹H NMR (500 MHz, Chloroform-d) δ 7.09 – 7.02 (m, 2H, H₆), 6.79 – 6.71 (m, 2H, H₇), 4.60 (s, 0.66H, H₉), 4.35 (s, 0.33H, H₉), 3.61 (m, 1H, H₄), 3.18 (m, 1H, H₄), 2.81 (s, 2H, H₁), 2.73 (s, 1H,

H₁), 2.37 – 2.30 (m, 0.56H, H_{12/13}), 2.29 – 2.13 (m, 1.69H, H_{12/13}), 1.95 (dd, *J* = 14.6, 5.1 Hz, 0.75H, H₁₂), 1.09 – 1.04 (m, 12H, H_{11&14}), 0.96 (s, 3H, H₁₁) – rotameric mixture

¹³C NMR (126 MHz, Chloroform-d) δ 171.00 (C₂), 155.04 (C₈), 154.70 (C₈), 149.19 (C₁₅), 147.17 (C₁₅), 131.58 (C₆), 131.45 (C₆), 126.96 (C₅), 126.40 (C₅), 115.09 (C₇), 114.97 (C₇), 82.76 (C₉), 73.60 (C₃), 71.76 (C₃), 46.20 (C₁₂), 46.04 (C₁₂), 42.22 (C₄), 39.18 (C₁₀), 38.82 (C₁₀), 38.05 (C₄), 31.58 (C₁), 31.24 (C₁), 27.76 (C₁₁), 27.30 (C₁₁), 25.08 (C₁₄), 24.97 (C₁₄), 24.84 (C₁₄), 24.66 (C₁₄), 23.75 (C₁₃), 23.56 (C₁₃) – rotameric mixture

HRMS-ESI (*m/z*) [M+Na]⁺ calc. for C₂₀H₂₉N₂O₃NaCl, 403.1759; found 403.1750



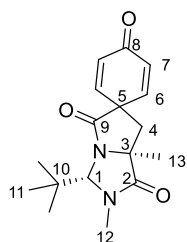
(2S,5S)-5-Benzyl-2-(tert-butyl)-5-(4-hydroxybenzyl)-3-methyl-4-oxoimidazolidine-1-carbonyl chloride (320)

To a solution of **315** (375 mg, 0.74 mmol) in THF (7.00 mL) under N₂, palladium on active carbon (10 wt. %) (74.0 mg, 20 % wt.) was added. The mixture was then stirred at room temperature for 4 hours under hydrogen atmosphere. The reaction mixture was filtered over a pad of celite and concentrated in *vacuo* to yield **320** (308 mg, Quant.) as a white powder.

¹H NMR (500 MHz, Chloroform-d) δ 7.45 – 7.41 (m, 1H, H₁₄), 7.36 (m, 1H, H₁₄), 7.31 – 7.29 (m, 1H, H₁₅), 7.28 – 7.21 (m, 2H, H_{15&16}), 7.11 – 7.01 (m, 2H, H₆), 6.76 (m, 2H, H₇), 4.89 (s, 0.51H, OH), 4.84 (s, 0.49H, OH), 4.32 (s, 0.49H, H₉), 4.14 (s, 1H, H₉), 3.75 (m, 1H, H_{4/12}), 3.58 (m, H_{4/12}), 3.55 – 3.44 (m, 1.51H, H_{4/12}), 3.17 (m, H_{4/12}), 3.01 (m, 0.49H, H_{4/12}), 2.71 (s, 1.47H, H₁), 2.65 (s, 1.53H, H₁), 0.66 (s, 4.45H, H₁₁), 0.40 (s, 4.55H, H₁₁) – rotameric mixture

¹³C NMR (126 MHz, Chloroform-d) δ 169.93 (C₂), 169.78 (C₂), 155.09 (C₈), 154.85 (C₈), 149.37 (C₁₇), 148.16 (C₁₇), 135.74 (C₁₃), 131.70 (C₆), 131.49 (C₆), 131.28 (C₁₄), 131.24 (C₁₄), 128.62 (C₁₅), 128.45 (C₁₅), 127.47 (C₁₆), 127.36 (C₁₆), 115.13 (C₇), 115.02 (C₇), 82.68 (C₉), 82.53 (C₉), 75.82 (C₃), 74.00 (C₃), 43.03 (C_{4/12}), 41.83 (C_{4/12}), 41.08 (C_{4/12}), 39.79 (C_{4/12}), 38.24 (C₁₀), 38.16 (C₁₀), 31.25 (C₁), 31.21 (C₁), 27.22 (C₁₁), 26.34 (C₁₁) – rotameric mixture

HRMS-ESI (*m/z*) [M+Na]⁺ calc. for C₂₃H₂₇N₂O₃NaCl, 437.1602; found 437.1617



(3'S,7a'S)-3'-(tert-Butyl)-2',7a'-dimethyl-2',3',7',7a'-tetrahydro-1'H,5'H-spiro[cyclohexane-1,6'-pyrrolo[1,2-c]imidazole]-2,5-diene-1',4,5'-trione (317)

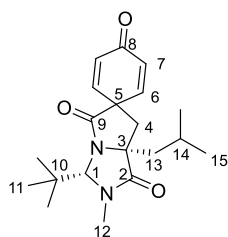
To a solution of **316** (200 mg, 0.60 mmol) in MeCN (3.00 mL), triethylamine (92 μ L, 0.66 mmol) was added. The mixture was then heated under microwave irradiation at 150 $^{\circ}$ C for 30 minutes. The reaction mixture was concentrated *in vacuo*, redissolved in dichloromethane (20 mL) and washed with water (10 mL). The aqueous phase was extracted with dichloromethane (3 x 10 mL). The combined organics were washed with brine (10 mL), dried over MgSO₄, filtered and concentrated *in vacuo* to yield **317** (180 mg, Quant.) as a yellow foam.

¹H NMR (500 MHz, Chloroform-d) δ 7.07 (dd, J = 10.0, 3.0 Hz, 1H, H₆), 6.64 (dd, J = 10.0, 3.0 Hz, 1H, H₆), 6.45 (dd, J = 10.0, 1.8 Hz, 1H, H₇), 6.40 (dd, J = 10.0, 1.8 Hz, 1H, H₇), 4.86 (s, 1H, H₁), 3.02 (s, 3H, H₁₂), 2.71 (d, J = 13.7 Hz, 1H, H₄), 2.36 (d, J = 13.7 Hz, 1H, H₄), 1.78 (s, 3H, H₁₃), 1.08 (s, 9H, H₁₁)

¹³C NMR (126 MHz, Chloroform-d) δ 184.66 (C₈), 177.32 (C₉), 174.12 (C₂), 147.22 (C₆), 144.73 (C₆), 131.90 (C₇), 130.77 (C₇), 83.48 (C₁), 63.17 (C₃), 53.94 (C₅), 45.39 (C₄), 36.52 (C₁₀), 31.31 (C₁₂), 27.02 (C₁₁), 26.66 (C₁₃)

R_f = 0.58 in 5% MeOH in DCM

HRMS-ESI (m/z) [M+Na]⁺ calc. for C₁₇H₂₂N₂NaO₃, 325.1523; found 325.1533



(3'S,7a'S)-3'-(tert-Butyl)-7a'-isobutyl-2'-methyl-2',3',7',7a'-tetrahydro-1'H,5'H-spiro[cyclohexane-1,6'-pyrrolo[1,2-c]imidazole]-2,5-diene-1',4,5'-trione (319)

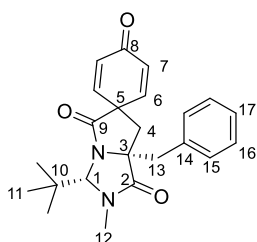
To a solution of **318** (192 mg, 0.41 mmol) in MeCN (2.00 mL), triethylamine (63 μ L, 0.45 mmol) was added. The mixture was then heated under microwave irradiation at 150 $^{\circ}$ C for 30 minutes. The reaction mixture was concentrated *in vacuo*, redissolved in dichloromethane (20 mL) and washed with water (10 mL). The aqueous phase was extracted with dichloromethane (3 x 10 mL). The combined organics were washed with brine (10 mL), dried over MgSO₄, filtered and concentrated *in vacuo* to yield **319** (142 mg, Quant.) as a yellow foam.

¹H NMR (500 MHz, Chloroform-d) δ 7.05 (dd, J = 10.0, 3.0 Hz, 1H, H₆), 6.67 (dd, J = 10.0, 3.0 Hz, 1H, H₆), 6.45 (dd, J = 10.0, 1.8 Hz, 1H, H₇), 6.42 (dd, J = 10.0, 1.8 Hz, 1H, H₇), 4.84 (s, 1H, H₁), 3.03 (s, 3H, H₁₂), 2.63 (s, 2H, H₄), 2.13 – 2.06 (m, 2H, H₁₃), 1.91 – 1.83 (m, 1H, H₁₄), 1.13 – 1.09 (m, 12H, H_{11&15}), 1.03 (d, J = 6.3 Hz, 3H, H₁₅)

¹³C NMR (126 MHz, Chloroform-d) δ 184.71 (C₈), 176.86 (C₉), 173.46 (C₂), 147.46 (C₆), 144.72 (C₆), 131.63 (C₇), 130.77 (C₇), 83.38 (C₁), 65.32 (C₃), 54.02 (C₅), 48.65 (C₁₃), 41.64 (C₄), 36.13 (C₁₀), 31.15 (C₁₂), 27.26 (C₁₁), 25.15 (C₁₄), 24.48 (C₁₅), 24.26 (C₁₅)

R_f = 0.73 in 5% MeOH in DCM

HRMS-ESI (m/z) [$M+Na$]⁺ calc. for C₂₀H₂₈N₂O₃Na, 367.1992; found 367.1985



(3'S,7a'S)-7a'-Benzyl-3'-(tert-butyl)-2'-methyl-2',3',7',7a'-tetrahydro-1'H,5'H-spiro[cyclohexane-1,6'-pyrrolo[1,2-c]imidazole]-2,5-diene-1',4,5'-trione (321)

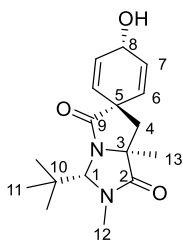
To a solution of **320** (308 mg, 0.74 mmol) in MeCN (4.00 mL), triethylamine (104 μ L, 0.81 mmol) was added. The mixture was then heated under microwave irradiation at 150 °C for 30 minutes. The reaction mixture was concentrated *in vacuo*, redissolved in dichloromethane (20 mL) and washed with water (10 mL). The aqueous phase was extracted with dichloromethane (3 x 10 mL). The combined organics were washed with brine (10 mL), dried over MgSO₄, filtered and concentrated *in vacuo* to yield **321** (275 mg, 98 %) as an orange foam.

¹H NMR (500 MHz, Chloroform-d) δ 7.46 – 7.32 (m, 5H, H_{15,16&17}), 6.49 (dd, J = 10.0, 3.0 Hz, 1H, H₆), 6.28 (dd, J = 10.0, 1.8 Hz, 1H, H₇), 5.89 (dd, J = 10.1, 1.8 Hz, 1H, H₇), 5.04 (dd, J = 10.1, 3.0 Hz, 1H, H₆), 4.91 (s, 1H, H₁), 3.28 (d, J = 14.5 Hz, 1H, H₁₃), 3.19 (d, J = 14.5 Hz, 1H, H₁₃), 3.09 (s, 3H, H₁₂), 2.55 (s, 2H, H₄), 1.25 (s, 9H, H₁₁)

¹³C NMR (126 MHz, Chloroform-d) δ 184.57 (C₈), 178.92 (C₉), 174.20 (C₂), 147.70 (C₆), 144.31 (C₆), 134.94 (C₁₄), 131.16 (C_{15/16}), 130.85 (C₇), 129.80 (C₇), 129.34 (C_{15/16}), 128.29 (C₁₇), 85.24 (C₁), 66.80 (C₃), 53.13 (C₅), 43.16 (C₁₃), 38.97 (C₄), 36.62 (C₁₀), 31.39 (C₁₂), 27.42 (C₁₁)

R_f = 0.70 in 5% MeOH in DCM

HRMS-ESI (m/z) [$M+Na$]⁺ calc. for C₂₃H₂₆N₂ONa₃, 401.1836; found 401.1837



(1s,3'S,4R,7a'S)-3'-(tert-Butyl)-4-hydroxy-2',7a'-dimethyl-2',3',7',7a'-tetrahydro-1'H,5'H-spiro[cyclohexane-1,6'-pyrrolo[1,2-c]imidazole]-2,5-diene-1',5'-dione (322)

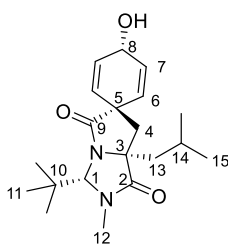
To a solution of **317** (180 mg, 0.60 mmol) in dry methanol (6.00 mL) under N₂, cerium(III) chloride heptahydrate (335 mg, 0.90 mmol) was added and stirred for 15 minutes at room temperature. The reaction mixture was then cooled to 0 °C and sodium borohydride (45.0 mg, 1.20 mmol) was added. The resultant mixture was left to stir for a further 30 minutes and then quenched with water (5 mL). The mixture was then diluted with EtOAc (20 mL) and washed with water (15 mL). The aqueous phase was extracted with EtOAc (3 x 10 mL) and brine (10 mL). The combined organics were dried over MgSO₄, filtered and concentrated *in vacuo*. Purification was carried out by column chromatography on silica gel eluting with 0-10% MeOH in dichloromethane to yield **322** (140 mg, 77 %) as a clear oil.

¹H NMR (400 MHz, Chloroform-d) δ 6.19 (m, 1H, H₆), 6.15 – 6.04 (m, 2H, H_{6&7}), 5.59 (m, 1H, H₇), 4.80 (s, 1H, H₁), 4.45 (m, 1H, H₈), 2.98 (s, 3H, H₁₂), 2.40 (d, *J* = 13.6 Hz, 1H, H₄), 2.23 (d, *J* = 13.6 Hz, 1H, H₄), 2.12 – 2.04 (m, 1H, OH), 1.71 (s, 3H, H₁₃), 1.06 (s, 9H, H₁₁)

¹³C NMR (101 MHz, Chloroform-d) δ 181.32 (C₂), 174.81 (C₉), 131.26 (C_{6/7}), 130.80 (C_{6/7}), 130.48 (C_{6/7}), 129.51 (C_{6/7}), 83.25 (C₁), 62.98 (C₃), 61.35 (C₈), 50.52 (C₅), 47.47 (C₄), 36.39 (C₁₀), 31.15 (C₁₂), 27.01 (C₁₁), 26.93 (C₁₃)

R_f = 0.55 in 5% MeOH in DCM

HRMS-ESI (*m/z*) [M+Na]⁺ calc. for C₁₇H₂₄N₂O₃Na, 327.1679; found 327.1670



(1s,3'S,4R,7a'S)-3'-(tert-Butyl)-4-hydroxy-7a'-isobutyl-2'-methyl-2',3',7',7a'-tetrahydro-1'H,5'H-spiro[cyclohexane-1,6'-pyrrolo[1,2-c]imidazole]-2,5-diene-1',5'-dione (324)

To a solution of **319** (140 mg, 0.40 mmol) in dry methanol (4 mL) under N₂, cerium(III) chloride heptahydrate (224 mg, 0.60 mmol) was added and stirred for 15 minutes at room temperature. The reaction mixture was then cooled to 0 °C and sodium borohydride (31 mg, 0.8 mmol) was added. The resultant mixture was left to stir for a further 30 minutes and then quenched with water

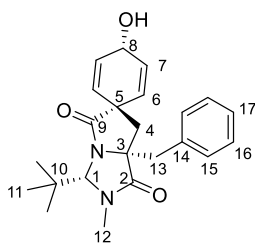
(10 mL). The mixture was then diluted with EtOAc (20 mL) and washed with water (15 mL). The aqueous phase was extracted with EtOAc (3 x 10 mL) and brine (10 mL). The combined organics were dried over MgSO₄, filtered and concentrated *in vacuo*. Purification was carried out by column chromatography on silica gel eluting with 0-10% MeOH in dichloromethane to yield **324** (70.0 mg, 50 %) as a yellow oil.

¹H NMR (500 MHz, Chloroform-d) δ 6.19 (m, 1H, H₆), 6.14 (m, 1H, H₆), 6.06 – 6.02 (m, 1H, H₇), 5.61 (m, 1H, H₇), 4.76 (s, 1H, H₁), 4.45 (m, 1H, H₈), 2.97 (s, 3H, H₁₂), 2.51 (d, J = 13.9 Hz, 1H, H₄), 2.30 (d, J = 13.9 Hz, 1H, H₄), 2.10 – 2.04 (m, 1H, H₁₄), 2.00 (dd, J = 14.2, 5.6 Hz, 1H, H₁₃), 1.80 (dd, J = 14.2, 6.2 Hz, 1H, H₁₃), 1.09 – 1.06 (m, 13H, H_{11&15}), 0.99 (d, J = 6.5 Hz, 3H, H₁₅)

¹³C NMR (126 MHz, Chloroform-d) δ 180.95 (C₂), 174.07 (C₉), 131.05 (C_{6/7}), 130.96 (C_{6/7}), 130.73 (C_{6/7}), 129.56 (C_{6/7}), 83.25 (C₁), 65.20 (C₃), 61.20 (C₈), 50.60 (C₅), 48.63 (C₁₃), 43.47 (C₄), 35.95 (C₁₀), 30.92 (C₁₂), 27.19 (C₁₁), 24.86 (C₁₄), 24.34 (C₁₅), 24.25 (C₁₅)

R_f = 0.53 in 5% MeOH in DCM

HRMS-ESI (m/z) [M+H]⁺ calc. for C₂₀H₃₀N₂O₃, 369.2149; found 369.2150



(1s,3'S,4R,7a'S)-7a'-Benzyl-3'-(tert-butyl)-4-hydroxy-2'-methyl-2',3',7',7a'-tetrahydro-1'H,5'H-spiro[cyclohexane-1,6'-pyrrolo[1,2-c]imidazole]-2,5-diene-1',5'-dione (326)

To a solution of **321** (275 mg, 0.73 mmol) in dry methanol (7.00 mL) under N₂, cerium(III) chloride heptahydrate (406 mg, 1.10 mmol) was added and stirred for 15 minutes at room temperature. The reaction mixture was then cooled to 0 °C and sodium borohydride (55 mg, 1.45 mmol) was added. The resultant mixture was left to stir for a further 30 minutes and then quenched with water (10 mL). The mixture was then diluted with EtOAc (20 mL) and washed with water (15 mL). The aqueous phase was extracted with EtOAc (3 x 10 mL) and brine (10 mL). The combined organics were dried over MgSO₄, filtered and concentrated *in vacuo*. Purification was carried out by column chromatography on silica gel eluting with 0-10% MeOH in dichloromethane to yield **326** (205 mg, 74 %) as a pale-yellow oil.

¹H NMR (500 MHz, Chloroform-d) δ 7.41 – 7.30 (m, 5H, H_{15,16&17}), 6.09 (m, 1H, H₆), 5.73 (m, 1H, H₇), 5.50 (m, 1H, H₇), 4.84 (s, 1H, H₁), 4.34 (dd, J = 9.9, 2.3 Hz, 1H, H₆), 4.26 (t, J = 4.1 Hz, 1H, H₈), 3.28 – 3.11 (m, 2H, H₁₃), 3.05 (s, 3H, H₁₂), 2.45 (d, J = 14.5 Hz, 1H, H₄), 2.28 (d, J = 14.5 Hz, 1H, H₄), 1.22 (s, 9H, H₁₁)

^{13}C NMR (126 MHz, Chloroform- d) δ 183.01 (C_2), 174.67 (C_9), 135.16 (C_{14}), 132.17 (C_7), 131.07 ($\text{C}_{15/16}$), 130.68 (C_6), 129.74 (C_7), 129.15 (C_6), 128.86 ($\text{C}_{15/16}$), 127.76 (C_{17}), 84.96 (C_1), 66.60 (C_3), 60.74 (C_8), 50.19 (C_5), 43.38 (C_{13}), 41.17 (C_4), 36.44 (C_{10}), 31.19 (C_{12}), 27.33 (C_{11})

R_f = 0.65 in 5% MeOH in DCM

HRMS-ESI (m/z) [$\text{M}+\text{Na}$] $^+$ calc. for $\text{C}_{23}\text{H}_{28}\text{N}_2\text{O}_3\text{Na}$, 403.1992; found 403.1998

6. References

- (1) Maeda, H.; Dudareva, N. *Annu. Rev. Plant Biol.* **2012**, *63*, 73.
- (2) Dewick, P. M. *Nat. Prod. Rep.* **1998**, *15*, 17.
- (3) Coggins, J. R. *Herbic. Plant Metab.* **1989**, *38*, 97.
- (4) Jensen, R.; Fischer, R. *Methods Enzymol.* **1987**, *142*, 472.
- (5) Stenmark, S. L.; Pierson, D. L.; Jensen, R. A.; Glover, G. I. *Nature* **1974**, *247*, 290.
- (6) Zamir, L. O.; Jensen, R. A.; Arison, B. H.; Douglas, A. W.; Albersschonberg, G.; Bowen, J. R. *J. Am. Chem. Soc.* **1980**, *102*, 4499.
- (7) Fazel, A. M.; Bowen, J. R.; Jensen, R. A. *Proc. Natl. Acad. Sci. U. S. A.* **1980**, *77*, 1270.
- (8) Ocallaghan, D.; Maskell, D.; Liew, F. Y.; Easmon, C. S. F.; Dougan, G. *Infect. Immun.* **1988**, *56*, 419.
- (9) Baylis, A. D. *Pest Manag. Sci.* **2000**, *56*, 299.
- (10) Rippert, P.; Matringe, M. *Eur. J. Biochem.* **2002**, *269*, 4753.
- (11) Legrand, P.; Dumas, R.; Seux, M.; Rippert, P.; Ravelli, R.; Ferrer, J. L.; Matringe, M. *Structure* **2006**, *14*, 767.
- (12) Christendat, D.; Saridakis, V. C.; Turnbull, J. L. *Biochemistry* **1998**, *37*, 15703.
- (13) Hermes, J. D.; Tipton, P. A.; Fbher, M. A.; Morrison, J. F.; Cleland, W. W. *Biochemistry* **1984**, *23*, 6263.
- (14) Forouzesh, A.; Zand, E.; Soufizadeh, S.; Samadi Foroushani, S. *Weed Res.* **2015**, *55*, 334.
- (15) Steinrücken, H. C.; Amrhein, N. *Biochem. Biophys. Res. Commun.* **1980**, *94*, 1207.
- (16) Schönbrunn, E.; Eschenburg, S.; Shuttleworth, W. A.; Schloss, J. V.; Amrhein, N.; Evans, J. N.; Kabsch, W. *Proc. Natl. Acad. Sci. U. S. A.* **2001**, *98*, 1376.
- (17) Franz, J. E.; Mao, M. K.; Sikorski, J. A. Glyphosate: a unique global herbicide. *Am. Chem. Soc.* **1997**, *12*, 564.
- (18) Franz, J. E. N-phosphonomethyl-glycine phytotoxicant compositions. US 3799758 A, **1974**.
- (19) Benbrook, C. M. *Environ. Sci. Eur.* **2016**, *28*, 3.
- (20) Barry, G. F.; Kishore, G. M.; Padgett, S. R.; Stallings, W. C. Glyphosate-tolerant 5-enolpyruvylshikimate-3-phosphate synthases. US5633435 A, 1997.
- (21) International Agency for Research on Cancer (World Health Organisation) <https://www.iarc.fr/en/media-centre/iarcnews/pdf/MonographVolume112.pdf> (accessed July 28, 2020).
- (22) Temple, W. Environmental Protection Agency. <https://www.epa.govt.nz/assets/Uploads/Documents/Everyday-Environment/Publications/EPA-glyphosate-review.pdf> (accessed July 28, 2020).
- (23) Kniss, A. R.; Hulting, A. G.; Rocque, L. M.; Vendômois, J. S. de; Séralini, G. E. *Nat.*

Commun. **2017**, 8, 14865.

- (24) Zhang, L.; Rana, I.; Shaffer, R. M.; Taioli, E.; Sheppard, L. *Mutation Research - Reviews in Mutation Research*. Elsevier B.V. **2019**, 186.
- (25) Jensen, R. A.; Pierson, D. A. *Nature* **1975**, 254, 667.
- (26) Rubin, J. L.; Jensen, R. A. *Plant Physiol.* **1979**, 64, 727.
- (27) Byng, G.; Whitaker, R.; Flick, C.; Jensen, R. A. *Phytochemistry* **1981**, 20, 1289.
- (28) Fazel, A. M.; Bowen, J. R.; Jensen, R. A. *Proc. Natl. Acad. Sci. U. S. A.* **1980**, 77, 1270.
- (29) Fazel, A. M.; Jensen, R. A. *J. Bacteriol.* **1979**, 140, 580.
- (30) Fazel, A. M.; Jensen, R. A. *J. Bacteriol.* **1979**, 138, 805.
- (31) Siehl, D. L.; Connelly, J. A.; Conn, E. E. *Z. Naturforsch. C.* **1986**, 41, 79.
- (32) Bode, R.; Casper, P.; Kunze, G. *Biochem. und Physiol. der Pflanz.* **1983**, 178, 457.
- (33) Jung, E.; Zamir, L. O.; Jensen, R. A. *PNAS* **1986**, 83, 7231.
- (34) Cho, M. H.; Corea, O. R. A.; Yang, H.; Bedgar, D. L.; Laskar, D. D.; Anterola, A. M.; Moog-Anterola, F. A.; Hood, R. L.; Kohalmi, S. E.; Bernards, M. A.; Kang, C.; Davin, L. B.; Lewis, N. G. *J. Biol. Chem.* **2007**, 282, 30827.
- (35) Ehlting, J.; Mattheus, N.; Aeschliman, D. S.; Li, E.; Hamberger, B.; Cullis, I. F.; Zhuang, J.; Kaneda, M.; Mansfield, S. D.; Samuels, L.; Ritland, K.; Ellis, B. E.; Bohlmann, J.; Douglas, C. J. *Plant J.* **2005**, 42, 618.
- (36) Danishefsky, S.; Morris, J.; Clizbe, L. A. *J. Am. Chem. Soc.* **1981**, 103, 1602.
- (37) Crossley, M. J.; Reid, R. C. *J. Chem. Soc. Chem. Commun.* **1994**, 2237.
- (38) Marshall, J. L.; Erickson, K. C.; Folsom, T. K. *Tetrahedron Lett.* **1970**, 11, 4011.
- (39) Hempel, C.; Weckenmann, N. M.; Maichle-Moessmer, C.; Nachtsheim, B. J. *Org. Biomol. Chem* **2012**, 10.
- (40) Brice, H.; Clayden, J.; Hamilton, S. D. *Beilstein J. Org. Chem.* **2010**, 6, 22.
- (41) Senczyszyn, J.; Brice, H.; Clayden, J. *Org. Lett.* **2013**, 15, 1922.
- (42) D. Ginn, J.; Padwa, A. *Org. Lett.* **2002**, 4, 1515.
- (43) He, W.; Huang, J.; Sun, X.; Frontier, A. J. *J. Am. Chem. Soc.* **2008**, 130, 300.
- (44) Baran, P. S.; Shenvi, R. A. *J. Am. Chem. Soc.* **2006**, 128, 14028.
- (45) Trzupek, J. D.; Lee, D.; Crowley, B. M.; Marathias, V. M.; Danishefsky, S. J. *J. Am. Chem. Soc.* **2010**, 132, 8506.
- (46) Siegel, D. R.; Danishefsky, S. J. *J. Am. Chem. Soc.* **2006**, 128, 1048.
- (47) Dai, M.; Danishefsky, S. J. *Tetrahedron Lett.* **2008**, 49, 6610.
- (48) Clayden, J.; Hamilton, S. D.; Mohammed, R. T. *Org. Lett.* **2005**, 7, 3673.
- (49) Arnott, G.; Brice, H.; Clayden, J.; Blaney, E. *Org. Lett.* **2008**, 10, 3089.
- (50) Brice, H.; Clayden, J. *Chem. Commun.* **2009**, No. 15, 1964.
- (51) Senczyszyn, J.; Brice, H.; Clayden, J. *Org. Lett.* **2013**, 15, 1922.
- (52) Roche, S. P.; Porco, J. A. *Angew. Chemie Int. Ed.* **2011**, 50, 4068.

- (53) Pouységou, L.; Deffieux, D.; Quideau, S. *Tetrahedron* **2010**, *66*, 2235.
- (54) Dohi, T.; Minamitsuji, Y.; Maruyama, A.; Hirose, S.; Kita, Y. *Org. Lett.* **2008**, *10*, 3559.
- (55) Snyder, S. A.; Sherwood, T. C.; Ross, A. G. *Angew. Chemie Int. Ed.* **2010**, *49*, 5146.
- (56) McGrath, N. A.; Bartlett, E. S.; Sittihan, S.; Njardarson, J. T. *Angew. Chemie Int. Ed.* **2009**, *48*, 8543.
- (57) Nicolaou, K. C.; Edmonds, D. J.; Li, A.; Tria, G. S. *Angew. Chemie Int. Ed.* **2007**, *46*, 3942.
- (58) Unsworth, W. P.; Cuthbertson, J. D.; Taylor, R. J. K. *Org. Lett.* **2013**, *15*, 3306.
- (59) Fu, J.-J.; Qin, J.-J.; Zeng, Q.; Huang, Y.; Jin, H. Z.; Zhang, W. D. *Chem. Pharm. Bull.* **2010**, *58*, 1263.
- (60) Ge, H. M.; Xu, C.; Wang, X. T.; Huang, B.; Tan, R. X. *European J. Org. Chem.* **2006**, *71*, 5551.
- (61) Gilbert, B.; Gilbert, M. E. A.; De Oliveira, M. M.; Ribeiro, O.; Wenkert, E.; Wickberg, B.; Hollstein, U.; Rapoport, H. *J. Am. Chem. Soc.* **1964**, *86*, 694.
- (62) Lemièrre, G.; Sedehizadeh, S.; Toueg, J.; Fleary-Roberts, N.; Clayden, J. *Chem. Commun.* **2011**, *47*, 3745.
- (63) Angelie, E. R.; Stessman, C. C.; Crew, P. *J. Nat. Prod.* **2003**, *66*, 939.
- (64) Chabaud, L.; Hromjakova, T.; Rambla, M.; Retailleau, P.; Guillou, C. *Chem. Commun. Chem. Commun* **2013**, *49*, 11542.
- (65) Honda, T.; Shigehisa, H. *Org. Lett.* **2006**, *8*, 657.
- (66) Nicolaou, K. C.; Edmonds, D. J.; Li, A.; Tria, G. S. *Angew. Chemie Int. Ed.* **2007**, *46*, 3942.
- (67) Nicolaou, K. C.; Li, A.; Edmonds, D. J.; Tria, G. S.; Ellery, S. P. *J. Am. Chem. Soc.* **2009**, *131*, 16905.
- (68) Schwartz, M. A.; Pham, P. T. K. *J. Org. Chem* **1988**, *53*, 2318.
- (69) Braun, N. A.; Ciufolini, M. A.; Peters, K.; Peters, E. M. *Tetrahedron Lett.* **1998**, *39*, 4667.
- (70) Tamura, Y.; Yakura, T.; Haruta, J. ichi; Kita, Y. *J. Org. Chem.* **1987**, *52*, 3927.
- (71) Tohma, H.; Harayama, Y.; Hashizume, M.; Iwata, M.; Kiyono, Y.; Egi, M.; Kita, Y. *J. Am. Chem. Soc.* **2003**, *125*, 11235.
- (72) Tohma, H.; Harayama, Y.; Hashizume, M.; Iwata, M.; Egi, M.; Kita, Y. *Angew. Chemie Int. Ed.* **2002**, *41*, 348.
- (73) Dohi, T.; Minamitsuji, Y.; Maruyama, A.; Hirose, S.; Kita, Y. *Org. Lett.* **2008**, *10*, 3559.
- (74) Ficht, S.; Mülbaier, M.; Giannis, A. *Tetrahedron* **2001**, *57*, 4863.
- (75) Rama Rao, A. V.; Gurjar, M. K.; Sharma, P. A. *Tetrahedron Lett.* **1991**, *32*, 6613.
- (76) Wipf, P.; Kim, Y.; Fritch, P. C. *J. Org. Chem.* **1993**, *58*, 7195.
- (77) Green, S. P.; Whiting, D. A.; Liang, K. S. Y.; Perkins, M. J.; Tezuka, Y.; Kikuchi, T.; Chan, D. F.; Xu, G. J.; Hori, T.; Extine, M.; Mizuno, H. *J. Chem. Soc. Perkin Trans. 1*

- 1998**, 113, 193.
- (78) Topiwala, U. P.; Luszniak, M. C.; Whiting, D. A.; Perkins, M. J.; Will, G.; Kirfel, A.; Langen, R. *J. Chem. Soc. Perkin Trans. 1* **1998**, 21, 1185.
 - (79) Turiso, F. G. L.; Curran, D. P. **2005**, 7, 151.
 - (80) Hamamoto, H.; Anilkumar, G.; Tohma, H.; Kita, Y. *Chem. - A Eur. J.* **2002**, 8, 5377.
 - (81) Millá N-Ortiz, A.; Ló Pez-Valdez, G.; Cortez-Guzmán, F.; Miranda, L. D. *Chem. Commun* **2015**, 51, 8345.
 - (82) Masamune, S. *J. Am. Chem. Soc.* **1961**, 83, 1009.
 - (83) McChesney, J. D.; Swanson, R. A. *J. Org. Chem.* **1982**, 47, 5201.
 - (84) Gajewski, R. P. *Tetrahedron Lett.* **1976**, 17, 4125.
 - (85) Hares, O.; Hobbs-Mallyon, D.; Whiting, D. A.; Seitz, S. P.; Johnston, J. O.; Robinson, C. *H. J. Chem. Soc. Perkin Trans. 1* **1993**, 69, 1481.
 - (86) Hobbs-Mallyon, D.; Whiting, D. A.; Coulson, D. R.; Whiting, D. A. *J. Chem. Soc. Perkin Trans. 1* **1991**, 96, 2277.
 - (87) Rousseaux, S.; García-Fortanet, J.; Del Aguila Sanchez, M. A.; Buchwald, S. L. *J. Am. Chem. Soc.* **2011**, 133, 9282.
 - (88) Qian, P. C.; Liu, Y.; Song, R. J.; Xiang, J. N.; Li, J. H. *Synlett* **2015**, 26, 1213.
 - (89) Wu, W. T.; Xu, R. Q.; Zhang, L.; You, S. L. *Chem. Sci.* **2016**, 7, 3427.
 - (90) Nemoto, T.; Wu, R.; Zhao, Z.; Yokosaka, T.; Hamada, Y. *Tetrahedron* **2013**, 69, 3403.
 - (91) Dohi, T.; Nakae, T.; Ishikado, Y.; Kato, D.; Kita, Y. *Org. Biomol. Chem.* **2011**, 9, 6899.
 - (92) Clarke, A. K.; Liddon, J. T. R.; Cuthbertson, J. D.; Taylor, R. J. K.; Unsworth, W. P.; J. *Org. Biomol. Chem.* **2017**, 15, 233.
 - (93) Nemoto, T.; Ishige, Y.; Yoshida, M.; Kohno, Y.; Kanematsu, M.; Hamada, Y. *Org. Lett.* **2010**, 12, 5020.
 - (94) Yin, Q.; You, S. L. *Org. Lett.* **2012**, 14, 3526.
 - (95) Wu, Q. F.; Liu, W. B.; Zhuo, C. X.; Rong, Z. Q.; Ye, K. Y.; You, S. L. *Angew. Chemie Int. Ed.* **2011**, 50, 4455.
 - (96) Pati, L. C.; Roy, A.; Mukherjee, D. *Tetrahedron Lett.* **2000**, 41, 10353.
 - (97) Pati, L. C.; Roy, A.; Mukherjee, D. *Tetrahedron* **2002**, 58, 1773.
 - (98) Nemoto, T.; Wu, R.; Zhao, Z.; Yokosaka, T.; Hamada, Y. *Tetrahedron* **2013**, 9, 3403.
 - (99) Hashmi, A. S. K.; Schwarz, L.; Bolte, M. *Tetrahedron Lett.* **1998**, 39, 8969.
 - (100) Magnus, P.; Marks, K. D.; Meis, A. *Tetrahedron* **2015**, 71, 3872.
 - (101) Dohi, T.; Nakae, T.; Ishikado, Y.; Kato, D.; Kita, Y.; Fujioka, H.; Caemmerer, S.; Kita, Y.; Nakata, M. *Org. Biomol. Chem.* **2011**, 9, 6899.
 - (102) Wu, W. T.; Xu, R. Q.; Zhang, L.; You, S. L.; Toste, F. D.; Hashmi, A. S. K.; Luan, X.; Luan, X.; Jones, G. B. *Chem. Sci.* **2016**, 7, 3427.
 - (103) Luo, L.; Zheng, H.; Liu, J.; Wang, H.; Wang, Y.; Luan, X. *Org. Lett.* **2016**, 18, 2082.

- (104) Yin, Q.; You, S. L. *Org. Lett.* **2012**, *14*, 3526.
- (105) Nemoto, T.; Ishige, Y.; Yoshida, M.; Kohno, Y.; Kanematsu, M.; Hamada, Y. *Org. Lett.* **2010**, *12*, 5020.
- (106) Atkinson, R. C.; Fernandez-Nieto, F.; Rosello, J. M.; Clayden, J. *Angew. Chemie-International Ed.* **2015**, *54*, 8961.
- (107) Seebach, D.; Fadel, A. *Helv. Chim. Acta* **1985**, *68*, 1243.
- (108) Atkinson, R. C.; Fernández-Nieto, F.; Mas Roselló, J.; Clayden, J. *Angew. Chemie Int. Ed.* **2015**, *54*, 8961.
- (109) Fadel, A.; Salaün, J. *Tetrahedron Lett.* **1987**, *28*, 2243.
- (110) Alonso, F.; Davies, S. G.; Elend, A. S.; Smith, A. D.; Schlatter, V.; Smith, A. D.; Thomson, J. E.; Shen, S.; Lee, H.; Farina, V.; Irwin, J. I.; Locher, R.; Maestro, M.; Maetzke, T.; Mourino, A.; Pfammatter, E.; Plattner, D. A.; Schickli, C.; Schweizer, W. B.; Seiler, P.; Stucky, G. *Org. Biomol. Chem.* **2009**, *7*, 518.
- (111) Seebach, D.; Sting, A. R.; Hoffmann, M. *Angew. Chemie Int. Ed. English* **1996**, *35*, 2708.
- (112) Amer, M. M.; Abas, H.; Leonard, D. J.; Ward, J. W.; Clayden, J. *J. Org. Chem.* **2019**, *84*, 7199.
- (113) Amer, M. M.; Carrasco, A. C.; Leonard, D. J.; Ward, J. W.; Clayden, J. *Org. Lett.* **2018**, *20*, 7977.
- (114) Zamir, L. O.; Tiberio, R.; Jung, E.; Jensen, R. A. *J. Biol. Chem.* **1983**, 258.
- (115) Legrand, P.; Dumas, R.; Seux, M.; Rippert, P.; Ravelli, R.; Ferrer, J.-L.; Matringe, M. *Structure* **2006**, *14*, 767.
- (116) Butts, C. P.; Jones, C. R.; Harvey, J. N. *Chem. Commun* **2011**, *47*, 1193.
- (117) Naganawa, Y.; Kawagishi, M.; Ito, J.; Nishiyama, H. *Angew. Chemie Int. Ed.* **2016**, *55*, 6873.
- (118) Yang, H.; Liu, X.; Li, Q.; Li, L.; Zhang, J. R.; Tang, Y. *Org. Biomol. Chem* **2016**, *14*, 198.
- (119) Jonathan Clayden; Nick Greeves; Stuart Warren. *Organic Chemistry*; Oxford University Press: Oxford, 2012.
- (120) Abas, H.; Amer, M. M.; Olaizola, O.; Clayden, J. *Org. Lett.* **2019**, *21*, 1908.
- (121) Zamir, L. O.; Tiberio, R.; Jung, E.; Jensen, R. A. *J. Biol. Chem. Print. m U. S. A* **1983**, 258.
- (122) Rippert, P.; Matringe, M. *Eur. J. Biochem.* **2002**, *269*, 4753.
- (123) Alpert, A. J. *J. Chromatogr.* **1990**, *499*, 177.
- (124) Buszewski, B.; Noga, S. *Anal. Bioanal. Chem.* **2012**, *402*, 231.
- (125) Thermo Fisher <https://assets.thermofisher.com/TFS-Assets/CMD/Specification-Sheets/TG-20394-Method-Development-Guide-Hypercarb-Columns-TG20394-EN.pdf> (accessed July 28, 2020)
- (126) Thermo Fisher https://www.hplc.eu/Downloads/Thermo_Hypercarb.pdf (accessed July 28, 2020)

- (127) Thermo Fisher https://www.pragolab.cz/documents/hypercarb_technical.pdf (accessed July 28, 2020)
- (128) Shaikh, A. C.; Banerjee, S.; Mule, R. D.; Bera, S.; Patil, N. T. *J. Org. Chem.* **2019**, *84*, 4120.
- (129) Boger, D. L.; Boyce, C. W. *J. Org. Chem.* **2000**, *65*, 4088.
- (130) Murashige, R.; Hayashi, Y.; Ohmori, S.; Torii, A.; Aizu, Y.; Muto, Y.; Murai, Y.; Oda, Y.; Hashimoto, M. *Tetrahedron* **2011**, *67*, 641.
- (131) Lister, T.; Sharma, R.; Zabawa, T.; Robert, Z. Polymyxin Analogs Useful As Antibiotic Potentiators. WO/2017/189866, **2017**
- (132) Raffier, L.; Piva, O. *Beilstein J. Org. Chem.* **2011**, *7*, 151.
- (133) Amer, M. M.; Carrasco, A. C.; Leonard, D. J.; Ward, J. W.; Clayden, J. *Org. Lett.* **2018**, *20*, 7977.
- (134) Cerezo, V.; Amblard, M.; Martinez, J.; Verdié, P.; Planas, M.; Feliu, L. *Tetrahedron* **2008**, *64*, 10538.
- (135) Knör, S.; Laufer, B.; Kessler, H. *J. Org. Chem.* **2006**, *71*, 5625.
- (136) Quiroz-Florentino, H.; Hernández-Benitez, R. I.; Aviña, J. A.; Burgueño-Tapia, E.; Tamariz, J. *Synthesis* **2011**, *7*, 1106.